Dysregulated mRNA Translation in Autism Spectrum Disorders

Mehdi Hooshmandi

Integrated Program of Neuroscience

McGill University, Montreal, Quebec

A thesis submitted to McGill University in partial fulfillment of the requirements of the degree of Doctor of Philosophy

Table of contents

Abstract

Deviation from the optimal level of proteostasis has been causally associated with a variety of clinical disorders, including autistic phenotypes in fragile X syndrome (FXS). Elevated levels of general protein synthesis have been reported in FXS animal models and patients. Despite the well-known contributions of the mechanistic target of rapamycin complex 1 (mTORC1) and extracellular signal-regulated kinase (ERK) pathways in the development of autistic symptoms, the significance of the integrated stress response (ISR), another key mRNA translational control pathway, in autism remains elusive. The highly conserved ISR pathway responds to cellular stress by suppressing general protein synthesis via phosphorylation of the α-subunit of eukaryotic translation initiation factor 2 (p-eIF2α). Lowering p-eIF2α promotes general protein synthesis. We found a concomitant reduction in p-eIF2α and an increase in general protein synthesis exclusively in excitatory neurons, but not inhibitory neurons, in the brain of the FXS mouse model, the fragile X mental retardation 1 knockout mouse (*Fmr*1$^{-/y}$). We also found that the ISR suppression is mediated by enhanced mTORC1 activity. The genetic decrease of p-eIF2α in excitatory neurons is sufficient to produce social impairments and repetitive behaviors, two core symptoms of autism. Consistently, correction of p-eIF2α selectively in excitatory neurons, using a viral approach, rescued the electrophysiological, behavioral, and biochemical impairments in *Fmr*1$^{-/y}$ mice. Thus, excitatory neuron-specific suppression of the ISR contributes to the exaggerated general protein synthesis and autistic-like behaviors in *Fmr*1$^{-/y}$ mice.

Aside from the proven involvement of mTORC1 in autism-like phenotypes in several areas of the brain such as hippocampus and cortex, recent studies have revealed that selective ablation of the mTORC1 negative regulator tuberous sclerosis proteins 1 and 2 (TSC1 and 2) or phosphatase and tensin homolog (PTEN) in cerebellar Purkinje cells (PCs) causes autistic-like

behavior in mice. However, the molecular mechanisms by which the cerebellar PC-specific mTORC1 overactivation causes autistic symptoms remain unknown. We observed that mice with PC-selective deletion of the eukaryotic translation initiation factor 4E-binding protein 2 (4E-BP2), a major downstream effector of mTORC1 and translational repressor, show loss of PC's, increased PC action potential firing rate regularity, and impaired motor learning. Surprisingly, despite the spatial memory deficits in the Morris water maze test, these mice showed no autistic-like behaviors. These findings suggest that mTORC1/4E-BP2 signaling in the cerebellar PCs mediates spatial memory and social behaviors via distinct mechanisms.

RÉSUMÉ

Une déviation par rapport au niveau optimal de protéostase dévoile un lien de causalité avec une variété de troubles clinique, incluant certains phénotypes autistiques appartenant au syndrome de l'X fragile (SXF). Des niveaux élevés de synthèse générale de protéine ont été observés dans des modèles de SXF animaux et humain. Malgré les contributions reconnues du mechanistic target of rapamycin complex 1 (mTORC1) et les voies de signalisation par la kinase ERK dans le développement de symptômes autistiques, l'importance de la réaction intégrée au stress (RIS), une autre voie fondamentale au contrôle de traduction d'ARN, dans l'autisme demeure floue. La voie RIS hautement conservée réagit au stress cellulaire en supprimant la synthèse générale de protéine via la phosphorylation du sous-unité alpha du facteur 2 eucaryote d'initiation de traduction d'ARN messager (p-eIF2α). Cette réduction de p-eIF2α favorise la synthèse générale de protéine. Nous avons trouvé une réduction concomitante de p-eIF2α et une croissance de synthèse générale de protéine exclusivement dans les neurones excitateurs, et non dans les inhibiteurs, dans le cerveau des modèles SXF de souris *Fmr1*$^{-/y}$ (« fragile mental retardation 1 knockout mouse »). Nous avons aussi trouvé que la suppression de la RIS est modérée par une activité accrue de mTORC1. La diminution

génétique de p-eIF2α dans les neurones excitateurs est suffisante pour produire des troubles sociaux et des comportements répétitifs, deux symptômes fondamentaux de l'autisme. Systématiquement, la correction de niveaux de p-eIF2α dans les neurones excitateurs avec une méthode utilisant des virus a corrigé les déficiences électrophysiologiques, comportementales, et biochimiques des souris *Fmr1*$^{-/y}$. Ainsi, la suppression spécifique des neurones excitateurs de la RIS contribue à la synthèse générale exagérée de protéine et aux comportements de type autiste dans les souris *Fmr1*$^{-/y}$.

Autre que l'implication avérée de mTORC1 dans les phénotypes de type autiste dans plusieurs zones du cerveau comme l'hippocampe et le cortex, des études récentes dévoilent que l'ablation sélective des protéines régulatrices négatives de sclérose tubéreuse (TSC1 et 2) de mTORC1, ou de la phosphatase et de l'homologue la tensine (PTEN) dans les cellules Purkinje cérébelleuses (PCs) suscite un comportement de type autiste parmi les souris. Cependant, les mécanismes moléculaires par lesquels l'hyperactivation de mTORC1 spécifique au PC cérébelleuses cause ces symptômes de type autiste demeures inconnus. Nous avons observé que des souris avec une délétion spécifique aux PC du facteur eucaryote d'initiation de traduction d'ARN 4E-BP2 (« 4E-binding protein 2 »), une protéine majeure en aval de mTORC1 et une inhibitrice de traduction, démontre une perte de PC, augmente la régularité des potentiels d'action des PC, et compromet l'apprentissage moteur. Étonnamment, malgré les déficits de mémoire spatiale dans le test « Morris water maze », ces souris n'ont pas présenté de comportements de type autiste. Ces résultats proposent que la signalisation de mTORC1/4E-BP2 dans les PC cérébelleuses modère la mémoire spatiale et les comportements sociaux via des mécanismes distingués.

Acknowledgments

I would first like to extend my sincere gratitude to my supervisor, Dr. Arkady Khoutorsky, for your unwavering support, mentorship, and encouragement throughout this long journey and, importantly, the opportunity you provided me to join your lab, where I could master multiple techniques, systematically troubleshoot potential errors, and formulate a scientific question with the appropriate study design and methodology. Regardless of the project-related obstacles and challenges, you have always been supportive and patient while offering your best insights and feedback on the project.

Next, I am profoundly grateful to the members of my advisory committee: Dr. Nahum Sonenberg and Dr. Wayne S. Sossin, and my mentor Dr. Kenneth E M Hastings. Through your valuable comments and conversations at our annual advisory meetings, you shaped my project into what it is today. You taught me to be critical when it comes to experimenting, collecting, analyzing, interpreting, and presenting data.

I would greatly thank our collaborators in both manuscripts who generously contributed to the project and kindly offered us their time and efforts. I would also like to extend my deep appreciation to my colleagues, Jieyi Yang, Calvin Wong, Dr. Carolina Thörn Perez, Dr. Patricia Roque, Patricia Stecum, Weihua Cai, Kevin Lister, Nicole Brown, Alba Guzman, Shilan Heshmati, Emma Nadler, Georgio Mansour Nehmo and Amirah-Iman Hicks who made such an incredible atmosphere in the lab.

I am extremely grateful to the funding agencies, Brain Canada and Transforming Autism Care Consortium (TACC) graduate fellowships, Quebec Autism Research Training (QART)

Program, and Simons Foundation (SFARI, award #611773) which financially supported this project.

A special thanks to Vahideh, my wife, who has always been supporting me, especially during my Ph.D. You have gone through a lot of hardship due to immigration, yet you have pretended that everything is absolutely fine and kept encouraging me. I am eternally grateful to my parents and my sibling for their unconditional love and consistent support over my entire life.

Contribution to original knowledge

In the first chapter, we showed that, in parallel with the established translational control pathways such as mTORC1 and ERK, reduced activity of the integrated stress response signaling also significantly contributes to the autistic-like behaviors in the mouse model of fragile X syndrome. These findings revealed a putative signaling pathway that could be targeted to alleviate autistic symptoms. Furthermore, this study showed that in *Fmr*1$^{-/y}$ mice the dysregulated ISR is restricted to excitatory neurons, but not inhibitory neurons. These findings suggest that future manipulations and therapies should target certain types of neurons in the brain rather than non-selectively exposing all neurons to medication.

It has been reported that overactivation of mTORC1 in the cerebellar Purkinje cells through loss of PTEN or TSC1/2, two negative inhibitors of mTORC1, results in an autistic-like phenotype in mice. In the second manuscript, we showed that these effects are not mediated through the main downstream effector of mTORC1, 4E-BP2. However, we found that mice lacking 4E-BP2 in cerebellar Purkinje cells exhibit impaired spatial memory in the Morris water maze task. These results suggest that mTORC1 hyperactivation in Purkinje cells engenders autistic-like behaviors through other mTORC1 downstream effectors such as ribosomal S6K.

Manuscript 1: Mehdi Hooshmandi, Vijendra Sharma, Carolina Thörn Perez, Rapita Sood, Konstanze Simbriger, Calvin Wong, Emma Nadler, Patricia Margarita Roque, Ilse Gantois, Jelena Popic, Maxime Lévesque, Randal J. Kaufman, Massimo Avoli, Elisenda Sanz, Karim Nader, Mauro Costa-Mattioli, Jean-Claude Lacaille, Nahum Sonenberg, Christos G. Gkogkas, and Arkady Khoutorsky. *The integrated stress response pathway in excitatory neurons controls autism-related features.* The manuscript is under review in ***Neuron*.** We plan to resubmit it in November 2022.

Manuscript 2: Mehdi Hooshmandi, Vinh Tai Truong, Eviatar Fields, Riya Elizabeth Thomas, Calvin Wong, Vijendra Sharma, Ilse Gantois, Patricia Soriano Roque, Kleanthi Chalkiadaki, Neil Wu, Anindyo Chakraborty, Soroush Tahmasebi, Masha Prager-Khoutorsky, Nahum Sonenberg, Aparna Suvrathan, Alanna J. Watt, Christos G. Gkogkas, Arkady Khoutorsky. *4E-BP2-dependent translation in cerebellar Purkinje cells controls spatial memory but not autism-like behaviors*, ***Cell Reports***, Volume 35, Issue 4, 2021, 109036, ISSN 2211-1247, https://doi.org/10.1016/j.celrep.2021.109036.
(https://www.sciencedirect.com/science/article/pii/S221112472100352

Contribution of authors

These two manuscripts were completed with the help of many researchers, as follows:

In the first chapter: Mehdi Hooshmandi, Dr. Arkady Khoutorsky, Dr. Nahum Sonenberg, and Dr. Christos G. Gkogkas contributed to the study conception and design, writing/editing. Mehdi Hooshmandi: conducting biochemistry, behaviors, field potential recordings, and surgical experiments. Vijendra Sharma: intellectually influenced the manuscript and contributed to the methodology. Rapita Sood: helped with the animal colony. Konstanze Simbriger: analyzed the bioinformatics data. Calvin Wong, Emma Nadler, Patricia Margarita Roque, Ilse Gantois, Jelena Popic, and Maxime Lévesque: helped with methodology and scoring behaviors, and quantifications. Jean-Claude Lacaille and Carolina Thörn Perez: electrophysiological design and conducted patch clamp recording. Randal J. Kaufman, Massimo Avoli, Elisenda Sanz, Karim Nader, Mauro Costa-Mattioli, and all co-authors helped with study design and editing the manuscript.

In the second chapter: Mehdi Hooshmandi, Vinh Tai Truong*, Nahum Sonenberg, Masha Prager-Khoutorsky, Soroush Tahmasebi, Christos G. Gkogkas, and Arkady Khoutorsky conceived the project, designed experiments, supervised the research, and wrote the manuscript. Mehdi Hooshmandi performed immunohistochemistry and biochemistry experiments, assessed motor and ASD-like behaviors, analyzed the data, and generated the figures. Vijendra Sharma performed the MWM experiment. The electrophysiological recordings were carried out by Eviatar Fields, Riya Elizabeth Thomas, Aparna Suvrathan, and Alanna J. Watt. Calvin Wong, Ilse Gantois, Patricia Soriano Roque, Kleanthi Chalkiadaki, Neil Wu, and Anindyo Chakraborty assisted with behavioral quantifications and mouse colony management. All authors contributed to editing the manuscript.

*Vinh Tai Truong is co-first on the project.

List of abbreviations

mTOR: Mammalian Target of Rapamycin

ERK: Extracellular ligand-Regulated Kinases

FXS: Fragile X Syndrome

PTEN: Phosphatase and Tensin Homolog

TSC: Tuberous Sclerosis Complex

4E-BP2: Eukaryotic Translation Initiation Factor 4E-Binding Protein 2

PC: Purkinje Cell

IRES: Internal Ribosome Entry Sites

eIF: Eukaryotic Initiation Factor

PIC: Pre-Initiation Complex

PI3K: Phosphoinositide 3-Kinase

PIP2: Phosphatidylinositol 4,5-bisphosphate

PIP3: Phosphatidylinositol (3,4,5)-trisphosphate

PDK1: Pyruvate Dehydrogenase Kinase 1

Rheb: Ras Homolog Enriched in Brain

FKBP38: FK506-Binding Protein 38

S6K1: Ribosomal Protein S6 Kinase Beta-1

eEFK2: Eukaryotic Elongation Factor 2 Kinase

PKR: Double-Stranded RNA-dependent Protein Kinase R

GCN2: General Control Non-depressible 2

HRI: Heme-Regulated Inhibitor

PERK: PKR-like Endoplasmic Reticulum Kinase

EIF2AK3: Eukaryotic Translation Initiation Factor 2 Alpha Kinase 3

EIF2AK2: Eukaryotic Translation Initiation Factor 2 Alpha Kinase 2

dsRNA: Double-Stranded RNA

EIF2AK4: Eukaryotic Translation Initiation Factor 2 Alpha Kinase 4

EIF2AK1: Eukaryotic Translation Initiation Factor 2 Alpha Kinase 1

ATF4: Activating Transcription Factor 4

CHOP: C/EBP Homologous Protein

GADD34: Growth Arrest and DNA Damage-Inducible Protein

ORF: Open Reading Frame

UTR: Untranslated Region

IRES: Internal Ribosome Entry Sites

PP1: Protein Phosphatase 1

PPP1R15A: Protein Phosphatase 1 Regulatory Subunit 15A

PPP1R15B: Protein Phosphatase 1 Regulatory Subunit 15B

PDD-NOS: Pervasive Developmental Disorders Not Otherwise Specified

ASD: Autism Spectrum Disorder

OCD: Obsessive-Compulsive Disorder

ADHD: Attention-Deficit Hyperactivity Disorder

DZ: Dizygotic

MZ: Monozygotic

CNV: Copy Number Variations

FXS: Fragile X Syndrome

MeA: Medial Amygdala

FMRP: Fragile X Mental Retardation Protein

FXTAS: Fragile X-Associated Tremor/Ataxia Syndrome

FXPOI: Fragile X-Associated Primary Ovarian Insufficiency

FXAND: Fragile X-Associated Neuropsychiatric Disorders

RGG: Arginine-Glycine-Glycine

NES: Nuclear Export Signal

NLS: Nuclear Localization Signal

TD1: Tudor Domain 1

DDR: DNA Damage Response

RIP: Ribonucleoprotein Coimmunoprecipitation

G4: G-quadruplex

HITS-CLIP: High-Throughput Sequencing of RNA Isolated by Crosslinking and Immunoprecipitation

CDS: Coding Sequence

DHPG: (S)-3,5-Dihydroxyphenylglycine

Brd4: Bromodomain-containing protein 4

CYFIP1: Cytoplasmic FMRP Interacting Protein 1

AGS: Audiogenic Seizure

LTD: Long-Term Depression

LTP: Long-Term Potentiation

mGluR: Metabotropic Glutamate Receptor

AMPAR: α-Amino-3-hydroxy-5-Methyl-4-isoxazolepropionic Acid Receptor

PP-LFS: Paired-Pulse Low-Frequency Stimulation

PIKE: Phosphatidylinositol 3-Kinase Enhancer Protein

MAPK: Mitogen-Activated Protein Kinase

PET: Positron Emission Tomography

SUnSET: SUrface SEnsing of Translation

SYNGAP1: Synaptic Ras GTPase-Activating Protein 1

NF1: Neurofibromin 1

ISRIB: Integrated Stress Response Inhibitor

DS: Down Syndrome

Chapter 1: General introduction

1.1 Protein synthesis

Protein synthesis, also referred to as mRNA translation, is a vital and energy-consuming biological process in which the mRNAs are converted into polypeptides by the ribosome machinery. In eukaryotes, this process occurs outside the nucleus in the cytoplasm. mRNA translation consists of three key phases: initiation, elongation, and termination. Translation is tightly regulated in an optimum range by several signaling pathways and is modulated in response to a wide range of external and internal stimuli. This high-precision regulation can be exerted at any stage of the translation process; however, translation is predominantly regulated at the initiation stage. Deviations from the optimum level of translational regulation is associated with numerous disorders and diseases (Taylor and Brameld 1999, Jackson, Hellen et al. 2010).

1.2 The initiation phase of translation

The initiation phase of mRNA translation can be cap-dependent or cap-independent. Cap-dependent initiation is the canonical pathway of translation initiation in eukaryotes. Unlike viruses, eukaryotic mRNAs contain a 5´ cap structure that is essential for the effective binding of the initiation factors (Richter and Sonenberg 2005). On the other hand, cap-independent initiation relies on the internal ribosome entry sites (IRESs) on the mRNA to recruit ribosomes to the internal region of the mRNA to initiate translation. This pathway was first discovered in the Picornaviridae family of viruses (Pelletier and Sonenberg 1988). However, this mechanism of initiation has also been observed in cellular mRNA under cellular stress conditions (Komar and Hatzoglou 2011). The 5´ cap, referred to as a 7-methylguanylate cap (m7G), consists of guanosine that is methylated at position 7 (Sonenberg and Gingras 1998). The initiation phase first begins with the formation of the 43S pre-initiation complex (PIC). This complex is composed of recycled 40S ribosomal small subunits from the previous cycle of translation and

the eIF2 (eukaryotic initiation factors 2) ternary complex (eIF2-GTP-Met-tRNA$^{Met}_i$). The 40S subunit contains three sites: an unoccupied P site, and blocked A and E sites with eIF1A and eIF1, respectively. The eIF3 additionally prevents the 40S from being activated. The GTP-coupled eIF2 transfers the initiator tRNA to the 40S subunit to generate the 43S PIC (Hershey, Sonenberg et al. 2019). Second, the mRNA is activated by the eIF4F complex and eIF4B in an ATP-dependent manner and attaches to the 43S PIC. The eIF4F complex is composed of three subunits: eIF4E (an mRNA cap-binding protein), eIF4A (a RNA helicase), and eIF4G, a large scaffolding protein linking eIF4E to eIF4A (Marcotrigiano, Gingras et al. 1997). The abundance of eIF4E is exceedingly low among all initiation factors and therefore eIF4E activity is the rate-limiting factor for translation (Marcotrigiano, Gingras et al. 1997). Third, the scanning step starts from 5′ to 3′ to identify the initiation codon, AUG. Once the initiation codon is recognized, the GTP-bound to eIF2 is hydrolyzed and the initiator tRNA is appropriately positioned at the P site, and eIF2-GDP is released. The complex is now called 48S initiation complex. Fourth, the large ribosomal subunit 60S is assembled to the 48S complex, assisted by eIF5B-GTP. Following the attachment of the 60S to the 48S complex, all initiation factors including eIF5B, eIF1, eIF1A, and eIF3 are released, and the 80S enters the elongation phase of translation (Jackson, Hellen et al. 2010).

The availability of the GTP-bound ternary complex via eIF2α phosphorylation and eIF4E via eIF4E-binding proteins (eIF4E-BPs) are two major translational control mechanisms that are rate-limiting steps in translation initiation (Gebauer and Hentze 2004). The mammalian target of rapamycin complex 1 (mTORC1), extracellular ligand-regulated kinase (ERK), and the integrated stress response (ISR) are three major signaling pathways that tightly control translation, primarily at the initiation phase. These pathways link numerous extracellular cues and intracellular stimuli to the translation machinery to maintain cellular homeostasis.

1.3 The mTORC1 pathway

mTORC1 is a complex and multifunctional protein kinase. mTORC1 integrates a broad range of extracellular and intracellular signaling inputs (growth factors, amino acids, energy, oxygen, and signals from membrane receptors) to regulate a wide variety of cellular functions including anabolism, catabolism, and autophagy via its downstream effectors. Importantly, mTORC1 along with the ERK and ISR pathways regulate the rate of the mRNA translation, thereby affecting cell growth and proliferation (Saxton and Sabatini 2017). Upstream signaling of mTORC1 in the brain is often initiated by G-protein-coupled neurotransmitter receptors such as mGluR5 or receptors with tyrosine kinase activity such as the insulin receptor. When these receptors are activated by its respective ligand, phosphoinositide 3-kinase (PI3K) is activated and transforms Phosphatidylinositol 4,5-bisphosphate (PIP2) into Phosphatidylinositol (3,4,5)-trisphosphate (PIP3). Conversely, PIP3 can be dephosphorylated by the phosphatase and tensin homolog (PTEN) (Maehama and Dixon 1998). PIP3 then activates pyruvate dehydrogenase kinase 1 (PDK1), and PDK1 phosphorylates protein kinase B (AKT) at threonine 308 (Engelman, Luo et al. 2006). AKT then directly phosphorylates tuberous sclerosis protein 2 (TSC2) (Manning, Tee et al. 2002) thereby removing TSC2's inhibitory effect on the GTP-binding protein known as ras homolog enriched in brain (Rheb). Next, Rheb, in a GTP-dependent manner, activates mTORC1 by preventing FK506-binding protein 38 (FKBP38) from interacting with mTOR (Bai, Ma et al. 2007). While PI3K, AKT, and Rheb activate mTORC1, PTEN and TSC2 inhibit mTORC1 activity.

mTORC1 also controls protein synthesis via two essential downstream effectors: S6K and 4E-BP2. eIF4E-binding proteins (4E-BPs) include three paralogs: 4E-BP1, BP2, and BP3, and BP2 is the most abundant in the brain. The 4E-BPs compete with eIF4G for the shared binding site on the surface of eIF4E, thereby preventing eIF4F complex formation and translation initiation. When upstream signaling pathways activate mTORC1, it phosphorylates

4E-BP2. As a result, eIF4E escapes 4E-BP2 repression, enabling eIF4G and eIF4A to bind and form the eIF4F complex thereby facilitating the initiation phase of translation (Bidinosti, Ran et al. 2010). Ribosomal protein S6 kinase 1 (S6K1) is the second major downstream effector of mTORC1. Once S6K1 is phosphorylated by mTORC1, S6K phosphorylates eIF4B and this, in turn, enhances eIF4E interaction with eIF4G and eIF4A helicase activity (Gingras, Raught et al. 2001, Shahbazian, Parsyan et al. 2010). S6K also phosphorylates eukaryotic elongation factor 2 kinase (eEFK2) and thereby contributes to the elongation phase of translation (Figure. 1) (Wang, Li et al. 2001).

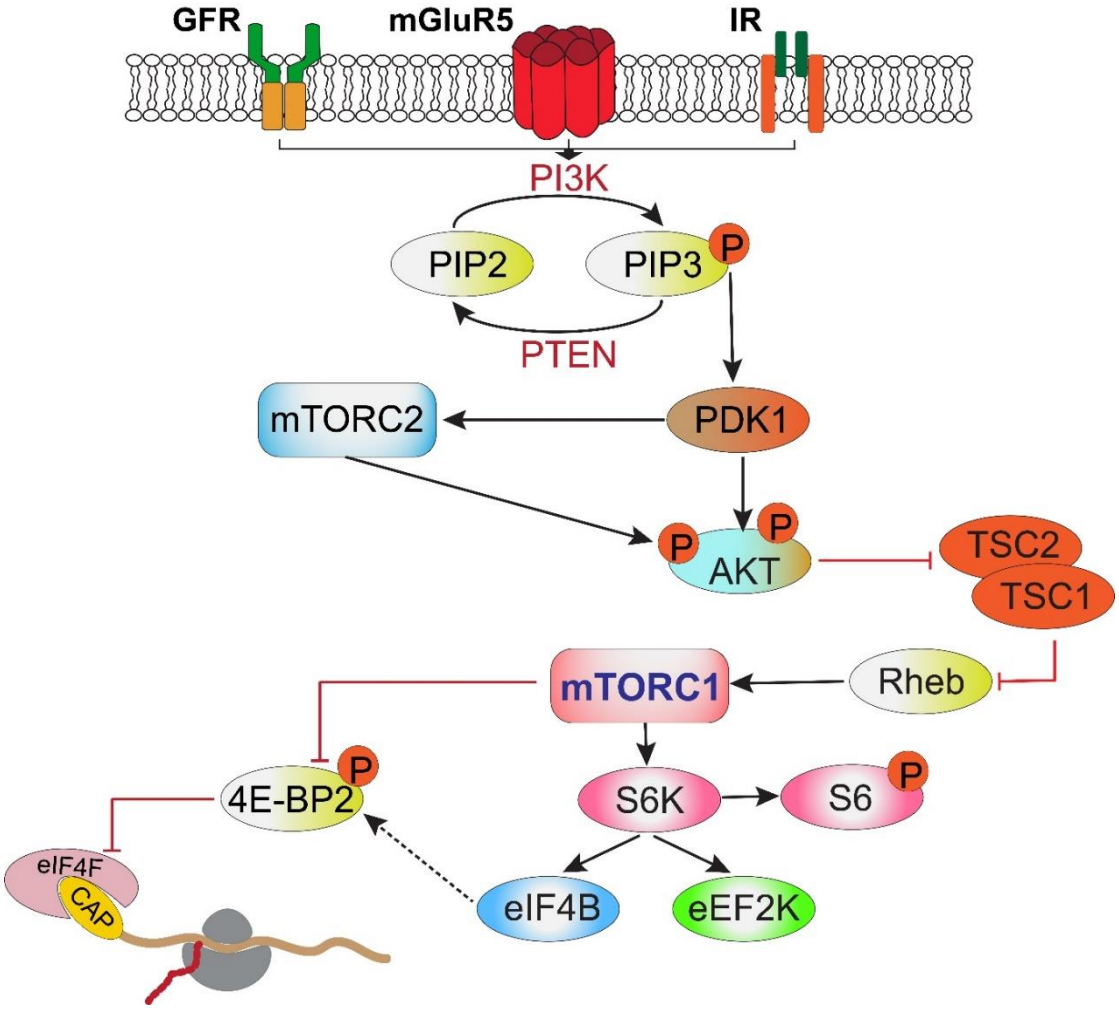

1.3.1 Figure 1. The mTORC1 pathway.

A schematic illustration depicting the mTORC1 pathway. The mTORC1 pathway is often activated by G-protein coupled receptors. When these receptors are activated, PI3K

phosphorylates PIP2 to activate PIP3. PIP3 then activates AKT, either directly through PDK1 or indirectly through mTORC2, and AKT activates Rheb by inhibiting TSC1/2. As a result, mTORC1 is activated and phosphorylates 4E-BPs, allowing the formation of the eIF4F complex and enhanced mRNA translation. mTORC1 also phosphorylates and activates ribosomal S6K which promotes biogenesis of the ribosome and translation elongation.

1.4 The MAPK/ERK pathway

The MAPK/ERK pathway plays a crucial role in the regulation of mRNA translation along with the mTORC1 pathway. A number of proteins within this pathway, including Ras, Raf, Mek1/2, ERK1/2, and Mnk1/2 receive and integrate the signals from membrane receptors to control mRNA translation, among other functions. The MAPK/ERK pathway either directly or indirectly regulates *de novo* protein synthesis. In direct signaling, the serine/threonine protein kinase ERK phosphorylates and activates the mitogen-activated protein kinase (MAPK) interacting protein kinases 1 and 2 (Mnk1/2) and Mnk1/2, in turn, phosphorylates eIF4E, modulating *de novo* protein synthesis (Wang, Flynn et al. 1998). This pathway also indirectly regulates protein synthesis by interacting with the mTORC1 pathway. ERK has been shown to phosphorylate TSC1/2 (Huang and Manning 2008) and Raptor (Carriere, Romeo et al. 2011), thereby enhancing mTORC1 activity. Furthermore, ERK phosphorylates and activates S6K, resulting in activation of eEF2K and eIF4B (Shahbazian, Roux et al. 2006). In conjunction with mTORC1, the ERK pathway modulates the rate of mRNA translation and mutations in proteins within this pathway cause a variety of disorders, including developmental conditions associated with autism.

1.5 The integrated stress response (ISR)

The ISR is the third major signaling pathway that controls mRNA translation to maintain cellular proteostasis in response to a broad range of physiological and pathological stimuli,

including amino acid deprivation, viral infection, and accumulation of unfolded proteins. The common checkpoint for activating the ISR is phosphorylation of the α-subunit of eIF2 at Serine-51. The key function of this signaling pathway is to cope with cellular stress and preserve cellular resources by inhibiting general protein synthesis and paradoxically facilitating the translation of stress-related mRNAs and their encoded proteins, such as activating transcription factor 4 (ATF4) (Pakos-Zebrucka, Koryga et al. 2016, Costa-Mattioli and Walter 2020).

1.6 The eukaryotic initiation factor 2 (eIF2) protein

The eIF2 is a heterotrimer protein composed of three subunits: α (subunit 1), β (subunit 2), and γ (subunit 3). The α-subunit, known as the regulatory subunit, contains serine at position 51, which is the only phosphorylation site on eIF2 (Erickson, Harding et al. 1997). The β-subunit interacts with the guanine nucleotide exchange factor eIF2B through the binding domain located at its C-terminus (Kimball, Heinzinger et al. 1998) and also contributes to the formation of 43S PIC (Jennings, Kershaw et al. 2016). The γ-subunit is the primary docking subunit for GTP/GDP and also has a specific site for tRNA binding (Alone and Dever 2006). Translation begins with the formation of the ternary complex comprising eIF2-GTP and the initiator Met-tRNA$_i$. As explained earlier, once the ternary complex is formed, it binds to the 40S small subunit to form 43S PIC and the cycle of translation repeats. When the Met-tRNA$_i$ is placed in the P site by hydrolyzing eIF2 bound GTP, the eIF2-GDP is released and the guanine exchanger factor, eIF2B loads the eIF2 with another GTP and makes it available for another cycle of ternary complex formation and translation initiation. eIF2B is the main target of phosphorylated eIF2α. Indeed, p-eIF2α is a competitive inhibitor of the eIF2B and thus controls the formation of the ternary complex. Therefore, the formation of the ternary complex

is the first rate-limiting steps at the initiation phase of translation (Figure. 2) (Hershey, Sonenberg et al. 2019).

1.6 Activation of the ISR

When exposed to stress, four serine/threonine kinases (double-stranded RNA-dependent protein kinase R (PKR), general control non-depressible 2 (GCN2), heme-regulated inhibitor (HRI), and PKR-like endoplasmic reticulum kinase (PERK)) become activated via autophosphorylation or dimerization to phosphorylate a serine 51 on the alpha subunit of eIF2 (Liu, Schröder et al. 2000, Bauer, Rafie-Kolpin et al. 2001, Narasimhan, Staschke et al. 2004). In contrast to the similarity in the catalytic domain, the regulatory domains of kinases are different, allowing them to respond to a variety of distinct stimuli (Donnelly, Gorman et al. 2013).

In humans, PERK kinase is encoded by eukaryotic translation initiation factor 2 alpha kinase 3 (*EIF2AK3*). PERK plays a key role in linking unfolded protein-induced stress inside the lumen of the endoplasmic reticulum (ER) to the protein synthesis machinery to prevent further general protein synthesis and assist in cell recovery (Marciniak, Garcia-Bonilla et al. 2006). PKR is encoded by eukaryotic translation initiation factor 2 alpha kinase 2 (EIF2AK2) and primarily inhibits protein synthesis in response to viral infection (Eiermann, Haneke et al. 2020) and double-stranded RNA (dsRNA) (Lemaire, Anderson et al. 2008). It has recently been shown that dsRNA may leak from the mitochondria even in the absence of viral infection and activate PKR (Kim, Park et al. 2018). GCN2 is encoded by eukaryotic translation initiation factor 2 alpha kinase 4 (EIF2AK4) and is expressed in various tissues, with higher expression in the brain and liver (Sood, Porter et al. 2000). GCN2 responds to multiple stimuli including UV radiation (Deng, Harding et al. 2002), heat shock (Taniuchi, Miyake et al. 2016), and, in particular, amino acid deprivation (Guo and Cavener 2007), most likely through sensing

accumulated amino acid-uncharged tRNAs (Dong, Qiu et al. 2000), or ribosome stalling (Harding, Ordonez et al. 2019, Wu, Peterson et al. 2020, Yan and Zaher 2021). Heme-regulated inhibitor (HRI) kinase is encoded by the eukaryotic translation initiation factor 2 alpha kinase 1 (EIF2AK1) and responds to heme deficiency (Chen 2000). While it is primarily expressed in erythrocytes, it is also expressed at low levels in neurons under physiological conditions (Alvarez-Castelao, tom Dieck et al. 2020). In addition, whereas each kinase distinctively responds to certain stressors, some stressors can simultaneously activate multiple kinases.

1.7 The eIF2α -ATF4 axis

When the level of p-eIF2α is increased, the translation of two clusters of mRNAs is paradoxically elevated. First are the mRNAs that contain an upstream open reading frame (ORF) (Hinnebusch, Ivanov et al. 2016). An uORF is an open reading frame (ORF) located at the 5´ UTR of the mRNA that regulates gene expression. Commonly, translation of the uORF has an inhibitory effect on the downstream expression of the primary ORF. For example, ATF4 has two upstream open reading frames (uORFs), uORF1 and 2 (Morris and Geballe 2000). Following translation of the uORF1, phosphorylated eIF2α reduces the rate of ribosomal re-initiation, allowing the inhibitory uORF2 to be bypassed. This, in turn, increases the translation of the ATF4 coding region (Young and Wek 2016). Second, the cluster of mRNAs employs a non-canonical mRNA translation initiation such as internal ribosome entry sites (IRESs) (Komar and Hatzoglou 2011).

In addition to the inhibitory effect of eIF2α phosphorylation on general translation, it increases the translation of the activating transcription factor 4 (ATF4) mRNA whose protein product is a transcriptional factor that plays a key role in fundamental adaptive responses (Harding, Novoa et al. 2000). ATF4 induces transcription of its target genes such as the C/EBP homologous protein (CHOP) or (GADD153). Moreover, ATF4 and CHOP induce the

expression of other genes such as the growth arrest and DNA damage-inducible protein (GADD34), and this, in turn, lead to a negative feedback loop to dephosphorylate p-eIF2α. Furthermore, ATF4 in combination with CHOP induces ATF5 expression which contributes to the ER stress response (Novoa, Zeng et al. 2001, Teske, Fusakio et al. 2013). ATF4 contributes to a multitude of cellular functions including apoptosis, oxidative stress, gene expression, metabolism, and protein folding (Harding, Zhang et al. 2003, Schröder and Kaufman 2005).

1.8 Termination of the stress response

Similar to phosphorylation, dephosphorylation of eIF2α also plays a critical role in the termination of the stress response and restoration of protein synthesis (Novoa, Zeng et al. 2001). eIF2α dephosphorylation is mediated by serine/threonine-protein phosphatase 1 (PP1). PP1 contains catalytic and regulatory subunits. The catalytic subunit is highly conserved across eukaryotes and can be assembled with different regulatory subunits (Goldberg, Huang et al. 1995, Armstrong, Browne et al. 1997). Protein phosphatase 1 regulatory subunit 15A (PPP1R15A, known as GADD34), and protein phosphatase 1 regulatory subunit 15B (PPP1R15B, known as CReP), are two regulatory subunits involved in dephosphorylation of eIF2α (Novoa, Zeng et al. 2001). During the stress response, GADD34, via the RVxF motif located at the C-terminal recruits PP1 to phosphorylate eIF2α and thereby terminates the stress response. Unlike GADD34, CReP is constitutively active and similarly recruits PP1 to eIF2α. CReP is responsible for maintaining an optimal level of p-eIF2α in cells with no stress or damage (Connor, Weiser et al. 2001, Harding, Zhang et al. 2009). The regulatory subunit of PP1 has been pharmacologically or genetically targeted to restore the cell's proteostasis. For instance, Guanabenz binds to GADD34 and selectively inhibits "stress-induced dephosphorylation" of p-eIF2α leading to reduced general protein synthesis, better folding, and

reduced accumulation of unfolded or misfolded proteins (Tsaytler, Harding et al. 2011). Likewise, the regulatory subunit 15B (CReP) has also been selectively targeted with Raphin 1 which guards cells against stress and slows the neurodegenerative process in the Huntington's disease mouse model (Vagnarelli and Alessi 2018). Salubrinal is another inhibitor that blocks both GADD34 and CReP, thereby reducing dephosphorylation of p-eIF2α (Boyce, Bryant et al. 2005). Multiple inhibitors have been utilized in previous studies to block p-eIF2 dephosphorylation in a cell-type non-specific manner. In our work, a viral cell-type-specific approach that inhibits dephosphorylation of p-eIF2 has been used to target the phosphatases (Figure. 2).

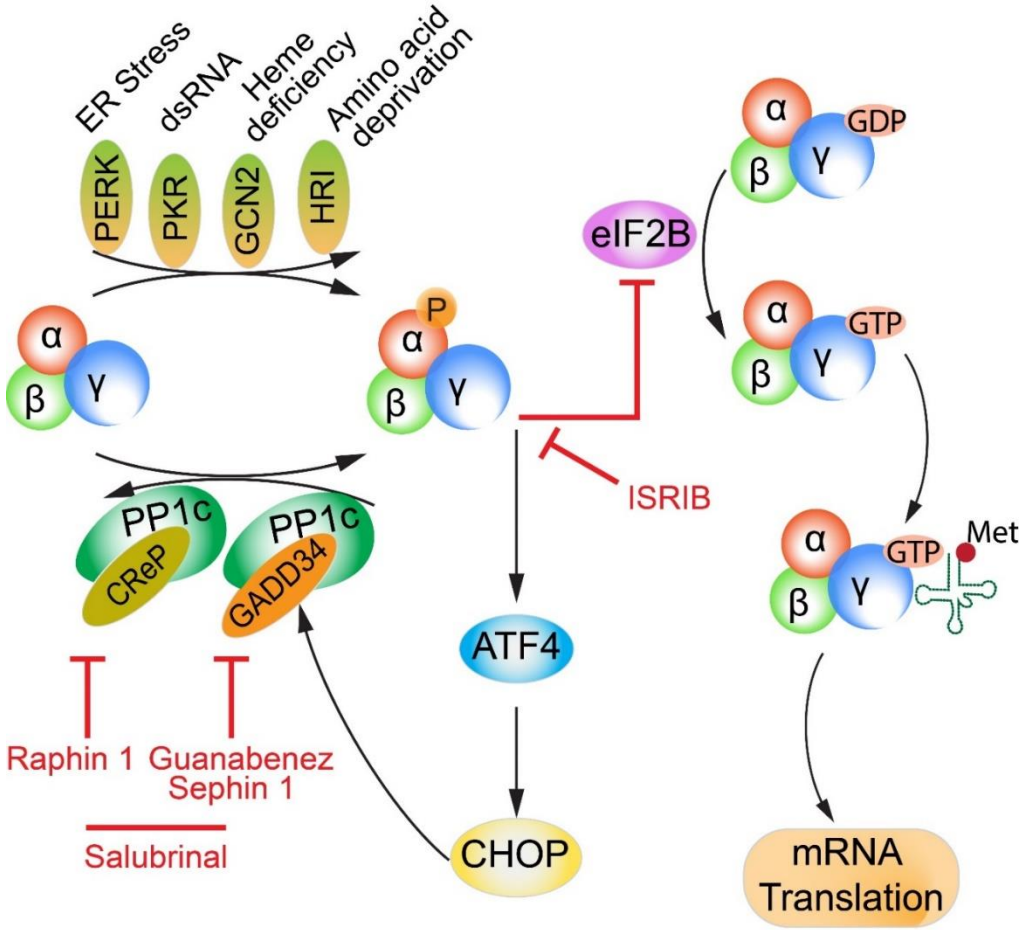

1.8.1 Figure 2. The integrated stress response (ISR).

The schematic illustrates the ISR pathway. eIF2α is activated by four kinases (PKR, PERK, HRI, and GCN2) and is dephosphorylated by protein phosphatase 1, which is recruited by CReP and GADD34 adaptor proteins. Phosphorylated eIF2α is a competitive inhibitor of eIF2B. Therefore, p-eIF2α blocks general translation by limiting the formation of the ternary complex (TC), but paradoxically enhances the translation of ATF4 and CHOP. CHOP, in turn, activates GADD34, thereby dephosphorylating p-eIF2α. Raphin 1, Sephin 1, Guanabenze, and Salubrinal block the activity of CReP and GADD34, resulting in increased p-eIF2α.

1.9 History of autism spectrum disorders (ASDs)

The term "autism" was first coined in 1911 by Eugen Bleuler to describe the introspective symptoms of adults suffering from schizophrenia. He characterized autism as an infantile desire to avoid unpleasant experiences in favor of hallucinations and unconscious imagination (Crespi 2010). Later, in the 1920s, Jean Piaget used the term “infantile autism” for the pre-verbal thought period of a child’s life. He used this term for normal kids, though (Evans 2013). However, Leo Kanner documented autistic traits in a group of children previously diagnosed with mental retardation. He observed that these children did not socially interact with peers, performed repetitive activities, and had difficulty developing speech and changing their routines. Finally, in 1943, Kanner published his observations and described the symptoms as “infantile autism”. Despite Jean Piaget’s notion, Kanner's description of “infantile autism” was used beyond the “pre-verbal period” of the child’s life. In the 1940s, autism and schizophrenia were used interchangeably (Harris 2018). However, in 1971, Israel Kolvin disproved the notion that autistic individuals experience hallucinations. In 1944, Hans Asperger reported a less severe type of autism called Asperger. Since the paper was written in German, the term Asperger remained unknown until 1981, when Lorna Wing coined the condition “Asperger

Syndrome" to describe a milder form of autism. In the Diagnostic and Statistical Manual of Mental Disorders (DSM III) published in 1980, autism was categorized as a pervasive developmental disorder. In the DSM IV, published in 1994, four subcategories of autism were defined, and now patients could be diagnosed with 1) Autistic Disorder, 2) Asperger's Syndrome, 3) Childhood Disintegrative Disorder, and 4) Pervasive Developmental Disorders Not Otherwise Specified (PDD-NOS). In 2013, DSM V was released, and all four autism subcategories defined in DSM IV were used under the umbrella of ASDs (Feinstein 2011, Volkmar and Reichow 2013).

1.10 ASD symptoms and comorbidities

ASDs are a set of persistent and heterogenous neurodevelopmental disorders with two core symptoms: difficulty in social communication and restricted/repetitive pattern of behaviors. The ASDs symptoms usually appear before age three, and many of the symptoms such as those related to social performance and cognitive ability persist into adulthood. Autistic individuals may also suffer from a range of comorbidities including intellectual disability, epilepsy, developmental delay, sleep disorders, obsessive-compulsive disorder (OCD), anxiety, attention-deficit hyperactivity disorder (ADHD), and gastrointestinal (GI) complications. The likelihood of developing certain comorbidities such as epilepsy is notably higher in individuals with ASDs. Individuals with Asperger's syndrome, in contrast, may experience fewer comorbidities. For instance, they benefit from normal speech development and average or above-average intelligence (Zafeiriou, Ververi et al. 2007, Bauman 2010).

1.11 Autism epidemiology

Considering the variabilities in data from different studies and countries, it is estimated that 1 in 160 children are diagnosed with ASD. According to the National Autism Spectrum Disorder

Surveillance System (NASS) report in 2018, approximately 1 in 66 children and youth were diagnosed with ASD in Canada including 1 in 42 males and 1 in 165 females (Ofner, Coles et al. 2018). Moreover, according to the Centre for Disease Control's Autism and Developmental Disabilities Monitoring (ADDM) Network, 1 in 44 children are diagnosed with ASDs. Males are four times more likely to be diagnosed with autism than females. No difference in prevalence was found in terms of ethnicity, socioeconomic level, and race. The prevalence of autism in many developing countries and those with low income is yet to be studied. Considering the variability of the estimated prevalence rate among studies and countries, the sheer number of children with ASDs is alarmingly high, irrespective of better diagnostic tools and awareness or the actual prevalence rate (Maenner, Shaw et al. 2021).

1.12 Autism etiology

ASD has a multifactorial etiology with both genetic and environmental components. ASD is generally categorized as syndromic and non-syndromic (idiopathic or primary). Unlike non-syndromic ASD, with rather unidentified etiology, syndromic ASD is frequently associated with monogenic mutations such as mutations in *Fmr1* and *MECP2* genes and chromosomal abnormalities. Although the exact ASD etiology remains relatively elusive, Dizygotic (DZ) and Monozygotic (MZ) twins' studies provide a great platform for assessing the relative contribution of environmental factors versus genetic factors in the expression of ASDs traits. Despite previous twin studies indicating that heritability accounts for 80 %–90 % of differences in autistic traits, recent reports have shown that up to 50 % of the variances in autism liability are determined by environmental factors (Modabbernia, Velthorst et al. 2017). The current

studies even show less than 50 % concordance rate for MZ twins. Among environmental factors, advanced parental age is highly associated with the risk of ASD in offspring (Durkin, Maenner et al. 2008). Altogether, a combination of genetic and environmental factors plays a role in the development of ASD, particularly in non-syndromic ASDs. In contrast to the environmental factors that are more complicated to study, some genetic abnormalities such as monogenic mutations are valuable tools to study the underlying biological mechanisms of ASD.

1.13 Autism genetic architecture

Identification of hundreds ASD risk genes has proved that the genetic component significantly contributes to ASD pathophysiology (Ruzzo, Pérez-Cano et al. 2019, Paulsen, Velasco et al. 2022). The genetic landscape of ASDs is extremely complicated because it is mainly shaped by an interaction between common and rare genetic mutations on one side, and environmental factors on the other side, and this complexity, in turn, results in heterogeneity across individuals with ASDs (Gardener, Spiegelman et al. 2011). However, the common denominator for a large number of ASD risk genes is that they converge on a limited number of common biological signaling pathways involved in protein synthesis, synaptic function, signal transduction, and transcription and chromatin remodeling (Cook Jr, Lindgren et al. 1997, Bourgeron 2009, Toro, Konyukh et al. 2010). Collectively, four categories of rare genetic risk factors have been shown to be associated with ASDs. The first group is rare penetrant genes such as *NLGN3, NRXN1, SHANK1-3,* and *CNTNAP2*. The estimated contribution of the rare genes in ASDs is ~5%. The penetrance of some of these rare genes is high enough to be sufficient to cause ASD phenotype as a monogenic factor. The second group is rare copy number variations (CNVs) which account

for ~5% of ASD causality. CNVs can have a large penetrance such as 15q11–q13 duplication while others can have a milder impact such as 15q11.2 deletion, which may require other risk factors like environmental stressors to significantly contribute to the ASD expression. The third group is rare chromosomal abnormalities such as trisomy 21, 47XYY, 47XXY, and maternal 15q11–q13 duplication. It is estimated that this group's contribution to autism expression is ~5%. The last group, which has a higher net share at ~10% in ASD causality, is ASD-related syndromes, including Tuberous Sclerosis, Rett syndromes, Timothy syndrome, and fragile X syndrome (FXS), which is the most common inherited cause of ASD accounting for 5% of all cases of ASD (Muhle, Trentacoste et al. 2004, Schaefer and Mendelsohn 2008). Studying FXS is beneficial to better understand the underpinning mechanisms of ASD. First, many individuals with FXS also meet at least one ASD criteria. Second, in contrast to ASD, which is diagnosed based on behaviors, FXS is diagnosed based on laboratory DNA tests. Third, unlike ASD with multifactorial etiology, FXS has a monogenic cause allowing to study the underlying mechanisms of ASD.

1.14 Autism neuroanatomy

Several areas of the brain are affected by ASDs. These findings have been generated mainly with structural magnetic resonance imaging (MRI) and post-mortem studies on autistic individuals. Although there are discrepancies among different studies and most of them are limited by small sample sizes, alterations in some areas of the brain such as the prefrontal cortex, amygdala, cerebellum, and hippocampus have been highlighted in ASDs. Enlarged hippocampal volume (Schumann, Hamstra et al. 2004, Barnea-Goraly, Frazier et al. 2014) and changes in the shape (Dager, Wang et al. 2007) of the hippocampus have been found in children with ASD. Moreover, alterations in white matter fibers between the hippocampus and fusiform gyrus have been observed (Conturo, Williams et al. 2008). The hippocampal-fusiform gyrus

tract functions in face recognition (Conturo, Williams et al. 2008) which is essential for social interactions. The amygdala is involved in the processing of emotions such as pleasure, aggression, fear, and anxiety and also modulates conditional fear learning. Impaired social interaction in autistic individuals may be indicative of amygdala alterations (Davis and Whalen 2001). Likewise, lesions in the amygdala lead to impaired recognition of facial emotions, resembling amygdala-driven difficulties in autistic individuals (Koelkebeck, Bauer et al. 2021). Enlarged right and left amygdala volume also has been observed in children with autism but not in adolescents (~12–18 years old) (Schumann, Hamstra et al. 2004). In a functional cell-type-specific study, Hong et al. pharmacologically and optogenetically manipulated two separate subpopulations of neurons (GABAergic and glutamatergic neurons) in the medial amygdala (MeA). They found that GABAergic neurons in the posterior dorsal medial amygdala engender aggression, social grooming, and mating behaviors. In contrast, manipulation of the adjacent glutamatergic populations caused social behaviors and self-grooming. Furthermore, they observed that inhibition of social interactions by the glutamatergic subpopulation was independent of promoting self-grooming effect of these neurons (Hong, Kim et al. 2014). Since the frontal cortex plays a pivotal role in executive functions such as working memory, learning, social behavior, emotions, and communication, it has been at the center of attention in autism studies. The general consensus is that an overgrowth and enlargement of the frontal cortex has been reported in autistic children that is restricted to the first few years, although later on, will shift toward normal growth (Carper and Courchesne 2005, Courchesne, Campbell et al. 2011, Courchesne, Mouton et al. 2011). Lastly, the cerebellum is a brain area that is consistently found to be affected in autism (Fatemi, Halt et al. 2002). The cerebellum is interconnected with the brain areas involved in processing social interaction (Jissendi, Baudry et al. 2008, Jack and Pelphrey 2015), reward processing (Snider and Maiti 1976), and executive function (Middleton and Strick 2000). Therefore, it is conceivable that cerebellar abnormalities found in individuals

with autism can potentially be a root cause for a range of behavioral abnormalities. Decreased number of Purkinje cells in the cerebellum of autistic individuals has been reported by numerous post-mortem studies (Fatemi, Halt et al. 2002, Bauman and Kemper 2005). Similarly, manipulation of proteins controlling protein synthesis in Purkinje cells was sufficient to cause autistic-like behavior in mice (Tsai, Hull et al. 2012, Cupolillo, Hoxha et al. 2016). Interestingly, in an analysis of 26 autistic mouse models, abnormal cerebellar cortex was uniformly detected (Ellegood, Anagnostou et al. 2015).

1.15 Fragile X Syndrome (FXS)

Fragile X syndrome (FXS) is the leading genetic cause of intellectual disability and the most common monogenetic cause of ASDs. It is estimated that 1 in 5000 males and 1 in 8000 females suffer from FXS. Males usually experience more severe symptoms than females. FXS is a genetic condition that is mainly caused by mutations in the fragile X mental retardation 1 gene (*FMR1*) located on chromosome Xq27.3. The *FMR*1 gene sequence is highly conserved across different species and is composed of 17 exons with ~ 40 kilobases (kb) in length (Fig. 1). In healthy individuals, there is an expansion of CGG trinucleotide repeats (5–44 repeats) in the 5´ untranslated region of the *FMR1* gene. Depending on the size of CGG expansion repeat in the 5´UTR of the *FMR1* gene, four key types of alleles are discernible. Excessive expanded CGG repeats (≥ 200) or full mutation of the *FMR1* gene leads to DNA hypermethylation and transcriptional silencing, impeding gene expression, and consequently, causing a reduction or loss of the *FMR1* product, fragile X mental retardation protein (FMRP). Normal expansion with 6–50 CGG repeats, intermediate expansion size or "grey zone" with ~ 45–60 repeats, and longer CGG expansion (~55–200 repeats) is termed premutation. Individuals with 55–200 repeats or premutation carriers might be affected by delayed fragile X-associated tremor/ataxia syndrome (FXTAS), fragile X-associated primary ovarian insufficiency (FXPOI), fragile X-

associated neuropsychiatric disorders (FXAND), and neurodegenerative disorders (Figure. 3). Clinical manifestation of FXS can include macroorchidism, macrocephaly, prominent ears and jaw, long face, hyperexcitable joints, soft skin, flat feet, high arched palate, and facial hypoplasia. Behavioural symptoms include hyperactivity, seizures, repetitive behaviors, and language and executive function problems. Autism-like behaviors such as poor or lack of eye contact may be also presented. FMRP, the product of the *FMR1* gene, is highly expressed in the brain and testes. There is a negative correlation between the level of FMRP and the severity of the symptoms. The excessively low level or absence of FMRP is associated with severe neurological and developmental disorders such as intellectual disability (Abbeduto, Thurman et al. 2019).

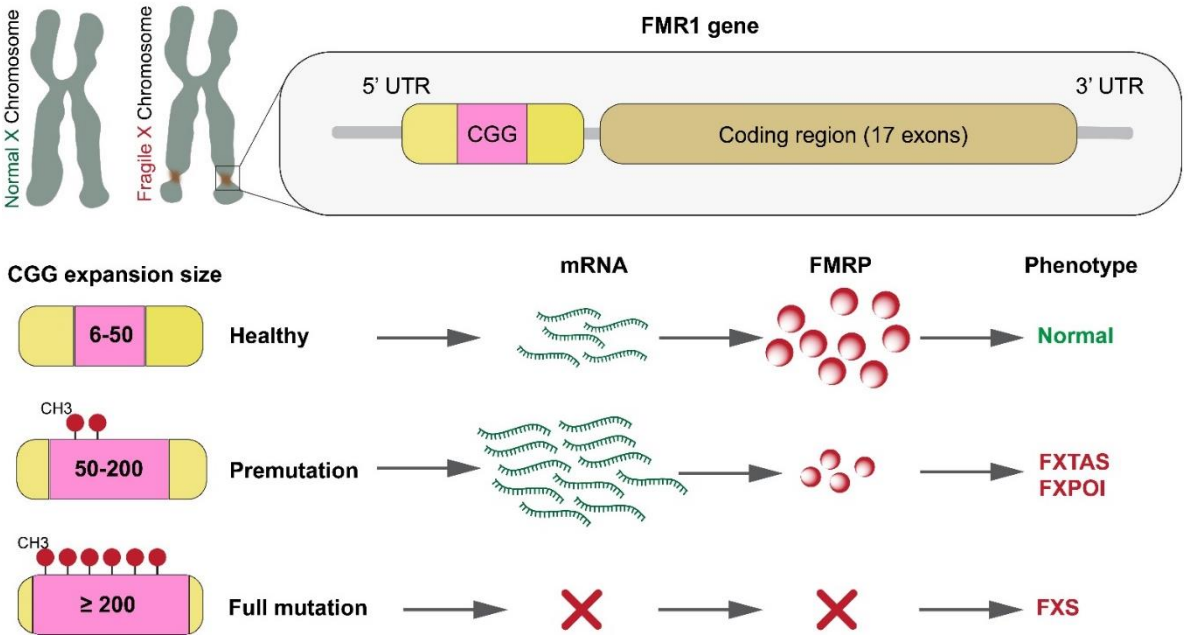

1.15.1 Figure 3. The FMR1 gene structure and the CGG expansion-related phenotypes.

The schematic shows the FMR1 gene structure, as well as the phenotypes triggered by the different number of CGG repeats in the gene's 5′ UTR. The FMR1 gene is located on the X chromosome and is composed of 17 exons. The FMR1 gene promoter normally contains 6–50

CGG expansion repeats. CGG expansion repeats greater than 50 are related to late-onset clinical symptoms, and more than 200 is a full mutation, which is common in FXS [modified from Zalfa et al.] (Zalfa and Bagni 2004).

1.16 Fragile X mental retardation protein (FMRP) structure and expression

Fragile X mental retardation protein (FMRP) is a multi-domain RNA binding protein with several key functions. FMRP has three canonical RNA binding domains including two hnRNP K-homology (KH1 and KH2) and one arginine-glycine-glycine (RGG) rich domain (Ashley Jr, Wilkinson et al. 1993, Siomi, Siomi et al. 1993) and it contains five additional newly discovered domains: KH0, nuclear export signal (NES), nuclear localization signal (NLS), and two tandem Agenet domains (Chen and Joseph 2015, Myrick, Hashimoto et al. 2015). Through these RNA binding domains (KH1, KH2, and RGG box), (Figure. 4). FMRP selectively regulates the translation of mRNA targets (Ashley Jr, Wilkinson et al. 1993). The KH1 and KH2 domains are suggested to bind single-stranded RNAs (Darnell, Mostovetsky et al. 2005). Moreover, *in vitro* studies suggest that the RGG box domain binds and stabilizes G-quadruplexes (secondary structures are formed by guanine-rich sequences) (Phan, Kuryavyi et al. 2011). The KH0 domain, which is located at the N-terminal, is deemed to bind RNA by creating a basic surface patch with Tudor domain 1 (TD1) (D'Annessa, Cicconardi et al. 2019). It has been reported that individuals with a single point mutation (R138Q) within the KH0 domain exhibited the FXS phenotype (Myrick, Deng et al. 2015). FMRP regulates chromatin remodeling and thereby plays a role in the DNA damage response (DDR) via tandem Agenet domains (Alpatov, Lesch et al. 2014). FMRP also harbors two nuclear localization and export signals (NSL and NES) (Eberhart, Malter et al. 1996) thereby, FMRP shuffles in and out of the nucleus (Feng, Gutekunst et al. 1997). It is highly localized in the cytoplasm of all neurons

(Bakker, de Diego Otero et al. 2000), and it is expressed in the dendrite, axon, and axonal terminals of the cortical pyramidal neurons (Feng, Gutekunst et al. 1997). In several areas of the mouse brain including the hippocampus, cortical areas, and cerebellum, FMRP is expressed in different types of neurons throughout development, however, its expression in astrocytes, microglia, and oligodendrocyte cells is limited to early and mid-postnatal stages of the brain development in those areas of the brain (Gholizadeh, Halder et al. 2015).

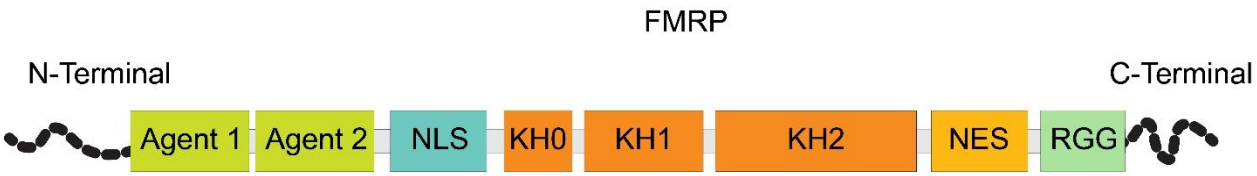

1.16.1 Figure 4. The FMRP structure.

The schematic of the FMRP structure depicts different domains of the protein. FMRP contains three centrally located KH domains, two nuclear localization and export signal domains, and two tandem agenet domains located at the N-terminal.

1.17 Fragile X mental retardation protein (FMRP) targets

In a study by Brown et. al., the authors coimmunoprecipitated the complex of FMRP-mRNAs with ribonucleoprotein coimmunoprecipitation assay (RIP) followed by microarrays analysis (Brown, Jin et al. 2001, Richter and Zhao 2021). They detected 432 FMRP-associated mRNAs from the mouse brain. Interestingly, majority of the mRNA targets included G-quadruplex (G4) structure (Brown, Jin et al. 2001), leading the authors to conclude that FMRP mainly binds mRNAs containing G4 structure. Darnell. et al., utilized high-throughput sequencing of RNA isolated by crosslinking and immunoprecipitation (HITS-CLIP), identifying 842 FMRP mRNA targets. The main findings of this study were: 1) the identified FMRP mRNA targets did not harbor G4 structure, 2) a highly significant overlap was found between the 117 SFARI autism

candidate genes (Basu, Kollu et al. 2009) and 24 of the FMRP identified mRNA targets including well-studied autism genes such as SHANK3, PTEN, TSC2, and NLGN3. 3) in contrast to the majority of RNA-binding proteins, FMRP mainly interacts with the coding sequence (CDS) of the mRNA targets, 4) FMRP tends to bind mRNAs associated with autism; therefore, it is conceivable that FXS and autism have some common molecular mechanisms, 5) there was a significant overlap between FMRP targets and pre or post-synaptic proteome (Darnell, Van Driesche et al. 2011, Richter and Zhao 2021). Although FMRP is expressed in all neurons, recent CLIP studies have reported a cell-type-specific role for the FMRP in CA1 pyramidal neurons in regulating the transcripts related to autism and memory (Ceolin, Bouquier et al. 2017, Sawicka, Hale et al. 2019).

1.18 Fragile X mental retardation protein (FMRP) functions

Canonically, FMRP has been thought of as an mRNA translation repressor. However recently, using analysis of whole translatome and transcriptome in both human and mouse models of FXS, a range of diverse functions of FMRP have been proposed. It is thought that approximately 4% of the human fetal brain mRNAs are regulated by FMRP (Brown, Jin et al. 2001). Therefore, it is crucial to understand how FMRP interacts with the mRNA targets.

First, FMRP can modulate the half-life and accordingly the stability of mRNAs either by preventing or expediting mRNAs degradation (De Rubeis and Bagni 2010). FMRP also influences its target mRNAs through epigenetic N^6-Methyladenosine (m6A)-dependent mechanisms (Edens, Vissers et al. 2019). 92% of 174 downregulated FMRP targets mRNAs in *Fmr1* KO mouse cerebral cortex contained m^6A (Zhang, Kang et al. 2018). There are several lines of evidence supporting the stabilizing role of FMRP. In the hippocampus of the *Fmr1* KO mice, Eberwine et al. showed reduced expression of GRK4 and p40/LRP mRNAs (Miyashiro, Beckel-Mitchener et al. 2003). Moreover, in FMRP-deficient neurons, decreased expression of

$GABA_A$ δ subunit mRNA has been reported (Gantois, Vandesompele et al. 2006). Furthermore, PSD-95 mRNA is protected against degradation by the C-terminus domain of FMRP which recognizes a G-rich sequence in the 3´ UTR of the PSD-95 mRNA (Todd, Mack et al. 2003, Muddashetty, Kelić et al. 2007). Second, FMRP not only regulates mRNA transportation from the cell body to the distal compartment such as dendrites, spines, and axonal growth cones, but also plays a key role in activity-dependent docking of the mRNA targets in the dendritic spines. Upon activation of group I metabotropic glutamate receptors (mGluR I), synaptic abundance of FMRP is increased as (S)-3,5-Dihydroxyphenylglycine (DHPG), the mGluR agonist, enhances the transport of FMR1 mRNA alongside dendrites (Antar, Afroz et al. 2004, Ferrari, Mercaldo et al. 2007, Kao, Aldridge et al. 2010). Dendritic expression of FMRP mRNA targets such as Map1b, Sapap4, and CaMKIIα is dysregulated in hippocampal neurons of *Fmr1* KO mice (Dictenberg, Swanger et al. 2008).

Third, recent findings suggest that FMRP also modulates the biological processes in the nucleus such as DNA damage response, gene transcription, and splicing. By analyzing the previous CLIP data, it was found that a significant number of FMRP targets interact with chromatin-related processes including histone methylation and acetylation. Moreover, in the absence of FMRP in mice, broad changes in chromatin and dysregulated gene expression were found. In line with this idea, inhibition of Bromodomain-containing protein 4 (Brd4), a chromatin associated protein and FMRP target, using JQ1 inhibitor, improved many of the FXS phenotypes in *Fmr1* KO mice (Korb, Herre et al. 2017). Another FMRP target is a chromatin modulator protein known as SETD2—which catalyses trimethylation of lysine 36 on histone H3 (H3K36me3)— was elevated in *Fmr1* KO hippocampus (Shah, Molinaro et al. 2020), and dysregulated alternative splicing was found in these animals due to elevated expression of H3K36me3 (Shah, Molinaro et al. 2020).

Fourth, FMRP directly interacts with ion channels, such as the sodium-activated potassium channel Slack (Brown, Kronengold et al. 2010). FMRP increased the mean opening time of the channel via direct interaction with the C-terminal tail of the channel (Brown, Kronengold et al. 2010). In addition, transcriptomic analysis in the brain revealed that many of the FMRP targets encode ion channels (Darnell, Van Driesche et al. 2011). Voltage-gated potassium channels are identified among the FMRP targets (Gross, Yao et al. 2011). FMRP also interacts with N-type voltage-gated calcium channels (Ferron, Nieto-Rostro et al. 2014).

Fifth, many effects of FMRP on cellular phenotypes are mediated via modulation of protein synthesis. Although a few studies have provided evidence that FMRP enhances mRNA translation (Greenblatt and Spradling 2018), the majority of findings favor the inhibitory role of the FMRP over protein synthesis. Among studies showing that FMRP enhances protein synthesis is a study titled "Fragile X mental retardation 1 gene enhances the translation of large autism-related proteins" by Greenblatt et. al. In Drosophila oocytes, they reported that FMR1 enhances the translation of stored mRNAs which significantly overlap with the FMRP targets. Ribosome profiling assay detected 20 and 30 targets that were associated with intellectual disability and neurodevelopmental dysfunction, respectively (Greenblatt and Spradling 2018). However, unlike humans carrying two paralogs of FMR1, FXR1 and FXR2, drosophila have only one FMR1 gene known as dFMR1(Drozd, Bardoni et al. 2018).

There are two lines of ideas supporting the inhibitory function of FMRP in regulating mRNA translation. The first is demonstrating that FMRP interacts with the proteins involved in the initiation phase of the translation, and the second one emphasizes the elongation phase as the target of FMRP. Several studies support the notion that FMRP suppresses the initiation phase of translation. In 2001, Laggerbauer et. al., added FMRP to a cycloheximide-incubated reticulocyte lysate to probe the phase of mRNA translation that FMRP acts upon. Interestingly, the amount of mRNA coupled with ribosomes was decreased by over 50% measured by the

sucrose density gradients assay. Therefore, formation of the 80S initiation complex is prevented to a great extent by FMRP (Laggerbauer, Ostareck et al. 2001). Consistent with this finding, Napoli et. al., revealed Cytoplasmic FMRP Interacting Protein 1 (CYFIP1)— also known as Specifically Rac1 Activated protein 1 (SRA-1)— functions as an eIF4E-binding protein (Napoli, Mercaldo et al. 2008). In their proposed model (Figure. 5), CYFIP1 is considered an eIF4E-binding protein (4E-BP) in neurons. Similar to 4E-BPs, CYFIP1 sequesters the cap-binding protein eIF4E and thereby inhibits eIF4F complex formation and represses mRNA translation (Napoli, Mercaldo et al. 2008). Therefore, the FMRP-CYFIP1-eIF4E complex suppresses mRNA translation and upon stimulation of synaptoneurosomes by application of DHPG or brain-derived neurotrophic factor (BDNF), eIF4E is released from CYFIP1 to form eIF4F complex and thereby enhance translation. Interestingly, the FMRP-CYFIP1-eIF4E complex has been detected at synapses and along dendrites, and its inhibitory effect on translation can be inverted following neuronal activation (Napoli, Mercaldo et al. 2008). Moreover, elevated levels of FMRP target MAP1B (~25%), CamKIIα (~70%), and APP (~90%) proteins in the brain extracted from CYFIP1 heterozygote mice ($CYFIP1^{+/-}$) further support the proposed model by Napoli et. al. (Napoli, Mercaldo et al. 2008).

Other studies have suggested that FMRP regulates mRNA translation at the elongation phase. The idea that FMRP suppresses mRNA translation at the elongation phase originally stems from studies that have demonstrated that FMRP co-sediments with polyribosomes in non-neuronal tissues (Khandjian, Corbin et al. 1996), in cultured neurons (Khandjian, Corbin et al. 1996, Ceman, O'donnell et al. 2003, Stefani, Fraser et al. 2004), and the brain of adult mice (Khandjian, Huot et al. 2004). The elongation hypothesis was further supported by an innovative study by Darnell et. al. In this study, using ultra-violet light, FMRP was crosslinked with its mRNA targets followed by immunoprecipitation (CLIP). Probing 842 identified mRNA targets, it was shown that FMRP, for the majority of its targets (66%), binds

predominantly to the coding region as opposed to the untranslated region (UTR) of mRNAs. Association of FMRP with the stalled ribosomes was re-validated with ribosomal run-off assay in the presence of puromycin and sodium azide, non-specific blockers of the initiation step (Darnell, Van Driesche et al. 2011). In line with the elongation theory, after blocking the initiation phase of the translation using hippuristanol in lysates extracted from *Fmr1* KO mice, Udagawa et al., showed an increase in elongation-specific global protein synthesis, indicating that FMRP represses the elongation phase of translation (Udagawa, Farny et al. 2013). This theory is further supported by a study by Chen et al. where they found that FMRP directly interacts with ribosomes through its KH1 and 2 domains (Chen, Sharma et al. 2014). Moreover, transgenic Flag-tagged FMRP suppresses mRNA translation throughout the elongation phase in dividing fibroblast cultured cells (Ceman, O'donnell et al. 2003). Considering both initiation and elongation theories and the supportive findings regarding the role of FMRP, these mechanisms need to be further elaborated in cell-type, spatial, and temporal-specific manner. For example, are these mechanisms restricted to a certain compartment of the cell such as dendritic spines or cell body? In conclusion, a combination of both theories can be involved depending on the spatial and temporal regulation of translation by FMRP.

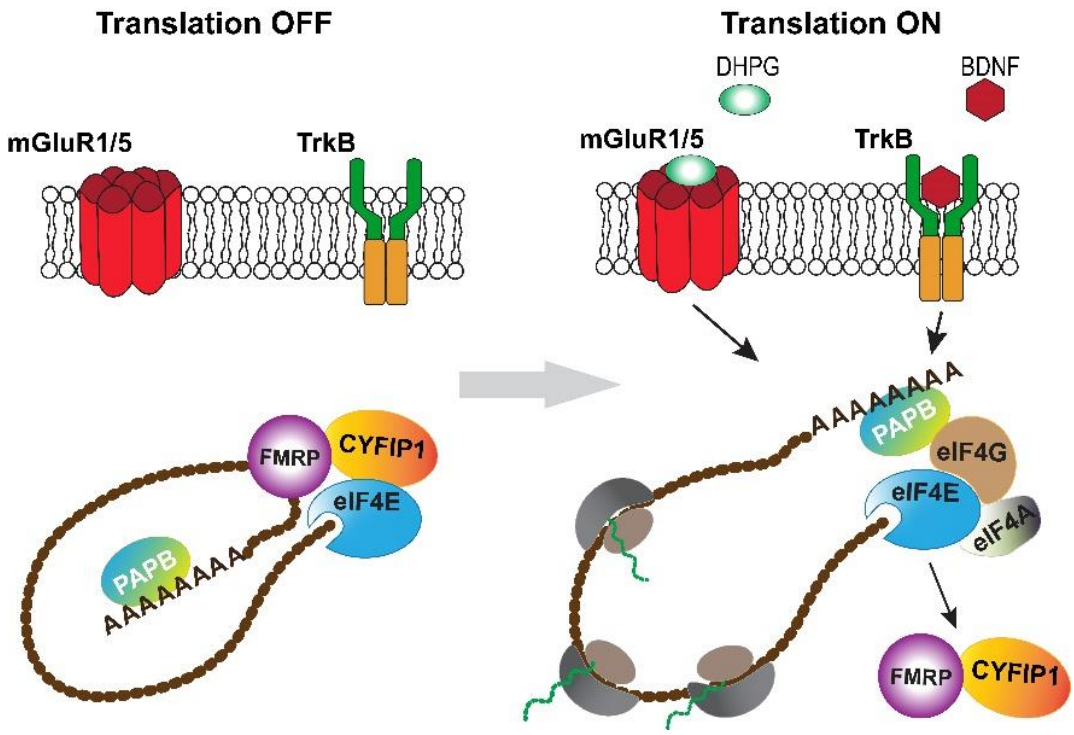

1.18.1 Figure 5. FMRP-CYFIP1-eIF4E complex in translationally silent and active mRNA.

The schematic illustration depicts how the inhibitory FMRP-CYFIP1-eIF4E complex regulates mRNA translation with and without stimulants (DHPG and BDNF) [modified from Rubeis et al.] (De Rubeis and Bagni 2011).

1.19 *Fmr1* KO mice

The *Fmr1* KO mouse was first generated and characterized by the Dutch-Belgian Fragile X Consortium. In this mouse model, the wild-type *Fmr1* gene is replaced with a non-functional *Fmr1* gene. Therefore, similar to FXS, the mouse does not produce FMRP, the protein product of the *Fmr1* gene (Consorthium, Bakker et al. 1994). The KO mouse exhibits a range of phenotypes; however, some discrepancies have been detected in different labs. One source of such discrepancies is the different genetic backgrounds of the mice (Spencer, Alekseyenko et

al. 2011). Likewise, it has been proposed that differences in behaviors, including autistic-like behaviors, are mainly due to the various genetic backgrounds (Kooy 2003). Despite the discrepancies in the *Fmr1* KO behaviors, this model is well-characterized and valuable for understating the underpinning mechanisms of FXS and ASD. This mouse line recapitulates many of the key features of FXS patients including higher susceptibility to seizures, elevated protein synthesis, macroorchidism, autistic-like behaviors, aberrant morphology and impaired synaptic function, cognitive impairments, and facial deformities.

1.19.1 Morphological abnormalities of dendritic spines

A dendritic spine is a miniature membranous protuberance on the neurons' dendrite. The number of spines on a single dendrite can be hundred of thousands. Most of the spines are composed of a large and thin shaft (neck) and a button-like head. Canonically, spines are categorized as mushroom, stubby, thin, and filopodium based on their shapes (Hayashi and Majewska 2005). The key functions of spines are memory storage, electrical signal transmission, and modulating connectivity between neurons (Alvarez and Sabatini 2007). Dendritic spine abnormalities are present in a range of cognitive disabilities including intellectual disability, autism, and FXS (Hutsler and Zhang 2010, Penzes, Cahill et al. 2011). Therefore, spine morphology has been taken into consideration as a potential biomarker to assess the progress of mental and cognitive disabilities or probe the efficacy of applied treatments and prescribed medications. Most of the studies have detected increased density of spines in the brain of the *Fmr1* KO mice. However, some studies observed no alterations in the morphology of the spines or conversely have shown a decrease in spine density. The decrease in spine density was observed in *Fmr1* KO mouse cultured hippocampal neurons (Braun and Segal 2000). According to the literature, it appears that the increased density of spines idea has been supported by more studies. Analyzing primary dendrites in mitral cells in *Fmr1* KO with

two genetic backgrounds, FVB and C57BL/6 revealed that *Fmr1* KO on the FVB background had significantly higher dendrites compared to controls, while no difference was detected in *Fmr1* KO on the C57BL/6 background (Galvez, Smith et al. 2005). Consistently, analyzing pyramidal neurons in visual cortices of *Fmr1* KO on the C57BL/6 background revealed a significantly higher number of longer spines and spines with immature morphology, while there was a fewer shorter spines and spines with mature morphology. Overall, the spine density in *Fmr1* KO mice was notably greater than controls (McKinney, Grossman et al. 2005). Shorter spines also have been reported in the hippocampus of 2-week-old *Fmr*1 KO mice (Pop, Levenga et al. 2014). Moreover, in the CA1 of 3-month-old *Fmr1* KO mice, a significantly higher spine density has been observed (Gantois, Khoutorsky et al. 2017). In summary, observed alterations in spine morphology in different studies suggest that this phenotype significantly depends on the developmental stage of the animal, mouse strain, *in vitro* versus *in vivo* analysis, and the technique used to image and analyze spine morphology.

1.19.2 Decreased GABAergic transmission

A mounting number of studies have shown alterations in the GABAergic system, including significant changes in GABA expression in the brain of *Fmr1* KO mice (El Idrissi, Ding et al. 2005, d'Hulst, De Geest et al. 2006). A dramatic change in GABA transmission was observed in the amygdala of *Fmr1* KO mice. Further assessment revealed a significant decline in both frequency and amplitude of tonic inhibitory currents, phasis IPSCs, and the total number of inhibitory synapses, while the number of inhibitory neurons did not change (Olmos-Serrano, Paluszkiewicz et al. 2010). Similarly, a considerable weakening in GABAergic transmission was observed in the hippocampus of *Fmr1* KO mice. The more detailed analysis revealed a dramatic reduction in both mRNA and protein expression of $GABA_A$ β1 and δ subunits and spontaneous, evoked, and miniature IPSCs in the CA1 pyramidal neurons (Sabanov, Braat et

al. 2017). Collectively, reduced inhibitory tone of the GABAergic system is considered an important landmark in *Fmr1* KO and patients with FXS pathology, and several clinical trials are being conducted to target this system to ameliorate symptoms.

1.19.3 Autistic-like behaviors

Impaired social interaction is one of the core features of ASDs. To assess this behavior in an autistic mouse model such as *Fmr1* KO, scientists have utilized different behavioral paradigms ranging from tube dominancy test to open field, direct reciprocal interaction, and indirect social interaction (three-chamber social) tests. The indirect social interaction followed by direct social interaction tests is the frequently used paradigm. Several studies have shown that *Fmr1* KO mice exhibit impaired social interaction in the three-chamber social test, which is assessed by spending less time interacting with the novel mouse (Gantois, Khoutorsky et al. 2017). In contrast, others have shown no preference for the novel mouse. Repetitive behavior is another key symptom of ASD and is assessed through self-grooming and marble burying tests.

Fmr1 KO mice exhibit significantly higher levels of self-grooming (time and bouts) compared to controls (Gantois, Khoutorsky et al. 2017). Moreover, *Fmr1* KO bury significantly more marbles (Veeraragavan, Graham et al. 2012, Gholizadeh, Arsenault et al. 2014).

1.19.4 Higher susceptibility to seizures

Hyperexcitable brain circuits is one of the salient symptoms in FXS and the associated mouse model, *Fmr*1 KO (Chuang, Zhao et al. 2005, Zhang, Bonnan et al. 2014, Contractor, Klyachko et al. 2015). Consistently, epileptic seizure activity has been observed in approximately 10–25% of patients with FXS (Berry-Kravis 2002, Hara 2007). Seizure is one of the most robust and reproducible phenotypes in the mouse model of FXS (Musumeci, Bosco et al. 2000, Gonzalez, Tomasek et al. 2019). Although *Fmr1* KO mice do not exhibit spontaneous seizures, seizures can be elicited by applying a high-pitch acoustic stimulation (~120 dB) causing

audiogenic seizure (AGS). Seizure phenotype has four stages starting from wild running, which proceeds to clonic seizure followed by the most severe stage, tonic seizure, and ultimately ending in respiratory arrest and death. Induction of audiogenic seizures, similar to many other phenotypes, depends on genetic background, developmental stage of the animal, and the intensity of the acoustic noise. AGS can be induced in as high as 90% of *Fmr1* KO mice at PND 22 and with a lower percentage in other ages ranging from 17 days to 45 days (Musumeci, Bosco et al. 2000). Interestingly, a recent study has shown a region and cell-type-specific pattern in AGS in the brain of *Fmr*1 KO mice. Genetic deletion of the *Fmr*1 gene in glutamatergic neurons located in subcortical areas of the brain is sufficient and necessary to produce AGSs (Gonzalez, Tomasek et al. 2019).

1.19.5 Exaggerated mGluR-dependent LTD

Long-term depression (LTD) is considered an one of the basic mechanisms involved in memory and learning and data storage, which primarily prevents synaptic saturation. In other words, LTD weakens the synaptic strength via various mechanisms, and thereby contributes to synaptic plasticity. Depending on the brain region and age, the fundamental mechanisms of LTD are different (Collingridge, Peineau et al. 2010). LTD plays a key role in a range of brain functions such as learning and memory and cognitive ability, as well as pathologies such as mental retardation and neurodegenerative disorders (Collingridge, Peineau et al. 2010). LTD has been studied in several areas of the brain, particularly in the hippocampus and cerebellum. While in the cerebellum, LTD can be elicited by a strong synaptic stimulation, regulating motor learning, in the hippocampus, it can be induced by prolonged weak synaptic stimulation and functions in learning and memory (Nicholls, Alarcon et al. 2008). In the cortex and hippocampus, LTD is mainly dependent on metabotropic glutamate receptors (mGluR) and NMDA receptors (Collingridge, Peineau et al. 2010). LTD can be induced either by electrical

(persistent low-frequency stimuli) or pharmacological stimulation (mGluR agonist) and regardless of the induction protocol, in both electrical and pharmacological LTD, the underlying mechanisms involve dephosphorylation of α-amino-3-hydroxy-5-methyl-4-isoxazolepropionic acid (AMPA) receptor and internalization of the receptors (Pinar, Fontaine et al. 2017). Unlike NMDA-dependent LTD, mGluR-dependent LTD, which is induced by activation of group 1 metabotropic glutamate receptors either with application of the selective agonist (DHPG) (Palmer, Irving et al. 1997) or paired-pulse low-frequency stimulation (PP-LFS) (Huber, Kayser et al. 2000), is dependent on *de novo* protein synthesis. This type of LTD is blocked in the presence of mRNA translation inhibitors (Huber, Roder et al. 2001). Enhanced mGluR-LTD has been reported in the hippocampus (Bhattacharya, Kaphzan et al. 2012, Michalon, Sidorov et al. 2012) and cerebellum (Koekkoek, Yamaguchi et al. 2005) of *Fmr*1 KO mice. The mGluR theory is founded on several lines of evidence including: 1) Stimulation of mGluR1 results in elevated levels of FMRP mRNAs and proteins (Weiler, Irwin et al. 1997), 2) FMRP represses *de novo* protein synthesis (Bassell and Warren 2008), whereas postnatal genetic overexpression of FMRP alleviates the elevated mGluR-LTD in *Fmr*1 KO (Hou, Antion et al. 2006), 3) The mGluR-LTD is exaggerated in *Fmr*1 KO mice (Huber, Gallagher et al. 2002), 4) In the absence of FMRP, AMPAR internalization, which is mediated by mGluR5, is exaggerated (Nakamoto, Nalavadi et al. 2007). In summary, while activation of mGluR1 enhances protein synthesis, FMRP inhibits protein synthesis, thereby maintaining the synaptic plasticity and LTD at an optimum level. However, in the absence of FMRP, the protein synthesis escapes from the inhibitory effect of FMRP and consequently, LTD is uncontrollably amplified. Activation of mGluR1 usually brings about diverse effects mainly because mGluR 1 interacts with several distinct downstream pathways.

Activation of mGluR5 in the hippocampus of WT mice causes the scaffolding protein homer to bind to the phosphatidylinositol 3-kinase enhancer protein (PIKE) (Ronesi and Huber

2008) and this, in turn, activates phosphatidylinositol 3-kinase (PI3K) and protein kinase B (AKT) (Hou and Klann 2004, Ronesi, Collins et al. 2012). AKT then stimulates mTORC1 and as a result, eIF4E-BP2 is phosphorylated by mTORC1 leading to the formation of the eIF4F complex and enhancement of the cap-dependent translation initiation and enhanced protein synthesis (Hou and Klann 2004, Klann and Dever 2004). One product protein is FMRP, which conversely represses the translation either in the initiation or elongation phase and thereby inhibits excessive protein synthesis (Darnell, Van Driesche et al. 2011). In contrast, in the absence of FMRP, the activity of PIKE, AKT, and mTORC1 is elevated in the hippocampus of *Fmr*1 KO mice (Sharma, Hoeffer et al. 2010, Liu, Huang et al. 2012, Huber, Klann et al. 2015). However, it has been shown that blocking mTORC1 activity using rapamycin does not rescue the exaggerated mGluR5-LTD in the hippocampus of *Fmr*1 KO mice (Sharma, Hoeffer et al. 2010) which suggests that it may be due to accumulation of the required proteins for mGluR5-LTD in the hippocampus of these mice (Huber, Klann et al. 2015).

The second mGluR5 downstream signaling pathway is through activation of mitogen-activated protein kinase (MAPK) and its downstream cascades including ERK and Mnk1. Mnk1 phosphorylates eIF4E and thereby modulates mRNA translation. In the brain of *Fmr*1 KO mice, there are some controversies related to the activity of the MAPK pathway (Sawicka, Pyronneau et al. 2016). While some studies have not observed any alterations in the activity of MEK and ERK in the hippocampus of young and adult *Fmr*1 KO mice (Liu, Huang et al. 2012, Ronesi, Collins et al. 2012), others have reported elevated MEK and ERK activity in the hippocampus and prefrontal cortex of adult (Gantois, Khoutorsky et al. 2017) and neocortex of ~30 day old *Fmr*1 KO mice (Sawicka, Pyronneau et al. 2016) (Figure. 6).

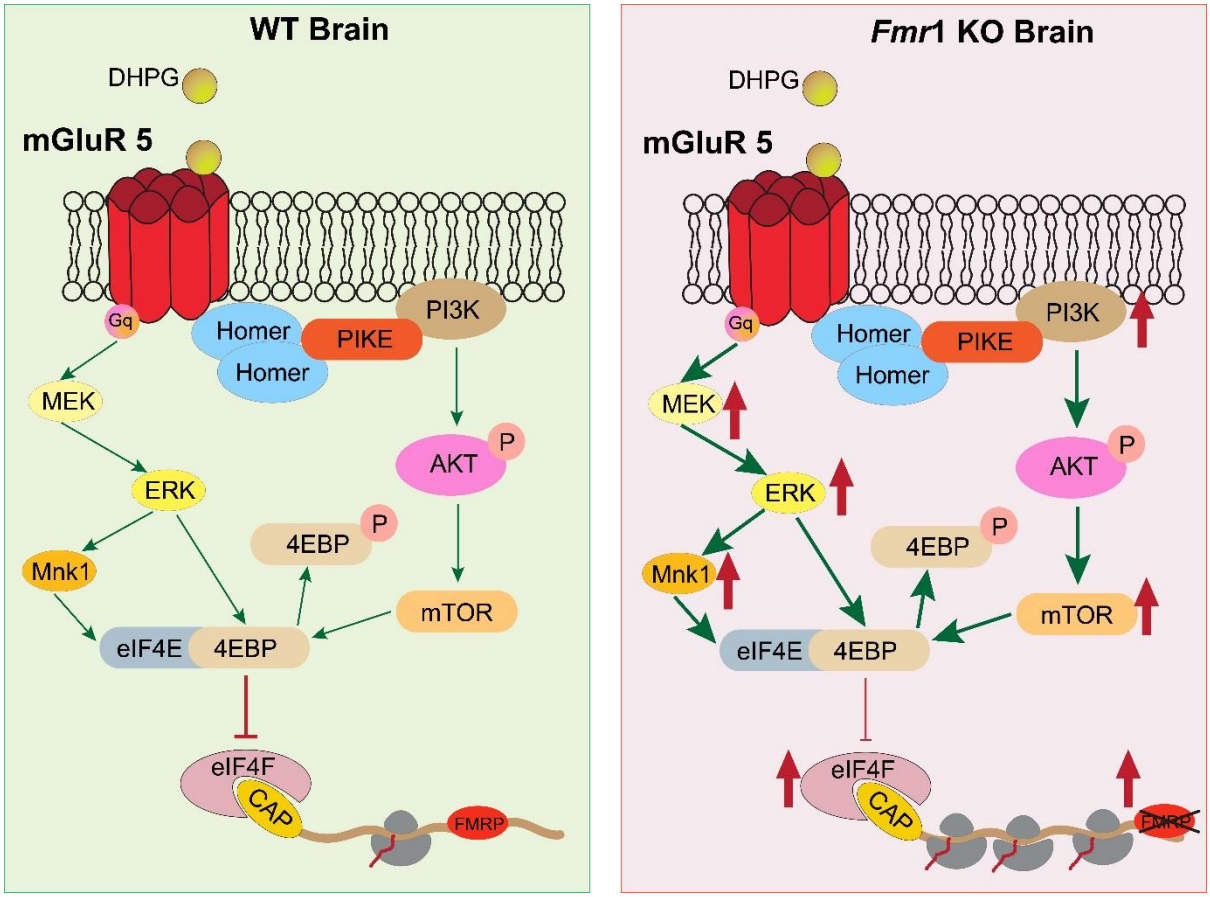

1.19.6 Figure 6. mGluR5 downstream pathway.

The mTORC1 and ERK pathways are depicted in the brains of WT and *Fmr*1 KO mice. In the absence of FMRP, the mTORC1 and ERK/MAPK pathways are hyperactive, resulting in increased protein synthesis.

1.19.6 Elevated level of global protein synthesis

Dysregulated global protein synthesis is believed to be a key symptom of FXS. The augmented rate of protein synthesis was initially reported by Qin et al., in the brain of adult *Fmr*1 KO mice. In this study, protein synthesis was measured using radiolabeled tracer L-[1-^{14}C] leucine in awake animals and elevated protein synthesis was observed in areas of the brain including the frontal association region, thalamus, and hippocampus (Qin, Kang et al. 2005). Contrary to *Fmr*1 KO mice, the rate of cerebral protein synthesis measured by L-[1-^{11}C] leucine positron emission tomography (PET) in sedated FXS patients was lower than in healthy controls. It was then hypothesized that propofol could be the cause of discrepancies in the rate of protein synthesis between *Fmr*1 KO and FXS. To this end, the rate of protein synthesis was measured in the brain of the sedated *Fmr*1 KO mice and WTs. The rate of protein synthesis diminished in the sedated *Fmr*1 KO mice but not WT animals, suggesting that in the absence of FMRP, propofol can affect protein synthesis (Qin, Schmidt et al. 2013). Likewise, Jacquemont et al., reported an increased rate of protein synthesis in fibroblasts from FXS individuals and in both fibroblasts and primary neurons of *Fmr*1 KO mice. In this study, using Surface Sensing of Translation (SUnSET) assay, they examined the rate of protein synthesis in fibroblasts derived from 32 patients with FXS and 17 healthy individuals in parallel with fibroblasts and primary neurons extracted from–27 *Fmr*1 KO and 20 control mice. However, in some fibroblasts either from FXS individuals or *Fmr*1 KO mice, they did not observe any increase in protein synthesis. Therefore, they concluded the variability in protein synthesis among individuals could be the reason some patients do not benefit from common clinical treatments (Jacquemont, Pacini et al. 2018). Consistently, in an *in vitro* study using ^{35}S-Met/Cys labeling assay on the hippocampal sections of the *Fmr*1 KO mice, enhanced basal protein synthesis was detected. It was further shown that this elevated level of protein synthesis is dependent on ERK1/2 and mGluR5 activity. Therefore, acute inhibition of ERK1/2 or mGluR5 normalized the elevated

protein synthesis in the hippocampus of *Fmr*1 KO mice (Osterweil, Krueger et al. 2010). In line with these findings, FMRP-deficient human neuronal cells had approximately 50% higher protein synthesis in comparison to control cells, which was related to enhanced AKT and ERK1/2 activity. Metformin treatment corrected the excessive rate of protein synthesis in these cells (Utami, Yusof et al. 2020). Elevated protein synthesis in the absence of FMRP is a widely established concept, and treatments that directly or indirectly inhibit protein synthesis can rescue the key symptoms of FXS in animal models.

1.20 Dysregulated mTORC1 and ERK pathways in ASDs

Mutations in several genes whose protein products regulate mRNA translation via mTORC1, ERK, and ISR pathways have been associated with an increased risk of autism spectrum disorders. Furthermore, the activity of the translational control pathways such as mTORC1 and ERK is dysregulated in both autistic individuals and animal models (Faridar, Jones-Davis et al. 2014, Winden, Ebrahimi-Fakhari et al. 2018). Interestingly, in autistic animal models, pharmacological or genetic manipulation of mRNA translation ameliorates the core symptoms of autism, indicating a causal association between autism and translational dysregulation. Hyperactivation of mTORC1 is a well-established landmark in autism, and inhibition of mTORC1 using pharmacological inhibitors such as rapamycin improves the autistic features (Huber, Klann et al. 2015, Sato 2016). Mutations in TSC1/2 and PTEN, two negative regulators of mTORC1, have been associated with an elevated risk of autism, and deletion of these genes in animals results in autism-like phenotypes (Smalley 1998, Zhou and Parada 2012, Reith, McKenna et al. 2013). Likewise, mutations in the downstream effectors of mTORC1 also lead to autistic-like behaviors in animals. Clinical findings have shown that gain-of-function mutations in eIF4E are correlated with ASD. Likewise, deletion of 4E-BP2, the eIF4E repressor, or overexpression of eIF4E in mice, is sufficient to generate the key symptoms of

ASD. Application of 4EGI-1, which disrupts the formation of the eIF4F complex, rescues core symptoms of autism in animals (Gkogkas, Khoutorsky et al. 2013, Santini, Huynh et al. 2013). The mouse model of FXS, *Fmr*1 KO, shows elevated activity of the mTORC1 pathway, indicated by increased levels of PIKE and p-S6 (Sharma, Hoeffer et al. 2010). Inactivation of S6K in this mouse model ameliorates the core autistic syndromes (Bhattacharya, Kaphzan et al. 2012). Dysregulation of the ERK/MAPK pathway has also been connected to the development of ASD (Satoh, Endo et al. 2011). In mice, genetic deletion of ERK2 or pharmacological suppression of ERK results in abnormalities in social interactions that are development-dependent (Satoh, Endo et al. 2011). Synaptic Ras GTPase-activating protein 1 (SYNGAP1) and neurofibromin (NF1) are typical negative regulators of the Ras-GTPase and hence the ERK/MAPK pathway. Mutations in genes encoding for SYNGAP1 and NF1 have been linked with autistic phenotype in patients and animal models. Heterozygous NF1 ablation in mice increases MAPK pathway activity, as indicated by elevated p-ERK in the brain and impaired social interactions (Chisholm, Anderson et al. 2018, Toft 2019).

1.21 Integrated stress response and cognitive disorders

Dysregulation of the ISR has been associated with many cognitive and psychiatric illnesses such as Parkinson's disease (Hoozemans, Van Haastert et al. 2007), Alzheimer's diseases (Ma, Trinh et al. 2013), and multiple sclerosis (Lin, Bailey et al. 2007), The eIF2 pathway has been widely studied in the context of learning and memory, establishing that high levels of p-eIF2 induce memory impairment, whereas lowering the phosphorylated form of eIF2 or blocking the action of p-eIF2 using integrated stress response inhibitor (ISRIB) improves memory function in rodents (Costa-Mattioli, Gobert et al. 2005, Costa-Mattioli, Gobert et al. 2007, Placzek, Di Prisco et al. 2016). Furthermore, p-eIF2 influences memory in a cell-type-specific manner (Sharma, Sood et al. 2020). Elevated levels of p-eIF2α—indicative of ISR activation—

have been observed in the hippocampus of the mouse model of Down Syndrome (DS) and post-mortem brain tissue from patients with DS. This increase in p-eIF2α levels is accompanied by a reduction in global protein synthesis (Zhu, Khatiwada et al. 2019). It has also been demonstrated that suppressing the PKR increases epileptic activity in the brain, measured by higher network excitability in the brains of PKR deficient mice (Zhu, Huang et al. 2011). Moreover, activation of the ISR has been detected in the brains of the offspring of the maternal immune activation (MIA) mouse model, and suppression of ISR activity reverses behavioral abnormalities such as impaired social interaction and marble burying, and cortical network activity in MIA offspring. Surprisingly, ISR activation was only observed in male offspring and not females. (Kalish, Kim et al. 2021). Kabir et al. observed a connection between the ISR pathway and autism. They discovered an increased level of p-eIF2 in the prefrontal cortex of *Cacna1c* conditional KO mice and found that blockade of p-eIF2 with ISRIB could correct lowered protein synthesis, a higher excitation/inhibition ratio, impaired social interaction, and anxiety-like behaviors in this model (Kabir, Che et al. 2017).

1.22 Cerebellum and autism

Aside from the well-established role of the cerebellum in motor learning and balance, a growing body of evidence suggests that the cerebellum also plays a major role in mediating higher functions and cognitive abilities such as memory and sociability (Schmahmann and Pandya 1995, Riva and Giorgi 2000). Several lines of evidence have emerged in recent years to support the cerebellum-autism link. First, both autistic individuals and some autistic animal models bear anatomical and functional abnormalities in the cerebellum. Purkinje cell (PC) loss is one of the most widely reported morphological changes in post-mortem brain tissue of autistic individuals (Palmen, van Engeland et al. 2004, Whitney, Kemper et al. 2008). Second, a higher prevalence of autistic traits has been reported in patients with cerebellar injuries

(Wang, Kloth et al. 2014). Third, selective deletion of distinct autism risk genes in the rodents' cerebellum results in autistic-like behaviors. For example, selective ablation of TSC1, a mTORC1 negative regulator, in mouse cerebellar PCs produces the core symptoms of ASDs, including impaired social interactions, difficulty in vocalizations, and repetitive behaviors. Furthermore, PCs are hypoexcitable in these mice. Interestingly, the morphological and functional abnormalities were rescued by rapamycin, a mTORC1 inhibitor (Tsai, Hull et al. 2012). Similarly, the major autistic symptoms were also detected in mice with TSC2 loss only in cerebellar PCs. (Reith, McKenna et al. 2013). In line with these findings, mice with deleted PTEN in their cerebellar PCs exhibited autistic-like behaviors, motor disabilities, decreased excitability, and a range of morphological changes in the cerebellum network, including deficits in axons, dendrites, climbing fiber synapses, and parallel fiber synapses. (Cupolillo, Hoxha et al. 2016).

In addition, the involvement of the cerebellum in spatial memory and place learning has been supported by several studies. For example, in adult rats, selective destruction of cerebellar PCs with the anti-neuronal immunotoxin OX7-saporin (OX7-saporin) impeded the acquisition phase of the Morris water maze. (Gandhi, Kelly et al. 2000). Consistently, spatial memory impairment has been reported in cerebellar mutant mice such as *Grid2*^{LC}, *Rora*^{sg}, *Nna1*^{pcd}, and *nervous* (Lalonde and Strazielle 2003).

1.24 References

Abbeduto, L., et al. (2019). "ASD comorbidity in fragile X syndrome: Symptom profile and predictors of symptom severity in adolescent and young adult males." Journal of autism and developmental disorders 49(3): 960-977.

Alone, P. V. and T. E. Dever (2006). "Direct binding of translation initiation factor eIF2γ-G domain to its GTPase-activating and GDP-GTP exchange factors eIF5 and eIF2Bϵ." Journal of Biological Chemistry **281**(18): 12636-12644.

Alpatov, R., et al. (2014). "A chromatin-dependent role of the fragile X mental retardation protein FMRP in the DNA damage response." Cell **157**(4): 869-881.

Alvarez-Castelao, B., et al. (2020). "The switch-like expression of heme-regulated kinase 1 mediates neuronal proteostasis following proteasome inhibition." Elife **9**: e52714.

Alvarez, V. A. and B. L. Sabatini (2007). "Anatomical and physiological plasticity of dendritic spines." Annu. Rev. Neurosci. **30**: 79-97.

Antar, L. N., et al. (2004). "Metabotropic glutamate receptor activation regulates fragile x mental retardation protein and FMR1 mRNA localization differentially in dendrites and at synapses." Journal of Neuroscience **24**(11): 2648-2655.

Antoine, M. W., et al. (2019). "Increased excitation-inhibition ratio stabilizes synapse and circuit excitability in four autism mouse models." Neuron **101**(4): 648-661. e644.

Armstrong, C. G., et al. (1997). "PPP1R6, a novel member of the family of glycogen-targetting subunits of protein phosphatase 1." FEBS letters **418**(1-2): 210-214.

Ashley Jr, C. T., et al. (1993). "FMR1 protein: conserved RNP family domains and selective RNA binding." Science **262**(5133): 563-566.

Bai, X., et al. (2007). "Rheb activates mTOR by antagonizing its endogenous inhibitor, FKBP38." Science **318**(5852): 977-980.

Bakker, C. E., et al. (2000). "Immunocytochemical and biochemical characterization of FMRP, FXR1P, and FXR2P in the mouse." Experimental cell research **258**(1): 162-170.

Banko, J. L., et al. (2006). "Regulation of eukaryotic initiation factor 4E by converging signaling pathways during metabotropic glutamate receptor-dependent long-term depression." Journal of Neuroscience **26**(8): 2167-2173.

Banko, J. L., et al. (2005). "The translation repressor 4E-BP2 is critical for eIF4F complex formation, synaptic plasticity, and memory in the hippocampus." Journal of Neuroscience **25**(42): 9581-9590.

Barnea-Goraly, N., et al. (2014). "A preliminary longitudinal volumetric MRI study of amygdala and hippocampal volumes in autism." Progress in Neuro-Psychopharmacology and Biological Psychiatry **48**: 124-128.

Bassell, G. J. and S. T. Warren (2008). "Fragile X syndrome: loss of local mRNA regulation alters synaptic development and function." Neuron **60**(2): 201-214.

Basu, S. N., et al. (2009). "AutDB: a gene reference resource for autism research." Nucleic acids research **37**(suppl_1): D832-D836.

Bauer, B. N., et al. (2001). "Multiple autophosphorylation is essential for the formation of the active and stable homodimer of heme-regulated eIF2α kinase." Biochemistry **40**(38): 11543-11551.

Bauman, M. L. (2010). "Medical comorbidities in autism: challenges to diagnosis and treatment." Neurotherapeutics **7**(3): 320-327.

Bauman, M. L. and T. L. Kemper (2005). "Neuroanatomic observations of the brain in autism: a review and future directions." International journal of developmental neuroscience **23**(2-3): 183-187.

Bear, M. F., et al. (2004). "The mGluR theory of fragile X mental retardation." Trends in neurosciences **27**(7): 370-377.

Berry-Kravis, E. (2002). "Epilepsy in fragile X syndrome." Developmental medicine and child neurology **44**(11): 724-728.

Bhattacharya, A., et al. (2012). "Genetic removal of p70 S6 kinase 1 corrects molecular, synaptic, and behavioral phenotypes in fragile X syndrome mice." Neuron **76**(2): 325-337.

Bidinosti, M., et al. (2010). "Postnatal deamidation of 4E-BP2 in brain enhances its association with raptor and alters kinetics of excitatory synaptic transmission." Molecular cell **37**(6): 797-808.

Bourgeron, T. (2009). "A synaptic trek to autism." Current opinion in neurobiology **19**(2): 231-234.

Boyce, M., et al. (2005). "A selective inhibitor of eIF2α dephosphorylation protects cells from ER stress." Science **307**(5711): 935-939.

Braun, K. and M. Segal (2000). "FMRP involvement in formation of synapses among cultured hippocampal neurons." Cerebral cortex **10**(10): 1045-1052.

Brown, M. R., et al. (2010). "Fragile X mental retardation protein controls gating of the sodium-activated potassium channel Slack." Nature neuroscience **13**(7): 819-821.

Brown, V., et al. (2001). "Microarray identification of FMRP-associated brain mRNAs and altered mRNA translational profiles in fragile X syndrome." Cell **107**(4): 477-487.

Carper, R. A. and E. Courchesne (2005). "Localized enlargement of the frontal cortex in early autism." Biological psychiatry **57**(2): 126-133.

Carriere, A., et al. (2011). "ERK1/2 phosphorylate Raptor to promote Ras-dependent activation of mTOR complex 1 (mTORC1)." Journal of Biological Chemistry **286**(1): 567-577.

Ceman, S., et al. (2003). "Phosphorylation influences the translation state of FMRP-associated polyribosomes." Human molecular genetics **12**(24): 3295-3305.

Ceolin, L., et al. (2017). "Cell type-specific mRNA dysregulation in hippocampal CA1 pyramidal neurons of the fragile X syndrome mouse model." Frontiers in molecular neuroscience **10**: 340.

Chen, E. and S. Joseph (2015). "Fragile X mental retardation protein: a paradigm for translational control by RNA-binding proteins." Biochimie **114**: 147-154.

Chen, E., et al. (2014). "Fragile X mental retardation protein regulates translation by binding directly to the ribosome." Molecular cell **54**(3): 407-417.

Chen, J.-J. (2000). "Heme-regulated eIF2alpha kinase." COLD SPRING HARBOR MONOGRAPH SERIES **39**: 529-546.

Chisholm, A. K., et al. (2018). "Social function and autism spectrum disorder in children and adults with neurofibromatosis type 1: a systematic review and meta-analysis." Neuropsychology Review **28**(3): 317-340.

Chuang, S.-C., et al. (2005). "Prolonged epileptiform discharges induced by altered group I metabotropic glutamate receptor-mediated synaptic responses in hippocampal slices of a fragile X mouse model." Journal of Neuroscience **25**(35): 8048-8055.

Collingridge, G. L., et al. (2010). "Long-term depression in the CNS." Nature reviews neuroscience **11**(7): 459-473.

Connor, J. H., et al. (2001). "Growth arrest and DNA damage-inducible protein GADD34 assembles a novel signaling complex containing protein phosphatase 1 and inhibitor 1." Molecular and cellular biology **21**(20): 6841-6850.

Consorthium, T. D.-B. F. X., et al. (1994). "Fmr1 knockout mice: a model to study fragile X mental retardation." Cell **78**(1): 23-33.

Contractor, A., et al. (2015). "Altered neuronal and circuit excitability in fragile X syndrome." Neuron **87**(4): 699-715.

Conturo, T. E., et al. (2008). "Neuronal fiber pathway abnormalities in autism: an initial MRI diffusion tensor tracking study of hippocampo-fusiform and amygdalo-fusiform pathways." Journal of the International Neuropsychological Society **14**(6): 933-946.

Cook Jr, E. H., et al. (1997). "Autism or atypical autism in maternally but not paternally derived proximal 15q duplication." American journal of human genetics **60**(4): 928.

Costa-Mattioli, M., et al. (2005). "Translational control of hippocampal synaptic plasticity and memory by the eIF2α kinase GCN2." Nature **436**(7054): 1166-1170.

Costa-Mattioli, M., et al. (2007). "eIF2α phosphorylation bidirectionally regulates the switch from short-to long-term synaptic plasticity and memory." Cell **129**(1): 195-206.

Costa-Mattioli, M. and P. Walter (2020). "The integrated stress response: From mechanism to disease." Science **368**(6489): eaat5314.

Courchesne, E., et al. (2011). "Brain growth across the life span in autism: age-specific changes in anatomical pathology." Brain research **1380**: 138-145.

Courchesne, E., et al. (2011). "Neuron number and size in prefrontal cortex of children with autism." Jama **306**(18): 2001-2010.

Crespi, B. J. (2010). "Revisiting Bleuler: relationship between autism and schizophrenia." The British Journal of Psychiatry **196**(6): 495-495.

Cupolillo, D., et al. (2016). "Autistic-like traits and cerebellar dysfunction in Purkinje cell PTEN knock-out mice." Neuropsychopharmacology **41**(6): 1457-1466.

D'Annessa, I., et al. (2019). "Handling FMRP and its molecular partners: Structural insights into Fragile X Syndrome." Progress in Biophysics and Molecular Biology **141**: 3-14.

d'Hulst, C., et al. (2006). "Decreased expression of the GABAA receptor in fragile X syndrome." Brain research **1121**(1): 238-245.

Dager, S. R., et al. (2007). "Shape mapping of the hippocampus in young children with autism spectrum disorder." American journal of neuroradiology **28**(4): 672-677.

Darnell, J., et al. "Fraser Ce, Stone eF, Chen C, Fak JJ, Chi Sw, Licatalosi DD, Richter JD, Darnell RB (2011) FMRP stalls ribosomal translocation on mRNAs linked to synaptic function and autism." Cell **146**(2): 247-261.

Darnell, J. C., et al. (2005). "FMRP RNA targets: identification and validation." Genes, Brain and Behavior **4**(6): 341-349.

Darnell, J. C., et al. (2011). "FMRP stalls ribosomal translocation on mRNAs linked to synaptic function and autism." Cell **146**(2): 247-261.

Davis, M. and P. J. Whalen (2001). "The amygdala: vigilance and emotion." Molecular psychiatry **6**(1): 13-34.

De Rubeis, S. and C. Bagni (2010). "Fragile X mental retardation protein control of neuronal mRNA metabolism: Insights into mRNA stability." Molecular and Cellular Neuroscience **43**(1): 43-50.

De Rubeis, S. and C. Bagni (2011). "Regulation of molecular pathways in the Fragile X Syndrome: insights into Autism Spectrum Disorders." Journal of Neurodevelopmental Disorders **3**(3): 257-269.

Deng, J., et al. (2002). "Activation of GCN2 in UV-irradiated cells inhibits translation." Current Biology **12**(15): 1279-1286.

Di Prisco, G. V., et al. (2014). "Translational control of mGluR-dependent long-term depression and object-place learning by eIF2α." Nature neuroscience **17**(8): 1073-1082.

Dictenberg, J. B., et al. (2008). "A direct role for FMRP in activity-dependent dendritic mRNA transport links filopodial-spine morphogenesis to fragile X syndrome." Developmental cell **14**(6): 926-939.

Dong, J., et al. (2000). "Uncharged tRNA activates GCN2 by displacing the protein kinase moiety from a bipartite tRNA-binding domain." Molecular cell **6**(2): 269-279.

Donnelly, N., et al. (2013). "The eIF2α kinases: their structures and functions." Cellular and molecular life sciences **70**(19): 3493-3511.

Drozd, M., et al. (2018). "Modeling fragile X syndrome in Drosophila." Frontiers in molecular neuroscience **11**: 124.

Durkin, M. S., et al. (2008). "Advanced parental age and the risk of autism spectrum disorder." American journal of epidemiology **168**(11): 1268-1276.

Eberhart, D. E., et al. (1996). "The fragile X mental retardation protein is a ribonucleoprotein containing both nuclear localization and nuclear export signals." Human molecular genetics **5**(8): 1083-1091.

Edens, B. M., et al. (2019). "FMRP modulates neural differentiation through m6A-dependent mRNA nuclear export." Cell reports **28**(4): 845-854. e845.

Eiermann, N., et al. (2020). "Dance with the devil: stress granules and signaling in antiviral responses." Viruses **12**(9): 984.

El Idrissi, A., et al. (2005). "Decreased GABAA receptor expression in the seizure-prone fragile X mouse." Neuroscience letters **377**(3): 141-146.

Ellegood, J., et al. (2015). "Clustering autism: using neuroanatomical differences in 26 mouse models to gain insight into the heterogeneity." Molecular psychiatry **20**(1): 118-125.

Engelman, J. A., et al. (2006). "The evolution of phosphatidylinositol 3-kinases as regulators of growth and metabolism." Nature Reviews Genetics **7**(8): 606-619.

Erickson, F., et al. (1997). "Functional analysis of homologs of translation initiation factor 2γ in yeast." Molecular and General Genetics MGG **253**(6): 711-719.

Evans, B. (2013). "How autism became autism: The radical transformation of a central concept of child development in Britain." History of the human sciences **26**(3): 3-31.

Faridar, A., et al. (2014). "Mapk/Erk activation in an animal model of social deficits shows a possible link to autism." Molecular autism **5**(1): 1-12.

Fatemi, S. H., et al. (2002). "Purkinje cell size is reduced in cerebellum of patients with autism." Cellular and molecular neurobiology **22**(2): 171-175.

Fehlow, P., et al. (1993). "Early infantile autism and excessive aerophagy with symptomatic megacolon and ileus in a case of Ehlers-Danlos syndrome." Padiatrie und Grenzgebiete **31**(4): 259-267.

Feinstein, A. (2011). A history of autism: Conversations with the pioneers, John Wiley & Sons.

Feng, Y., et al. (1997). "Fragile X mental retardation protein: nucleocytoplasmic shuttling and association with somatodendritic ribosomes." Journal of Neuroscience **17**(5): 1539-1547.

Ferrari, F., et al. (2007). "The fragile X mental retardation protein–RNP granules show an mGluR-dependent localization in the post-synaptic spines." Molecular and Cellular Neuroscience **34**(3): 343-354.

Ferron, L., et al. (2014). "Fragile X mental retardation protein controls synaptic vesicle exocytosis by modulating N-type calcium channel density." Nature communications **5**(1): 1-14.

Galvez, R., et al. (2005). "Olfactory bulb mitral cell dendritic pruning abnormalities in a mouse model of the Fragile-X mental retardation syndrome: further support for FMRP's involvement in dendritic development." Developmental Brain Research **157**(2): 214-216.

Gandhi, C. C., et al. (2000). "Impaired acquisition of a Morris water maze task following selective destruction of cerebellar purkinje cells with OX7-saporin." Behavioural brain research **109**(1): 37-47.

Gandin, V., et al. (2016). "mTORC1 and CK2 coordinate ternary and eIF4F complex assembly." Nature communications **7**(1): 1-15.

Gantois, I., et al. (2017). "Metformin ameliorates core deficits in a mouse model of fragile X syndrome." Nature medicine **23**(6): 674-677.

Gantois, I., et al. (2006). "Expression profiling suggests underexpression of the GABAA receptor subunit δ in the fragile X knockout mouse model." Neurobiology of disease **21**(2): 346-357.

Gao, R. and P. Penzes (2015). "Common mechanisms of excitatory and inhibitory imbalance in schizophrenia and autism spectrum disorders." Current molecular medicine **15**(2): 146-167.

Gardener, H., et al. (2011). "Perinatal and neonatal risk factors for autism: a comprehensive meta-analysis." Pediatrics **128**(2): 344-355.

Gebauer, F. and M. W. Hentze (2004). "Molecular mechanisms of translational control." Nature reviews Molecular cell biology **5**(10): 827-835.

Gholizadeh, S., et al. (2014). "Reduced phenotypic severity following adeno-associated virus-mediated Fmr1 gene delivery in fragile X mice." Neuropsychopharmacology **39**(13): 3100-3111.

Gholizadeh, S., et al. (2015). "Expression of fragile X mental retardation protein in neurons and glia of the developing and adult mouse brain." Brain research **1596**: 22-30.

Gingras, A.-C., et al. (2001). "Regulation of translation initiation by FRAP/mTOR." Genes & development **15**(7): 807-826.

Gkogkas, C. G., et al. (2013). "Autism-related deficits via dysregulated eIF4E-dependent translational control." Nature **493**(7432): 371-377.

Goldberg, J., et al. (1995). "Three-dimensional structure of the catalytic subunit of protein serine/threonine phosphatase-1." Nature **376**(6543): 745-753.

Gonzalez, D., et al. (2019). "Audiogenic seizures in the Fmr1 knock-out mouse are induced by Fmr1 deletion in subcortical, VGlut2-expressing excitatory neurons and require deletion in the inferior colliculus." Journal of Neuroscience **39**(49): 9852-9863.

Greenblatt, E. J. and A. C. Spradling (2018). "Fragile X mental retardation 1 gene enhances the translation of large autism-related proteins." Science **361**(6403): 709-712.

Gross, C., et al. (2011). "Fragile X mental retardation protein regulates protein expression and mRNA translation of the potassium channel Kv4. 2." Journal of Neuroscience **31**(15): 5693-5698.

Guo, F. and D. R. Cavener (2007). "The GCN2 eIF2α kinase regulates fatty-acid homeostasis in the liver during deprivation of an essential amino acid." Cell metabolism **5**(2): 103-114.

Guo, W., et al. (2015). "Elevated CaMKIIα and hyperphosphorylation of Homer mediate circuit dysfunction in a fragile X syndrome mouse model." Cell reports **13**(10): 2297-2311.

Hara, H. (2007). "Autism and epilepsy: a retrospective follow-up study." Brain and Development **29**(8): 486-490.

Harding, H. P., et al. (2000). "Regulated translation initiation controls stress-induced gene expression in mammalian cells." Molecular cell **6**(5): 1099-1108.

Harding, H. P., et al. (2019). "The ribosomal P-stalk couples amino acid starvation to GCN2 activation in mammalian cells." Elife **8**: e50149.

Harding, H. P., et al. (2009). "Ppp1r15 gene knockout reveals an essential role for translation initiation factor 2 alpha (eIF2α) dephosphorylation in mammalian development." Proceedings of the National Academy of Sciences **106**(6): 1832-1837.

Harding, H. P., et al. (2003). "An integrated stress response regulates amino acid metabolism and resistance to oxidative stress." Molecular cell **11**(3): 619-633.

Harris, J. (2018). "Leo Kanner and autism: a 75-year perspective." International Review of Psychiatry **30**(1): 3-17.

Harvey, R. F., et al. (2019). "Signaling from mTOR to eIF2α mediates cell migration in response to the chemotherapeutic doxorubicin." Science Signaling **12**(612): eaaw6763.

Hayashi, Y. and A. K. Majewska (2005). "Dendritic spine geometry: functional implication and regulation." Neuron **46**(4): 529-532.

Hays, S. A., et al. (2011). "Altered neocortical rhythmic activity states in Fmr1 KO mice are due to enhanced mGluR5 signaling and involve changes in excitatory circuitry." Journal of Neuroscience **31**(40): 14223-14234.

Hershey, J. W., et al. (2019). "Principles of translational control." Cold Spring Harbor Perspectives in Biology **11**(9): a032607.

Hinnebusch, A. G., et al. (2016). "Translational control by 5′-untranslated regions of eukaryotic mRNAs." Science **352**(6292): 1413-1416.

Hong, W., et al. (2014). "Antagonistic control of social versus repetitive self-grooming behaviors by separable amygdala neuronal subsets." Cell **158**(6): 1348-1361.

Hoozemans, J., et al. (2007). "Activation of the unfolded protein response in Parkinson's disease." Biochemical and biophysical research communications **354**(3): 707-711.

Hou, L., et al. (2006). "Dynamic translational and proteasomal regulation of fragile X mental retardation protein controls mGluR-dependent long-term depression." Neuron **51**(4): 441-454.

Hou, L. and E. Klann (2004). "Activation of the phosphoinositide 3-kinase-Akt-mammalian target of rapamycin signaling pathway is required for metabotropic glutamate receptor-dependent long-term depression." Journal of Neuroscience **24**(28): 6352-6361.

Huang, J. and B. D. Manning (2008). "The TSC1–TSC2 complex: a molecular switchboard controlling cell growth." Biochemical Journal **412**(2): 179-190.

Huber, K. M., et al. (2002). "Altered synaptic plasticity in a mouse model of fragile X mental retardation." Proceedings of the National Academy of Sciences **99**(11): 7746-7750.

Huber, K. M., et al. (2000). "Role for rapid dendritic protein synthesis in hippocampal mGluR-dependent long-term depression." Science **288**(5469): 1254-1256.

Huber, K. M., et al. (2015). "Dysregulation of mammalian target of rapamycin signaling in mouse models of autism." Journal of Neuroscience **35**(41): 13836-13842.

Huber, K. M., et al. (2001). "Chemical induction of mGluR5-and protein synthesis–dependent long-term depression in hippocampal area CA1." Journal of neurophysiology **86**(1): 321-325.

Hutsler, J. J. and H. Zhang (2010). "Increased dendritic spine densities on cortical projection neurons in autism spectrum disorders." Brain research **1309**: 83-94.

Ishimura, R., et al. (2016). "Activation of GCN2 kinase by ribosome stalling links translation elongation with translation initiation." Elife **5**: e14295.

Jack, A. and K. A. Pelphrey (2015). "Neural correlates of animacy attribution include neocerebellum in healthy adults." Cerebral cortex **25**(11): 4240-4247.

Jackson, R. J., et al. (2010). "The mechanism of eukaryotic translation initiation and principles of its regulation." Nature reviews Molecular cell biology **11**(2): 113-127.

Jacquemont, S., et al. (2018). "Protein synthesis levels are increased in a subset of individuals with fragile X syndrome." Human molecular genetics **27**(12): 2039-2051.

Jennings, M. D., et al. (2016). "eIF2β is critical for eIF5-mediated GDP-dissociation inhibitor activity and translational control." Nucleic acids research **44**(20): 9698-9709.

Jissendi, P., et al. (2008). "Diffusion tensor imaging (DTI) and tractography of the cerebellar projections to prefrontal and posterior parietal cortices: a study at 3T." Journal of Neuroradiology **35**(1): 42-50.

Kabir, Z., et al. (2017). "Rescue of impaired sociability and anxiety-like behavior in adult cacna1c-deficient mice by pharmacologically targeting eIF2α." Molecular psychiatry **22**(8): 1096-1109.

Kalish, B. T., et al. (2021). "Maternal immune activation in mice disrupts proteostasis in the fetal brain." Nature neuroscience **24**(2): 204-213.

Kao, D.-I., et al. (2010). "Altered mRNA transport, docking, and protein translation in neurons lacking fragile X mental retardation protein." Proceedings of the National Academy of Sciences **107**(35): 15601-15606.

Kelleher III, R. J. and M. F. Bear (2008). "The autistic neuron: troubled translation?" Cell **135**(3): 401-406.

Khandjian, E. W., et al. (1996). "The fragile X mental retardation protein is associated with ribosomes." Nature genetics **12**(1): 91-93.

Khandjian, E. W., et al. (2004). "Biochemical evidence for the association of fragile X mental retardation protein with brain polyribosomal ribonucleoparticles." Proceedings of the National Academy of Sciences **101**(36): 13357-13362.

Kim, J., et al. (2011). "AMPK and mTOR regulate autophagy through direct phosphorylation of Ulk1." Nature cell biology **13**(2): 132-141.

Kim, Y., et al. (2018). "PKR senses nuclear and mitochondrial signals by interacting with endogenous double-stranded RNAs." Molecular cell **71**(6): 1051-1063. e1056.

Kimball, S. R., et al. (1998). "Identification of interprotein interactions between the subunits of eukaryotic initiation factors eIF2 and eIF2B." Journal of Biological Chemistry **273**(5): 3039-3044.

Klann, E. and T. E. Dever (2004). "Biochemical mechanisms for translational regulation in synaptic plasticity." Nature reviews neuroscience **5**(12): 931-942.

Koekkoek, S., et al. (2005). "Deletion of FMR1 in Purkinje cells enhances parallel fiber LTD, enlarges spines, and attenuates cerebellar eyelid conditioning in Fragile X syndrome." Neuron **47**(3): 339-352.

Koelkebeck, K., et al. (2021). "Case of Asperger's Syndrome and Lesion of the Right Amygdala: Deficits in Implicit and Explicit Fearful Face Recognition." Frontiers in Psychology **12**.

Komar, A. A. and M. Hatzoglou (2011). "Cellular IRES-mediated translation: the war of ITAFs in pathophysiological states." Cell cycle **10**(2): 229-240.

Kooy, R. F. (2003). "Of mice and the fragile X syndrome." Trends in genetics **19**(3): 148-154.

Korb, E., et al. (2017). "Excess translation of epigenetic regulators contributes to fragile X syndrome and is alleviated by Brd4 inhibition." Cell **170**(6): 1209-1223. e1220.

Laggerbauer, B., et al. (2001). "Evidence that fragile X mental retardation protein is a negative regulator of translation." Human molecular genetics **10**(4): 329-338.

Lalonde, R. and C. Strazielle (2003). "The effects of cerebellar damage on maze learning in animals." The Cerebellum **2**(4): 300-309.

Lemaire, P. A., et al. (2008). "Mechanism of PKR Activation by dsRNA." Journal of molecular biology **381**(2): 351-360.

Levisohn, P. M. (2007). "The autism-epilepsy connection." Epilepsia **48**: 33-35.

Lin, W., et al. (2007). "The integrated stress response prevents demyelination by protecting oligodendrocytes against immune-mediated damage." The Journal of clinical investigation **117**(2): 448-456.

Liu, C. Y., et al. (2000). "Ligand-independent dimerization activates the stress response kinases IRE1 and PERK in the lumen of the endoplasmic reticulum." Journal of Biological Chemistry **275**(32): 24881-24885.

Liu, Z.-H., et al. (2012). "Lithium reverses increased rates of cerebral protein synthesis in a mouse model of fragile X syndrome." Neurobiology of disease **45**(3): 1145-1152.

Lovelace, J. W., et al. (2020). "Deletion of Fmr1 from forebrain excitatory neurons triggers abnormal cellular, EEG, and behavioral phenotypes in the auditory cortex of a mouse model of fragile X syndrome." Cerebral cortex **30**(3): 969-988.

Lu, R., et al. (2004). "The fragile X protein controls microtubule-associated protein 1B translation and microtubule stability in brain neuron development." Proceedings of the National Academy of Sciences **101**(42): 15201-15206.

Ma, T., et al. (2013). "Suppression of eIF2α kinases alleviates Alzheimer's disease–related plasticity and memory deficits." Nature neuroscience **16**(9): 1299-1305.

Maehama, T. and J. E. Dixon (1998). "The tumor suppressor, PTEN/MMAC1, dephosphorylates the lipid second messenger, phosphatidylinositol 3, 4, 5-trisphosphate." Journal of Biological Chemistry **273**(22): 13375-13378.

Maenner, M. J., et al. (2021). "Prevalence and characteristics of autism spectrum disorder among children aged 8 years—autism and developmental disabilities monitoring network, 11 sites, United States, 2018." MMWR Surveillance Summaries **70**(11): 1.

Manning, B. D., et al. (2002). "Identification of the tuberous sclerosis complex-2 tumor suppressor gene product tuberin as a target of the phosphoinositide 3-kinase/akt pathway." Molecular cell **10**(1): 151-162.

Marciniak, S. J., et al. (2006). "Activation-dependent substrate recruitment by the eukaryotic translation initiation factor 2 kinase PERK." The Journal of cell biology **172**(2): 201-209.

Marcotrigiano, J., et al. (1997). "Cocrystal structure of the messenger RNA 5′ cap-binding protein (eIF4E) bound to 7-methyl-GDP." Cell **89**(6): 951-961.

McKinney, B. C., et al. (2005). "Dendritic spine abnormalities in the occipital cortex of C57BL/6 Fmr1 knockout mice." American Journal of Medical Genetics Part B: Neuropsychiatric Genetics **136**(1): 98-102.

Michalon, A., et al. (2012). "Chronic pharmacological mGlu5 inhibition corrects fragile X in adult mice." Neuron **74**(1): 49-56.

Middleton, F. A. and P. L. Strick (2000). "Basal ganglia and cerebellar loops: motor and cognitive circuits." Brain research reviews **31**(2-3): 236-250.

Miyashiro, K. Y., et al. (2003). "RNA cargoes associating with FMRP reveal deficits in cellular functioning in Fmr1 null mice." Neuron **37**(3): 417-431.

Modabbernia, A., et al. (2017). "Environmental risk factors for autism: an evidence-based review of systematic reviews and meta-analyses." Molecular autism **8**(1): 1-16.

Morris, D. R. and A. P. Geballe (2000). "Upstream open reading frames as regulators of mRNA translation." Molecular and cellular biology **20**(23): 8635-8642.

Muddashetty, R. S., et al. (2007). "Dysregulated metabotropic glutamate receptor-dependent translation of AMPA receptor and postsynaptic density-95 mRNAs at synapses in a mouse model of fragile X syndrome." Journal of Neuroscience **27**(20): 5338-5348.

Muhle, R., et al. (2004). "The genetics of autism." Pediatrics **113**(5): e472-e486.

Mullins, C., et al. (2016). "Unifying views of autism spectrum disorders: a consideration of autoregulatory feedback loops." Neuron **89**(6): 1131-1156.

Musumeci, S. A., et al. (2000). "Audiogenic seizures susceptibility in transgenic mice with fragile X syndrome." Epilepsia **41**(1): 19-23.

Myrick, L. K., et al. (2015). "Independent role for presynaptic FMRP revealed by an FMR1 missense mutation associated with intellectual disability and seizures." Proceedings of the National Academy of Sciences **112**(4): 949-956.

Myrick, L. K., et al. (2015). "Human FMRP contains an integral tandem Agenet (Tudor) and KH motif in the amino terminal domain." Human molecular genetics **24**(6): 1733-1740.

Nakamoto, M., et al. (2007). "Fragile X mental retardation protein deficiency leads to excessive mGluR5-dependent internalization of AMPA receptors." Proceedings of the National Academy of Sciences **104**(39): 15537-15542.

Napoli, I., et al. (2008). "The fragile X syndrome protein represses activity-dependent translation through CYFIP1, a new 4E-BP." Cell **134**(6): 1042-1054.

Narasimhan, J., et al. (2004). "Dimerization is required for activation of eIF2 kinase Gcn2 in response to diverse environmental stress conditions." Journal of Biological Chemistry **279**(22): 22820-22832.

Nicholls, R. E., et al. (2008). "Transgenic mice lacking NMDAR-dependent LTD exhibit deficits in behavioral flexibility." Neuron **58**(1): 104-117.

Niere, F., et al. (2012). "Evidence for a fragile X mental retardation protein-mediated translational switch in metabotropic glutamate receptor-triggered Arc translation and long-term depression." Journal of Neuroscience **32**(17): 5924-5936.

Novoa, I., et al. (2001). "Feedback inhibition of the unfolded protein response by GADD34-mediated dephosphorylation of eIF2α." The Journal of cell biology **153**(5): 1011-1022.

Ofner, M., et al. (2018). Autism spectrum disorder among children and youth in Canada 2018, Public Health Agency of Canada Ottawa, ON.

Olmos-Serrano, J. L., et al. (2010). "Defective GABAergic neurotransmission and pharmacological rescue of neuronal hyperexcitability in the amygdala in a mouse model of fragile X syndrome." Journal of Neuroscience **30**(29): 9929-9938.

Osterweil, E. K., et al. (2010). "Hypersensitivity to mGluR5 and ERK1/2 leads to excessive protein synthesis in the hippocampus of a mouse model of fragile X syndrome." Journal of Neuroscience **30**(46): 15616-15627.

Pakos-Zebrucka, K., et al. (2016). "The integrated stress response." EMBO reports **17**(10): 1374-1395.

Palmen, S. J., et al. (2004). "Neuropathological findings in autism." Brain **127**(12): 2572-2583.

Palmer, M., et al. (1997). "The group I mGlu receptor agonist DHPG induces a novel form of LTD in the CA1 region of the hippocampus." Neuropharmacology **36**(11-12): 1517-1532.

Paulsen, B., et al. (2022). "Autism genes converge on asynchronous development of shared neuron classes." Nature **602**(7896): 268-273.

Pelletier, J. and N. Sonenberg (1988). "Internal initiation of translation of eukaryotic mRNA directed by a sequence derived from poliovirus RNA." Nature **334**(6180): 320-325.

Penzes, P., et al. (2011). "Dendritic spine pathology in neuropsychiatric disorders." Nature neuroscience **14**(3): 285-293.

Phan, A. T., et al. (2011). "Structure-function studies of FMRP RGG peptide recognition of an RNA duplex-quadruplex junction." Nature structural & molecular biology **18**(7): 796-804.

Pinar, C., et al. (2017). "Revisiting the flip side: long-term depression of synaptic efficacy in the hippocampus." Neuroscience & Biobehavioral Reviews **80**: 394-413.

Placzek, A. N., et al. (2016). "eIF2α-mediated translational control regulates the persistence of cocaine-induced LTP in midbrain dopamine neurons." Elife **5**: e17517.

Pop, A. S., et al. (2014). "Rescue of dendritic spine phenotype in Fmr1 KO mice with the mGluR5 antagonist AFQ056/Mavoglurant." Psychopharmacology **231**(6): 1227-1235.

Poultney, C. S., et al. (2013). "Identification of small exonic CNV from whole-exome sequence data and application to autism spectrum disorder." The American Journal of Human Genetics **93**(4): 607-619.

Qin, M., et al. (2005). "Postadolescent changes in regional cerebral protein synthesis: an in vivo study in the FMR1 null mouse." Journal of Neuroscience **25**(20): 5087-5095.

Qin, M., et al. (2013). "Altered cerebral protein synthesis in fragile X syndrome: studies in human subjects and knockout mice." Journal of Cerebral Blood Flow & Metabolism **33**(4): 499-507.

Reith, R. M., et al. (2013). "Loss of Tsc2 in Purkinje cells is associated with autistic-like behavior in a mouse model of tuberous sclerosis complex." Neurobiology of disease **51**: 93-103.

Richter, J. D. and X. Zhao (2021). "The molecular biology of FMRP: new insights into fragile X syndrome." Nature reviews neuroscience 22(4): 209-222.

Richter, J. D. and N. Sonenberg (2005). "Regulation of cap-dependent translation by eIF4E inhibitory proteins." Nature **433**(7025): 477-480.

Riva, D. and C. Giorgi (2000). "The cerebellum contributes to higher functions during development: evidence from a series of children surgically treated for posterior fossa tumours." Brain **123**(5): 1051-1061.

Ronesi, J. A., et al. (2012). "Disrupted Homer scaffolds mediate abnormal mGluR5 function in a mouse model of fragile X syndrome." Nature neuroscience **15**(3): 431-440.

Ronesi, J. A. and K. M. Huber (2008). "Homer interactions are necessary for metabotropic glutamate receptor-induced long-term depression and translational activation." Journal of Neuroscience **28**(2): 543-547.

Ruzzo, E. K., et al. (2019). "Inherited and de novo genetic risk for autism impacts shared networks." Cell **178**(4): 850-866. e826.

Sabanov, V., et al. (2017). "Impaired GABAergic inhibition in the hippocampus of Fmr1 knockout mice." Neuropharmacology **116**: 71-81.

Santini, E., et al. (2013). "Exaggerated translation causes synaptic and behavioural aberrations associated with autism." Nature **493**(7432): 411-415.

Sato, A. (2016). "mTOR, a potential target to treat autism spectrum disorder." CNS & Neurological Disorders-Drug Targets (Formerly Current Drug Targets-CNS & Neurological Disorders) **15**(5): 533-543.

Satoh, Y., et al. (2011). "ERK2 contributes to the control of social behaviors in mice." Journal of Neuroscience **31**(33): 11953-11967.

Sawicka, K., et al. (2019). "FMRP has a cell-type-specific role in CA1 pyramidal neurons to regulate autism-related transcripts and circadian memory." Elife **8**: e46919.

Sawicka, K., et al. (2016). "Elevated ERK/p90 ribosomal S6 kinase activity underlies audiogenic seizure susceptibility in fragile X mice." Proceedings of the National Academy of Sciences **113**(41): E6290-E6297.

Saxton, R. A. and D. M. Sabatini (2017). "mTOR signaling in growth, metabolism, and disease." Cell **168**(6): 960-976.

Schaefer, G. B. and N. J. Mendelsohn (2008). "Genetics evaluation for the etiologic diagnosis of autism spectrum disorders." Genetics in Medicine **10**(1): 4-12.

Schmahmann, J. D. and D. N. Pandya (1995). "Prefrontal cortex projections to the basilar pons in rhesus monkey: implications for the cerebellar contribution to higher function." Neuroscience letters **199**(3): 175-178.

Schröder, M. and R. J. Kaufman (2005). "The mammalian unfolded protein response." Annu. Rev. Biochem. **74**: 739-789.

Schumann, C. M., et al. (2004). "The amygdala is enlarged in children but not adolescents with autism; the hippocampus is enlarged at all ages." Journal of Neuroscience **24**(28): 6392-6401.

Shah, S., et al. (2020). "FMRP control of ribosome translocation promotes chromatin modifications and alternative splicing of neuronal genes linked to autism." Cell reports **30**(13): 4459-4472. e4456.

Shahbazian, D., et al. (2010). "eIF4B controls survival and proliferation and is regulated by proto-oncogenic signaling pathways." Cell cycle **9**(20): 4106-4109.

Shahbazian, D., et al. (2006). "The mTOR/PI3K and MAPK pathways converge on eIF4B to control its phosphorylation and activity." The EMBO journal **25**(12): 2781-2791.

Sharma, A., et al. (2010). "Dysregulation of mTOR signaling in fragile X syndrome." Journal of Neuroscience **30**(2): 694-702.

Sharma, V., et al. (2020). "eIF2α controls memory consolidation via excitatory and somatostatin neurons." Nature **586**(7829): 412-416.

Siomi, H., et al. (1993). "The protein product of the fragile X gene, FMR1, has characteristics of an RNA-binding protein." Cell **74**(2): 291-298.

Smalley, S. L. (1998). "Autism and tuberous sclerosis." Journal of autism and developmental disorders **28**(5): 407-414.

Snider, R. S. and A. Maiti (1976). "Cerebellar contributions to the Papez circuit." Journal of neuroscience research **2**(2): 133-146.

Sonenberg, N. and A.-C. Gingras (1998). "The mRNA 5′ cap-binding protein eIF4E and control of cell growth." Current opinion in cell biology **10**(2): 268-275.

Sood, R., et al. (2000). "A mammalian homologue of GCN2 protein kinase important for translational control by phosphorylation of eukaryotic initiation factor-2α." Genetics **154**(2): 787-801.

Spencer, C. M., et al. (2011). "Modifying behavioral phenotypes in Fmr1KO mice: Genetic background differences reveal autistic-like responses." Autism research **4**(1): 40-56.

Sragovich, S., et al. (2017). "ADNP plays a key role in autophagy: from autism to schizophrenia and Alzheimer's disease." Bioessays **39**(11): 1700054.

Stefani, G., et al. (2004). "Fragile X mental retardation protein is associated with translating polyribosomes in neuronal cells." Journal of Neuroscience **24**(33): 7272-7276.

Takarae, Y. and J. Sweeney (2017). "Neural hyperexcitability in autism spectrum disorders." Brain sciences **7**(10): 129.

Taniuchi, S., et al. (2016). "Integrated stress response of vertebrates is regulated by four eIF2α kinases." Scientific reports **6**(1): 1-11.

Taylor, P. and J. Brameld (1999). "Mechanisms and regulation of transcription and translation." PUBLICATION-EUROPEAN ASSOCIATION FOR ANIMAL PRODUCTION **96**: 25-50.

Teske, B. F., et al. (2013). "CHOP induces activating transcription factor 5 (ATF5) to trigger apoptosis in response to perturbations in protein homeostasis." Molecular biology of the cell **24**(15): 2477-2490.

Thomson, S. R., et al. (2017). "Cell-type-specific translation profiling reveals a novel strategy for treating fragile X syndrome." Neuron **95**(3): 550-563. e555.

Todd, P. K., et al. (2003). "The fragile X mental retardation protein is required for type-I metabotropic glutamate receptor-dependent translation of PSD-95." Proceedings of the National Academy of Sciences **100**(24): 14374-14378.

Toft, A. K. H. (2019). "Impact of two autism related genes on amygdala physiology."

Toro, R., et al. (2010). "Key role for gene dosage and synaptic homeostasis in autism spectrum disorders." Trends in genetics **26**(8): 363-372.

Trinh, M. A., et al. (2014). "The eIF2α kinase PERK limits the expression of hippocampal metabotropic glutamate receptor-dependent long-term depression." Learning & memory **21**(5): 298-304.

Tsai, P. T., et al. (2012). "Autistic-like behaviour and cerebellar dysfunction in Purkinje cell Tsc1 mutant mice." Nature **488**(7413): 647-651.

Tsaytler, P., et al. (2011). "Selective inhibition of a regulatory subunit of protein phosphatase 1 restores proteostasis." Science **332**(6025): 91-94.

Udagawa, T., et al. (2013). "Genetic and acute CPEB1 depletion ameliorate fragile X pathophysiology." Nature medicine **19**(11): 1473-1477.

Utami, K. H., et al. (2020). "Elevated de novo protein synthesis in FMRP-deficient human neurons and its correction by metformin treatment." Molecular autism **11**(1): 1-11.

Vagnarelli, P. and D. R. Alessi (2018). "PP1 phosphatase complexes: undruggable no longer." Cell **174**(5): 1049-1051.

Valentinova, K. and M. Mameli (2016). "mGluR-LTD at excitatory and inhibitory synapses in the lateral habenula tunes neuronal output." Cell reports **16**(9): 2298-2307.

Veeraragavan, S., et al. (2012). "Genetic reduction of muscarinic M4 receptor modulates analgesic response and acoustic startle response in a mouse model of fragile X syndrome (FXS)." Behavioural brain research **228**(1): 1-8.

Volkmar, F. R. and B. Reichow (2013). "Autism in DSM-5: progress and challenges." Molecular autism **4**(1): 1-6.

Wang, S. S.-H., et al. (2014). "The cerebellum, sensitive periods, and autism." Neuron **83**(3): 518-532.

Wang, X., et al. (1998). "The phosphorylation of eukaryotic initiation factor eIF4E in response to phorbol esters, cell stresses, and cytokines is mediated by distinct MAP kinase pathways." Journal of Biological Chemistry **273**(16): 9373-9377.

Wang, X., et al. (2001). "Regulation of elongation factor 2 kinase by p90RSK1 and p70 S6 kinase." The EMBO journal **20**(16): 4370-4379.

Waung, M. W. and K. M. Huber (2009). "Protein translation in synaptic plasticity: mGluR-LTD, Fragile X." Current opinion in neurobiology **19**(3): 319-326.

Weiler, I. J., et al. (1997). "Fragile X mental retardation protein is translated near synapses in response to neurotransmitter activation." Proceedings of the National Academy of Sciences **94**(10): 5395-5400.

Whitney, E. R., et al. (2008). "Cerebellar Purkinje cells are reduced in a subpopulation of autistic brains: a stereological experiment using calbindin-D28k." The Cerebellum **7**(3): 406-416.

Winden, K. D., et al. (2018). "Abnormal mTOR activation in autism." Annual review of neuroscience **41**: 1-23.

Wu, C. C.-C., et al. (2020). "Ribosome collisions trigger general stress responses to regulate cell fate." Cell **182**(2): 404-416. e414.

Xu, Z.-X., et al. (2020). "Elevated protein synthesis in microglia causes autism-like synaptic and behavioral aberrations." Nature communications **11**(1): 1-17.

Yan, L. L. and H. S. Zaher (2021). "Ribosome quality control antagonizes the activation of the integrated stress response on colliding ribosomes." Molecular cell **81**(3): 614-628. e614.

Young, S. K. and R. C. Wek (2016). "Upstream open reading frames differentially regulate gene-specific translation in the integrated stress response." Journal of Biological Chemistry **291**(33): 16927-16935.

Zafeiriou, D. I., et al. (2007). "Childhood autism and associated comorbidities." Brain and Development **29**(5): 257-272.

Zalfa, F. and C. Bagni (2004). "Molecular insights into mental retardation: multiple functions for the Fragile X mental retardation protein?" Current issues in molecular biology **6**(2): 73-88.

Zhang, F., et al. (2018). "Fragile X mental retardation protein modulates the stability of its m6A-marked messenger RNA targets." Human molecular genetics **27**(22): 3936-3950.

Zhang, Y., et al. (2014). "Dendritic channelopathies contribute to neocortical and sensory hyperexcitability in Fmr1−/y mice." Nature neuroscience **17**(12): 1701-1709.

Zhou, J. and L. F. Parada (2012). "PTEN signaling in autism spectrum disorders." Current opinion in neurobiology **22**(5): 873-879.

Zhu, P. J., et al. (2011). "Suppression of PKR promotes network excitability and enhanced cognition by interferon-γ-mediated disinhibition." Cell **147**(6): 1384-1396.

Zhu, P. J., et al. (2019). "Activation of the ISR mediates the behavioral and neurophysiological abnormalities in Down syndrome." Science **366**(6467): 843-849.

Chapter 2: The integrated stress response pathway in excitatory neurons controls autistic features

Mehdi Hooshmandi[1], Vijendra Sharma[2], Carolina Thörn Perez[1], Rapita Sood[2], Konstanze Simbriger[3], Calvin Wong[1], Emma Nadler[1], Patricia Margarita Roque[1], Ilse Gantois[2], Jelena Popic[2], Maxime Lévesque[4], Randal J. Kaufman[5], Massimo Avoli[4], Elisenda Sanz[6], Karim Nader[7], Mauro Costa-Mattioli[8], Jean-Claude Lacaille[9], Nahum Sonenberg[2,*], Christos G. Gkogkas[10,*], and Arkady Khoutorsky[1,11,*].

The manuscript is under review in ***Neuron*.** We plan to resubmit it in November 2022.

2.1 Abstract

Dysregulation of protein synthesis is one of the key mechanisms underlying autism spectrum disorders (ASDs). However, the role of a major pathway controlling protein synthesis, the integrated stress response (ISR), in ASDs remains poorly understood. Here, we demonstrate that the main arm of the ISR, eIF2α phosphorylation (p-eIF2α), is significantly suppressed in excitatory but not inhibitory neurons in a mouse model of fragile X syndrome (FXS; *Fmr1*$^{-/y}$). We further show that the decrease in p-eIF2α is mediated via activation of the mTORC1. Genetic reduction of p-eIF2α only in excitatory neurons is sufficient to increase general protein synthesis and cause autism-like phenotypes. In *Fmr1*$^{-/y}$ mice, genetic restoration of p-eIF2α only in excitatory neurons reverses elevated protein synthesis and rescues autistic features. Thus, we reveal a previously unknown causal relationship between excitatory neuron-specific translational control via the ISR pathway, general protein synthesis and core autism-like phenotypes in a mouse model of FXS.

Keywords: mRNA translation, integrated stress response, autism, fragile X syndrome.

2.2 Introduction

Dysregulation of protein synthesis is thought to underlie autism-related phenotypes in fragile X syndrome (FXS) (Hagerman et al., 2017) and several other neurodevelopmental disorders (Bagni and Zukin, 2019; Barnes et al., 2015; Hornberg et al., 2020; Kelleher and Bear, 2008; Torossian et al., 2021). Increased general protein synthesis in FXS, which has been reported in humans (Jacquemont et al., 2018; Utami et al., 2020) and animal models (Auerbach et al., 2011; Qin et al., 2005), is believed to critically contribute to FXS pathophysiology. However, the mechanism driving the robust stimulation of global protein synthesis in FXS is not well understood. On the other hand, several studies have investigated cell-type-specific changes in mRNA translation (Ceolin et al., 2017; Sawicka et al., 2019; Thomson et al., 2017), yet

strikingly it is unclear whether elevated global protein synthesis in FXS is observed in all brain cell types. This is highly relevant for autism spectrum disorders, as recently single-cell genomics of patient cortex revealed that excitatory neurons are amongst the main cell types preferentially affected in autism (Velmeshev et al., 2019). Previous studies have largely focused on the upregulation of the mechanistic/mammalian target of rapamycin complex 1 (mTORC1) pathway as the main driver of elevated protein synthesis and distinct behavioural deficits in animal models of FXS (Bhattacharya et al., 2012; Hoeffer et al., 2012; Rosina et al., 2019; Sharma et al., 2010). However, the role of a major signaling pathway controlling general protein synthesis, the integrated stress response (ISR) (Costa-Mattioli and Walter, 2020; Trinh and Klann, 2013), in mediating autistic features in *Fmr1*$^{-/y}$ mice, a commonly used FXS model, is unknown. The ISR is a highly conserved cellular mechanism that suppresses general protein synthesis during stress via phosphorylation of the α-subunit of eukaryotic translation initiation factor 2 (p-eIF2α) (Costa-Mattioli and Walter, 2020; Harding et al., 2000; Walter and Ron, 2011). Conversely, a decrease in p-eIF2α stimulates general protein synthesis. Here, we showed that the ISR is suppressed in the brain of *Fmr1*$^{-/y}$ mice. Unexpectedly, we reveal that the p-eIF2α is reduced only in excitatory but not inhibitory neurons. The decrease in p-eIF2α in *Fmr1*$^{-/y}$ mice is mediated via excitatory neuron-specific upregulation of the mTORC1 activity and is accompanied by an elevation of general protein synthesis selectively in excitatory neurons. Using mouse genetics, we show that low levels of p-eIF2α in excitatory neurons, but not all cell types, are sufficient to cause core autism-like phenotypes. In *Fmr1*$^{-/y}$, low p-eIF2α in excitatory neurons strongly contributes to molecular and behavioural deficits as normalization of p-eIF2α rescued elevated protein synthesis, exaggerated long-term depression (LTD) and impairment in social behaviour, and alleviated seizures. Thus, suppression of the ISR in excitatory neurons plays a major role in mediating core-autism like phenotypes in a mouse model of FXS.

2.3 Results

2.3.1 p-eIF2α is decreased in *Fmr1*$^{-/y}$ excitatory neurons

To assess the activity of the ISR pathway in *Fmr1*$^{-/y}$ mice, we measured p-eIF2α levels in tissue lysates from the cortex, hippocampus, and amygdala, which are brain areas implicated in autism spectrum disorders (ASD) (Endo et al., 2007; Weston, 2019). We found a significant decrease in p-eIF2α in *Fmr1*$^{-/y}$ mice in all three brain areas (percent decrease in p-eIF2α; hippocampus, 45%, Figures 1A and B; cortex, 52%, Figures 1C and D; amygdala, 23%, Figures 1E and F). Quantitative immunohistochemical (IHC) analysis showed that p-eIF2α is decreased in *Fmr1*$^{-/y}$ mice in excitatory neurons (labeled with Ca^{2+}-calmodulin-dependent protein kinase 2 (CAMK2α)) (hippocampus, Figures 1G and H; cortex, Figures 1I and J; amygdala, Figures S1A and B) but not inhibitory neurons (labeled with glutamic-acid decarboxylase 67 (GAD67)) (hippocampus, Figures 1K and L; cortex, Figures 1M and N; amygdala, Figures S1C and D). No difference was found in total eIF2α protein levels (Figures S1E-J). Phosphorylation of eIF2α decreases the availability of the translation preinitiation complex and inhibits translation initiation (Costa-Mattioli and Walter, 2020). Conversely, the reduction of p-eIF2α stimulates general translation. To study whether the decrease in p-eIF2α in excitatory neurons is accompanied by an increase in translation, we assessed general protein synthesis using azidohomoalanine (AHA)-based metabolic labeling (FUNCAT) (Dieterich et al., 2010) (Figure 1O). Mice were injected with AHA intraperitoneally, and AHA incorporation into nascent polypeptides in the brain was assessed 3 hrs later (Figure 1P). The validity of this approach was confirmed by showing that the protein synthesis inhibitor anisomycin blocks AHA incorporation (Figure S1K). Consistent with the decrease in p-eIF2α, general protein synthesis was increased in excitatory neurons (percent increase in AHA incorporation; hippocampus, 63.77%, Figures 1Q and R; cortex, 65.25%, Figures 1S and T; amygdala, 52.07%, Figures S1L and M) but not inhibitory neurons in the hippocampus, cortex, and amygdala (Figures 1U and

V, Figures 1W and X, and Figures S1N and O, respectively) in *Fmr1*$^{-/y}$ mice compared with wild-type animals.

Dephosphorylation of eIF2α causes an increase in general protein synthesis but paradoxically represses translation of distinct mRNAs, many of which are involved in the cellular stress response and harbor upstream open reading frame (uORF) in their 5′ untranslated region (5′ UTR) (Hinnebusch et al., 2016). Given the low level of p-eIF2α in excitatory neurons of *Fmr1*$^{-/y}$ mice, we hypothesized that translation of mRNAs containing 5′ UTR uORFs should be reduced in this cell type. Previous studies have examined the translational landscape in excitatory neurons of *Fmr1*$^{-/y}$ mice using excitatory neuron-specific translating ribosome affinity purification (TRAP) (Heiman et al., 2008). Analysis of the published datasets (Ceolin *et al.*, 2017; Sawicka *et al.*, 2019) revealed that mRNAs with uORFs were substantially enriched in the subset of genes downregulated in excitatory neurons of *Fmr1*$^{-/y}$ mice compared with control animals (Figure S1P-S, $p < 0.0001$, Fisher's exact test). Thus, consistent with the reduction of p-eIF2α in excitatory neurons of *Fmr1*$^{-/y}$ mice, general protein synthesis is increased and translation of mRNAs containing uORFs is decreased in excitatory neurons.

2.3.2 Hyperactivated mtorc1 downregulates p-eIF2α

We next investigated the mechanism underlying the reduction of p-eIF2α in *Fmr1*$^{-/y}$ mice. In the brain, the α subunit of eIF2 can be phosphorylated by stress-activated kinases GCN2, PERK, and PKR, and dephosphorylated by GADD34 and CReP phosphatases (Alvarez-Castelao et al., 2020; Costa-Mattioli and Walter, 2020; Trinh and Klann, 2013). Western blot analysis of lysates from hippocampus and cortex of *Fmr1*$^{-/y}$ mice showed an increase in GCN2 phosphorylation (Thr899, suggesting its activation (Liu et al., 2018), hippocampus, 54.2%, cortex, 61.3%, Figures S2A, B, G, and H), and no change in the phosphorylation status or expression level of PERK, and PKR (Figures S2C-F, 2I-L). The expression levels of GADD34

and CReP were also not altered in *Fmr1*$^{-/y}$ brain (Figure S2M-P). These results indicate that the activities of eIF2α kinases and phosphatases cannot explain the reduction in eIF2α phosphorylation in the brain of *Fmr1*$^{-/y}$ mice and thus suggest the involvement of another mechanism.

Previous work has established that the mTORC1 is activated in the brain of *Fmr1*$^{-/y}$ mice (Bhattacharya *et al.*, 2012; Hoeffer *et al.*, 2012; Sharma *et al.*, 2010). Furthermore, a study performed in non-neuronal cultures suggested that hyperactivation of mTORC1 can lead to eIF2α dephosphorylation (Gandin et al., 2016), although the precise molecular mechanism underlying this effect remains unknown. To investigate whether an increase in mTORC1 activity in the brain causes a decrease in p-eIF2α, we administered wild-type mice with a specific brain-penetrant mTORC1 activator, NV-5138 (Sengupta et al., 2019). As expected, NV-5138 increased the phosphorylation of the mTORC1 downstream effector S6 (p-S6) in hippocampal and cortical lysates 2 hours post-administration (Figures 2A-D), indicating mTORC1 activation. Notably, NV-5138 also significantly decreased p-eIF2α in the hippocampus (Figures 2A and B), and cortex (Figurges 2C and D), revealing a crosstalk between the mTORC1 and the ISR in the brain. To test if hyperactivation of mTORC1 is required for the decrease in p-eIF2α in *Fmr1*$^{-/y}$ mice, we suppressed mTORC1 in *Fmr1*$^{-/y}$ animals by systemic administration of the mTORC1 inhibitor, CCI-779 (7.5 mg/kg, i.p., daily over 3 days), which was previously shown to cross the blood-brain barrier (Kwon et al., 2003; Zhao et al., 2012). Inhibition of the enhanced mTORC1 activity in *Fmr1*$^{-/y}$ mice corrected reduced p-eIF2α in the brain of these animals (Figures 2E and F). Intriguingly, quantitative IHC analysis revealed that p-S6 in *Fmr1*$^{-/y}$ mice is elevated exclusively in excitatory but not inhibitory neurons in the hippocampus, cortex, and amygdala (excitatory neurons, Figures S3A-F; inhibitory neurons, Figures S3G-L). Altogether, these results suggest that in *Fmr1*$^{-/y}$

mice, a selective increase in mTORC1 activity in excitatory neurons leads to a decrease in p-eIF2α in this cell type.

2.3.3 Decreased p-eIF2α in excitatory neurons causes ASD traits

Elevated general protein synthesis has previously been associated with ASD (Gkogkas et al., 2013; Santini et al., 2013; Xu et al., 2020). To study whether the decrease in p-eIF2α, which causes an increase in general protein synthesis, is sufficient to engender autistic features, we generated conditional knock-in (cKI) mice with reduced eIF2α phosphorylation (~50% reduction) selectively in excitatory neurons, to mimic reduced p-eIF2α in *Fmr1*$^{-/y}$ mice. To this end, we crossed a transgenic mouse harboring one non-phosphorylatable Ser51Ala mutant *Eif2α* allele (*Eif2α*$^{S/A}$) and the wild-type (WT) *Eif2α* transgene flanked by two *lox*-P sites (Back et al., 2009) with a mouse expressing Cre recombinase under the excitatory neuron-specific *Camk2α* promoter (referred to as *Eif2α*$^{S/A}$ cKI^{Camk2α}, Figure S4A). Cre recombinase in *Eif2α*$^{S/A}$ cKI^{Camk2α} mouse leads to the excision of the WT transgene in excitatory neurons and induces eGFP expression. As expected, *Eif2α*$^{S/A}$ cKI^{Camk2α} animals showed a reduction in p-eIF2α and an upregulation of protein synthesis (AHA-incorporation) in excitatory (Figures 3A, B, and Figures 3C, D, respectively) but not inhibitory (Figures S4B-E) neurons. Behavioral analysis showed that *Eif2α*$^{S/A}$ cKI^{Camk2α} mice exhibit impaired social interaction in the novelty phase of the three-chamber social interaction test (Figures 3E-H) and reduced direct social interaction in the reciprocal social interaction test (Figures 3I, J). Moreover, *Eif2α*$^{S/A}$ cKI^{Camk2α} mice exhibited increased self-grooming (Figures 3K and L) and repetitive marble burying behaviors (Figures 3M and N). No anxiety phenotype was found in the elevated plus maze (EPM, Figures S4F-H), and no olfactory discrimination deficits were detected (Figures S4I and J) in these mice. We also generated mice with complete ablation of p-eIF2α in excitatory neurons (*Eif2α*$^{A/A}$ cKI^{Camk2α}) (Figure S5A). Like mice with partial elimination of p-eIF2α, *Eif2α*$^{A/A}$

cKI$^{Camk2\alpha}$ mice showed deficits in social interaction in three-chamber (Figures S5B and C) and direct social interaction (Figure S5D) tests and exhibited increased grooming (Figure S5E). No difference in marble-burying behaviors (Figures S5F) and anxiety (EPM, Figures S5G-I) was observed. These findings demonstrate that the selective reduction of p-eIF2α in excitatory neurons is sufficient to engender altered social and repetitive/stereotypic behaviors, which are reminiscent of autism.

Next, we tested mice with whole-body reduction of p-eIF2α (~50% reduction, *Eif2α*$^{S/A}$ KI, Figure 4A) (Scheuner et al., 2001). Surprisingly, *Eif2α*$^{S/A}$ KI animals showed no autistic-like traits as no change was found in social interaction (three-chamber social interaction, Figures 4B and C; direct social interaction, Figure 4D), grooming (Figure 4E), marble burying (Figure 4F), and anxiety (EPM, Figures 4G-I). Altogether, these results demonstrate that the activity of the ISR is reduced selectively in excitatory neurons in different brain areas of *Fmr1*$^{-/y}$ mice and this reduction is accompanied by an increase in general protein synthesis. Importantly, lowering p-eIF2α in excitatory neurons but not all cell types, engenders ASD-like behaviors.

2.3.4 Rescue of *Fmr1*$^{-/y}$ features by increasing p-eIF2α

To study whether normalization of the reduced p-eIF2α selectively in excitatory neurons in *Fmr1*$^{-/y}$ mice could rescue increased protein synthesis and ASD-like features, we developed a genetic strategy to upregulate p-eIF2α only in excitatory neurons of *Fmr1*$^{-/y}$ mice. To increase p-eIF2α, we knocked down a constitutive eIF2α phosphatase, CReP (encoded by the Protein Phosphatase 1 Regulatory Subunit 15B, *Ppp1r15b***)**, in excitatory neurons using intracerebroventricular (i.c.v.) administration of adeno-associated virus (AAV) expressing microRNA-adapted short hairpin RNA (shRNAmir) against *Ppp1r15b* under the excitatory neuron-specific *Camk2α* promoter (AAV9-Camk2α-GFP-*Ppp1r15b*-shRNAmir, Figures 5A

and B, and Figure S5J). We used a viral titer that elevated p-eIF2α in excitatory neurons of *Fmr1*$^{-/y}$ mice to the WT level (Figures 5C and D). Notably, normalization of p-eIF2α in excitatory neurons of *Fmr1*$^{-/y}$ mice corrected elevated protein synthesis (cortex, Figures 5E and F, hippocampus, Figures 5G and H).

We next studied whether correction of p-eIF2α in excitatory neurons rescues core deficits in *Fmr1*$^{-/y}$ mice. We first examined the effect of normalizing p-eIF2α in excitatory neurons on the exaggerated group 1 metabotropic glutamate receptor (mGluR)-dependent long-term depression (LTD), a key feature of *Fmr1*$^{-/y}$ mice (Huber et al., 2002). Whereas *Fmr1*$^{-/y}$ mice injected with the control virus (expressing scrambled sequence) exhibited enhanced LTD in response to DHPG administration, *Fmr1*$^{-/y}$ mice injected with AAV-CReP-shRNAmir exhibited intact mGluR-LTD (Figures 6A-D), demonstrating correction of this phenotype.

We next investigated whether correction of p-eIF2α rescues altered social and repetitive/stereotypic behaviors in *Fmr1*$^{-/y}$ mice. Remarkably, normalization of p-eIF2α in excitatory neurons of *Fmr1*$^{-/y}$ mice rescued social deficits in the three-chamber social interaction test (Figures 6E and F), and reversed the increased marble burying (Figure 6G) and grooming (Figure 6H) behavior. Moreover, the audiogenic seizure phenotype of *Fmr1*$^{-/y}$ mice was substantially alleviated upon correction of p-eIF2α (Figures 6I-K). Altogether, the results demonstrate that normalization of reduced p-eIF2α in excitatory neurons of *Fmr1*$^{-/y}$ mice corrects impaired social interaction and repetitive behaviors and ameliorates the audiogenic seizure phenotype.

2.4 Discussion

Dysregulation of protein synthesis is a central pathophysiological mechanism in FXS and several other neurodevelopmental disorders (Hornberg *et al.*, 2020; Kelleher and Bear, 2008; Santini *et al.*, 2013). Our study is the first to show that decreased activity of the ISR, associated

with reduced p-eIF2α and elevated general protein synthesis, is sufficient to engender social interaction deficits and repetitive behaviors. Moreover, we demonstrate that this mechanism critically contributes to core ASD-like phenotypes in a mouse model of FXS. Correction of reduced p-eIF2α in excitatory neurons of *Fmr1*$^{-/y}$ mice not only normalized enhanced protein synthesis, but also rescued social interaction deficits, repetitive behavior, and audiogenic seizure phenotypes.

Our study shows that p-eIF2*α* is decreased and protein synthesis is increased in excitatory but not inhibitory neurons in an animal model of FXS. Selective ablation of p-eIF2*α* in excitatory neurons leads to their hyperactivation (Sharma et al., 2020). This might cause an imbalance between excitatory and inhibitory neuronal circuits resulting in abnormal neuronal functioning and social dysfunction (Yizhar et al., 2011). This notion is supported by the finding that reduction of p-eIF2*α* in excitatory neurons (*Eif2α*$^{S/A}$ cKI^{Camk2α}) but not all cell types (*Eif2α*$^{S/A}$ KI), engenders autistic features.

The ISR pathway is differentially modulated in distinct neuronal cell types to control physiological processes such as memory formation (Sharma *et al.*, 2020) and skill learning (Helseth et al., 2021). Our work reveals cell-type-specific alterations of the ISR in a neurodevelopmental disorder. Moreover, we show that reduced activity of the ISR in excitatory neurons is sufficient to cause ASD features. These findings highlight the need to assess translational control pathways and rates of protein synthesis in disease states in a cell-type-specific manner as their evaluation in total cell lysates might dilute the effect of cell-type-specific alterations and mask underlying mechanisms. These results also imply that cell-type-specific interventions, targeting cell populations in which the ISR is dysregulated, may offer more effective treatments compared with current approaches targeting all cell types.

Our work shows that the activities of the two main translational control mechanisms, mediated via the mTORC1 and the ISR, are coordinated in the brain. We found that the stimulation of

mTORC1 in the brain leads to a downregulation of p-eIF2α, and mTORC1 inhibition in *Fmr1*$^{-/y}$ mice normalizes p-eIF2α, suggesting that enhanced mTORC1 activity contributes to reduced ISR in FXS. Future studies should investigate the molecular mechanism by which mTORC1 activation downregulates p-eIF2α in both neuronal and non-neuronal cells. Intriguingly, mTORC1 activity is increased in excitatory but not inhibitory neurons where it causes a selective downregulation of p-eIF2α. The neuronal cell type-specific interplay between mTORC1 and ISR underscores the intricacy of translational control mechanisms in the brain, demonstrating how changes in one signaling pathway can contribute to phenotypes by altering the homeostasis of another signaling cascade.

Although ablation of *Fmr1* in excitatory neurons is sufficient to cause core FXS phenotypes such as audiogenic seizures (Gonzalez et al., 2019), indicating a central role for excitatory neurons in FXS, changes in inhibition in *Fmr1*$^{-/y}$ mice and their important roles in FXS pathophysiology are well documented (Curia et al., 2009; Hagerman *et al.*, 2017; Olmos-Serrano et al., 2010; Van der Aa and Kooy, 2020). These changes are likely mediated via eIF2α-independent mechanisms.

In summary, we uncovered the role of excitatory neuron-specific suppression of the ISR pathway in engendering core ASD-like phenotypes in *Fmr1*$^{-/y}$ mice.

2.5 Acknowledgments

This work was supported by a grant from the Simons Foundation (SFARI, award #611773), and the Canadian Institutes of Health Research (CIHR, PJT-162412) to A.K., and a Hellenic Foundation for Research and Innovation (HFRI, #2556) grant to C.G.G. J.C.L. is supported by the Canada Research Chair in Cellular and Molecular Neurophysiology (CRC 950-231066). M.H. was supported by the Brain Canada and Transforming Autism Care Consortium (TACC) graduate fellowships. We thank Gottfried Simbriger for helping with the uORF analysis.

2.6 Author contributions

M.H., N.S., C.G.G., and A.K. conceived the project, designed experiments, and supervised the research. M.H. performed immunohistochemistry and biochemistry analyses, behavioral experiments, and LTD recordings. C.T.P. and J.C.L. assisted with electrophysiological studies. M.L., M.A., E.S., I.G., C.W., P.M.R., E.N., I.G., and J.P. helped with data analysis. K.N. and M.C.M. assisted with behavioural experiments and data interpretation. R.J.K., V.S., P.M.R., and R.S. assisted with the generation of transgenic animals. K.S. assisted with the analysis of previous TRAP studies. All the authors contributed to writing the manuscript.

2.7 Declaration of interests

The authors declare no competing interests.

2.8 Figures

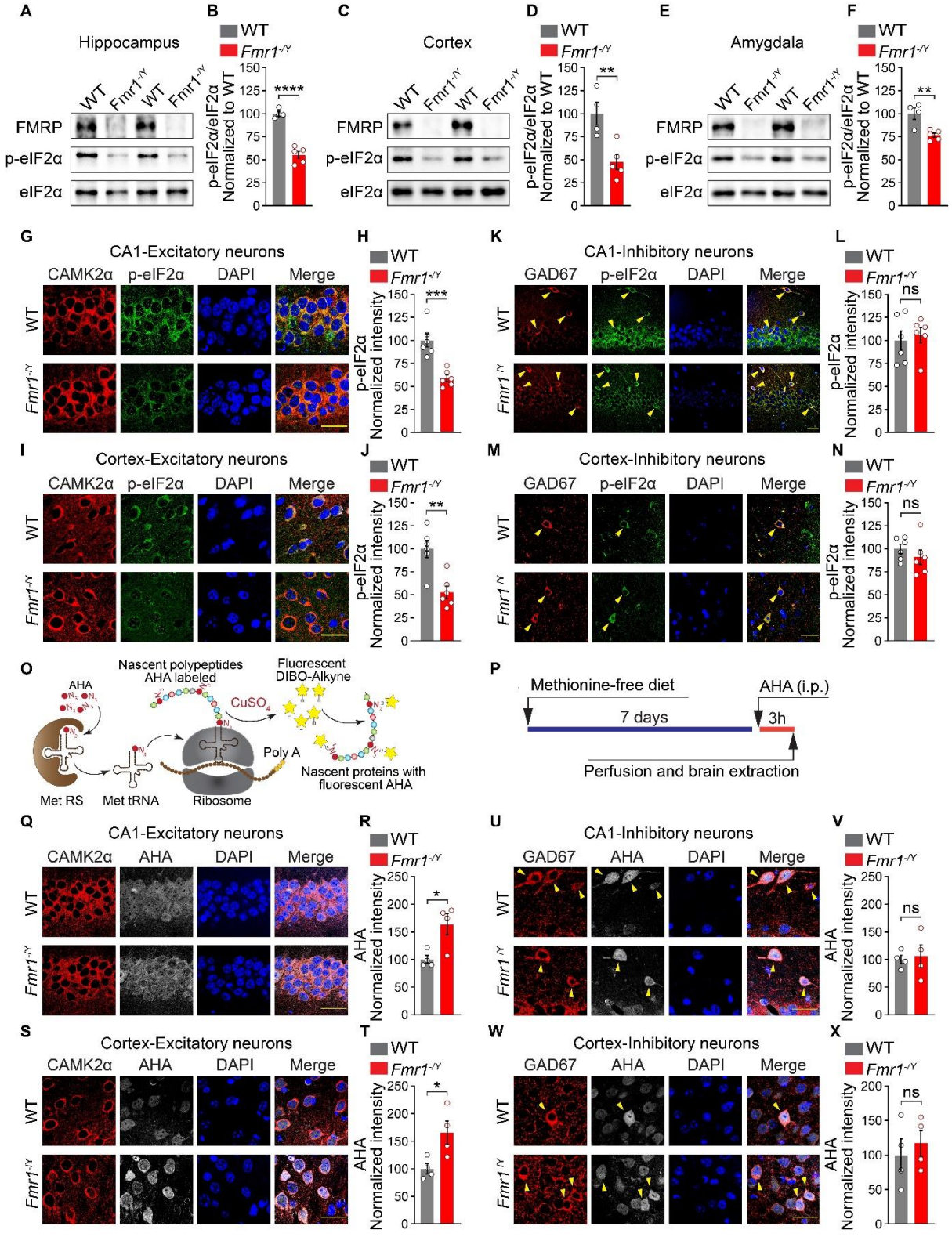
A
Hippocampus
WT
Fmr1-/Y
WT
Fmr1-/Y
FMRP
p-eIF2α
eIF2α
B
WT
Fmr1-/Y
p-eIF2α/eIF2α
Normalized to WT
****
C
Cortex
D
**
E
Amygdala
F
**
G
CA1-Excitatory neurons
CAMK2α
p-eIF2α
DAPI
Merge
H
***
K
CA1-Inhibitory neurons
GAD67
L
ns
I
Cortex-Excitatory neurons
J
**
M
Cortex-Inhibitory neurons
N
ns
O
AHA
Nascent polypeptides
AHA labeled
CuSO4
Fluorescent
DIBO-Alkyne
Poly A
Met RS
Met tRNA
Ribosome
Nascent proteins with
fluorescent AHA
P
Methionine-free diet
AHA (i.p.)
7 days
3h
Perfusion and brain extraction
Q
CA1-Excitatory neurons
AHA
R
*
U
CA1-Inhibitory neurons
V
ns
S
Cortex-Excitatory neurons
T
*
W
Cortex-Inhibitory neurons
X
ns

2.8.1 Figure 1. *Fmr1*$^{-/y}$ mice show a reduction in p-eIF2α and an increase in global protein synthesis in excitatory but not inhibitory neurons.

(A-F) Representative immunoblotting (left) and quantification (right) shows reduced p-eIF2α in *Fmr1*$^{-/y}$ mice (n = 5) as compared to WT mice (n = 4) in hippocampus (A, B**,** WT versus *Fmr1*$^{-/y}$, $t = 8.818$, $p < 0.0001$), cortex (C, D**,** WT versus *Fmr1*$^{-/y}$, $t = 3.681$, $p = 0.0078$), and amygdala (E, F**,** WT versus *Fmr1*$^{-/y}$, $t = 3.790$, $p = 0.0068$). (G-N) Immunofluorescent labelling against p-eIF2α (green) in excitatory (CAMK2α-positive, red) and inhibitory (GAD67-positive, red) neurons reveals reduced p-eIF2α in *Fmr1*$^{-/y}$ (n = 6) as compared to WT animals (n = 6) in excitatory neurons in CA1 (G, H**,** WT versus *Fmr1*$^{-/y}$, $t = 5.119$, $p < 0.0005$) and prefrontal cortex (I, J**,** WT versus *Fmr1*$^{-/y}$, $t = 4.084$, $p < 0.0022$), but not inhibitory neurons in CA1 (K, L**,** WT versus *Fmr1*$^{-/y}$, $t = 0.444$, $p > 0.05$) or prefrontal cortex (M, N**,** WT versus *Fmr1*$^{-/y}$, $t = 0.967$, $p > 0.05$). (O) Schematic illustration of the fluorescence non-canonical amino acid tagging (FUNCAT) and (P) experimental design. AHA incorporation (grey), indicating the level of the nascent protein synthesis, is significantly higher in excitatory (CAMK2α-positive, red) neurons in CA1 (Q, R**,** WT versus *Fmr1*$^{-/y}$, $t = 3.083$, $p = 0.0216$) and cortex (S, T, WT versus *Fmr1*$^{-/y}$, $t = 2.78$, $p = 0.032$) of *Fmr1*$^{-/y}$ (n = 4) as compared to WT (n = 4) mice. No significant differences were found in AHA incorporation in inhibitory (GAD67-positive, red) neurons in CA1 (U, V, WT versus *Fmr1*$^{-/y}$, $t(6) = 0.283$, $p > 0.05$) and cortex (W, X, WT versus *Fmr1*$^{-/y}$, $t = 0.567$, $p > 0.05$) of *Fmr1*$^{-/y}$ (n = 4) as compared to WT (n = 4) mice. Each data point represents an individual animal. All data are presented as mean ± s.e.m. *$p <$ 0.05, **$p < 0.01$, ***$p < 0.001$, ****$p < 0.0001$, and ns, not significant. Student's t-test was performed for all the experiments. Scale bars, 25 μm. See also Figure S1.

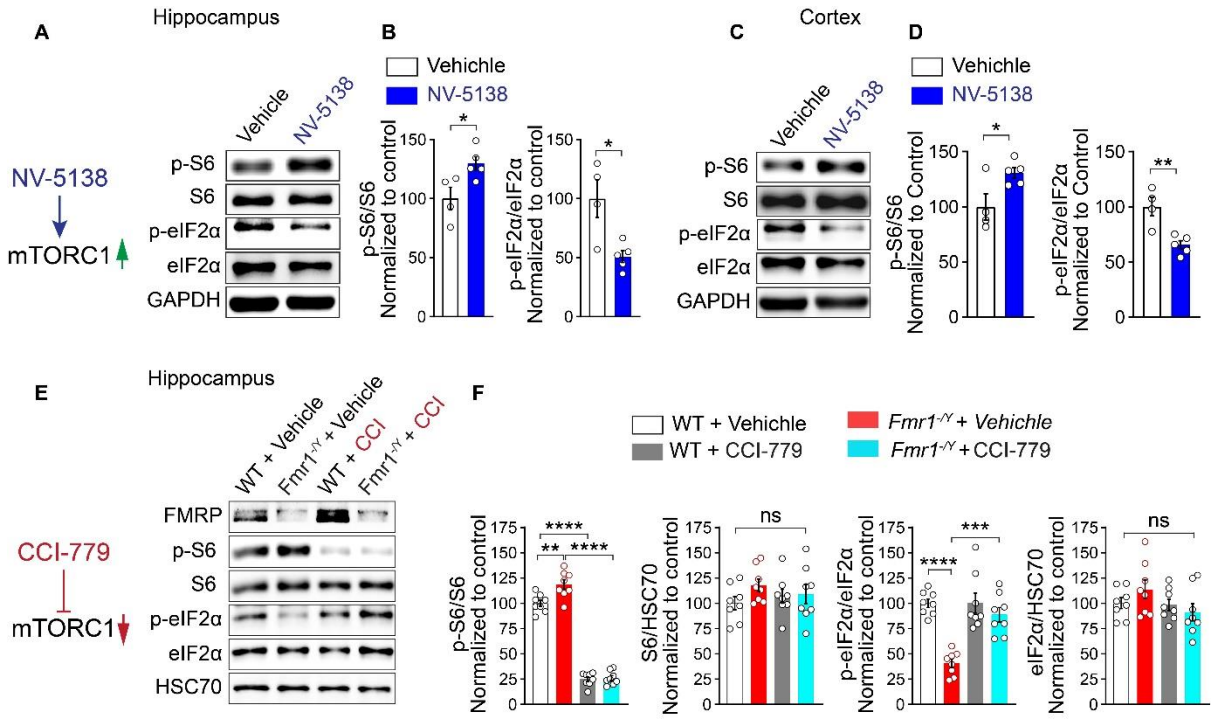

2.8.2 Figure 2. A crosstalk between mTORC1 and eIF2α pathways in the brain of *Fmr1*$^{-/y}$ mice.

(A-D) Oral administration of NV-5138 results in elevated p-S6 and decrease in p-eIF2α in hippocampal and cortical lysates. (A) A schematic shows mTORC1 activation by NV-5138. The brains were extracted from vehicle (n = 4) or NV-5138 (n = 5) treated mice 2 hours after receiving vehicle or NV-5138 (160 mg/kg). NV-5138 causes an increase in p-S6/S6 (B, left, hippocampus, $t = 2.567$, $p = 0.0372$; D, left, cortex, $t = 2.76$, $p = 0.0281$, Student's t-test) and a decrease in p-eIF2α/eIF2α (B, right, hippocampus, $t = 4.039$, $p = 0.0049$; D, right, cortex, $t = 3.211$, $p = 0.0148$, Student's t-test). (E, left) Inhibition of mTORC1 by CCI-779. Representative immunoblots (E, right) and (F) quantifications of p-S6/S6 and p-eIF2α/eIF2α in hippocampal lysates. Inhibition of mTORC1 with CCI-779 (7.5 mg/kg, daily over 3 days, i.p.) reduces p-S6/S6 in *Fmr1*$^{-/y}$ and WT animals ($F_{3, 28} = 228.4$, $p < 0.0001$, WT + Vehicle versus *Fmr1*$^{-/y}$ + Vehicle, $q_{28} = 5.734$, $p = 0.0019$; WT + Vehicle versus WT + CCI-779, $q_{28} = 23.17$, $p < 0.0001$; *Fmr1*$^{-/y}$ + Vehicle versus *Fmr1*$^{-/y}$ + CCI-779, $q_{28} = 28.54$, $p < 0.0001$, n = 8 per group). CCI-

779 increases p-eIF2α/eIF2α in *Fmr1*$^{-/y}$ mice ($F_{3, 28}$ = 17.84, p < 0.0001, WT + Vehicle versus *Fmr1*$^{-/y}$ + Vehicle, q_{28} = 8.838, p < 0.0001; *Fmr1*$^{-/y}$ + vehicle versus *Fmr1*$^{-/y}$ + CCI-779, q_{28} = 7.171, p = 0.0001, n = 8 per group, one-way ANOVA followed by Tukey's multiple comparisons post hoc test). No differences in S6 ($F_{3, 28}$ = 1.002, p > 0.05) or eIF2α ($F_{3, 28}$ = 1.652, p > 0.05) were observed (F, right, One-way ANOVA). Each data point represents an individual animal. Data are presented as mean ± s.e.m. *p < 0.05, **p < 0.01, ****p < 0.0001, ns, not significant. See also Figures S2 and S3.

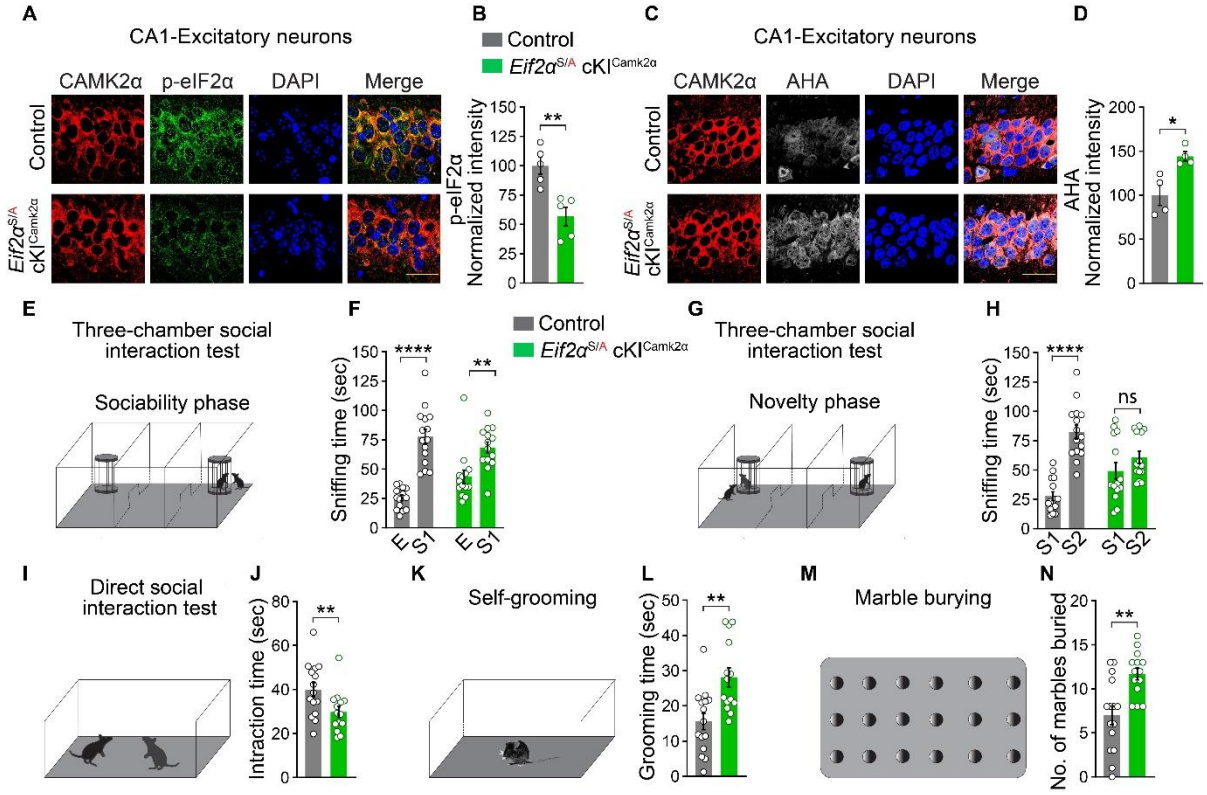

2.8.3 Figure 3. Mice with reduced phosphorylation of eIF2α in excitatory neurons exhibit autistic-like behaviors.

(A, B**)** Immunostaining of hippocampal sections from *Eif2α*$^{S/A}$ cKI^{Camk2α} mice shows a reduction in p-eIF2α in excitatory neurons (CAMK2α-positive, red) in CA1 area (control (n = 5) versus *Eif2α*$^{S/A}$ cKI^{Camk2α} (n = 5), t = 4.038, p = 0.0037, Student's t-test). *Eif2α*$^{S/S}$ *Camk2*^{Cre}

mouse line was used as control. (C, D) The global protein synthesis, measured by AHA incorporation, is increased in CA1 excitatory neurons in *Eif2α*$^{S/A}$ cKI^{Camk2α} mice as compared to the control mice (control (n = 4) versus *Eif2α*$^{S/A}$ cKI^{Camk2α} (n = 4), $t = 3.504$, $p = 0.0128$, Student's t-test). (E) Three-chamber social interaction test was used to measure indirect social interaction in *Eif2α*$^{S/A}$ cKI^{Camk2α} mice. (F) In the first 10-minutes phase of the test (sociability phase), both *Eif2α*$^{S/A}$ cKI^{Camk2α} and control mice preferred cage containing stranger (S1) mouse over empty cage (E) (Chamber time effect: $F_{(1, 54)} = 59.86$, $p < 0.0001$; Controls, n = 15, E sniffing time versus S1 time, $t_{54} = 7.528$, $p < 0.0001$), Eif*2α*$^{S/A}$ cKI^{Camk2α} mice (n = 14, E time versus S1 time, $t_{54} = 3.485$, $p = 0.0020$). Statistics are based on two-way ANOVA followed by Bonferroni's post hoc test. In the second phase (G, H**,** novelty seeking phase), *Eif2α*$^{S/A}$ cKI^{Camk2α} mice show no preference for novel mouse (S2) over familiar mouse (S1) (Chamber time effect; $F_{(1, 54)} = 34.90$, $p < 0.0001$; S1 time versus S2 time, $t_{54} = 1.446$, $p > 0.05$), contrary to control animals (S1 time versus S2 time, $t_{54} = 7.006$, $p < 0.0001$). Statistics are based on two-way ANOVA followed by Bonferroni's post hoc test. Direct social interaction test (I, J**)** reveals that *Eif2α*$^{S/A}$ cKI^{Camk2α} mice interact less with the stranger mouse than control mice (J, $t = 2.49$, $p = 0.019$, Student's t-test). *Eif2α*$^{S/A}$ cKI^{Camk2α} mice groom significantly more than controls (K, L**,** control (n = 15) versus *Eif2α*$^{S/A}$ cKI^{Camk2α} (n = 14), $t = 3.515$, $p = 0.0016$, Student's t-test) and bury more marbles in marble burying test (M, N, control (n = 15) versus *Eif2α*$^{S/A}$ cKI^{Camk2α} (n = 14), $t = 3.657$, $p = 0.0011$, Student's t-test). All data are shown as mean ± s.e.m. *$p < 0.05$, **$p < 0.01$, ***$p < 0.001$, ****$p < 0.0001$, and ns, not significant. Scale bars, 25 μm. See also Figure S4.

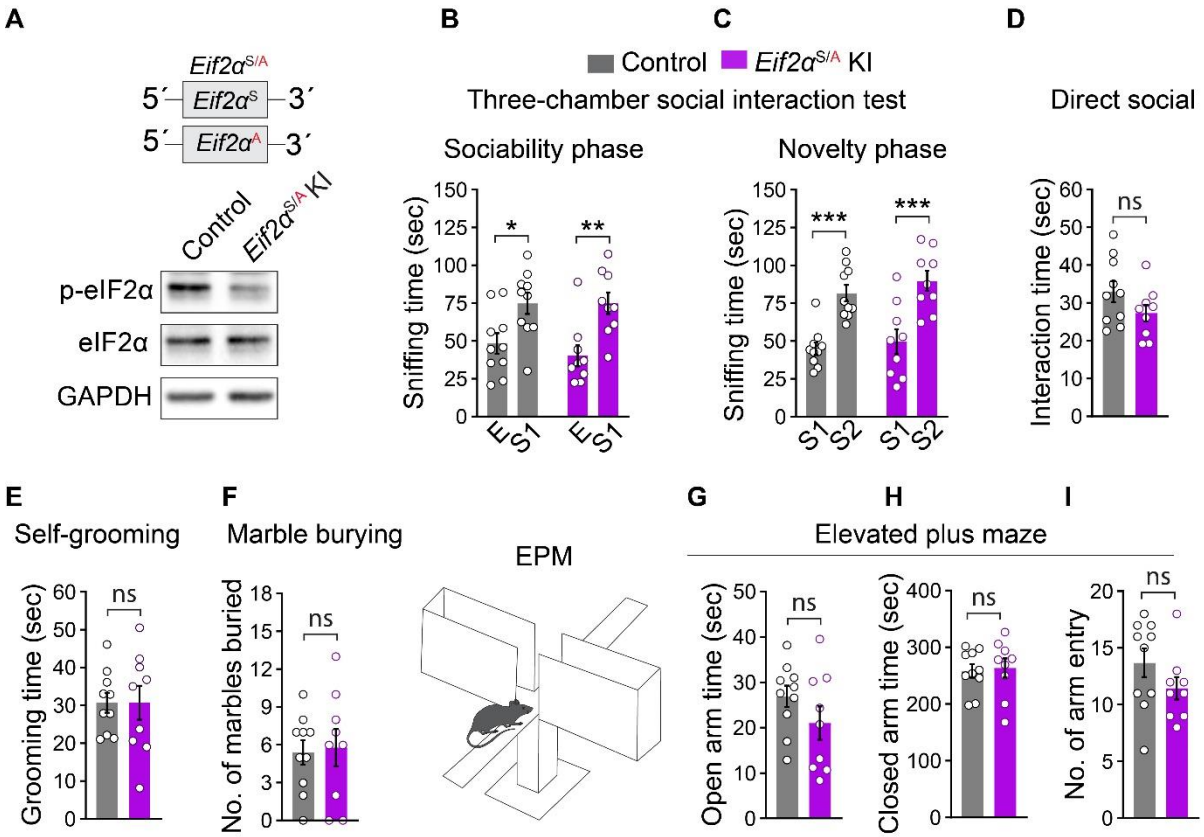

2.8.4 Figure 4. Heterozygous ablation of p-eIF2α in all cell types does not cause autism-like behaviors.

(A**,** top) A schematic illustration of alleles in *Eif2α*$^{S/A}$ knocking (KI) mouse line. (A**,** bottom) Representative immunoblot shows a reduction in p-eIF2α level in the brain of *Eif2α*$^{S/A}$ KI mice. (B**,** C) In three-chamber social interaction test, *Eif2α*$^{S/A}$ KI mice show no deficits in sociability ($F_{(1, 34)}$ = 0.337, p > 0.05; B, KI, n = 9; control, n = 10, sniffing time for empty cage (E) over stranger 1 (S1) for control, t_{34} = 2.766, p = 0.0182; KI mice t_{34} = 3.425, p = 0.0032, two-way ANOVA followed by Bonferroni's multiple comparisons test) or novelty phase (C, $F_{(1, 34)}$ = 0.082, p > 0.05, sniffing time for familiar mouse (S1) over novel mouse (S2) for control, t_{34} = 4.339, p = 0.0002; KI, t_{34} = 4.512, p = 0.0001, two-way ANOVA followed by Bonferroni's multiple comparisons test). Similar to control animals (n = 10), *Eif2α*$^{S/A}$KI mice (n = 9) showed no impairments in direct social interaction (D, t = 1.561, p > 0.05, Student's t-test), self-

grooming (F, t = 0.005, p > 0.05, Student's t-test), and marble burying (F, t = 0.218, p > 0.05, Student's t-test). (G-I) No anxiety-like behavior was found in *Eif2α*$^{S/A}$KI mice (Open arm time, t = 1.373, p > 0.05; Closed arm time, t = 0.2445, p > 0.05, and total number of arm entry, t = 1.396, p > 0.05, Student's t-test). Each data point represents an individual animal. All data are presented as mean ± s.e.m. *p < 0.05, **p < 0.01, and ***p < 0.001, and ns, not significant.

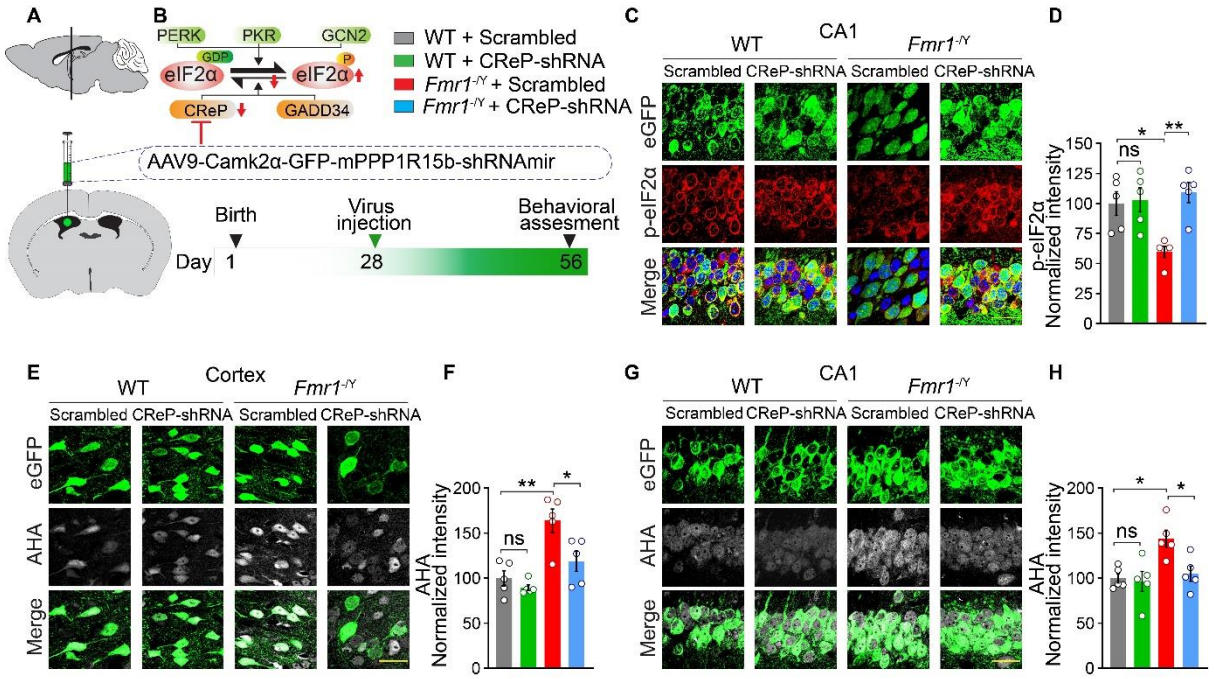

2.8.5 Figure 5. CReP-shRNA normalizes reduced eIF2α phosphorylation and corrects the elevated protein synthesis in excitatory neurons in *Fmr1*$^{-/y}$ mice.

(A) A schematic illustration of the virus injection site and the timeline for the virus injection and experiments. AAV9-Camk2α-GFP-*Ppp1r15b*-shRNAmir (CReP-shRNA) or scrambled virus was delivered via intracerebroventricular (i.c.v.) injection to ablate CReP in excitatory neurons. (B) In the brain, eIF2α is phosphorylated by PERK, PKR, and GCN2 kinases and dephosphorylated by CReP and GADD34 phosphatases. (C) Immunostaining of hippocampal sections for p-eIF2α in wild-type and *Fmr1*$^{-/y}$ animals injected with CReP-shRNA or scrambled

virus. (D) CReP-shRNAmir increases the p-eIF2α in excitatory neurons (eGFP-positive) in CA1 of *Fmr1*$^{-/y}$ mice to the control animal level ($F_{3, 16}$ = 7.054, p = 0.0031, *Fmr1*$^{-/y}$ + CReP-shRNA versus *Fmr1*$^{-/y}$ mice + Scrambled, t_{16} = 4.135, p = 0.0047; WT + Scrambled versus *Fmr1*$^{-/y}$ + Scrambled, t_{16} = 3.352, p = 0.0243, n = 5 for all groups. Statistics are based on one-way ANOVA followed by Tukey post hoc comparisons. (E-H) AHA incorporation (grey) in excitatory neurons (eGFP-positive, green) in cortex (E, F) and CA1 (G, H). CReP-shRNA virus normalizes the elevated protein synthesis in excitatory neurons in *Fmr1*$^{-/y}$ mice in cortex (F, $F_{3, 16}$ = 11.62, p = 0.0003, WT + Scrambled versus WT + CReP-shRNA, q_{16} = 1.085, p > 0.05; WT + Scrambled versus *Fmr1*$^{-/y}$ + Scrambled, q_{16} = 6.627, p = 0.0013; *Fmr1*$^{-/y}$ + Scrambled versus *Fmr1*$^{-/y}$ + CReP-shRNA, q_{16} = 4.688, p = 0.0205, one-way ANOVA followed by Tukey's multiple comparisons test, n = 5 for each group), and CA1 (H, $F_{3, 16}$ = 6.286, p = 0.005, WT + Scramble versus WT + CReP-shRNA, q_{16} = 0.411, p > 0.05; WT + Scrambled versus *Fmr1*$^{-/y}$ + Scrambled, q_{16} = 5.004, p = 0.0131; *Fmr1*$^{-/y}$ + Scrambled versus *Fmr1*$^{-/y}$ + CReP-shRNA, q_{16} = 4.424, p = 0.0297, one-way ANOVA followed by Tukey post hoc comparisons, n = 5 for each group). Each data point represents individual animal. Scale bar, 25 μm. All data are shown as mean ± s.e.m. *p < 0.05, **p < 0.01, ns, not significant. See also Figure S5.

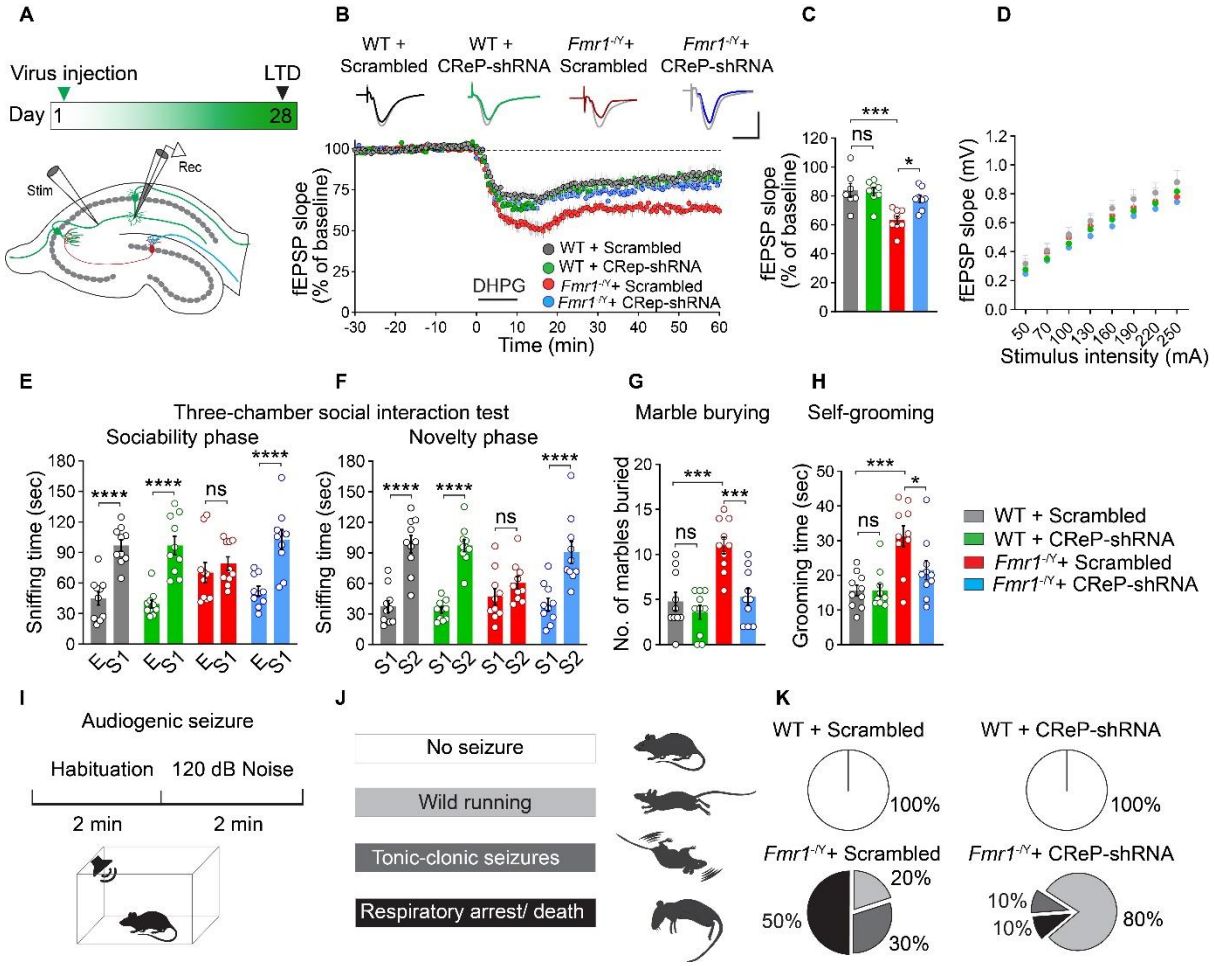

2.8.6 Figure 6. Correction of eIF2α phosphorylation in excitatory neurons rescues pathological phenotypes in *Fmr1*$^{-/y}$ mice.

(A-D) Ablation of CReP partially rescues exaggerated mGluR-LTD. (A) CReP-shRNA or Scrambled virus was injected ICV at postnatal day (PND) 1-2 and recording was performed at PND 28. Location of stimulating and recording electrodes is shown (bottom). (B) Representative traces from slices prepared from 4 groups (baseline in grey and recording at 1 hour in solid colors). (Bottom) LTD was induced by application of DHPG (50 µM for 10 min). Field excitatory postsynaptic potential (fEPSP) was recorded over a 60-min period after DHPG-induced LTD. (C) Bar graph shows the quantification of the fEPSP slope (% of baseline) during the last 10 min of the LTD recording. CReP-shRNA treatment reduced the exaggerated LTD in *Fmr1*$^{-/y}$ mice ($F_{3, 27}$ = 8.587, p = 0.0004, WT + Scrambled (n = 7 slices

from 7 mice) versus *Fmr1*$^{-/y}$ + Scrambled (n = 8 slices from 8 mice), $q_{27} = 6.196$, $p = 0.0009$; *Fmr1*$^{-/y}$ + Scrambled versus *Fmr1*$^{-/y}$ + CReP-shRNA (n = 8 slices from 8 mice), $q_{27} = 4.580$, $p = 0.0158$; one-way ANOVA followed by Tukey's multiple comparisons post hoc test). (D) No differences were observed between groups in input/output responses ($F_{21, 182} = 0.643$, $p > 0.05$, one-way ANOVA). **(**E, F**)** Three-chamber social interaction test, n = 10 per group. (E) In sociability phase, CReP-shRNA virus rescued the time *Fmr1*$^{-/y}$ mice interact with stranger animal (S1) over empty cage (E) (Chamber time effect, $F_{(1, 72)} = 66.10$, $p < 0.0001$; *Fmr1*$^{-/y}$ + CReP-shRNA, $t_{72} = 4.859$, $p < 0.0001$; WT + Scrambled, $t_{72} = 5.005$, $p < 0.0001$; *Fmr1*$^{-/y}$ + Scrambled, $t_{72} = 0.849$, $p > 0.5$; WT + CReP-shRNA, $t_{72} = 5.546$, $p < 0.0001$, one-way ANOVA followed by Bonferroni's multiple comparisons test). (F) In the novelty seeking phase, *Fmr1*$^{-/y}$ + CReP-shRNA group spent significantly more time interacting with novel moues (S2) than familiar one (S1) (Chamber time effect, $F_{(1, 72)} = 90.46$, $p < 0.0001$; Fmr*1*$^{-/y}$ + CReP-shRNA, $t_{72} = 5.137$, $p < 0.0001$; WT + Scrambled, $t_{72} = 6.147$, $p < 0.0001$; *Fmr1*$^{-/y}$ + Scrambled, $t_{72} = 1.343$, $p > 0.5$; WT + CReP-shRNA, $t_{72} = 6.394$, $p < 0.0001$, one-way ANOVA followed by Bonferroni's multiple comparisons test). (G) In marble burying test (n = 10 per group), CReP-shRNA reduced the number of buried marbles in *Fmr1*$^{-/y}$ mice ($F_{3, 36} = 13.20$, $p < 0.0001$, WT + Scrambled versus *Fmr1*$^{-/y}$ + Scrambled, $q_{36} = 6.836$, $p = 0.0001$; *Fmr1*$^{-/y}$ + Scrambled vs. *Fmr1*$^{-/y}$ + CReP-shRNA, $q_{36} = 6.285$, $p < 0.0005$, One-way ANOVA followed by Tukey's multiple comparisons test). (H) CReP-shRNA treatment reduced the time that *Fmr1*$^{-/y}$ mice spent grooming ($F_{3, 36} = 9.602$, $p < 0.0001$, WT + Scrambled versus *Fmr1*$^{-/y}$ + Scrambled, $q_{36} = 6.587$, $p = 0.0002$; *Fmr1*$^{-/y}$ + Scrambled versus *Fmr1*$^{-/y}$ + CReP-shRNA, $q_{36} = 4.108$, $p = 0.304$, One-way ANOVA, followed by Tukey's multiple comparisons test). (I-K) CReP-shRNA virus alleviated audiogenic seizures (AGS) in *Fmr1*$^{-/y}$ mice. (I) AGS induction protocol (top), and the apparatus (bottom) composed of a soundproof box and a speaker to generate 120 dB noise. (J) Different levels of seizure upon exposure to 120 dB noise ranging from no seizure

to wild running (WR), tonic-clonic (TC), and severe seizure which leads to respiratory arrest and death (RA). (K) Unlike WT + Scrambled (n = 10) and WT + CReP-shRNA (n = 10) groups which showed no seizure, 20% of *Fmr1*$^{-/y}$ mice (n = 10) experience wild running, 30% tonic-clonic and 50% of them showed the severe form of the seizure, respiratory arrest, and death. CReP-shRNA virus significantly reduced (X^2 (9)=545.3, $p < 0.0001$, Fisher's exact test) the severity of the seizure in *Fmr1*$^{-/y}$ + CReP-shRNA (n = 10), (WR: 80%, TC: 10%, RA: 10%). Each data point represents individual animal. All data are shown as mean ± s.e.m. *$p < 0.05$, ***$p < 0.001$, ****$p < 0.0001$, ns, not significant.

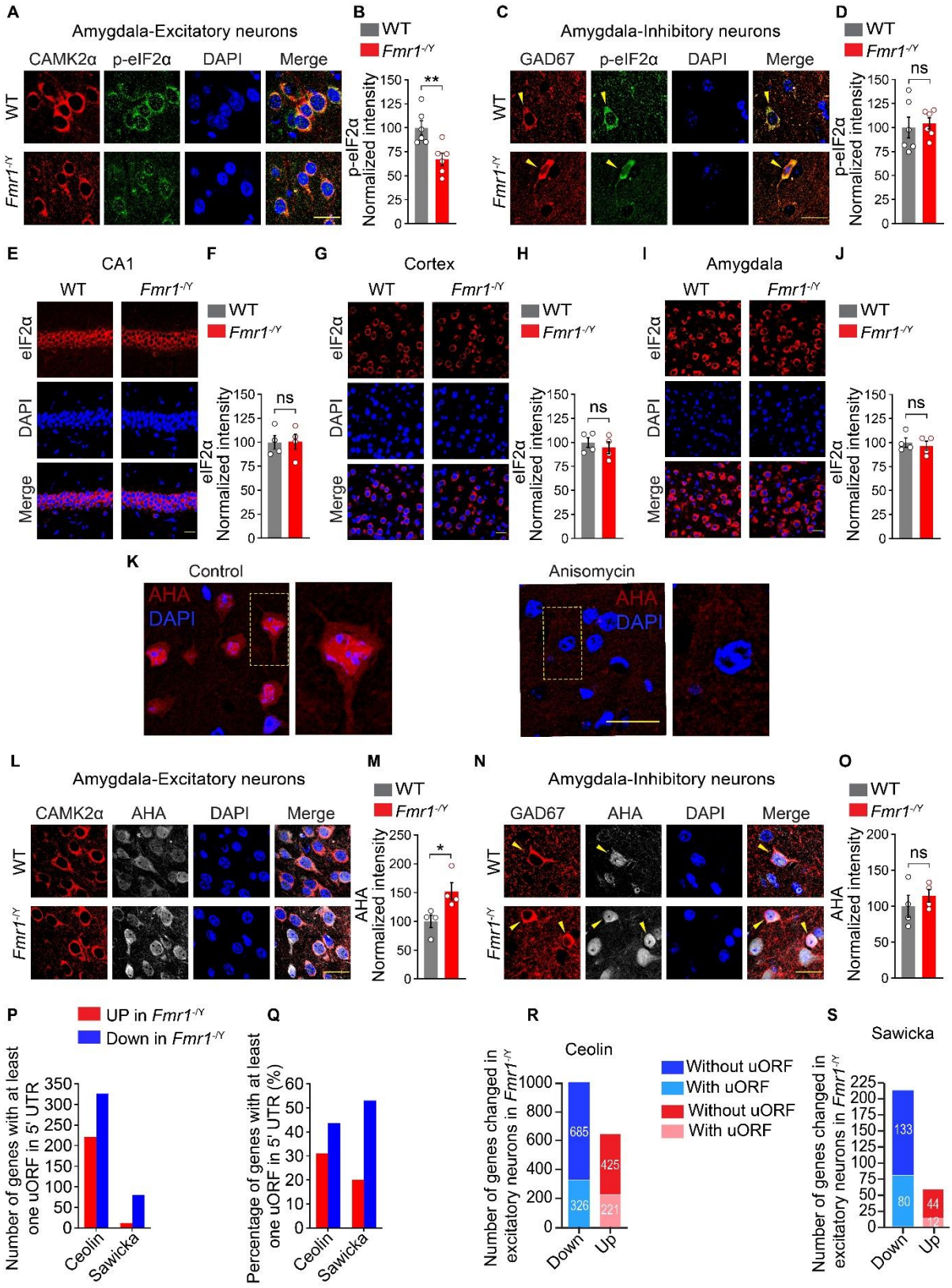
A
Amygdala-Excitatory neurons
CAMK2α
p-eIF2α
DAPI
Merge
WT
Fmr1-/Y
B
WT
Fmr1-/Y
**
p-eIF2α Normalized intensity
C
Amygdala-Inhibitory neurons
GAD67
p-eIF2α
DAPI
Merge
D
ns
E
CA1
F
G
Cortex
H
I
Amygdala
J
eIF2α
DAPI
Merge
K
Control
Anisomycin
AHA
DAPI
L
Amygdala-Excitatory neurons
CAMK2α
AHA
DAPI
Merge
M
*
AHA Normalized intensity
N
Amygdala-Inhibitory neurons
GAD67
O
P
UP in Fmr1-/Y
Down in Fmr1-/Y
Number of genes with at least one uORF in 5' UTR
Ceolin
Sawicka
Q
Percentage of genes with at least one uORF in 5' UTR (%)
R
Ceolin
Without uORF
With uORF
Without uORF
With uORF
Number of genes changed in excitatory neurons in Fmr1-/Y
685
326
425
221
Down
Up
S
Sawicka
133
80
44
12

2.8.7 Supplementary Figure 1. *Fmr1*$^{-/y}$ mice show a decrease in p-eIF2α and concomitant elevation in *de novo* protein synthesis in excitatory neurons.

(A, C) Representative immunostaining and (B, D) quantification of p-eIF2α expression in amygdala excitatory neuron in *Fmr1*$^{-/y}$ mice (n = 6) compared with WT (n = 6) show decreased p-eIF2α (B, $t = 3.409$, $p = 0.0067$, Student's t-test). No difference between *Fmr1*$^{-/y}$ (n = 6) and WT (n = 6) animals in inhibitory neurons in amygdala was observed (D, $t = 0.345$, $p > 0.05$, Student's t-test). (E-J) Representative immunostaining and quantification of total eIF2α expression in CA1, cortex, and amygdala showing no change in eIF2α in *Fmr1*$^{-/y}$ mice (n = 4) compared with WT animals (n = 4) (F, CA1, $t = 0.05$, $p > 0.05$; H, cortex, $t = 0.684$, $p > 0.05$; J, amygdala, $t = 0.511$, $p > 0.05$, Student's t-test). (K) AHA incorporation into newly synthesized polypeptides is sensitive to anisomycin, a protein synthesis inhibitor. (K, left, AHA in the control section is incorporated into newly synthesized proteins, whereas (right) pre-treatment with anisomycin blocks AHA incorporation. (L, N) Representative immunostaining and (M, O) quantification of AHA signal intensity in the amygdala shows that AHA incorporation is increased in excitatory neurons in *Fmr1*$^{-/y}$ mice (n = 4) compared with WT mice (n = 4), (M, $t = 2.793$, $p = 0.0314$, Student's t-test). In *Fmr1*$^{-/y}$ amygdala inhibitory neurons, no difference in AHA level was detected (O, $t = 0.567$, $p > 0.05$, Student's t-test, n = 4 for both group). Yellow arrows mark the inhibitory neurons. (P-S) Analysis of previously published TRAP data from excitatory neurons of *Fmr1*$^{-/y}$ mice (Ceolin(Ceolin *et al.*, 2017), Sawicka(Sawicka *et al.*, 2019)) shows a reduction in genes harboring uORF ($p < 0.0001$ for both datasets, two-sided Fisher's exact test). The bar graphs demonstrate the number (P) and the percentage (Q) of genes containing uORF in their 5′ UTR, and (R, S) the total number of upregulated and downregulated genes with and without uORF in the 5′ UTR in excitatory neurons in *Fmr1*$^{-/y}$ mice. Each data point represents an individual animal. All data are presented as mean ± s.e.m. *$p < 0.05$, **$p < 0.01$, and ns, not significant. Scale bars, 25 μm.

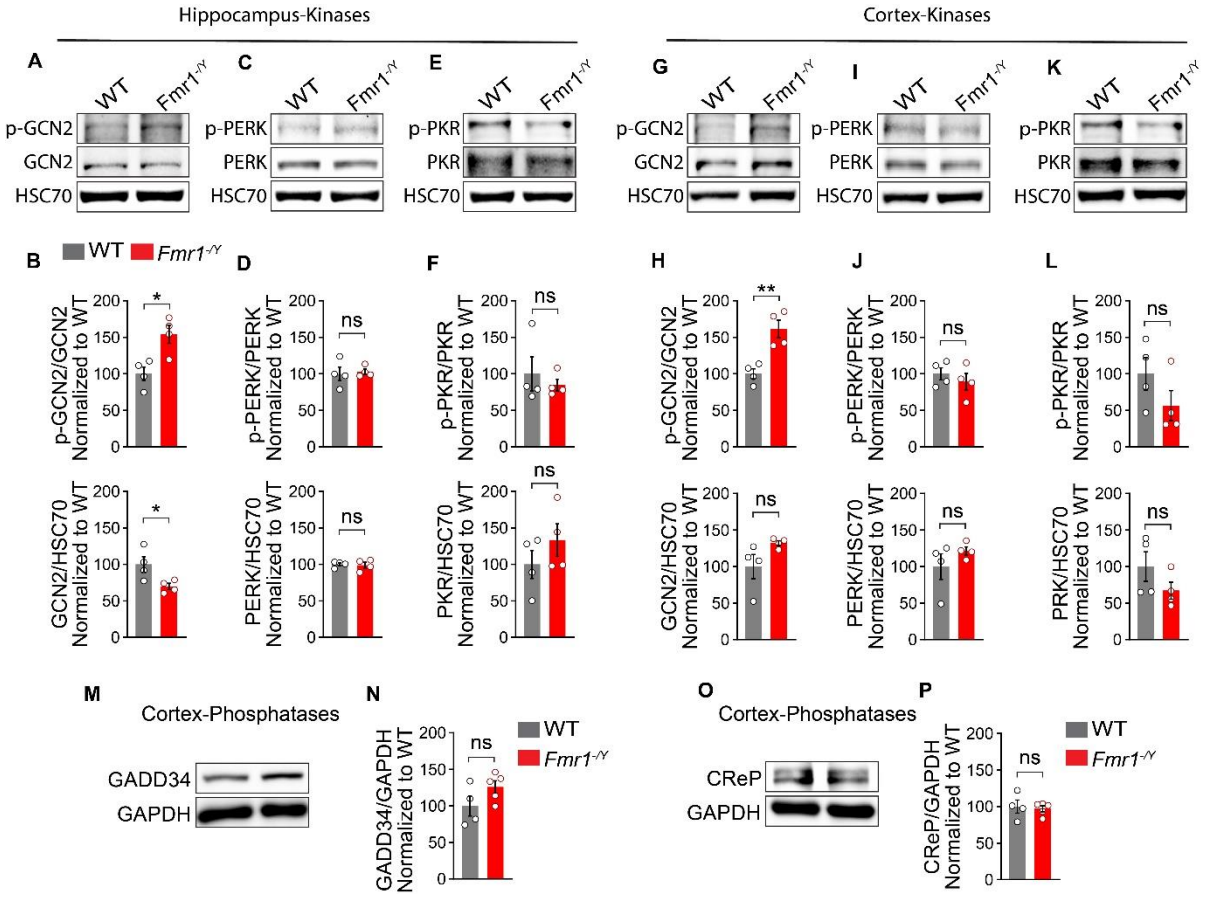

2.8.8 Supplementary Figure 2. eIF2α phosphatases and kinases in the brain of *Fmr1*$^{-/y}$ mice.

(A-L) Representative immunoblots and quantifications of p-GCN2, p-PERK, and p-PKR in hippocampal and cortical lysates extracted from *Fmr1*$^{-/y}$ (n = 4) in comparison to WT animals (n = 4) show increased p-GCN2 in the hippocampus (B, $t = 3.469$, $p = 0.0133$) and cortex (H, $t = 4.417$, $p = 0.0045$) of *Fmr1*$^{-/y}$ animals. There are no differences in p-PERK and p-PKR between *Fmr1*$^{-/y}$ and WT in the hippocampus (D, F, top, $p > 0.05$) and the cortex (J, L**,** top, $p > 0.05$). No differences in total PERK and PKR in the hippocampus (D, F, bottom, $p > 0.05$) or cortex (H-L, bottom, $p > 0.05$). The ratio of total GCN2 to loading control in hippocampus lysates of *Fmr1*$^{-/y}$ was lower than in WT mice (B, bottom, $t = 2.656$, $p = 0.0377$). Representative images (M, O) and quantification (N, P) of GADD34 and CReP phosphatases. The levels of GADD34 (N**,** $p > 0.05$) and CReP (P**,** $p > 0.05$) in *Fmr1*$^{-/y}$ (n = 4) cortical lysates are not

different comparing with WT (n = 4) animals. Each data point represents an individual animal. Data are presented as mean ± s.e.m. *$p < 0.05$, **$p < 0.01$, ns, not significant.

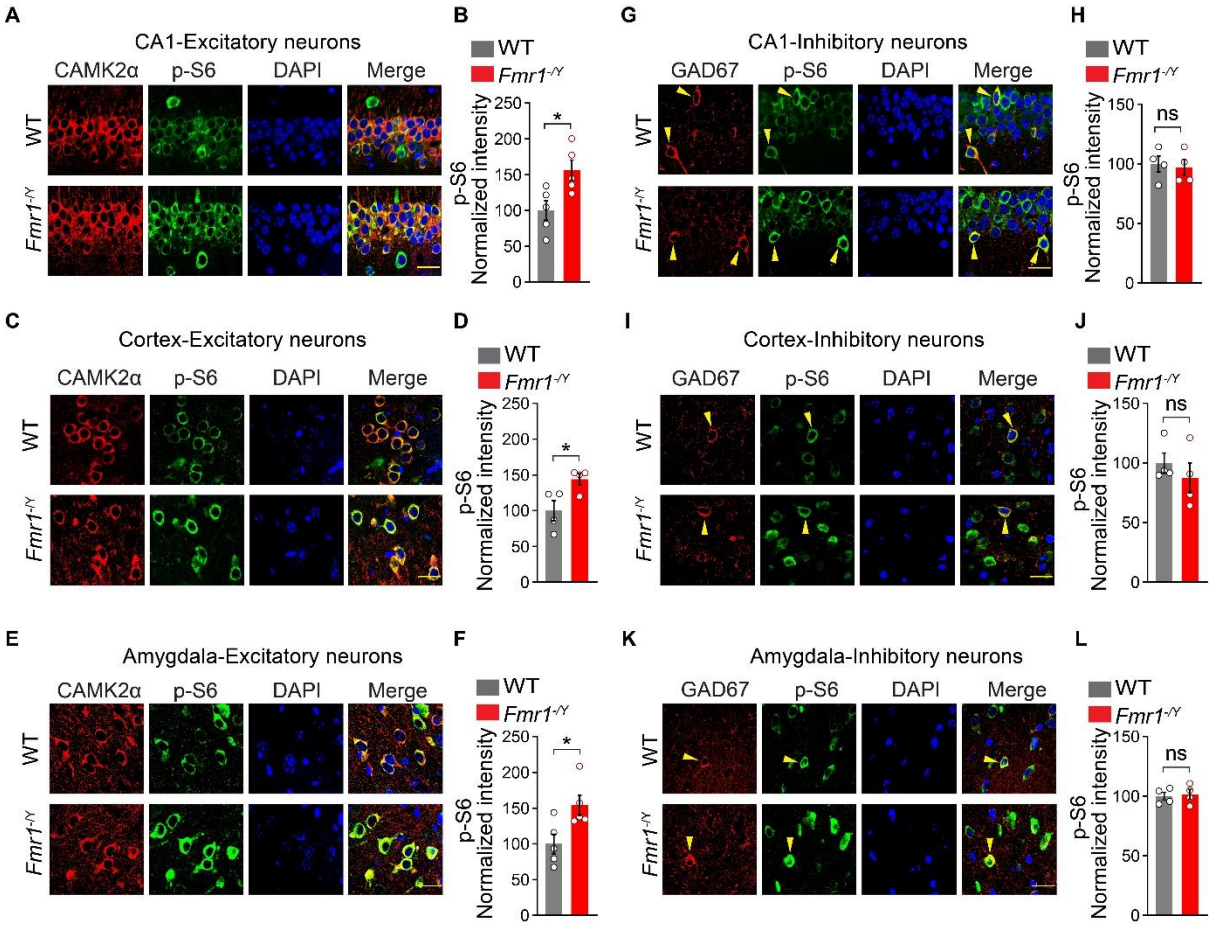

2.8.9 Supplementary Figure 3. Elevated p-S6 in excitatory neurons in the brain of *Fmr1*$^{-/y}$ mice.

(A-L) Representative images and quantification of p-S6 expression in excitatory and inhibitory neuron from *Fmr1*$^{-/y}$ and WT mice show that p-S6 is higher in *Fmr1*$^{-/y}$ excitatory neurons in hippocampus (B, $t = 2.845$, $p = 0.0217$, n = 5 for both groups), cortex (D, $t = 2.714$, $p = 0.0349$, n = 4 for either group) and amygdala (F, $t = 2.724$, $p = 0.0261$, n = 5 for either group) versus WT mice. No differences were observed in inhibitory neurons in p-S6 levels in hippocampus (H, $t = 0.293$, $p > 0.05$, n = 4 for both groups), cortex (J, $t = 0.833$, $p > 0.05$) and amygdala (L, $t = 0.247$, $p > 0.05$) in *Fmr1*$^{-/y}$ (n = 4) versus WT mice (n = 4). Yellow arrows show the

inhibitory neurons. The Student's t-test was performed for all analyses. Each data point represents an individual animal. All data are presented as mean ± s.e.m. *p < 0.05, ns, not significant. Scale bars, 25 µm.

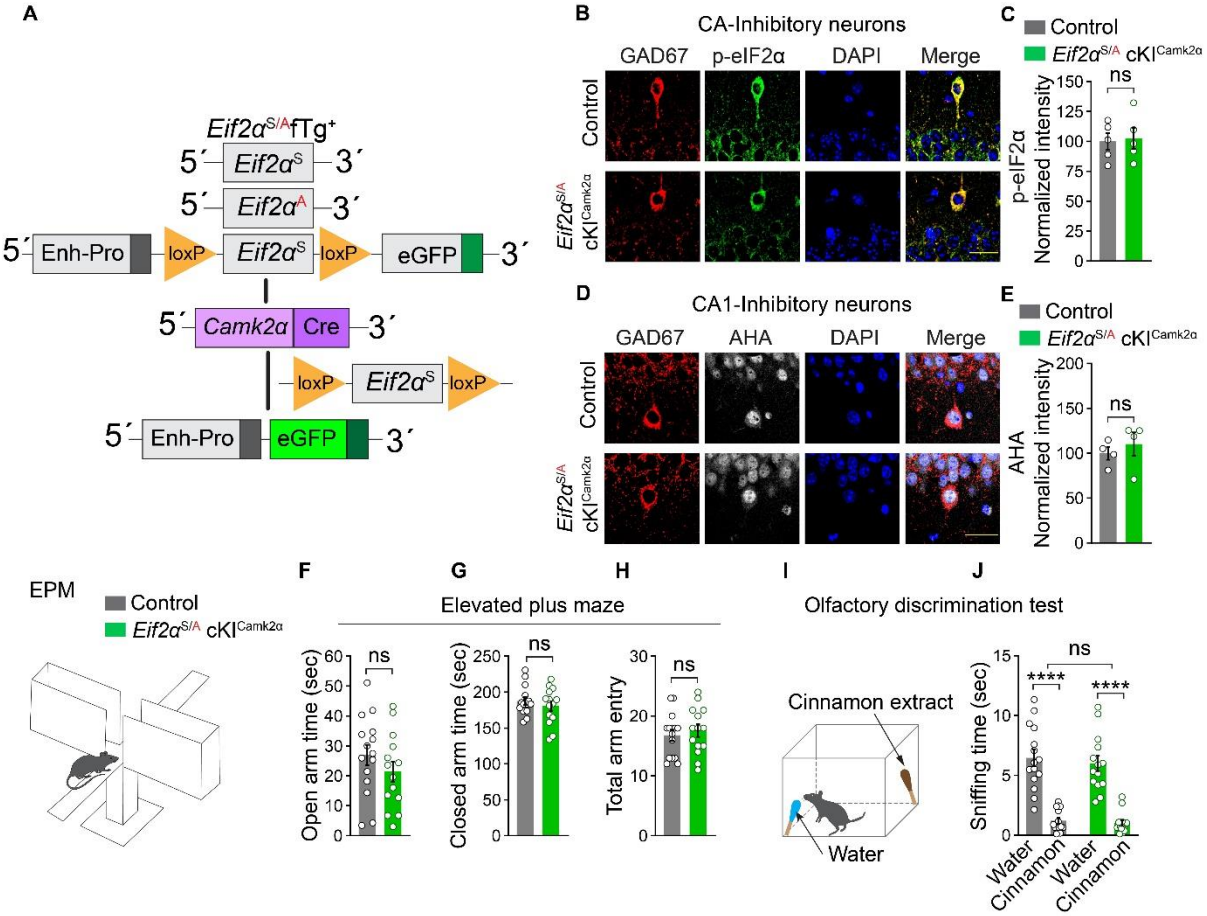

2.8.10 Supplementary Figure 4. No changes in p-eIF2α and global protein synthesis in inhibitory neurons of *Eif2α*$^{S/A}$ cKI^{Camk2α} mice.

(A) A schematic illustration depicts the generation of *Eif2α*$^{S/A}$ cKI^{Camk2α} mice (crossing the *Eif2α*$^{A/A}$*fTg*$^{+}$ mice with *Camk2*^{Cre} mice). Representative immunostaining and quantification of p-eIF2α (B, C) and AHA incorporation (D, E) in inhibitory neurons of hippocampal sections from *Eif2α*$^{S/A}$ cKI^{Camk2α} mice (n = 4) show no differences in p-eIF2α levels (C, t = 0.242, p > 0.05, Student's t-test) or AHA signal intensity (E, t = 0.679, p > 0.05, Student's t-test) compared

with control (*Camk2*^{Cre}) mice (n = 4). (F-H) *Eif2α*$^{S/A}$ cKI^{Camk2α} mice exhibit no anxiety-like behavior in an elevated plus maze test. *Eif2α*$^{S/A}$ cKI^{Camk2α} mice (n = 14) spent a comparable amount of time to controls (n = 15) in open arm (F**,** $p > 0.05$) and closed arm (G**,** $p > 0.05$), and entered both arms as frequent as controls (H**,** $p > 0.05$). Student's t-test was used for f-h. (I-J) *Eif2α*$^{S/A}$ cKI^{Camk2α} mice exhibit intact olfaction. (I) Mice were allowed to freely sniff either the water or cinnamon extract-dipped swab. *Eif2α*$^{S/A}$ cKI^{Camk2α} (n = 14) and control (n = 15) animals discriminated water over cinnamon extract, and no difference was found between the two groups (J, $F_{1, 54} = 0.4543$, $p > 0.05$, two-way ANOVA). Each data point represents an individual animal. All data are presented as mean ± s.e.m. ****$p < 0.0001$, and ns, not significant. Scale bars, 25 μm.

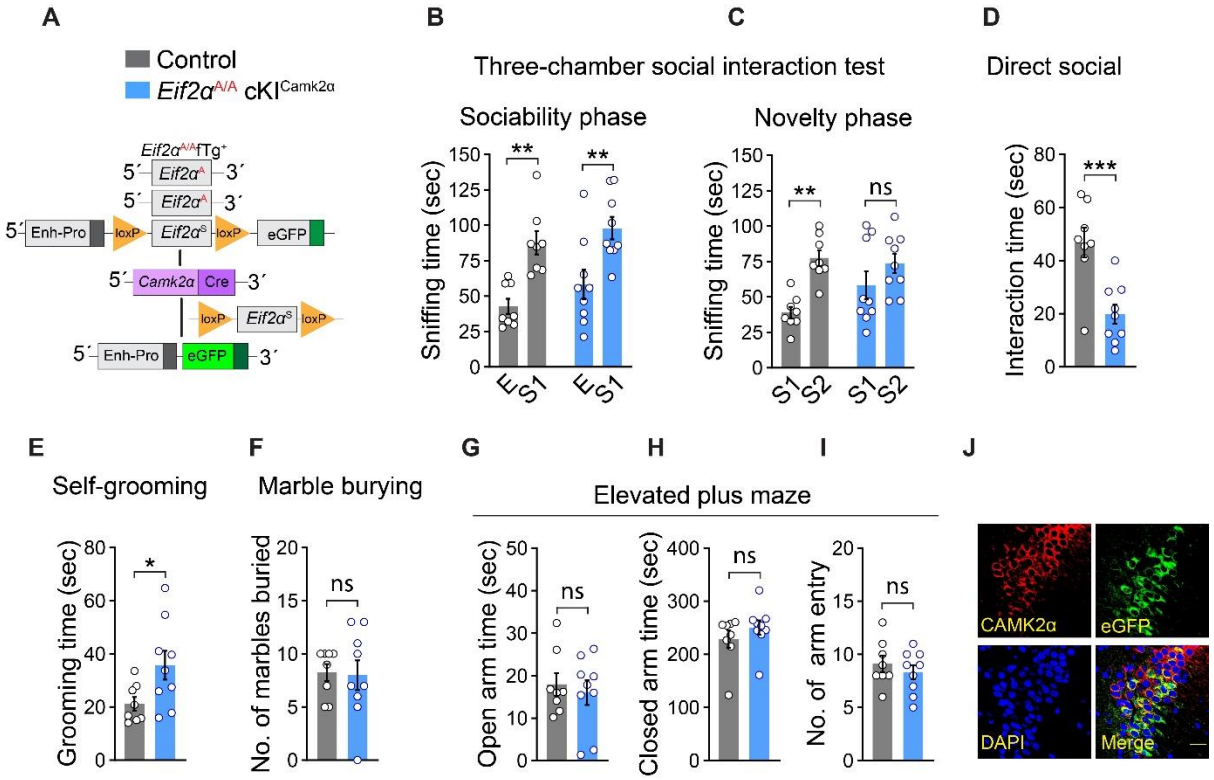

2.8.11 Supplementary Figure 5. Mice with complete ablation of p-eIF2*α* in excitatory neurons show autistic-like behaviors.

(A) A schematic illustration of *Eif2α*$^{A/A}$ cKI^{Camk2α} mice breeding strategy (crossing of *Eif2α*$^{A/A}$ *fTg*$^{+}$ mice with *Camk2α*^{Cre} mice). (B) In the sociability phase of the three-chamber social interaction test, *Eif2α*$^{A/A}$ cKI^{Camk2α} and control mice preferred stranger mouse (S1) over empty cage (E) (Control, n = 8, E versus S1 sniffing time, t_{30} = 3.7, p = 0.0017; *Eif2α*$^{A/A}$ cKI^{Camk2α}, n = 9, E versus S1 sniffing time, t_{30} = 3.48, p = 0.0031). (C) In the novelty phase, *Eif2α*$^{A/A}$ cKI^{Camk2α} mice did not show a significant preference for the novel mouse (S2) over the familiar one (S1) in comparison with control animals (Control, n = 8, S1 versus S2 sniffing time, t_{30} = 3.705, p = 0.0017; *Eif2α*$^{A/A}$ cKI^{Camk2α}, n = 9, S1 versus S2 sniffing time, t_{30} = 1.559, p > 0.05). Two-way ANOVA followed by Bonferroni's multiple comparisons test was applied. (D) In direct social interaction test, *Eif2α*$^{A/A}$ cKI^{Camk2α} mice (n = 9) spent less time interacting with the stranger mouse than controls (n = 8) (t = 4.099, p = 0.0009, Student's t-test). *Eif2α*$^{A/A}$ cKI^{Camk2α} mice (n = 9) spent more time than controls (n = 9) in self-grooming (E, t = 2.307, p = 0.0357, Student's t-test). (F) The total number of the buried marbles did not differ between *Eif2α*$^{A/A}$ cKI^{Camk2α} mice (n = 9) and controls (n = 8), (t = 0.149, p > 0.05, Student's t-test). (G-I) In elevate plus maze task, no differences between *Eif2α*$^{A/A}$ cKI^{Camk2α} and control mice were observed (p > 0.05, Student's t-test). (J) AAV9-Camk2α-GFP-Ppp1r15b-shRNAmir expression is restricted to excitatory neurons. Co-staining of virally expressed eGFP (green) and CAMK2α (red) confirms specific expression of the AAV in excitatory neurons. Scale bar 25 µm. Each data point represents an individual animal. All data are presented as mean ± s.e.m. *p < 0.05, **p < 0.01, and ***p < 0.001, and ns, not significant.

2.9 STAR Methods

2.9.1 Animals

The *Fmr1*$^{-/y}$ mice (Jackson Laboratories, stock #003025) and general heterozygous knock-in mice (*Eif2α*$^{S/A}$ KI)(Scheuner *et al.*, 2001; Scheuner et al., 2005) were maintained on the

C57BL/6 background. In this study only male mice have been used as the males show a pronounced autism-like phenotypes compared to females. To obtain the *Eif2α*$^{S/A}$ fTg^{+}; *Camk2α*$^{Cre+}$ (*Eif2α*$^{S/A}$ cKI^{Camk2α}) mice, *Eif2α*$^{A/A}$ fTg^{+} floxed mice(Back *et al.*, 2009) were bred with *Eif2α*$^{S/S}$ fTg^{+} *Camk2α*$^{Cre+}$ mice. The heterozygous knock-in *Eif2α*$^{S/A}$ fTg^{+}; *Camk2α*$^{Cre+}$ mice were then crossed with the same line to generate the homozygous mice *Eif2α*$^{A/A}$ fTg^{+}; *Camk2α*$^{Cre+}$ (*Eif2α*$^{A/A}$ cKI^{Camk2α}). All the mouse strains were maintained on the C57BL/6 background. *Eif2α*$^{A/A}$ fTg^{+} floxed, *Eif2α*$^{S/A}$ fTg^{+} floxed, and *Camk2α*$^{Cre+}$ mice were used as controls in behavioral experiments. No differences between these lines were observed, and the data were pooled and presented as "Control". All experiments were conducted on adult male mice (6–8-week-old), except for electrophysiology experiments in which young male mice (3–4-week-old) were used. All experiments were performed and analyzed by an experimenter blind to genotypes and treatments. Animals were housed in regular Plexiglas mouse cages with food and water available *ad libitum* and kept on a 12 h light/dark cycle (lights on at 7:00 AM). All procedures were compliant with the Canadian Council on Animal Care guidelines and approved by the McGill University's Animal Care Committee.

2.9.2 Stereotaxic surgery

Mice were deeply anesthetized (induced with 3% isoflurane and maintained on 1.5 % isoflurane) and placed in a stereotaxic frame (Kopf). The front teeth were placed in the incisor bar, and the head was secured using ear bars. The skull was exposed through a midline incision and drilled at the defined coordinates to microinject the virus into the lateral ventricles (i.c.v.) (anterior/posterior (AP): -0.55 mm, medial/lateral (ML): 1.1 mm, and dorsal/ventral (DV): -2.2 mm) or CA1 hippocampal area (AP: -1.90 mm, ML: ±1.0 mm, and DV: -1.50 mm). Using a 10 µl Hamilton syringe connected to a 23-gauge needle and mounted on a perfusion pump, mice received 7 µl of AAV9-Camk2α-GFP-*Ppp1r15b*-shRNAmir (3.8 x 10^{13} GC/mL) or

control AAV9-Camk2α-GFP-scrambled-shRNAmir (2.6 x 10^{13} GC/mL) via I.C.V. injection. The perfusion rate was set at 0.5 µl /min, and the needle was kept in place for additional 3 minutes before the withdrawal. Experiments were performed four weeks post-viral injection. For electrophysiology studies, pups at postnatal day 1 received 2 µl of AAV9-Camk2α-GFP-*Ppp1r15b*-shRNAmir or AAV9-Camk2α-GFP-scrambled-shRNAmir i.c.v. bilaterally. Two-fifths of the hypothetical line from lambda to eyes was marked as the coordinate for the i.c.v. microinjection site. Then, the virus was microinjected using a 5 µl Hamilton syringe connected to a 23-gauge needle. The needle was inserted 3 mm deep into the lateral ventricle.

2.9.3 AAV9-shRNAmir cloning and preparation

The microRNA-adapted short hairpin RNAs (shRNAmir) packaged in adeno-associated virus (AAV) were prepared by Vector Biolabs. The validate sequence targeting mouse *Ppp1r15b* was:

GCTGTGAACTCAGAGACTTCTGCACGTTTTGGCCACTGACTGACGTGCAGAACTCTGA GTTCACAG, and the scrambled sequence used as a control was: GCGAGTCTCCACGCGCAGTACATTTTAGTGAAGCCACAGATGTAAAATGTACTGC GCGTGGAGACCTGC

2.9.4 Western blotting

Mice were decapitated following deep anesthesia, and the brains were extracted and immediately placed in a dish containing ice-cold phosphate-buffered saline (PBS) to dissect the hippocampus, amygdala, and cortex. The extracted tissues were homogenized in a tissue homogenization buffer composed of 200 mM HEPES, 50 mM NaCl, 10% Glycerol, 1% Triton X-100, 1mM EDTA, 50 mM NaF, 2 mM Na3VO4, 25 mM β-glycerophosphate, and EDTA-free complete ULTRA tablets (Roche, Indianapolis, IN). Homogenized tissue was then

centrifuged (14000 rpm for 15 min at 4 ºC) to obtain the supernatant. Bradford protein assay was performed to measure protein concentration of the lysates. 30 µg of the lysates were loaded on a 12 % SDS-PAGE gel and ran at a constant current (0.03 A/per gel). The gel was then transferred to a nitrocellulose membrane overnight at a constant voltage (125 V). Next, the membrane was blocked for one h in 5% milk or BSA in TBS-T. The blocked membrane was incubated in primary antibodies (the list of antibodies is provided in the supplementary table 1) overnight at 4 °C. Primary antibody incubation was followed by three washes and incubation with HRP-conjugated secondary antibody (1:5000, Cat. No. NA931-1ML, Amersham) at room temperature. Then, the membrane was washed again, and the signal was enhanced using Enhanced Chemiluminescent (ECL) reagent and visualized using a ChemiDoc Imaging System (Bio-Rad). Antibody used in this study were: phospho-eIF2α (Ser51) (Cell Signaling Technology, Cat No. 3398), eIF2α (Cell Signaling Technology, Cat No. 9722), Anti-FMRP (Cell Signaling Technology, Cat No. 4317), GCN2 (phospho T899) (Abcam, Cat No. ab75836), GCN2 (Cell Signaling Technology, Cat NO. 3302), p-PERK (Thr 981), (Santa Cruz Biotechnology, Cat No. sc-32577), PERK (H-300), (Santa Cruz Biotechnology, Cat No. sc-13073), p-PKR (Thr 451) (Santa Cruz Biotechnology, Cat No. sc-101784), PKR (B-10) (Santa Cruz Biotechnology, Cat No. sc-6282), GAPDH (0411) (Santa Cruz Biotechnology, Cat No. sc-47724), GADD34 (Proteintech, Cat No. 10449-1-AP), CReP (PPP1R15B) (Proteintech, Cat No. 14634-1-AP), phospho-S6 ribosomal protein (Ser240/244) (Cell Signaling, Cat No. 5364), S6 ribosomal protein (5G10) (Cell Signaling Technology, Cat No. 2217), and HSC 70 (K-19) (Santa Cruz Biotechnology, Cat No. sc-1059.

2.9.5 Immunohistochemistry

Mice were transcardially perfused with 4% paraformaldehyde (PFA). The brains were postfixed in PFA 4% for 24 h following extraction. The fixed brains were sectioned using a

vibratome to acquire 50-µm-thick sections. After washing with PBS, sections were blocked using 10% normal goat serum (NGS) and 0.5% Triton-X100 in PBS for two hours. Next, the blocked sections were incubated in primary antibody (provided in the supplementary table 1) diluted in PBS containing 2% NGS overnight. Sections were washed three times with PBS and incubated for one hour at room temperature in secondary antibody diluted in PBS. DAPI (1:5000) was added to the solution in the last wash. Rinsed sections were mounted on glass slides, imaged using a confocal microscope (Zeiss LSM 880), and scored using ImageJ (NIH). In all experiments, confocal imaging with 63X Oil objective (NA 1.4) was used, except for the 20X objective for eIF2α imaging. Two sections per mouse from each brain area were imaged (n = 4-6 mice/group). All images were captured using Z-stack mode with 15-20 optical sections/stack. For excitatory neurons, integrated density of p-eIF2α and p-S6 signal in the cytoplasm of 40 neurons per mouse (2 sections per mouse, 20 neurons per section) in the hippocampus, prefrontal cortex, and basolateral amygdala were quantified using ImageJ on maximum intensity projection images. The values from 40 neurons per mouse were averaged to obtain a single value per mouse. For inhibitory neurons, 16-20 neurons per mouse (8-10 neurons per section) were quantified as described for excitatory neurons. Measurements were restricted to cytoplasm using nuclear DAPI stain. Antibody used in this study were: CaMKII-α (6G9) (Cell Signaling Technology, Cat No. 50049), GAD67 (Sigma-Aldrich, Cat No. MAB5406), EIF2S1 (phospho S51) (Abcam, Cat No. ab32157), eIF2α (L57A5) (Cell Signaling Technology, Cat No. 2103), and phospho-S6 ribosomal protein (Ser240/244) (Cell Signaling Technology, Cat No. 5364).

2.9.6 Marble burying test

After handling and habituation to the test environment, mice were individually placed on top of a 5 cm thick and leveled bedding with 18 shiny and clean marbles (distributed in 3 rows of

6 marbles) in a Plexiglas box (50 cm x 50 cm x 31 cm). Mice were allowed to explore and bury the marbles for 30 min. A marble was counted as buried if more than 2/3 of it were covered by bedding.

2.9.7 Self-grooming test

Mice were placed in a clean mouse cage with fresh beddings and allowed to habituate and explore the cage for 20 minutes. Grooming time in the last 10 min was scored and analyzed. Total time of self-grooming was measured using a manual stopwatch in the recorded video through a rigged camera in front of the cage.

2.9.8 Elevated plus maze

The handled mice were individually placed at the intersection of the four arms facing one of the closed arms and were allowed to explore the maze for 5 min while their motion path was filmed using a mounted camera over the maze. The maze comprises 4 Plexiglas arms (two closed and two open arms) raised 50 cm above the ground level with height: 30 cm, length: 50 cm, and width: 10 cm. The time spent in either arm and the total number of arms entries were scored.

2.9.9 Reciprocal male-male social interaction test

After five-min habituation in a clean mouse cage with fresh bedding, mice were individually exposed to an unfamiliar age and sex-matched mouse (WT) for 10 min. The recorded video was then analyzed offline to measure the total time of interaction between the test mouse and the unfamiliar one.

2.9.10 Three-chamber social interaction test

Three interconnected Plexiglas chambers (36 cm × 28 cm × 30 cm) divided by transparent walls were used. The experiment was conducted in three 10-min phases, including habituation, sociability, and novelty preferences. In the habituation phase, the test mice were individually placed in the middle chamber to freely explore all three chambers through doorways on the walls. In the sociability phase, the test mice were exposed to age, and sex-matched unfamiliar mice (stranger 1, C57BL/6J) which were confined in a small wire cage in one chamber, and the identical empty wire cage was located in the corresponding spot in the other chamber. In the novelty phase, the test mice were exposed to the same unfamiliar mouse (stranger 1) from the sociability phase, which is familiar now, and another age and sex-matched unfamiliar mouse (stranger 2, C57BL/6J) was placed in the empty wire cage. Once the doorways are opened, the test mice could explore both chambers containing stranger1 or stranger 2. All three phases were recorded using a mounted camera, and then the time spent sniffing of either empty or occupied wire cages, time spent in each chamber, and the total number of chamber entries were scored and analyzed. Any contact or sniffing when the test mouse approached as close as 1 cm of either empty or occupied wire cage was considered social interaction.

2.9.11 Olfactory discrimination test

For assessing the primary olfactory function, mice were placed in a mouse cage with either water or cinnamon extract-soaked swabs. The swabs were placed on either side of the clean mouse cage. The subject mice were allowed to sniff and explore the swabs for 4 min. The time spent sniffing each swab was measured and analyzed.

2.9.12 Fluorescent non-canonical amino acid tagging (FUNCAT)

Mice were kept on a low-methionine diet for seven days. The next day, mice received azidohomoalanine (AHA) intraperitoneally (100 µg/gbw, i.p., Click-IT™ AHA (L-Azidohomoalanine), Cat No. C10102, Thermo Fisher Scientific). After 3 hours, mice were anesthetized and perfused transcardially with 4% PFA. The extracted brains were kept overnight in PFA 4% at room temperature 4ºC for 24 h. Brains were then sectioned at 40 µm thickness. After washing, sections were blocked overnight at 4ºC in blocking solution composed of 10% normal goat serum, 0.5% Triton-X100, and 5% sucrose in PBS. Sections were then "clicked" overnight in click buffer containing 200 µM triazole ligand, 400 µM TCEP, 2 µM fluorescent Alexa Fluor 647 alkyne (Alexa Fluor™ 647 Alkyne, Cat No. A10278, Thermo Fisher Scientific), and 200 µM CuSO4 in PBS. Sections were then washed and mounted on glass slides, imaged using a confocal microscope (Zeiss, LSM 880), and analyzed using ImageJ. FUNCAT images were acquired using an Airyscan mode on the Zeiss confocal microscope (LSM880) with 63X/1.40 Oil DIC f/ELYRA objective from two sections per mouse. Quantification was performed as described for immunohistochemistry. Forty excitatory and 16-20 inhibitory neurons were quantified per mouse.

2.9.13 Pharmacological reagents

NV-5138 hydrochloride (Cat No. HY-114384B, MedChemExpress) was first dissolved in DMSO at 100 µg/µl. Then, it was further diluted in 5% Tween-80 and 40% PEG300 in saline (10.6 µg/µl) and administered via oral gavage at 160 mg/kg. Temsirolimus (CCI-779, Cat No. ab141999, Abcam) was first dissolved in DMSO at 50 µg/µl. Then, it was diluted in 5% Tween-80 and 5% PEG300 in saline (0.74 µg/µl) and injected at 7.5 mg/kg i.p. Anisomycin (Cat No.

A9789, Sigma-Aldrich) was first dissolved in DMSO at 40 mM and brain slices (maintained in oxygenated ACSF) were incubated with anisomycin (40 µM) for 1h before AHA application.

2.9.14 Audiogenic seizure test

Adult male mice were individually placed in a soundproof Plexiglas cage and allowed to habituate for 2 min. Then a high-pitch siren (120 dB) was remotely turned on for 2 minutes. The number of wild running, tonic-clonic seizures, and status epilepticus/reparatory arrests were counted, and the percentage of incidents was analyzed. Note that status epilepticus is followed by an immediate respiratory arrest and death.

2.9.15 Field potential recordings

Following anesthesia induced by isoflurane, brains of one-month-old male mice were rapidly extracted and dipped into an ice-cold sucrose-based cutting-solution (87 mM NaCl, 2.5 mM KCl, 1.25 mM NaH_2PO_4, 7 mM $MgSO_4$, 0.5 mM $CaCl_2$, 25 mM $NaHCO_3$, 25 mM glucose, and 75 mM sucrose) and bubbled with 95% O_2 and 5% CO_2. Brains were sectioned using a vibratome to acquire transverse sections of 400 µm thickness. A surgical cut was performed to disconnect CA1 and CA3 regions of the hippocampus. Free-floating sections were allowed to recover in oxygenated and 32°C artificial cerebrospinal fluid (ACSF; 124 mM NaCl, 5 mM KCl, 1.25 mM NaH_2PO_4, 2 mM $MgSO_4$, 2 mM $CaCl_2$, 26 mM $NaHCO_3$ and 10 mM glucose) for 2 h. One slice was then placed into the chamber and perfused with ACSF at 28 °C for an additional 30 min. Using a glass electrode (impedance; 2-4 MΩ) filled with ACSF, field excitatory postsynaptic potentials (fEPSP) were recorded from the CA1 stratum radiatum while the Schaffer collateral pathway was stimulated using a concentric bipolar tungsten stimulating electrode with 0.1 ms pulses at 0.033 Hz. The intensity was adjusted to evoke fEPSPs with 50% maximal amplitude. mGluR-dependent LTD was induced using group I mGluR agonist (S)-3,5-Dihydroxyphenylglycine (DHPG, Cat No. ab120007, Abcam) in ACSF perfusion (50

μM for 10 min). fEPSPs were recorded for one hour after induction of LTD. fEPSP slope between 10% and 90% of the maximal fEPSP amplitude was computed on Clampfit software. Fiber volley and population spikes were excluded from the analysis.

2.9.16 Statistical analysis

GraphPad Prism 9 (GraphPad Prism Software Inc., USA) was used for statistical analysis. Data are shown as mean ± s.e.m., and the significance level was set at 0.05 or $p < 0.05$. A two-tailed unpaired Student's t-test was performed to determine the differences between the two groups. Differences between multiple groups were determined using either one-way ANOVA or two-way ANOVA followed by either Tukey's or Bonferroni's post-tests. Fischer's exact test (two-sided) was performed to analyze differences in the percent of seizure incidents and TRAP data. Statistical details of individual experiments are presented in figure legends. All experiments were scored by an experimenter blind to genotypes and treatments. Data points in all graphs represent the number of animals.

2.10 Materials and Correspondence

Correspondence and requests for materials should be addressed to Nahum Sonenberg, Christos Gkogkas, and Arkady Khoutorsky. All data are available in the main text or supplementary materials.

2.11 References

Alvarez-Castelao, B., Tom Dieck, S., Fusco, C.M., Donlin-Asp, P., Perez, J.D., and Schuman, E.M. (2020). The switch-like expression of heme-regulated kinase 1 mediates neuronal proteostasis following proteasome inhibition. Elife *9*. 10.7554/eLife.52714.

Auerbach, B.D., Osterweil, E.K., and Bear, M.F. (2011). Mutations causing syndromic autism define an axis of synaptic pathophysiology. Nature *480*, 63-68. 10.1038/nature10658.

Back, S.H., Scheuner, D., Han, J., Song, B., Ribick, M., Wang, J., Gildersleeve, R.D., Pennathur, S., and Kaufman, R.J. (2009). Translation attenuation through eIF2alpha phosphorylation prevents oxidative stress and maintains the differentiated state in beta cells. Cell Metab *10*, 13-26. 10.1016/j.cmet.2009.06.002.

Bagni, C., and Zukin, R.S. (2019). A Synaptic Perspective of Fragile X Syndrome and Autism Spectrum Disorders. Neuron *101*, 1070-1088. 10.1016/j.neuron.2019.02.041.

Barnes, S.A., Wijetunge, L.S., Jackson, A.D., Katsanevaki, D., Osterweil, E.K., Komiyama, N.H., Grant, S.G., Bear, M.F., Nagerl, U.V., Kind, P.C., and Wyllie, D.J. (2015).

Convergence of Hippocampal Pathophysiology in Syngap+/- and Fmr1-/y Mice. J Neurosci *35*, 15073-15081. 10.1523/JNEUROSCI.1087-15.2015.

Bhattacharya, A., Kaphzan, H., Alvarez-Dieppa, A.C., Murphy, J.P., Pierre, P., and Klann, E. (2012). Genetic removal of p70 S6 kinase 1 corrects molecular, synaptic, and behavioral phenotypes in fragile X syndrome mice. Neuron *76*, 325-337. 10.1016/j.neuron.2012.07.022.

Ceolin, L., Bouquier, N., Vitre-Boubaker, J., Rialle, S., Severac, D., Valjent, E., Perroy, J., and Puighermanal, E. (2017). Cell Type-Specific mRNA Dysregulation in Hippocampal CA1 Pyramidal Neurons of the Fragile X Syndrome Mouse Model. Front Mol Neurosci *10*, 340. 10.3389/fnmol.2017.00340.

Costa-Mattioli, M., and Walter, P. (2020). The integrated stress response: From mechanism to disease. Science *368*. 10.1126/science.aat5314.

Curia, G., Papouin, T., Seguela, P., and Avoli, M. (2009). Downregulation of tonic GABAergic inhibition in a mouse model of fragile X syndrome. Cereb Cortex *19*, 1515-1520. 10.1093/cercor/bhn159.

Dieterich, D.C., Hodas, J.J., Gouzer, G., Shadrin, I.Y., Ngo, J.T., Triller, A., Tirrell, D.A., and Schuman, E.M. (2010). In situ visualization and dynamics of newly synthesized proteins in rat hippocampal neurons. Nat Neurosci *13*, 897-905. 10.1038/nn.2580.

Endo, T., Shioiri, T., Kitamura, H., Kimura, T., Endo, S., Masuzawa, N., and Someya, T. (2007). Altered chemical metabolites in the amygdala-hippocampus region contribute to autistic symptoms of autism spectrum disorders. Biol Psychiatry *62*, 1030-1037. 10.1016/j.biopsych.2007.05.015.

Gandin, V., Masvidal, L., Cargnello, M., Gyenis, L., McLaughlan, S., Cai, Y., Tenkerian, C., Morita, M., Balanathan, P., Jean-Jean, O., et al. (2016). mTORC1 and CK2 coordinate ternary and eIF4F complex assembly. Nat Commun *7*, 11127. 10.1038/ncomms11127.
Gkogkas, C.G., Khoutorsky, A., Ran, I., Rampakakis, E., Nevarko, T., Weatherill, D.B.,

Vasuta, C., Yee, S., Truitt, M., Dallaire, P., et al. (2013). Autism-related deficits via dysregulated eIF4E-dependent translational control. Nature *493*, 371-377. 10.1038/nature11628.

Gonzalez, D., Tomasek, M., Hays, S., Sridhar, V., Ammanuel, S., Chang, C.W., Pawlowski, K., Huber, K.M., and Gibson, J.R. (2019). Audiogenic Seizures in the Fmr1 Knock-Out Mouse Are Induced by Fmr1 Deletion in Subcortical, VGlut2-Expressing Excitatory Neurons and Require Deletion in the Inferior Colliculus. J Neurosci *39*, 9852-9863. 10.1523/JNEUROSCI.0886-19.2019.

Hagerman, R.J., Berry-Kravis, E., Hazlett, H.C., Bailey, D.B., Jr., Moine, H., Kooy, R.F., Tassone, F., Gantois, I., Sonenberg, N., Mandel, J.L., and Hagerman, P.J. (2017). Fragile X syndrome. Nat Rev Dis Primers *3*, 17065. 10.1038/nrdp.2017.65.

Harding, H.P., Novoa, I., Zhang, Y., Zeng, H., Wek, R., Schapira, M., and Ron, D. (2000). Regulated translation initiation controls stress-induced gene expression in mammalian cells. Mol Cell *6*, 1099-1108. 10.1016/s1097-2765(00)00108-8.

Heiman, M., Schaefer, A., Gong, S., Peterson, J.D., Day, M., Ramsey, K.E., Suarez-Farinas, M., Schwarz, C., Stephan, D.A., Surmeier, D.J., et al. (2008). A translational profiling approach for the molecular characterization of CNS cell types. Cell *135*, 738-748. 10.1016/j.cell.2008.10.028.

Helseth, A.R., Hernandez-Martinez, R., Hall, V.L., Oliver, M.L., Turner, B.D., Caffall, Z.F., Rittiner, J.E., Shipman, M.K., King, C.S., Gradinaru, V., et al. (2021). Cholinergic neurons constitutively engage the ISR for dopamine modulation and skill learning in mice. Science *372*. 10.1126/science.abe1931.

Hinnebusch, A.G., Ivanov, I.P., and Sonenberg, N. (2016). Translational control by 5'-untranslated regions of eukaryotic mRNAs. Science *352*, 1413-1416. 10.1126/science.aad9868.

Hoeffer, C.A., Sanchez, E., Hagerman, R.J., Mu, Y., Nguyen, D.V., Wong, H., Whelan, A.M., Zukin, R.S., Klann, E., and Tassone, F. (2012). Altered mTOR signaling and enhanced CYFIP2 expression levels in subjects with fragile X syndrome. Genes Brain Behav *11*, 332-341. 10.1111/j.1601-183X.2012.00768.x.

Hornberg, H., Perez-Garci, E., Schreiner, D., Hatstatt-Burkle, L., Magara, F., Baudouin, S., Matter, A., Nacro, K., Pecho-Vrieseling, E., and Scheiffele, P. (2020). Rescue of oxytocin response and social behaviour in a mouse model of autism. Nature *584*, 252-256. 10.1038/s41586-020-2563-7.

Huber, K.M., Gallagher, S.M., Warren, S.T., and Bear, M.F. (2002). Altered synaptic plasticity in a mouse model of fragile X mental retardation. Proc Natl Acad Sci U S A *99*, 7746-7750. 10.1073/pnas.122205699.

Jacquemont, S., Pacini, L., Jonch, A.E., Cencelli, G., Rozenberg, I., He, Y., D'Andrea, L., Pedini, G., Eldeeb, M., Willemsen, R., et al. (2018). Protein synthesis levels are increased in a subset of individuals with fragile X syndrome. Hum Mol Genet *27*, 3825. 10.1093/hmg/ddy291.

Kelleher, R.J., 3rd, and Bear, M.F. (2008). The autistic neuron: troubled translation? Cell *135*, 401-406. 10.1016/j.cell.2008.10.017.

Kwon, C.H., Zhu, X., Zhang, J., and Baker, S.J. (2003). mTor is required for hypertrophy of Pten-deficient neuronal soma in vivo. Proc Natl Acad Sci U S A *100*, 12923-12928. 10.1073/pnas.2132711100.

Liu, S., Yuan, J., Yue, W., Bi, Y., Shen, X., Gao, J., Xu, X., and Lu, Z. (2018). GCN2 deficiency protects against high fat diet induced hepatic steatosis and insulin resistance in mice. Biochim Biophys Acta Mol Basis Dis *1864*, 3257-3267. 10.1016/j.bbadis.2018.07.012.

Olmos-Serrano, J.L., Paluszkiewicz, S.M., Martin, B.S., Kaufmann, W.E., Corbin, J.G., and Huntsman, M.M. (2010). Defective GABAergic neurotransmission and pharmacological rescue of neuronal hyperexcitability in the amygdala in a mouse model of fragile X syndrome. J Neurosci *30*, 9929-9938. 10.1523/JNEUROSCI.1714-10.2010.

Qin, M., Kang, J., Burlin, T.V., Jiang, C., and Smith, C.B. (2005). Postadolescent changes in regional cerebral protein synthesis: an in vivo study in the FMR1 null mouse. J Neurosci *25*, 5087-5095. 10.1523/JNEUROSCI.0093-05.2005.

Rosina, E., Battan, B., Siracusano, M., Di Criscio, L., Hollis, F., Pacini, L., Curatolo, P., and Bagni, C. (2019). Disruption of mTOR and MAPK pathways correlates with severity in idiopathic autism. Transl Psychiatry *9*, 50. 10.1038/s41398-018-0335-z.

Santini, E., Huynh, T.N., MacAskill, A.F., Carter, A.G., Pierre, P., Ruggero, D., Kaphzan, H., and Klann, E. (2013). Exaggerated translation causes synaptic and behavioural aberrations associated with autism. Nature *493*, 411-415. 10.1038/nature11782.

Sawicka, K., Hale, C.R., Park, C.Y., Fak, J.J., Gresack, J.E., Van Driesche, S.J., Kang, J.J., Darnell, J.C., and Darnell, R.B. (2019). FMRP has a cell-type-specific role in CA1 pyramidal neurons to regulate autism-related transcripts and circadian memory. Elife *8*. 10.7554/eLife.46919.

Scheuner, D., Song, B., McEwen, E., Liu, C., Laybutt, R., Gillespie, P., Saunders, T., Bonner-Weir, S., and Kaufman, R.J. (2001). Translational control is required for the unfolded protein response and in vivo glucose homeostasis. Mol Cell *7*, 1165-1176. 10.1016/s1097-2765(01)00265-9.

Scheuner, D., Vander Mierde, D., Song, B., Flamez, D., Creemers, J.W., Tsukamoto, K., Ribick, M., Schuit, F.C., and Kaufman, R.J. (2005). Control of mRNA translation preserves endoplasmic reticulum function in beta cells and maintains glucose homeostasis. Nat Med *11*, 757-764. 10.1038/nm1259.

Sengupta, S., Giaime, E., Narayan, S., Hahm, S., Howell, J., O'Neill, D., Vlasuk, G.P., and Saiah, E. (2019). Discovery of NV-5138, the first selective Brain mTORC1 activator. Sci Rep *9*, 4107. 10.1038/s41598-019-40693-5.

Sharma, A., Hoeffer, C.A., Takayasu, Y., Miyawaki, T., McBride, S.M., Klann, E., and Zukin, R.S. (2010). Dysregulation of mTOR signaling in fragile X syndrome. J Neurosci *30*, 694-702. 10.1523/JNEUROSCI.3696-09.2010.

Sharma, V., Sood, R., Khlaifia, A., Eslamizade, M.J., Hung, T.Y., Lou, D., Asgarihafshejani, A., Lalzar, M., Kiniry, S.J., Stokes, M.P., et al. (2020). eIF2alpha controls memory consolidation via excitatory and somatostatin neurons. Nature *586*, 412-416. 10.1038/s41586-020-2805-8.

Thomson, S.R., Seo, S.S., Barnes, S.A., Louros, S.R., Muscas, M., Dando, O., Kirby, C., Wyllie, D.J.A., Hardingham, G.E., Kind, P.C., and Osterweil, E.K. (2017). Cell-Type-Specific Translation Profiling Reveals a Novel Strategy for Treating Fragile X Syndrome. Neuron *95*, 550-563 e555. 10.1016/j.neuron.2017.07.013.

Torossian, A., Sare, R.M., Loutaev, I., and Smith, C.B. (2021). Increased rates of cerebral protein synthesis in Shank3 knockout mice: Implications for a link between synaptic protein deficit and dysregulated protein synthesis in autism spectrum disorder/intellectual disability. Neurobiol Dis *148*, 105213. 10.1016/j.nbd.2020.105213.

Trinh, M.A., and Klann, E. (2013). Translational control by eIF2alpha kinases in long-lasting synaptic plasticity and long-term memory. Neurobiol Learn Mem *105*, 93-99. 10.1016/j.nlm.2013.04.013.

Utami, K.H., Yusof, N., Kwa, J.E., Peteri, U.K., Castren, M.L., and Pouladi, M.A. (2020). Elevated de novo protein synthesis in FMRP-deficient human neurons and its correction by metformin treatment. Mol Autism *11*, 41. 10.1186/s13229-020-00350-5.

Van der Aa, N., and Kooy, R.F. (2020). GABAergic abnormalities in the fragile X syndrome. Eur J Paediatr Neurol *24*, 100-104. 10.1016/j.ejpn.2019.12.022.

Velmeshev, D., Schirmer, L., Jung, D., Haeussler, M., Perez, Y., Mayer, S., Bhaduri, A., Goyal, N., Rowitch, D.H., and Kriegstein, A.R. (2019). Single-cell genomics identifies cell type-specific molecular changes in autism. Science *364*, 685-689. 10.1126/science.aav8130.

Walter, P., and Ron, D. (2011). The unfolded protein response: from stress pathway to homeostatic regulation. Science *334*, 1081-1086. 10.1126/science.1209038.

Weston, C.S.E. (2019). Four Social Brain Regions, Their Dysfunctions, and Sequelae, Extensively Explain Autism Spectrum Disorder Symptomatology. Brain Sci *9*. 10.3390/brainsci9060130.

Xu, Z.X., Kim, G.H., Tan, J.W., Riso, A.E., Sun, Y., Xu, E.Y., Liao, G.Y., Xu, H., Lee, S.H., Do, N.Y., et al. (2020). Elevated protein synthesis in microglia causes autism-like synaptic and behavioral aberrations. Nat Commun *11*, 1797. 10.1038/s41467-020-15530-3.

Yizhar, O., Fenno, L.E., Prigge, M., Schneider, F., Davidson, T.J., O'Shea, D.J., Sohal, V.S., Goshen, I., Finkelstein, J., Paz, J.T., et al. (2011). Neocortical excitation/inhibition balance in information processing and social dysfunction. Nature *477*, 171-178. 10.1038/nature10360.

Zhao, H., Cui, K., Nie, F., Wang, L., Brandl, M.B., Jin, G., Li, F., Mao, Y., Xue, Z., Rodriguez, A., et al. (2012). The effect of mTOR inhibition alone or combined with MEK inhibitors on brain metastasis: an in vivo analysis in triple-negative breast cancer models. Breast Cancer Res Treat *131*, 425-436. 10.1007/s10549-011-1420-7.

Connecting the text - chapter 2 to chapter 3

It has been established over a couple of decades that dysregulated mRNA translation is associated with an autistic phenotype in both autistic individuals and animal models. The three principal signaling pathways that predominantly regulate mRNA translation are mTORC1, integrated stress response (ISR), and MAPK/ERK. In the first chapter, we showed that the integrated stress response is dysregulated in a cell-type specific manner in the brain of *Fmr*1 KO mice. In the second chapter, we have investigated the mTORC1 pathway in a cell-type specific fashion to explore whether cell-specific ablation of 4E-BP2, a main downstream effector of mTORC1, can cause an autistic-like phenotype in mice.

Chapter 3: 4E-BP2-dependent translation in cerebellar Purkinje cells controls spatial memory but not autistic-like behaviors

Mehdi Hooshmandi[1,#], Vinh Tai Truong[2,#], Eviatar Fields[3,4], Riya Elizabeth Thomas[5], Calvin Wong[1], Vijendra Sharma[2], Ilse Gantois[2], Patricia Soriano Roque[1], Kleanthi Chalkiadaki[6], Neil Wu[1], Anindyo Chakraborty[1], Soroush Tahmasebi[7], Masha Prager-Khoutorsky[8], Nahum Sonenberg[2], Aparna Suvrathan[5], Alanna J. Watt[3], Christos G. Gkogkas[6,*] and Arkady Khoutorsky[1,9,*]

Cell Reports, https://doi.org/10.1016/j.celrep.2021.109036

3.1 Abstract

Recent studies have demonstrated that selective activation of mTORC1 in the cerebellum by deletion of mTORC1 upstream repressors TSC1 or PTEN in Purkinje cells (PCs) causes autistic-like features and cognitive deficits. However, the molecular mechanisms by which overactivated mTORC1 in the cerebellum engenders these behaviors remain unknown. The eukaryotic translation initiation factor 4E-binding protein 2 (4E-BP2) is a central translational repressor downstream of mTORC1. Here we show that mice with selective ablation of 4E-BP2 in PCs display a reduced number of PCs, increased regularity of PCs action potential firing, and deficits in motor learning. Surprisingly, while spatial memory is impaired in these mice, they exhibit normal social interaction and show no deficits in repetitive behavior. Together, our data suggest that downstream of mTORC1/4E-BP2, there are distinct cerebellar mechanisms independently controlling social behavior and memory formation.

Keywords: 4E-BP2, Purkinje cells, spatial memory, motor learning, autism spectrum disorders.

3.2 Introduction

Autism spectrum disorders (ASDs), which affect ~1% of the general population (Lai and Baron-Cohen, 2015), are a set of heterogeneous neurodevelopmental conditions characterized by a persistent impairment in social interaction, communication deficits, and the presence of repetitive activities, restricted interests, and stereotypic behaviors (Association, 2013). Although the etiology and pathogenicity of ASD remain largely unknown, mutations in genes encoding proteins involved in the regulation of mRNA translation and synaptic homeostasis are often associated with the monogenic forms of ASD (Santini and Klann, 2014).

Mammalian target of rapamycin complex 1 (mTORC1) is a master regulator of mRNA translation and is overactivated in several monogenic forms of ASD. Loss-of-function mutations in negative regulators of mTORC1, such as phosphatase and tensin homolog

(*PTEN)*, tuberous sclerosis complex 1/2 (*TSC1/*2), and neurofibromatosis 1 (*NF1*), lead to the hyperactivation of the PI3K-Akt-mTORC1 pathway and high rates of macrocephaly (Butler et al., 2005), cognitive deficits and ASD-related behaviors (Bilder et al., 2016; Huber et al., 2015). mTORC1 is also overactivated in patients diagnosed with fragile X syndrome (FXS) (Hoeffer et al., 2012), a leading cause of heritable intellectual disability and the most common monogenic cause of autism (Belmonte and Bourgeron, 2006; Wang et al., 2010), as well as in the brain of FXS mouse model, *Fmr1* knockout (KO) mice (Sharma et al., 2010).

mTORC1 regulates mRNA translation via its two main downstream effectors, p70 ribosomal protein S6 kinase (S6K) and eukaryotic initiation factor 4E-binding proteins (4E-BPs) (Hay and Sonenberg, 2004). 4E-BPs bind and repress the activity of the mRNA cap-binding protein eIF4E, which promotes translation initiation via binding to the mRNA 5' cap (7-methylguanosine triphosphate) and recruiting the ribosome to the mRNA (Sonenberg and Hinnebusch, 2009). mTORC1 phosphorylates 4E-BPs and thereby releases eIF4E from 4E-BP repression, leading to the activation of translation initiation. There are three 4E-BP isoforms in mammals (4E-BP1, 4E-BP2 and 4E-BP3) that are similar in function but vary in tissue distribution. 4E-BP2 is the predominant paralog in the brain (Banko et al., 2005a; Bidinosti et al., 2010), whereas 4E-BP3 is not expressed in the brain (Poulin et al., 1998). Since deletion of 4E-BP2 mimics mTORC1/eIF4E hyperactivation, *Eif4ebp2* knockout mice (4E-BP2 KO) constitute an attractive model for studying mTORC1 downstream mechanisms (Banko et al., 2005b; Gkogkas et al., 2013). 4E-BP2 whole body KO mice exhibit core ASD phenotypes, including impaired social interaction, communication deficits, and repetitive behaviors (Gkogkas et al., 2013). Conditional deletion of 4E-BP2 in excitatory and inhibitory neurons revealed that the ASD-like behaviors are mediated via inhibitory neurons, as mice with deletion of 4E-BP2 in GABAergic but not glutamatergic neurons show autistic traits (Wiebe et al., 2019). An important role of 4E-BP2/eIF4E in ASD is further supported by studies showing

that overexpression of eIF4E leads to ASD-associated behaviors (Santini et al., 2013) and gain-of-function mutations in eIF4E have been found in ASD patients (Neves-Pereira et al., 2009). 4E-BP2 is also involved in the regulation of memory formation, as 4E-BP2 KO mice exhibit impaired synaptic plasticity and long-term memory (Banko et al., 2005a).

Despite the traditional notion that cerebellar functions are limited to controlling motor learning, coordination, and balance, recent findings suggest that the cerebellum also plays a role in memory formation (Akshoomoff and Courchesne, 1992; Daum et al., 1993; Gandhi et al., 2000) and autistic behaviors (Fatemi et al., 2002; Kaufmann et al., 2003; Palmen et al., 2004). While the neocortex has historically been regarded as the principal brain region giving rise to ASDs, cerebellar injury at birth carries the largest single non-heritable risk for ASD (Wang et al., 2014), and loss of PCs is one of the salient anatomical pathologies in post-mortem brain samples of ASD patients (Palmen et al., 2004; Skefos et al., 2014; Wegiel et al., 2014). Neuronal activity has been observed in the posterior cerebellar hemispheres following cognitive tasks such as attention shifting or verbal working memory tasks (Allen et al., 1997; Desmond et al., 1997), indicating that damage to this region could underlie difficulties in problem solving and attention-shifting impairments, both of which are characteristics of autistic patients (Courchesne et al., 1994). Interestingly, emotional outbursts, difficulty understanding social cues, mood changes, and repetitive behaviors are also present in individuals with tumors, injuries, or congenital defects affecting the cerebellum (Bolduc et al., 2011). Recent studies have established a functional connection between enhanced mTORC1 activity in the cerebellum, and autistic behaviors in mice by showing that deletion of PTEN and TSC1 in PCs lead to core ASD features (impaired social interaction and repetitive behaviors) (Cupolillo et al., 2016; Reith et al., 2011; Tsai et al., 2012), and rapamycin treatment reverses aberrant phenotypes in TSC1 conditional KO mice (Tsai et al., 2012).

To study whether 4E-BP2 mediates the effects of mTORC1 overactivation in PCs, we generated transgenic mice lacking 4E-BP2 in PCs. These mice displayed a reduction in the number of PCs, increased regularity of PCs firing, and exhibited impaired motor learning. Notably, the mice showed no ASD-like phenotypes but exhibited an impairment in spatial memory. Our results indicate that ASD-associated behaviors do not depend on cerebellar 4E-BP2, whereas spatial memory is 4E-BP2-dependent.

3.3 Results

3.3.1 Generation of mice with conditional deletion of 4E-BP2 in cerebellar Purkinje neurons.

Immunostaining of cerebellar sections for 4E-BP1 and 4E-BP2 showed that cerebellar PCs preferentially express 4E-BP2, whereas the levels of 4E-BP1 are lower in these cells. To study the role of 4E-BP2 in cerebellar PCs in ASD-like behaviors and memory formation, we generated transgenic mice with selective ablation of *Eif4ebp2* in cerebellar PCs (*Eif4ebp2*$^{f/f}$; L7^{Cre}, hereafter referred to as 4E-BP2 conditional KO (cKO)). Cre recombinase in L7^{Cre} mouse is expressed selectively in cerebellar PCs and its expression was detected starting at postnatal day 6 (P6) (Barski et al., 2000). Western blot analysis of cerebellum tissue from 4E-BP2 cKO mice showed a decrease of ~61% in the levels of 4E-BP2 (Fig. 1A; control: 1 ± 0.06, 4E-BP2 cKO: 0.39 ± 0.04, $t(7) = 7.96$, $p = 0.0001$, Student's *t*-test) and immunohistochemistry revealed an almost complete absence of 4E-BP2 in PCs, identified by immunostaining for calbindin (Fig. 1B; control: 100 ± 5.8, 4E-BP2 cKO: 5.23 ± 1.2, $t(4) = 15.97$, $p = 0.0001$, Student's *t*-test). No reductions in 4E-BP2 levels were detected in hippocampal or prefrontal cortex sections from 4E-BP2 cKO mice (Fig. 1C-hippocampus; control: 100 ± 5.40, 4E-BP2 cKO: 112.49 ± 9.23, $t(6) = 1.67$, $p = 0.2875$, Student's *t*-test, Fig. 1D-preforntal cortex; control: 100 ± 6.54, 4E-BP2 cKO: 85.91 ± 7.1, $t(6) = 1.2$, $p = 0.2753$, Student's *t*-test), indicating efficient

and highly specific elimination of 4E-BP2 in cerebellar PCs. Deletion of 4E-BP2 in PCs did not affect the expression of 4E-BP1 in these cells (Fig. 1F), however, it caused a more pronounced staining of 4E-BP1 in cells within the molecular layer, likely representing basket/stellate cells or Bergman glia (Fig. 1F).

To assess the activity of eIF4E in PCs lacking 4E-BP2, we immunostained against neuroligin 1, whose translation is eIF4E-sensitive (Gkogkas et al., 2013), and gephyrin, whose translation is eIF4E-insensitive (Gkogkas et al., 2013). Protein levels of neuroligin 1 in PCs of 4E-BP2 cKO mice were increased as compared to control animals (Fig. 1G; control: 100 ± 3.46, 4E-BP2 cKO: 128.50 ± 10.35, $t(6) = 2.61$, $p = 0.0399$, Student's t-test), whereas the expression of gephyrin was not altered (Fig. 1H). These results are consistent with the notion that the deletion of 4E-BP2 in PCs de-represses eIF4E activity. To determine the impact of 4E-BP2 ablation on general protein synthesis, we employed fluorescent non-canonical amino-acid tagging (FUNCAT) assay, based on azidohomoalanine (AHA, an analog of methionine) metabolic labeling (Tom Dieck et al., 2012). AHA incorporation was not different in PCs of 4E-BP2 cKO mice as compared to control animals (Fig. 1I; control: 100 ± 6.30, 4E-BP2 cKO: 93.31 ± 8.32, $t(6) = 0.64$, $p = 0.5435$, Student's t-test). Altogether, these results show that deletion of 4E-BP2 in cerebellar PCs does not alter general protein synthesis, but preferentially affects the expression of specific eIF4E-sensitive mRNAs.

3.3.2 Loss of Purkinje cells in 4E-BP2 cKO mice

Several studies have consistently shown a reduction in the number of cerebellar PCs in both ASD patients and autism animal models (Bauman and Kemper, 2005; Cupolillo et al., 2016; Fehlow et al., 1993). The loss of PCs has been reported in mice with PC-specific ablation of *Tsc1*. TSC1 is an upstream repressor of mTORC1 and its ablation leads to the activation of the mTORC1 pathway (Tsai et al., 2012). 4E-BP2 is the main downstream effector of mTORC1

(Hay and Sonenberg, 2004), and its deletion mimics mTORC1/eIF4E hyperactivation. To determine whether the number of cerebellar PCs was affected in the cerebellum of the 4E-BP2 cKO mice, we counted calbindin-labeled PCs and found that their number was significantly reduced in lobules VI and VII in the vermis area of 4E-BP2 cKO mice as compared to controls (Fig. 2; cells in lobules VI and VII, control: 131.8 ± 1.75, 4E-BP2 cKO: 84 ± 7.15, $t(6) = 6.48$, $p = 0.0006$, Student's *t*-test), but not in other lobules.

3.3.3 Purkinje cells in 4E-BP2 cKO mice fire action potentials at higher regularity than controls.

Purkinje cells spontaneously fire action potentials at frequencies of up to 200 Hz with pace-maker like precision in their timing in brain slices (Häusser and Clark, 1997; Watt et al., 2009). These regular, high-frequency action potentials are important for the maintenance of normal motor functions and distinct cognitive behaviors (Hourez et al., 2011; Jayabal et al., 2016; Stoodley et al., 2017). Several mouse models of ASD exhibit alterations in the intrinsic firing of PCs. For example, reduced PCs action potential firing rates, with no alteration in their regularity, have been reported in Purkinje cell-specific *Tsc1* (Tsai et al., 2012; Tsai et al., 2018) and *Pten* (Cupolillo et al., 2016) knockout mice. As mTORC1 is hyperactivated in both the *Tsc1* and *Pten* conditional knockout mice, we hypothesized that PCs firing rate might be altered in 4E-BP2 cKO mice. We performed non-invasive extracellular/loose cell-attached recordings from the soma of PCs in acute cerebellar slices from 4E-BP2 cKO and wild-type control mice (Fig. 3A). Fast excitatory and inhibitory synaptic transmissions were pharmacologically blocked to isolate the intrinsic conductance of the PCs. Surprisingly, in contrast to findings in the *Tsc1* and *Pten* conditional knockout mice, we found no significant differences in firing rate of PCs from control and 4E-BP2 cKO mice (Fig. 3B, C; control: 48.49 ± 21.39 Hz, $n = 51$; 4E-BP2 cKO: 55 ± 29.52 Hz, $n = 60$; $p = 0.3074$, Mann-Whitney *U* Test; Fig. 3E - lobule III;

Fig. 3F - lobule VI). However, we found that the coefficient of variation (CV) of the inter-spike interval of simple spikes was reduced in 4E-BP2 cKO mice as compared to controls (Fig. 3G; control: 0.076 ± 0.05, n = 51; 4E-BP2 cKO: 0.065 ± 0.03, n = 60; p = 0.003, Mann-Whitney U Test). Plotting the distribution of the CV from both groups revealed a left-ward shift in the distribution of the CV of 4E-BP2 cKO PCs as compared to controls (Fig. 3H). A decrease in the CV showed regional specificity as it was detected in PCs located in lobule III (Fig. 3I) but not lobule VI (Fig. 3J). A protein synthesis-dependent form of long-term depression (LTD), induced by pairing of parallel fiber stimulation with depolarization of PCs, was not different between control and 4E-BP2 cKO cerebellar slices (Fig. 3K-M). Altogether, these results indicate that a subpopulation of 4E-BP2 KO PCs fire with higher regularity than control PCs.

3.3.4 Ablation of 4E-BP2 in PCs impairs motor learning

Cerebellar PCs play a pivotal role in motor coordination and learning (Nguyen-Vu et al., 2013). To study the role of 4E-BP2 in cerebellum-dependent motor functions, we subjected 4E-BP2 cKO mice to an accelerated mode of the rotarod test 3 times per day for 4 consecutive days. We observed no differences in basal motor functions on day 1 (Fig. 4A and B; t(60) = 0.375, p = 0.992). However, ablation of 4E-BP2 in cerebellar PCs caused an impairment in motor learning, since the mice learned less over the four days of training, and stayed on the rotarod for a significantly shorter duration compared to control animals (Fig. 4A and B; 4E-BP2 cKO: 51.5 ± 14.91 s, controls: 144.55 ± 25.35 s, two-way ANOVA, main effect of genotype, F(1, 15) = 4.7, p = 0.0446, Bonferroni's post hoc test for day 4, p = 0.0003).

3.3.5 Ablation of 4E-BP2 in cerebellar PCs does not cause autistic-like behaviors.

Enhanced activity of mTORC1 and eIF4E is implicated in several forms of ASD in humans (Kassai et al., 2014) and is recapitulated in animal models (Huang et al., 2016; Zhou et al.,

2009). Moreover, the whole body (Gkogkas et al., 2013) or GABAergic neuron-specific (Wiebe et al., 2019) deletion of 4E-BP2 engender ASD-like phenotypes. Because hyperactivation of mTORC1 induces ASD-like phenotypes in *TSC1*$^{f/f}$; L7^{Cre} mice and *PTEN*$^{f/f}$; L7^{Cre} mice (Cupolillo et al., 2016; Tsai et al., 2012), and PCs are GABAergic neurons, we hypothesized that 4E-BP2 in PCs might regulate phenotypes reminiscent of ASD. To test this hypothesis, we subjected 4E-BP2 cKO and control mice to a battery of behavioral assays to examine ASD-like behaviors. The open field test revealed no significant differences in total distance traveled over 10 minutes (Fig. 5A; control: 3.03 ± 0.13 m, 4E-BP2 cKO: 3.25 ± 0.2 m, $t(15) = 0.92$, $p = 0.3740$, Student's *t*-test), suggesting intact basal locomotor functions and activity. 4E-BP2 cKO and control mice spent similar time in the middle of the arena, demonstrating no anxiety phenotype in 4E-BP2 cKO mice (Fig. 5A; inside zone time, control: 28.36 ± 1.88 s, 4E-BP2 cKO: 29.69 ± 2.75 s, $t(15) = 0.48$, $p = 0.6892$). Elevated plus maze (EPM) test confirmed the lack of anxiety phenotype as 4E-BP2 cKO and control animals spent a similar amount of time in either the open or closed arms (Fig. 5B; open arm time, control: 53.33 ± 8.25 s and 4E-BP2 cKO: 56.63 ± 9.99 s, $t(15) = 0.25$, $p = 0.8013$; closed arm time, control: 212.4 ± 9.57 s and 4E-BP2 cKO: 212 ± 9.64 s, $t(15) = 0.03$, $p = 0.9752$, Student's *t*-test test for all parameters). No differences were detected between 4E-BP2 cKO and control mice in marble burying and self-grooming tests (Fig. 5C; marble burying, control: 3.78 ± 0.97, 4E-BP2 cKO: 4.86 ± 1.07, $t(15) = 0.76$, $p = 0.4591$, Student's *t*-test, Fig. 5D; self-grooming, control: 45.63 ± 10.66 s and 4E-BP2 cKO: 46.36 ± 12 s, $t(15) = 0.05$, $p = 0.9643$, Student's *t*-test), indicating no effect on repetitive/stereotypic behaviors.

Impaired social interaction is one of the core symptoms of ASDs (Grzadzinski et al., 2013). To evaluate social interaction in mice lacking 4E-BP2 in cerebellar PCs, we first assessed indirect social interaction using three-chamber sociability and social novelty test (Winslow, 2003). In the sociability phase of the test, both experimental groups spent

significantly more time interacting with the social stimulus (mouse enclosed in a wire cage) as compared to the non-social stimulus (empty wire cage), but no differences were found between the genotypes (Fig. 5E; left, chamber main effect $F(1, 30) = 25.38$, $p = 0.0001$, two-way ANOVA, Bonferroni's post hoc test, control: Empty 54.76 ± 7.59 s vs. Stranger1 88.50 ± 7.36 s, $p = 0.0115$, 4E-BP2 cKO: Empty 42.79 ± 3.463 s vs. Stranger1 81.91 ± 8.43 s, $p = 0.0049$, genotype and chamber interaction $F(1, 30) = 0.1385$, $p = 0.7124$, effect of genotype $F(1, 30) = 1.647$, $p = 0.2092$). Similarly, in the social novelty phase of the test, 4E-BP2 cKO and control mice interacted with the novel mouse (stranger 2) more than with the familiar mouse (stranger1), but no differences were found between the two genotypes (Fig. 5E right, chamber main effect $F(1, 30) = 33.51$, $p = 0.0001$, two way ANOVA, Bonferroni's post hoc test, control: Stranger1, 44.58 ± 6.55 s vs. Stranger 2, 96.12 ± 11.36 s, $p = 0.0008$, 4E-BP2 cKO: Stranger1, 34.48 ± 6.43 s vs. Stranger 2, 82.35 ± 7.69 s, $p = 0.0036$, genotype and chamber interaction $F(1, 30) = 0.045$, $p = 0.8329$, effect of genotype $F(1, 30) = 1.93$, $p = 0.1750$).

We next assessed male-male reciprocal social interaction and scored the total time of interaction of a test mouse with a stranger mouse. 4E-BP2 cKO and control mice did not show differences in total interaction time (Fig. 5F right; direct social interaction, control: 59.39 ± 8.39 s and 4E-BP2 cKO: 60.90 ± 9.65 s, $t(15) = 0.118$, $p = 0.9076$, Student's *t*-test). Overall, our analysis of indirect and direct social interaction indicates that the ablation of 4E-BP2 in cerebellar PCs does not cause social interaction deficits.

3.3.6 Impairment of spatial reference memory in mice with cerebellar PC-specific deletion of 4E-BP2.

A growing body of evidence indicates that the cerebellum, in addition to its central role in motor learning and memory, is also involved in the regulation of cognitive functions, including spatial learning and memory (Passot et al., 2012). Selective destruction of cerebellar PCs

impairs memory acquisition in the Morris water maze (MWM) (Gandhi et al., 2000), a classical task for assessing spatial learning and memory (Morris, 1984). Since 4E-BP2 global deletion disrupts long-term spatial memory (Banko et al., 2005a) and selective hyperactivation of mTORC1 in cerebellar PCs impairs reversal learning in water T maze (Tsai et al., 2012), we next assessed the role of PCs 4E-BP2 in spatial learning and memory by subjecting 4E-BP2 cKO mice to the MWM test. Overall, the escape latencies to find the hidden platform were not different between 4E-BP2 cKO and control mice during the course of five days of training (Fig. 6A; $F(1, 18) = 3.66$, $p = 0.0715$, two-way ANOVA). However, on the fifth training day, 4E-BP2 cKO mice reached the hidden platform significantly slower than control mice, indicating impaired learning (control: 15.33 ± 2.5 s, 4E-BP2 cKO: 29.48 ± 2.9 s, $p< 0.05$, Student's *t*-test). A probe test, performed 24 hours after the last training session, confirmed impaired spatial memory in 4E-BP2 cKO mice as they exhibited no preference for the quadrant in which the hidden platform was located during the training (target quadrant), whereas control animals spent significantly more time in the target quadrant and crossed the platform location significantly more than 4E-BP2 cKO mice (Fig. 6B; two-way ANOVA, significant interaction between group and quadrant occupancy $F(3, 72) = 7.74$, $p = 0.0002$, and main effect for quadrant occupancy $F(3, 72) = 4.53$, $p = 0.0057$, Bonferroni's post hoc test control: 34.46 ± 3.16 s and 4E-BP2 cKO: 20.66 ± 2.40 s in the target quadrant, $p = 0.0012$, Fig. 6C, platform crossings; control: 3.60 ± 0.58 and 4E-BP2 cKO: 1.10 ± 0.34, $t(18) = 3.69$, $p = 0.0017$, Student's *t*-test). Importantly, mice from both groups travelled a comparable distance (control: 2341 ± 33.32 cm, 4E-BP2 cKO: 2187 ± 84.36 cm, $t(18) =1.69$, $p = 0.19$, Fig. 6D) and exhibited similar thigmotaxis (swimming near the pool wall; control: 22.63 ± 4.18%, 4E-BP2 cKO: 31.16 ± 4.71%, $p = 0.19$), indicating unaltered motor functions and anxiety. 4E-BP2 cKO mice performed similarly to control animals in the visible version of the MWM test (control: 17.60 ± 2.95 s, 4E-BP2 cKO: 19.1 ± 3.28 s, $t(18) = 0.34$, $p = 0.7382$, Student's t-test), suggesting

intact vision and unaltered motivation to find the platform. The hippocampus plays a central role in spatial learning and memory (Bannerman et al., 2014; Eichenbaum, 2017). To confirm that hippocampal functions are intact in mice with deletion of 4E-BP2 in cerebellar PCs, we subjected 4E-BP2 cKO mice to contextual fear conditioning, a hippocampus-dependent test. Pairing of a specific context to a foot shock leads to the formation of long-term contextual fear memory. 4E-BP2 cKO mice showed no differences in freezing behaviour as compared to control animals when reintroduced to the training context 24 hours post-learning (control: 34.09 ± 5.5%, 4E-BP2 cKO: 44.17 ± 6.5%, $t(19) = 1.24$, $p = 0.2301$, Student's t-test), indicating intact hippocampal functions. Collectively, these results show that spatial learning and memory are impaired in MWM task in mice with deletion of 4E-BP2 in cerebellar PCs.

3.4 Discussion

Our study reveals that 4E-BP2-dependent translational control in cerebellar Purkinje cells plays a role in the control of spatial memory but not of autism-associated behaviors. 4E-BP2, a key mTORC1 downstream effector, has been previously implicated in both memory formation and ASD as whole-body deletion of 4E-BP2 leads to memory deficits and ASD phenotypes (Banko et al., 2005b; Gkogkas et al., 2013). 4E-BP2 deletion engenders autistic features via GABAergic neurons, as ablation of 4E-BP2 in inhibitory (using GAD2 Cre) but not excitatory neurons produces ASD phenotypes (Wiebe et al., 2019). Although Purkinje cells are GABAergic (Hirano, 2018) and thus are included in this ablation, our results show that the activation of mTORC1/4E-BP2/eIF4E signaling in Purkinje cells is not sufficient to produce ASD traits. We cannot, however, exclude the possibility that differences in developmental onset of promoters used to drive Cre expression in a previous study (GAD2, embryonic) (Wiebe et al., 2019) and our study (L7, postnatal) are the reason for the lack of ASD-like phenotypes in 4E-BP2 cKO mice. A previous study linked the overactivation of the mTORC1

pathway in the cerebellum to ASD behaviors by showing that in PC-specific *TSC1* KOs, rapamycin reverses autistic phenotypes (Tsai et al., 2012). Since our results show that 4E-BP2 is not involved in the regulation of these phenotypes, it is conceivable that other mTORC1 effectors, such as S6Ks, mediate autistic behaviors in cerebellum-specific *TSC1* KO mice. Indeed, hyperactivation of S6K1 contributes to ASD-like behaviors in *Fmr1* KO mice, as S6K pharmacological inhibition and genetic deletion of S6K1 reversed ASD-like behaviors in these animals (Bhattacharya et al., 2012). The specific role of S6K1 in the cerebellum in other ASD disorders with overactivation of mTORC1, such as Tuberous Sclerosis (TSC1/2) and PTEN hamartoma tumor syndrome, remains unknown. Another mechanism by which overactivated mTORC1 might produce ASD traits is via modulation of autophagy (Tang et al., 2014). mTORC1 inhibits various steps of autophagy, thereby regulating the balance between protein production and degradation (Yoon et al., 2008). mTORC1-dependent impairment of autophagy in $TSC1^{+/-}$ mice was proposed to mediate ASD-like behaviors and defects in the pruning of dendritic spines during development (Tang et al., 2014). A recent study showed that memory and social deficits in *Pten* heterozygous mice are caused by increased activity of mTORC2 (Chen et al., 2019). This finding raises the possibility that mTORC2 hyperactivation contributes to cognitive dysfunction in other disorders associated with enhanced mTOR activity.

There is a growing body of evidence implicating the cerebellum in the regulation of higher brain functions, such as social behaviors and spatial memory (Deverett et al., 2019; Kloth et al., 2015). Excitatory projections from the cerebellum to the ventral tegmental area (VTA), which mediates social behaviors in animals, have been described (Carta et al., 2019). These projections show enhanced activity during social interaction, and their optogenetic activation is rewarding in animals (Carta et al., 2019; Gil et al., 2013), indicating that the cerebello-VTA pathway might be a potential neuronal circuit by which the cerebellum

modulates social behaviors. Functional connectivity between the cerebellum and the medial prefrontal cortex (mPFC), a brain area highly implicated in social behaviors and ASD, has been recently demonstrated (Kelly et al., 2020).

Previous studies have shown that vestibular information, which is processed by the cerebellum, is essential for spatial navigation, as disruption of vestibular inputs results in deficits in spatial acquisition in the Morris water maze task (Semenov and Bures, 1989). Cerebellar PCs transform vestibular information from head-centered to earth-centered spatial reference signals, which are necessary for spatial orientation and learning (Rochefort et al., 2011b; Yakusheva et al., 2007). Mice expressing pseudosubstrate protein kinase C inhibitor (PKCI) in Purkinje cells show deficient long-term depression (LTD) at synapses between parallel fibers and PCs and exhibit impaired self-motion-dependent activity of hippocampal place cells, and deficient spatial navigation (Rochefort et al., 2011b). Whether these neuronal circuits in the cerebellum mediate the effects of overactivation of the mTORC1/4E-BP2 pathway on social behavior and spatial memory remains unknown.

Previous studies have shown that 4E-BP2/eIF4E-dependent translational control mechanisms are important for long-term memory formation, and their dysregulation leads to impairment in social interaction and repetitive/stereotypic behaviors. Our results demonstrate that cerebellar mechanisms regulating memory and ASD phenotypes are differentially dependent on 4E-BP2/eIF4E-mediated translation. 4E-BP2/eIF4E promotes translation of distinct mRNAs enriched with complex secondary structures at their 5'UTRs (Pelletier and Sonenberg, 1985; Sonenberg and Gingras, 1998), or harboring 5'UTR *cis*-regulatory elements (e.g. Cytosine Enriched Regulator of Translation (CERT)) (Leppek et al., 2018), or 5′ terminal oligopyrimidine tracts (5′ TOPs) (Thoreen et al., 2012). The specific sets of differentially translated genes, however, might be regulated by developmental stage and activity, thereby differentially impacting neuronal functions in memory formation and ASD behaviors.

We observed a region-specific decrease in the number of PCs in 4E-BP2 cKOs in lobules VI and VII. Since 4E-BP2 cKO mice do not exhibit ASD traits, this finding suggests that the loss of PCs in these lobules is not sufficient to induce ASD-like phenotypes but may underlie memory and/or motor learning deficits. This is consistent with studies showing that loss of PCs in mice with Purkinje cell degeneration such as *pcd* and Lurcher mutant mice (*Lc/+*) causes severe impairments in spatial learning and memory (Goodlett et al., 1992; Lalonde et al., 1988). This finding is also consistent with a study showing that lobule VI plays a role in flexible learning (Badura et al., 2018).

We found that ablation of 4E-BP2 in PCs does not change their firing rate. This was surprising since PC firing frequency reductions have been observed in mTORC1-related models of ASD (*TSC1* and *PTEN* cKO mice) (Cupolillo et al., 2016; Tsai et al., 2012). Since rescuing these firing rate deficits restores ASD-related behavior (Stoodley et al., 2017), PC firing frequency deficits are a core cellular pathophysiology that is thought to contribute to ASD-like behavior. Intact social behavior in 4E-BP2 cKO mice concomitant with unaltered PC firing rate further support the hypothesis that deficits in PC firing frequency underlie social behavior deficits in ASD models.

We did, however, find that PCs in 4E-BP2 cKO mice fired action potentials at higher regularity than controls. In the absence of synaptic input, PCs fire pace-maker-like action potentials with high regularity (shown by a low CV) (Häusser and Clark, 1997; Watt et al., 2009), and maintaining both rate and regularity is important for normal motor control and learning (Hong et al., 2016), although the relative contributions of rate and regularity remain unclear (Hoebeek et al., 2005; Payne et al., 2019). Decreases in the rate and/or regularity of PC firing have been observed in several cerebellar ataxias, and restoring either of these deficits to wild-type levels rescues deficits in motor behaviors (Ady et al., 2018; Cook et al., 2020; Hansen et al., 2013; Hourez et al., 2011; Jayabal et al., 2016; Shakkottai et al., 2011; Stoyas et al.,

2020; Walter et al., 2006). Interestingly, there are several examples of enhanced PC firing regularity being associated with motor symptoms including reduced motor learning, such as in a mouse model of spinocerebellar ataxia (SCA) type 7 (Faisal et al., 2008a), the spontaneous *waddles* mouse ataxia model (White et al., 2016), when inhibitory synaptic input onto PCs is removed (Shakkottai et al., 2011), or after maternal exposure to cannabinoids (Shabani et al., 2011). This suggests that deviation from the tightly regulated firing of PC, whether an increase or decrease in regularity, can lead to behavioral deficits such as the motor learning impairment we observe in 4E-BP2 cKO mice. The mechanisms underlying increased firing regularity of PCs in 4E-BP2 cKO mice remain elusive. Preferential loss of a subpopulation of PCs exhibiting irregular firing could contribute to this phenotype or alternatively, the observed increase in firing regularity could be a compensatory response to a decrease in the number of PCs in 4E-BP2 cKO mice.

Variability in PC firing could be necessary for the normal output of the cerebellar circuit. Such "noise" can encode information (De Schutter and Steuber, 2009; Faisal et al., 2008b; Softky and Koch, 1993; Steuber et al., 2007) and was associated with higher cognitive functions such as sensory processing (Doron et al., 2014), selective attention (Ardid et al., 2010), and working memory (Hansel and Mato, 2013). The irregular firing of inferior olive neurons, the origin of climbing fibers, has been proposed to function as a dynamic form of working memory (Kistler and Zeeuw, 2002). Alterations in cerebellar outputs to the hippocampus (mediated via multi-synaptic pathways), which provide information on self-motion signals and are essential for hippocampal spatial representation and subsequent goal-directed navigation (Rochefort et al., 2011a; Rochefort et al., 2013), could contribute to the impaired spatial learning and memory of 4E-BP2 cKO in the MWM test.

The role of cerebellum in autism and the control of other higher brain functions such as memory formation is under intensive investigation (Badura et al., 2018; Kelly et al., 2020). Our finding

of cerebellar 4E-BP2 involvement in memory but not in ASD-like behaviors provides an important insight into the translational control mechanisms of cerebellar functions and how dysregulated translation in the cerebellum affects complex behaviors.

3.5 Acknowledgments.

This study was supported by the Canadian Institutes of Health Research (CIHR, PJT-162412) and SFARI to A.K, and a start-up grant from FORTH-IMBB BR to C.G.G.

3.6 Author Contributions

M.H., V.T.T., N.S., M.PK., S.T., C.G.G., and A.K. conceived the project, designed experiments and supervised the research. M.H. performed immunohistochemistry and biochemistry experiments and assessed motor and ASD-like behaviors. V.S performed MWM experiment. R.T., A.S., E.F., and A.J.W designed and performed electrophysiology recordings. C.W., I.G., P.S.R., N.W., and A.C. helped with data analysis and mouse colony management. All the authors contributed to writing he manuscript.

3.7 Declaration of Interests

The authors declare no competing interests.

3.8 Figures

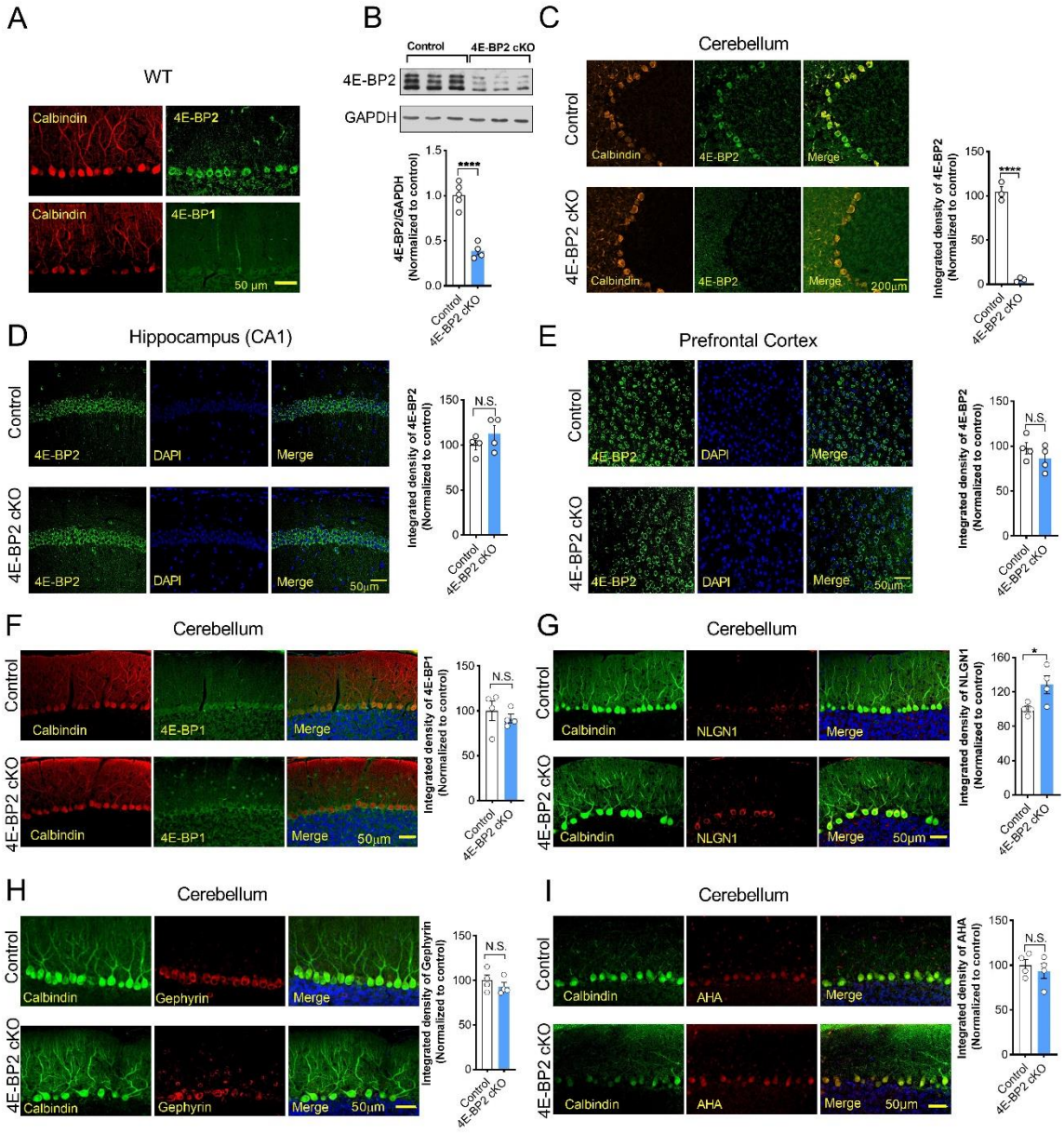

3.8.1 Figure 1. Deletion of 4E-BP2 in the cerebellar Purkinje cells.

(A) Immunostaining against 4E-BP1 and 4E-BP2 shows that 4E-BP2 is preferentially expressed in cerebellar Purkinje cells (labeled by calbindin). (B) Western blot analysis demonstrates a significant reduction in 4E-BP2 levels in tissue lysate extracted from the cerebellum of 4E-BP2 cKO mice (n=4) as compared to control mice (n=5), ****p<0.0001. (C) Immunohistochemistry shows an almost complete ablation of 4E-BP2 in calbindin-labeled cerebellar PCs in 4E-BP2 cKO mice (n=3) as compared to control animals (n=3), ****p<.0001.

(D and E) No significant differences in 4E-BP2 levels were found in the hippocampus and prefrontal cortex between 4E-BP2 cKO mice (n=4) and controls (n=4), p > 0.05. (F) Immunostaining against 4E-BP1 shows that the expression levels of 4E-BP1 in PCs remain unchanged in 4E-BP2 cKO mice, $p = 0.5059$. (G) Neuroligin 1 (NRLGN1) protein levels are increased in cerebellar PCs of 4E-BP2 cKO mice, $p = 0.0399$. (H) Gephyrin protein levels are not altered in PCs of 4E-BP2 cKO mice, $p = 0.3921$. (I) No change in AHA incorporation (FUNCAT) in cerebellar Purkinje cells in 4E-BP2 cKO mice, $p = 0.5435$. Unpaired student's *t*-test. Data points represent individual mice. Data are shown as mean ± SEM.

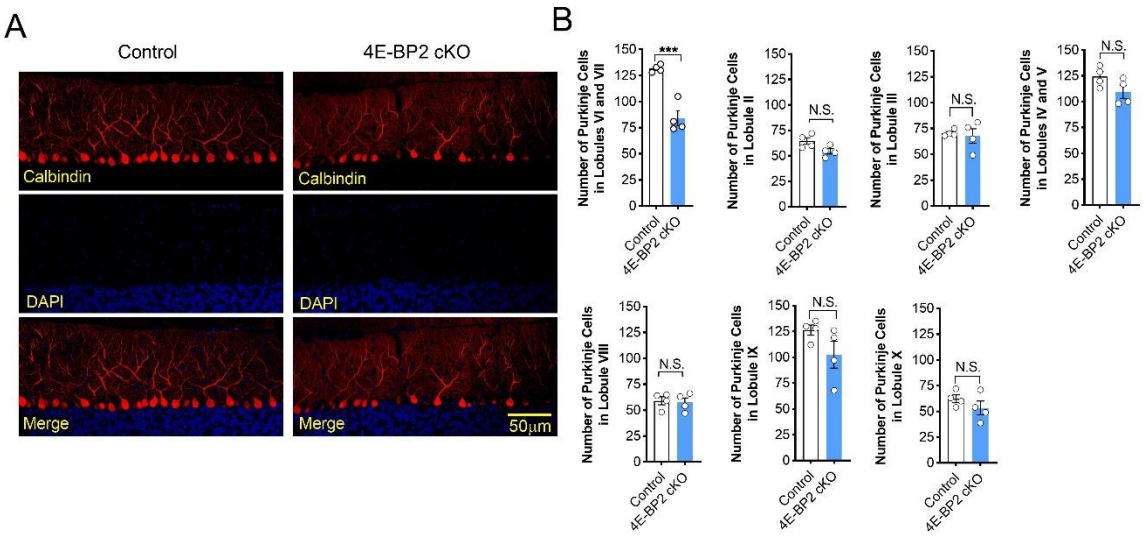

3.8.2 Figure 2. 4E-BP2 cKO mice exhibit a loss of Purkinje cells in the cerebellum.

Immunohistochemistry against calbindin (red) reveals a significant loss of PC in the cerebellum (lobules VI and VII) of 4E-BP2 cKO mice (n=4) as compared to controls (n=4), ***p < 0.001, unpaired student's *t*-test. No differences were found in other lobules (II, III, V, VIII, IX, and X). Sections were prepared from the vermis area of the cerebellum, and calbindin-labeled cells were counted. Data points represent individual mice. Data are shown as mean ± SEM.

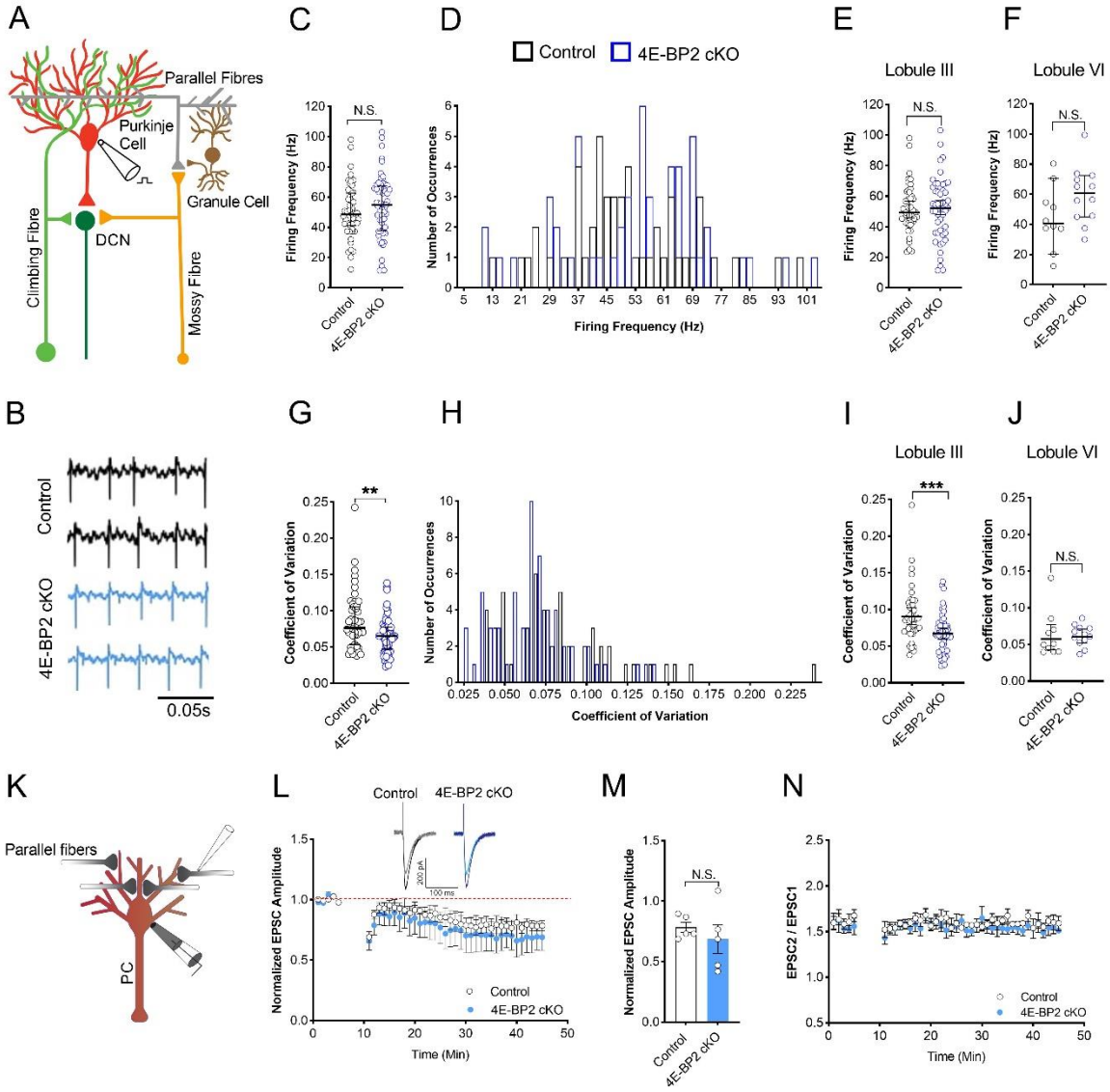

3.8.3 Figure 3. Purkinje cells from 4E-BP2 cKO animals fire action potentials at higher regularly than controls, with no change in the firing frequency and LTD.

(A) Loose cell-attached recordings were made in acute cerebellar slices from the soma of Purkinje cells, which constitute the sole output of the cerebellar cortex. (B) Sample traces from control (black) and 4E-BP2 cKO (blue) Purkinje cells. (C) No difference in Purkinje cell firing frequency was found between control (n= 51 cells from 5 animals, lobule III and VI) and 4E-BP cKO animals (n=60 cells from 5 animals, lobule III and VI), $p > 0.05$. (D) Frequency histogram depicting the distribution of firing frequency of PCs from control and 4E-BP2 cKO

mice. Cells were grouped into 55 bins of 2 Hz each. No differences in firing frequency of Purkinje cells in lobule III (E) and lobule VI (E). (G) 4E-BP2 cKO PCs (in lobule III and VI) fire action potentials at higher regularity than control PCs, **p < 0.01. (H) Frequency histogram depicting the distribution of coefficient of variation (CV) of PC firing from control and 4E-BP2 cKO mice. Cells were grouped into 50 bins, each with a CV of 0.005. Coefficient of variation (CV) of firing frequency was decreased in 4E-BP2 cKO PCs located in lobule III (I, ***p < 0.001) but not lobule VI (J). (K) Long-term depression (LTD) was induced at parallel fiber-to-Purkinje cell synapses, by pairing PF stimulation with PC depolarization (300 times at 1 Hz, from min 5-10, n = 5, 5). (L) Sample traces before and after LTD are shown. Black/grey traces show average EPSCs from 0-5 min and from 41-45 min for a representative cell from a wild-type mouse. Blue/light blue traces show average EPSCs from 0-5 min and from 41-45 min for a representative cell from a 4E-BP2 cKO mouse. Stimulus artifacts are truncated. (M) The amount of depression from min 41-45 is not different between cells from wild-type and 4E-BP2 cKO mice. (N) Paired-pulse ratio (PPR) after LTD is not altered in wild-type or 4E-BP2 cKO cells. Mann-Whitney *U* tests and Student's t test were performed for all comparisons. Significance was set at p<0.05. Data points represent individual PCs. Data are shown as median ± IQR or mean ± SEM.

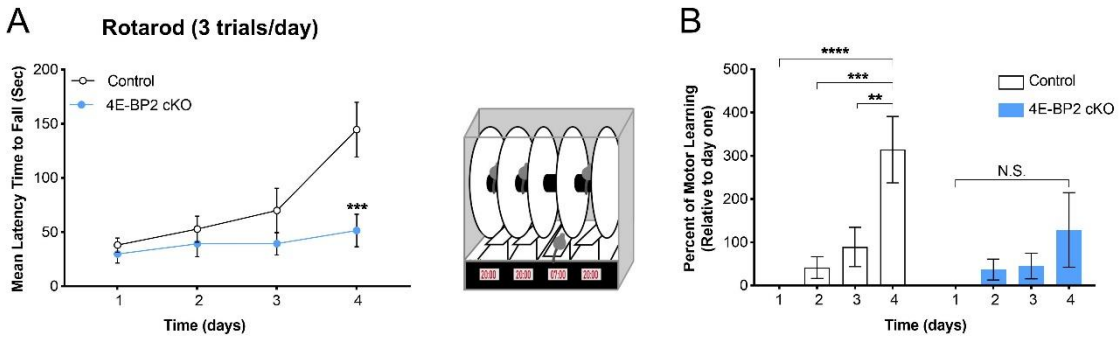

3.8.4 Figure 4. 4E-BP2 deletion in PC causes impaired motor learning.

Mice were subjected to an accelerating mode of rotarod for four consecutive days three times per day. (A) 4E-BP2 cKO mice (n=8) show a significant impairment in motor learning measured using a rotarod task as compared to controls (n=9), $F(1, 15) = 4.7$, *p < 0.05 and Bonferroni's post hoc test reveals a significant reduction in latency time to fall for 4E-BP2 cKO mice vs. controls on day 4, ***p < 0.001, two-way ANOVA. (B) Percent of motor learning relative to day 1. Data are shown as mean ± SEM.

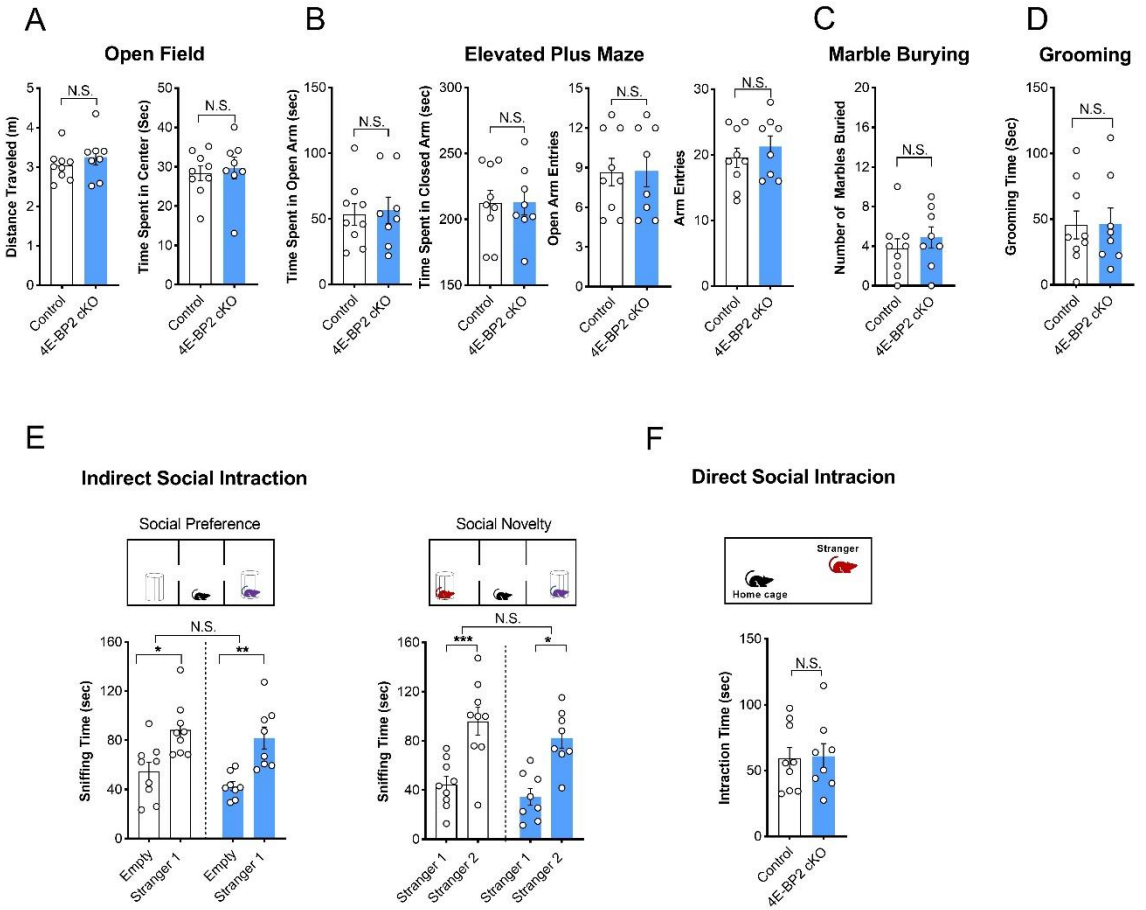

3.8.5 Figure 5. Ablation of 4E-BP2 in cerebellar PCs does not engender autistic behaviors.

(A) There was no significant difference between 4E-BP2 cKO animals and control littermates (n=8-9 per group) in the distance traveled (p > 0.05) or time spent in the center of the apparatus (p > 0.05) in the open field test. (B) 4E-BP2 cKO mice show no significant difference compared

to control littermates (n=8-9 per group) in time spent in open/closed arms ($p > 0.05$) in the elevated plus maze test. (C) No significant difference was observed between 4E-BP2 cKO animals and control littermates (n=8-9 per group) in the number of marbles buried in the marble burying test ($p > 0.05$). (D) Similarly, 4E-BP2 cKO mice display no significant difference as compared to control littermates (n=8-9 per group) in time spent grooming ($p > 0.05$). (E) There was no significant difference in the social preference (genotype and chamber interaction $F(1, 30) = 0.1385$, effect of genotype $F(1, 30) = 1.647$ and social novelty (genotype and chamber interaction $F(1, 30) = 0.045$, effect of genotype $F(1, 30) = 1.93$ phases of the indirect social interaction test between 4E-BP2 cKO animals and control littermates, $p > 0.05$. (F) No significant difference in interaction time was observed between 4E-BP2 cKO animals and control littermates (n=8-9 per group) in the direct social interaction test ($p > 0.05$). For statistical analysis, student's t-test was performed for all experiments aside E, where two-way ANOVA with Bonferroni's post hoc test was conducted. Significance was set at $p < 0.05$. Data points represent individual mice, and data are shown as mean ± SEM.

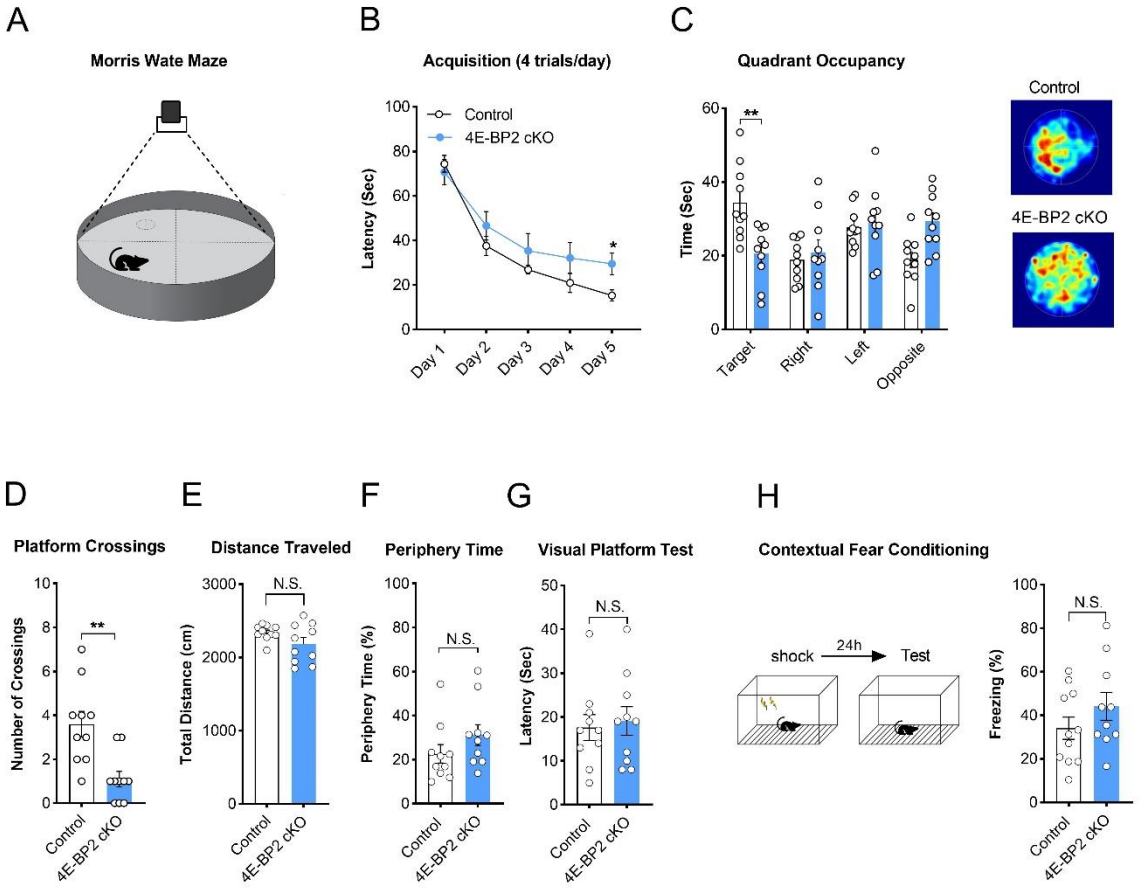

3.8.6 Figure 6. 4E-BP2 cKO animals show impairment in spatial learning and memory in the Morris water maze task.

(A-B) No significant difference was observed between 4E-BP2 cKO animals and control littermates (n=10 per group) in the 5-day acquisition trials ($F(1, 18) = 3.66$, $p = 0.0715$). However, on the fifth training day, 4E-BP2 cKO animals reached the hidden platform significantly slower than control littermates, $^{*}p < 0.05$. (C) Whereas control animals spent significantly more time in the target quadrant on day sixth (probe trial session without submerged platform) (n=10 per group), 4E-BP2 cKO mice did not show a preference for the target quadrant, $F(3, 72) = 4.53$, $^{**}p < 0.01$. Representative heat maps of locomotor activity in the Morris water maze are shown for control and 4E-BP2 cKO animals. (D) 4E-BP2 cKO animals cross the platform location significantly less as compared to control animals during

the probe trial (n=10 per group, **p < 0.01). There was no significant difference between 4E-BP2 cKO animals and control littermates (n=10 per group) in the total distance traveled, p > 0.05 (E), and the time spent swimming near the pool wall (thigmotaxis), p > 0.05, (F). No difference in escape latency was observed between the two groups in the visible version of the MWM, p > 0.05, (G). (H) 4E-BP2 cKO and control animals showed similar freezing behaviour in the contextual fear conditioning task 24 h post-training, p > 0.2301. For statistical analysis, a student's t-test was performed for D-H, and two-way ANOVA with Bonferroni's post hoc test was conducted for B and C. Significance was set at p<0.05. Data points represent individual mice, and data are shown as mean ± SEM.

3.9 STAR Methods, experimental model, and subject details.

3.9.1 Animals

Eif4ebp2$^{f/f}$ mice (Wiebe et al., 2019) were crossed with mice expressing L7^{Cre} (Cre recombinase) (both on C57BL6/J background) to generate the heterozygous mice for both alleles, which were then crossed to generate conditional knockout *Eif4ebp2*$^{f/f}$; L7^{Cre}. *Eif4ebp2*$^{+/+}$; L7^{Cre} mice were used as control. *Eif4ebp2* mutant and wild-type alleles were detected by PCR with the forward primer (5´-GTCGGTCTTCTGTAGATTGTGAGT-3´) and the reverse primer (5´-GGCGATCCCTAGAAAATAAAGCCT-3´) to amplify the wild-type allele (276 bp) and BP2 conditional allele (379 bp). Cre expression was detected by PCR with the forward primer (5´-GATCTCCGGTATTGAAACTC-3´) and the reverse primer (5´-GCTAAACATGCTTCATCGTC-3´), which amplify a 300 bp fragment. All experiments were conducted on 8-12-week-old male mice. Food and water were available *ad libitum*. Mice were kept on a 12-hr light/dark cycle (lights on at 7:00 AM). Mice were handled for three days before the test day, and on the test day, they were allowed to habituate to the test environment for 30 min. Behavioral experiments were conducted during the light phase of the cycle (09:00 -

15:00h). All procedures were compliant with the Canadian Council on Animal Care guidelines and approved by the McGill University's downtown Animal Care Committee.

3.10 Method details

3.10.1 Open field

Mice were placed in an illuminated (~1,200 lx) white non-porous plastic square box (50 cm x 50 cm x 31 cm) and were allowed to explore the apparatus freely for 10 min. Behaviors were recorded and analyzed using the Noldus EthoVision XT video tracking software. Time spent inside the defined zone and the total distance traveled were analyzed.

3.10.2 Elevated plus maze

An elevated plus maze consisting of four arms (two open and two enclosed), arranged to form a plus shape (height: 30 cm, length: 50 cm and width: 10 cm, Plexiglas) was used. All four arms were at a distance of 50 cm above ground level. Mice were placed in the intersection of four arms, facing one of the closed arms and were allowed to explore for 5 min, while the movement path was filmed using a camera mounted over the maze. The number of entries and time spent in the open and closed arms were scored.

3.10.3 Self-Grooming

Mice were placed in a clean Plexiglas cage filled with 1 cm of fresh bedding. They were allowed to habituate and explore the cage for 20 min, but only the last 10 min were scored and analyzed. Self-grooming behavior was recorded with a camera located in front of the cage. The total time of grooming was scored using a manual stopwatch.

3.10.4 Marble burying

Mice were placed into a corner of a Plexiglas cage (50 cm x 50 cm x 31 cm) containing 5 cm of bedding material with 20 shiny clear marbles on top of the leveled bedding (distributed in 5 rows of 4 marbles) and were allowed to bury the marbles for 30 min. The marble was considered buried if 2/3 of it were covered by the bedding.

3.10.5 Three-chamber social interaction test

The social apparatus consisted of a Plexiglas box divided into three identical chambers (36 cm × 28 cm × 30 cm) by two transparent walls. Each wall had a removable doorway allowing access into chambers. The test consisted of three 10-min phases, including habituation, sociability, and novelty preference. Before each phase, the test mouse was maintained in the middle chamber while two doorways were closed. In the first phase, the test mouse was allowed to habituate in the three-chamber arena for 10 min. In the second sociability phase, the test mouse was exposed to an age-matched unfamiliar male mouse (stranger 1, C57BL/6J) confined in a wire cage, which was located in one of the chambers, and an identical empty wire cage was placed at the corresponding spot in the opposite chamber. In the third novelty preference phase, an age and sex-matched novel mouse (stranger 2, C57BL/6J) was enclosed in the empty wire cage, and the test mouse was allowed to roam between chambers containing familiar mouse (stranger 1) and novel mouse (stranger 2). All sessions were recorded using an overhead mounted camera. The time spent sniffing each wire cage, the total time spent in each chamber, and the total number of entries into the chambers were scored. Sniffing time was measured when the test mouse climbed the wire cages or approached either the empty wire cage or enclosed mouse as close as less than 1cm between the mouse nose and the wire cages.

3.10.6 Reciprocal male-male social interaction

Mice were individually placed in a mouse cage with fresh bedding material and were allowed to habituate for 5 min. Immediately after, the subject mouse was exposed to an unfamiliar mouse (sex- and age-matched) for 10 min. The experiment was recorded by a camera mounted above the cage. The total contact time between the subject mouse and the unfamiliar was scored.

3.10.7 Rotarod

IITC Life Science Rotarod was used for evaluating motor learning and coordination. Mice were mounted on a mouse-specific drum (1¼ inch diameter). On the first day, mice were trained to stay on the constantly rotating (5 rpm) drum for 2 min. Next, mice were placed on the drum rotating at a gradually accelerating speed (starting at 5 rpm and accelerating by 0.2 rpm per second) for a maximum of 5 minutes or until they fell. This was repeated three times per day over four consecutive days. For each mouse, the average latency to fall in three trials per day was calculated.

3.10.8 Morris water maze

Mice were placed in a circular opaque pool (100 cm diameter, 23 °C) with a submerged platform (10 cm diameter) and were allowed to search for the hidden platform for 60 sec. Mice were trained three times per day with a 30 min intertrial interval for five consecutive days. If the mouse did not find the platform within 60 sec, it was gently guided to the platform and remained there for 10 sec before being returned to the cage. On the probe test day (day 6), mice were allowed to swim for 60 sec, while the platform was removed. The mouse swimming was recorded using a video tracking system and the latency to find the platform over training days and the total time spent in the target quadrant, the total number of crossing the platform

location, and the total distance/speed traveled in the probe day were analyzed. In the visible version of the MWM test, mice had three trials of 60 s to locate a visible platform marked with a distinct flag in an opposite quadrant.

3.10.9 Contextual fear conditioning

After three consecutive days of handling, mice were subjected to a contextual fear conditioning which included a 2-min period of context exploration, followed by two 0.7 mA foot shocks with a 60 s interval. Mice were returned to their home cage 1 min. after the last foot shock. Contextual fear memory was tested 24 h post-training by placing the mice in the conditioning context and measuring percent of freezing for 4 min. Freezing was assessed every 5 s as either "freezing" or "not freezing", and the percent of freezing was calculated as the number of 5-s intervals with freezing divided by the total number of 5-s intervals.

3.10.10 Immunohistochemistry

Mice were deeply anesthetized, transcardially perfused with 4% paraformaldehyde (Cat. No. P6148, Sigma-Aldrich) in PBS (PH: 7.4) and their brains were extracted. The extracted brains were post-fixed for 24 hours and sectioned at 50 µm using a vibratome (Leica VT1200 S, Biosystems). Coronal sections of both the hippocampus and prefrontal cortex and sagittal sections from the vermis area of the cerebellum were collected. Sections were blocked with 10% normal goat serum (NGS) and 0.05% Triton-100x in PBS for 1h at room temperature. The blocked sections were incubated in primary antibodies diluted in PBS-T containing 5% NGS (overnight, 4 °C). Antibodies against calbindin (1:1000, Cat. No. C9848, Sigma-Aldrich and 1:400, Cat: #13176T, Cell Signaling), neuroligin 1 (1:50, Synaptic System, Cat: # 129 111), gephyrin (1:200, Synaptic System, Cat: #147318), 4E-BP2 (1:50, Cat. No. 2845S, Cell Signaling Technology), and 4E-BP1 (1:100, Cell Signaling, Cat: #9644**)** were used. Sections

were washed in PBS-T and incubated with secondary antibodies (1:800, 2 h at room temperature), Alexa Fluor 568 rabbit anti-mouse IgG (Cat. No. 31194, Thermo Fisher Scientific) and Alexa Fluor 488 goat anti-rabbit IgG (Cat. No. A11034, Thermo Fisher Scientific). Finally, sections were washed three times and incubated with DAPI (1:5000, Cat. No. D1306, Thermo Fisher Scientific) for 5 min and mounted on glass histology slides, cover-slipped and visualized using a confocal laser scanning microscope (Zeiss LSM880). Image quantification was performed using ImageJ (NIH). Integrated density of fluorescent signal was measured in 10 PCs per section and in two sections per animal, and average of all data points per animal was calculated. The integrated density of fluorescent signal was measured in lobules III, VI, and VII, where changes in electrophysiological activity and PC count have been observed.

3.10.11 Acute cerebellar slice preparation

Acute cerebellar slices were prepared as previously described (Watt et al., 2009; Ady et al., 2018). Briefly, mice were deeply anesthetized in a home-made anesthesia chamber using isoflurane, rapidly decapitated and their brains extracted into the ice-cold artificial cerebrospinal fluid (ACSF) containing (in mM:) 125 NaCl, 2.5 KCl, 2 $CaCl_2$, 1 $MgCl_2$, 1.25 NaH_2PO_4, 26 $NaHCO_3$ and 20 glucose, bubbled with 95% O_2 and 5% CO_2 to maintain pH at 7.3; Osmolality 320 ± 5 mOsm). Acute sagittal slices (200 μm thick) were cut from the cerebellar vermis as previously described (Jayabal et al., 2016, 2017; Ady et al., 2018) using a Leica VT1000S microtome (Leica Microsystems, Wetzlar, Germany). Slices were then incubated in ACSF at 37°C for 35-40 minutes before being removed and incubated at room temperature (~25°C) in continuously oxygenated ACSF for up to an additional 4 hours. All chemicals were purchased from Sigma-Aldrich (Oakville, ON, Canada).

3.10.12 Electrophysiology

The spontaneous firing was recorded from PCs using the non-invasive extracellular/loose cell-attached recording techniques. Briefly, slices were bathed in ACSF at 30-33°C in the presence of a cocktail of synaptic blockers that included SR-95531 (GABAzine; 10 μm), 6,7-dinitroquinoxaline-2,3-dione (DNQX; 10 μm) and 2-amino-5-phosphonopentanoate (AP-V; 50 μm) to block fast excitatory and inhibitory synaptic transmission to the PCs. PCs were identified using an upright microscope (Scientifica, Uckfield, UK), and extracellular recordings were obtained using a BVC-700A Voltage Clamp Amplifier (Dagan Corporation, Minnesota, USA). Custom-designed acquisition and data analysis software run in Igor Pro software (Wavemetrics, Portland, OR, USA) was used to determine PC firing frequency and coefficient of variation (CV) of the inter-spike interval of simple spikes. Recordings were done in anterior lobules III and VI using electrodes pulled with a P-1000 puller (Sutter Instruments, Novato, CA, USA) filled with ACSF. All chemicals were purchased from Sigma-Aldrich (Oakville, ON, Canada).

LTD experiments: Cerebellar slice recordings for long-term plasticity experiments were performed using 21-35 days old mice. Mice were anesthetized with isoflurane, cervically dislocated and decapitated. The brain was extracted, and the cerebellum dissected out in ice cold artificial cerebrospinal fluid (aCSF (concentration in mM): NaCl(119), KCl(2.5), NaH2PO4(1), NaHCO3(26.2), MgCl2(1.3), CaCl2(2.5), D-Glucose(10), bubbled with carbogen (95% O2, 5% CO2, Praxair)). Parasagittal cerebellar slices of 300 μm thickness were made using a Leica VT1200S vibratome. The slices were allowed to recover at 34°C for 20-30 minutes followed by recovery at room temperature for at least 1 hr.

Recordings: Slices were transferred to a recording chamber on an Olympus BX61W1 upright microscope and visualized using differential interference contrast optics. The recording chamber was provided with a continuous flow of carbogen-bubbled aCSF at room temperature.

50 μM picrotoxin (Abcam) was added to the aCSF to block GABAA channels. The cells were recorded in the whole-cell configuration. Stimulation of the parallel fibers was performed using aCSF-filled bipolar stimulation electrode made from theta glass (World Precision Instruments), with the stimulation electrode placed in the outer third of the molecular layer. Patch electrodes were made pulled to a resistance of 3-7 MOhms from borosilicate glass tubing (Harvard Apparatus) and filled with an internal solution containing (concentration in mM): Cs-gluconate(145), CsCl(5),MgCl2(2), EGTA(0.5), Mg-ATP(2), Na-GTP(0.5), pH adjusted to 7.3 with CsOH, osmolarity 290-305 mOsm. The cells were voltage clamped at -70 mV. Signals were acquired at a sampling rate of 20 kHz using a Multiclamp 700B amplifier and low-pass filtered at 5 kHz. Access resistance was maintained below 25 MOhms and both input and access resistance were monitored for stability throughout the recording. All aCSF reagents were obtained from Sigma-Aldrich, except KCl which was from Thermo- Fisher Scientific. Slice physiology data were analyzed in pCLAMP 11.1 (Clampfit). Purkinje cells were recorded in voltage clamp and the strength of parallel fiber synapses was monitored by parallel fiber stimulation (100 μs) at 0.05 Hz. Long-term plasticity was induced by a single parallel (PF) fiber stimulation paired with a 100 ms depolarization of the Purkinje cell to 0 mV, repeated 300 times at 1 Hz. PF-alone stimulation (0.05 Hz) was resumed for 35 min after plasticity induction. Input and access resistance were monitored throughout the recording. Although transient changes in input resistance did occur immediately after the plasticity induction protocol, it was ensured that the access resistance did not change by more than 25% or input resistance by 20% compared to the baseline, at the time the percentage of LTD was measured (Min 41-45, Fig. 3L). EPSC amplitude was measured in Clampfit. For 9/10 cells paired pulse ratios were monitored through the pre-LTD and post-LTD baselines. Each PF stimulation was paired with a second PF stimulation 100 ms later for 9/10 cells. The amplitude of the first EPSC was used for the plasticity measurements mentioned above. The EPSC amplitude reported for

any minute was the average amplitude of the three EPSC traces acquired during that minute. The ratio of the amplitude of the second EPSC to that of the first EPSC (paired pulse ratio = amplitude of EPSC 2/amplitude of EPSC1) was measured at each point in the baselines.

3.10.13 Western blotting

Extracted tissues were homogenized in ice-cold RIPA lysis buffer (Cat. No. R0278, Sigma-Aldrich), EDTA-free protease inhibitor (Cat. No. 4693132001, Sigma-Aldrich), phosphatase inhibitor cocktail 2 (1:100, Cat. No. P5726-1ML, Sigma-Aldrich), and cocktail 3 (1:100, Cat. No. P0044-1ML, Sigma-Aldrich). Concentrations were measured using the Bradford protein assay. 30 μg of protein was loaded on 12% SDS-PAGE gel and transferred to a nitrocellulose membrane. The membrane was blocked in 5% BSA and TBS-T (1 h, room temperature) and incubated (overnight, 4 °C) with a rabbit polyclonal antibody against 4E-BP2 (1:500, Cat. No. 2845S, Cell Signaling Technology). Following three washes with TBS-T, membranes were incubated in a HRP-conjugated secondary antibody (1:5000, Cat. No. NA931-1ML, Amersham) for 1h at room temperature. Finally, the membranes were washed (3 times in TBS-T), treated with Enhanced Chemiluminescent (ECL) reagent, and visualized using a ChemiDoc Imaging System (Bio-Rad).

3.10.14 Measurement of de novo protein synthesis

To measure the rate of de novo protein synthesis in PCs, fluorescent non-canonical amino-acid tagging (FUNCAT) in conjunction with immunohistochemistry were used. Following a 7-day low-methionine diet, mice received an intraperitoneal injection of 100 μg/gbw azidohomoalanine (AHA). Three hours after AHA injection, mice were anesthetized and perfused transcardially with 4% PFA. The cerebellum was sliced sagittally at 40-μm thickness. After washing with PBS, cerebral sections were incubated overnight at 4 °C in a blocking

solution composed of 10% normal goat serum, 5% sucrose, and 0.5% Triton-100X in PBS. The sections were washed again and incubated in click buffer consisting of 400 μM TCEP, 200 μM triazole ligand, 200 μM CuSO4, and 2 μM fluorescent Alexa Fluor 555 alkyne in PBS overnight. After the "click" reaction, sections were processed using the regular immunohistochemistry protocol to stain against calbindin. Sections were washed with PBS, mounted on slides, and imaged using Zeiss LSM880 confocal microscope. The images were quantified using ImageJ (NIH). Integrated density was measured in 10 PCs per section in 2 sections per animal and all data points from the same animal were averaged.

3.10.15 Quantification and statistical analysis

All behavioral experiments were conducted and scored by the experimenter blinded to the genotype. Data are reported as mean ± SEM, except for electrophysiology data, which are non-normally distributed and thus reported as median ± IQR, and all were analyzed using GraphPad Prism 8. The level of significance was set *a priori* at $p < 0.05$. Unpaired student's *t*-tests were used to analyze the data from different experiments except for the acquisition sessions of Morris water maze, rotarod, and three-chamber test, which were analyzed with a two-way ANOVA followed by Bonferroni's post-hoc tests, and the PC firing frequency and CV, which were analyzed using Mann-Whitney *U* tests and graphed in Igor Pro and Inkscape: Open Source Scalable Vector Graphics Editor.

3.11 References

Ady, V., Toscano-Márquez, B., Nath, M., Chang, P.K., Hui, J., Cook, A., Charron, F., Larivière, R., Brais, B., and McKinney, R.A. (2018). Altered synaptic and firing properties of cerebellar Purkinje cells in a mouse model of ARSACS. The Journal of physiology *596*, 4253-4267.

Akshoomoff, N.A., and Courchesne, E. (1992). A new role for the cerebellum in cognitive operations. Behavioral neuroscience *106*, 731.

Allen, G., Buxton, R.B., Wong, E.C., and Courchesne, E. (1997). Attentional activation of the cerebellum independent of motor involvement. Science *275*, 1940-1943.

Ardid, S., Wang, X.-J., Gomez-Cabrero, D., and Compte, A. (2010). Reconciling coherent oscillation with modulationof irregular spiking activity in selective attention: gamma-range synchronization between sensoryand executive cortical areas. Journal of Neuroscience *30*, 2856-2870.

Association, A.P. (2013). Diagnostic and statistical manual of mental disorders (DSM-5®) (American Psychiatric Pub).

Badura, A., Verpeut, J.L., Metzger, J.W., Pereira, T.D., Pisano, T.J., Deverett, B., Bakshinskaya, D.E., and Wang, S.S. (2018). Normal cognitive and social development require posterior cerebellar activity. Elife *7*.

Banko, J.L., Poulin, F., Hou, L., DeMaria, C.T., Sonenberg, N., and Klann, E. (2005a). The translation repressor 4E-BP2 is critical for eIF4F complex formation, synaptic plasticity, and memory in the hippocampus. Journal of Neuroscience *25*, 9581-9590.

Banko, J.L., Poulin, F., Hou, L., DeMaria, C.T., Sonenberg, N., and Klann, E. (2005b). The translation repressor 4E-BP2 is critical for eIF4F complex formation, synaptic plasticity, and memory in the hippocampus. J Neurosci *25*, 9581-9590.

Bannerman, D.M., Sprengel, R., Sanderson, D.J., McHugh, S.B., Rawlins, J.N., Monyer, H., and Seeburg, P.H. (2014). Hippocampal synaptic plasticity, spatial memory and anxiety. Nat Rev Neurosci *15*, 181-192.

Barski, J.J., Dethleffsen, K., and Meyer, M. (2000). Cre recombinase expression in cerebellar Purkinje cells. genesis *28*, 93-98.

Bauman, M.L., and Kemper, T.L. (2005). Neuroanatomic observations of the brain in autism: a review and future directions. International journal of developmental neuroscience *23*, 183-187.

Belmonte, M.K., and Bourgeron, T. (2006). Fragile X syndrome and autism at the intersection of genetic and neural networks. Nature neuroscience *9*, 1221-1225.

Bhattacharya, A., Kaphzan, H., Alvarez-Dieppa, A.C., Murphy, J.P., Pierre, P., and Klann, E. (2012). Genetic removal of p70 S6 kinase 1 corrects molecular, synaptic, and behavioral phenotypes in fragile X syndrome mice. Neuron *76*, 325-337.

Bidinosti, M., Ran, I., Sanchez-Carbente, M.R., Martineau, Y., Gingras, A.-C., Gkogkas, C., Raught, B., Bramham, C.R., Sossin, W.S., and Costa-Mattioli, M. (2010). Postnatal deamidation of 4E-BP2 in brain enhances its association with raptor and alters kinetics of excitatory synaptic transmission. Molecular cell *37*, 797-808.

Bilder, D.A., Bakian, A.V., Stevenson, D.A., Carbone, P.S., Cunniff, C., Goodman, A.B., McMahon, W.M., Fisher, N.P., and Viskochil, D. (2016). Brief Report: The Prevalence of Neurofibromatosis Type 1 among Children with Autism Spectrum Disorder Identified by the Autism and Developmental Disabilities Monitoring Network. J Autism Dev Disord *46*, 3369-3376.

Bolduc, M.E., Du Plessis, A.J., Sullivan, N., Khwaja, O.S., Zhang, X., Barnes, K., Robertson, R.L., and Limperopoulos, C. (2011). Spectrum of neurodevelopmental disabilities in children with cerebellar malformations. Dev Med Child Neurol *53*, 409-416.

Butler, M.G., Dasouki, M.J., Zhou, X.-P., Talebizadeh, Z., Brown, M., Takahashi, T.N., Miles, J.H., Wang, C., Stratton, R., and Pilarski, R. (2005). Subset of individuals with autism spectrum disorders and extreme macrocephaly associated with germline PTEN tumour suppressor gene mutations. Journal of medical genetics *42*, 318-321.

Carta, I., Chen, C.H., Schott, A.L., Dorizan, S., and Khodakhah, K. (2019). Cerebellar modulation of the reward circuitry and social behavior. Science *363*, eaav0581.

Chen, C.J., Sgritta, M., Mays, J., Zhou, H., Lucero, R., Park, J., Wang, I.C., Park, J.H., Kaipparettu, B.A., Stoica, L., *et al.* (2019). Therapeutic inhibition of mTORC2 rescues the behavioral and neurophysiological abnormalities associated with Pten-deficiency. Nat Med *25*, 1684-1690.

Cook, A.A., Fields, E., and Watt, A.J. (2020). Losing the beat: contribution of Purkinje cell firing dysfunction to disease, and its reversal. Neuroscience.

Courchesne, E., Saitoh, O., Townsend, J.P., Yeung-Courchesne, R., Press, G.A., Lincoln, A.J., Haas, R.H., and Schriebman, L. (1994). Cerebellar hypoplasia and hyperplasia in infantile autism. Lancet *343*, 63-64.

Cupolillo, D., Hoxha, E., Faralli, A., De Luca, A., Rossi, F., Tempia, F., and Carulli, D. (2016). Autistic-like traits and cerebellar dysfunction in Purkinje cell PTEN knock-out mice. Neuropsychopharmacology *41*, 1457-1466.

Daum, I., Ackermann, H., Schugens, M.M., Reimold, C., Dichgans, J., and Birbaumer, N. (1993). The cerebellum and cognitive functions in humans. Behavioral neuroscience *107*, 411.
De Schutter, E., and Steuber, V. (2009). Patterns and pauses in Purkinje cell simple spike trains: experiments, modeling and theory. Neuroscience *162*, 816-826.

Desmond, J.E., Gabrieli, J.D., Wagner, A.D., Ginier, B.L., and Glover, G.H. (1997). Lobular patterns of cerebellar activation in verbal working-memory and finger-tapping tasks as revealed by functional MRI. The Journal of neuroscience : the official journal of the Society for Neuroscience *17*, 9675-9685.

Deverett, B., Kislin, M., Tank, D.W., and Wang, S.S. (2019). Cerebellar disruption impairs working memory during evidence accumulation. Nat Commun *10*, 3128.
Doron, G., Von Heimendahl, M., Schlattmann, P., Houweling, A.R., and Brecht, M. (2014). Spiking irregularity and frequency modulate the behavioral report of single-neuron stimulation. Neuron *81*, 653-663.

Eichenbaum, H. (2017). The role of the hippocampus in navigation is memory. J Neurophysiol *117*, 1785-1796.

Faisal, A.A., Selen, L.P., and Wolpert, D.M. (2008a). Noise in the nervous system. Nature reviews neuroscience *9*, 292-303.

Faisal, A.A., Selen, L.P., and Wolpert, D.M. (2008b). Noise in the nervous system. Nat Rev Neurosci *9*, 292-303.

Fatemi, S.H., Halt, A.R., Realmuto, G., Earle, J., Kist, D.A., Thuras, P., and Merz, A. (2002). Purkinje cell size is reduced in cerebellum of patients with autism. Cellular and molecular neurobiology *22*, 171-175.

Fehlow, P., Bernstein, K., Tennstedt, A., and Walther, F. (1993). Early infantile autism and excessive aerophagy with symptomatic megacolon and ileus in a case of Ehlers-Danlos syndrome. Padiatrie und Grenzgebiete *31*, 259-267.

Gandhi, C.C., Kelly, R.M., Wiley, R.G., and Walsh, T.J. (2000). Impaired acquisition of a Morris water maze task following selective destruction of cerebellar purkinje cells with OX7-saporin. Behavioural brain research *109*, 37-47.

Gil, M., Nguyen, N.T., McDonald, M., and Albers, H.E. (2013). Social reward: interactions with social status, social communication, aggression, and associated neural activation in the ventral tegmental area. European journal of neuroscience *38*, 2308-2318.

Gkogkas, C.G., Khoutorsky, A., Ran, I., Rampakakis, E., Nevarko, T., Weatherill, D.B., Vasuta, C., Yee, S., Truitt, M., and Dallaire, P. (2013). Autism-related deficits via dysregulated eIF4E-dependent translational control. Nature *493*, 371-377.

Goodlett, C.R., Hamre, K.M., and West, J.R. (1992). Dissociation of spatial navigation and visual guidance performance in Purkinje cell degeneration (pcd) mutant mice. Behavioural brain research *47*, 129-141.
Grzadzinski, R., Huerta, M., and Lord, C. (2013). DSM-5 and autism spectrum disorders (ASDs): an opportunity for identifying ASD subtypes. Molecular autism *4*, 12.

Hansel, D., and Mato, G. (2013). Short-term plasticity explains irregular persistent activity in working memory tasks. Journal of Neuroscience *33*, 133-149.

Hansen, S.T., Meera, P., Otis, T.S., and Pulst, S.M. (2013). Changes in Purkinje cell firing and gene expression precede behavioral pathology in a mouse model of SCA2. Human molecular genetics *22*, 271-283.

Häusser, M., and Clark, B.A. (1997). Tonic synaptic inhibition modulates neuronal output pattern and spatiotemporal synaptic integration. Neuron *19*, 665-678.

Hay, N., and Sonenberg, N. (2004). Upstream and downstream of mTOR. Genes & development *18*, 1926-1945.

Hirano, T. (2018). Purkinje Neurons: Development, Morphology, and Function. Cerebellum *17*, 699-700.

Hoebeek, F., Stahl, J., Van Alphen, A., Schonewille, M., Luo, C., Rutteman, M., Van den Maagdenberg, A., Molenaar, P., Goossens, H., and Frens, M. (2005). Increased noise level of purkinje cell activities minimizes impact of their modulation during sensorimotor control. Neuron *45*, 953-965.

Hoeffer, C.A., Sanchez, E., Hagerman, R.J., Mu, Y., Nguyen, D.V., Wong, H., Whelan, A.M., Zukin, R.S., Klann, E., and Tassone, F. (2012). Altered mTOR signaling and enhanced CYFIP2 expression levels in subjects with fragile X syndrome. Genes Brain Behav *11*, 332-341.

Hong, S., Negrello, M., Junker, M., Smilgin, A., Thier, P., and De Schutter, E. (2016). Multiplexed coding by cerebellar Purkinje neurons. Elife *5*, e13810.

Hourez, R., Servais, L., Orduz, D., Gall, D., Millard, I., de Kerchove d'Exaerde, A., Cheron, G., Orr, H.T., Pandolfo, M., and Schiffmann, S.N. (2011). Aminopyridines correct early dysfunction and delay neurodegeneration in a mouse model of spinocerebellar ataxia type 1. Journal of Neuroscience *31*, 11795-11807.

Huang, W.-C., Chen, Y., and Page, D.T. (2016). Hyperconnectivity of prefrontal cortex to amygdala projections in a mouse model of macrocephaly/autism syndrome. Nature communications *7*, 1-15.

Huber, K.M., Klann, E., Costa-Mattioli, M., and Zukin, R.S. (2015). Dysregulation of Mammalian Target of Rapamycin Signaling in Mouse Models of Autism. J Neurosci *35*, 13836-13842.

Jayabal, S., Chang, H.H.V., Cullen, K.E., and Watt, A.J. (2016). 4-aminopyridine reverses ataxia and cerebellar firing deficiency in a mouse model of spinocerebellar ataxia type 6. Scientific reports *6*, 29489.

Kassai, H., Sugaya, Y., Noda, S., Nakao, K., Maeda, T., Kano, M., and Aiba, A. (2014). Selective activation of mTORC1 signaling recapitulates microcephaly, tuberous sclerosis, and neurodegenerative diseases. Cell reports *7*, 1626-1639.

Kaufmann, W.E., Cooper, K.L., Mostofsky, S.H., Capone, G.T., Kates, W.R., Newschaffer, C.J., Bukelis, I., Stump, M.H., Jann, A.E., and Lanham, D.C. (2003). Specificity of cerebellar vermian abnormalities in autism: a quantitative magnetic resonance imaging study. Journal of child neurology *18*, 463-470.

Kelly, E., Meng, F., Fujita, H., Morgado, F., Kazemi, Y., Rice, L.C., Ren, C., Escamilla, C.O., Gibson, J.M., Sajadi, S., *et al.* (2020). Regulation of autism-relevant behaviors by cerebellar-prefrontal cortical circuits. Nat Neurosci.

Kistler, W.M., and Zeeuw, C.I.D. (2002). Dynamical working memory and timed responses: the role of reverberating loops in the olivo-cerebellar system. Neural computation *14*, 2597-2626.

Kloth, A.D., Badura, A., Li, A., Cherskov, A., Connolly, S.G., Giovannucci, A., Bangash, M.A., Grasselli, G., Penagarikano, O., Piochon, C., *et al.* (2015). Cerebellar associative sensory learning defects in five mouse autism models. Elife *4*, e06085.

Lai, M.-C., and Baron-Cohen, S. (2015). Identifying the lost generation of adults with autism spectrum conditions. The Lancet Psychiatry *2*, 1013-1027.

Lalonde, R., Lamarre, Y., and Smith, A.M. (1988). Does the mutant mouse lurcher have deficits in spatially oriented behaviours? Brain research *455*, 24-30.

Leppek, K., Das, R., and Barna, M. (2018). Functional 5' UTR mRNA structures in eukaryotic translation regulation and how to find them. Nature reviews Molecular cell biology *19*, 158-174.

Morris, R. (1984). Developments of a water-maze procedure for studying spatial learning in the rat. Journal of neuroscience methods *11*, 47-60.

Neves-Pereira, M., Muller, B., Massie, D., Williams, J.H., O'Brien, P.C., Hughes, A., Shen, S.B., Clair, D.S., and Miedzybrodzka, Z. (2009). Deregulation of EIF4E: a novel mechanism for autism. J Med Genet *46*, 759-765.

Nguyen-Vu, T.B., Kimpo, R.R., Rinaldi, J.M., Kohli, A., Zeng, H., Deisseroth, K., and Raymond, J.L. (2013). Cerebellar Purkinje cell activity drives motor learning. Nature neuroscience *16*, 1734.

Palmen, S.J., van Engeland, H., Hof, P.R., and Schmitz, C. (2004). Neuropathological findings in autism. Brain *127*, 2572-2583.

Passot, J.-B., Sheynikhovich, D., Duvelle, É., and Arleo, A. (2012). Contribution of cerebellar sensorimotor adaptation to hippocampal spatial memory. PloS one *7*.

Payne, H.L., French, R.L., Guo, C.C., Nguyen-Vu, T.B., Manninen, T., and Raymond, J.L. (2019). Cerebellar Purkinje cells control eye movements with a rapid rate code that is invariant to spike irregularity. Elife *8*, e37102.

Pelletier, J., and Sonenberg, N. (1985). Insertion mutagenesis to increase secondary structure within the 5' noncoding region of a eukaryotic mRNA reduces translational efficiency. Cell *40*, 515-526.

Poulin, F., Gingras, A.C., Olsen, H., Chevalier, S., and Sonenberg, N. (1998). 4E-BP3, a new member of the eukaryotic initiation factor 4E-binding protein family. J Biol Chem *273*, 14002-14007.

Reith, R.M., Way, S., McKenna III, J., Haines, K., and Gambello, M.J. (2011). Loss of the tuberous sclerosis complex protein tuberin causes Purkinje cell degeneration. Neurobiology of disease *43*, 113-122.

Rochefort, C., Arabo, A., Andre, M., Poucet, B., Save, E., and Rondi-Reig, L. (2011a). Cerebellum shapes hippocampal spatial code. Science *334*, 385-389.

Rochefort, C., Arabo, A., André, M., Poucet, B., Save, E., and Rondi-Reig, L. (2011b). Cerebellum shapes hippocampal spatial code. Science *334*, 385-389.

Rochefort, C., Lefort, J.M., and Rondi-Reig, L. (2013). The cerebellum: a new key structure in the navigation system. Front Neural Circuits *7*, 35.

Santini, E., Huynh, T.N., MacAskill, A.F., Carter, A.G., Pierre, P., Ruggero, D., Kaphzan, H., and Klann, E. (2013). Exaggerated translation causes synaptic and behavioural aberrations associated with autism. Nature *493*, 411-415.

Santini, E., and Klann, E. (2014). Reciprocal signaling between translational control pathways and synaptic proteins in autism spectrum disorders. Sci Signal *7*, re10-re10.

Semenov, L., and Bures, J. (1989). Vestibular stimulation disrupts acquisition of place navigation in the Morris water tank task. Behavioral and neural biology *51*, 346-363.

Shabani, M., Hosseinmardi, N., Haghani, M., Shaibani, V., and Janahmadi, M. (2011). Maternal exposure to the CB1 cannabinoid agonist WIN 55212–2 produces robust changes in motor function and intrinsic electrophysiological properties of cerebellar Purkinje neurons in rat offspring. Neuroscience *172*, 139-152.

Shakkottai, V.G., do Carmo Costa, M., Dell'Orco, J.M., Sankaranarayanan, A., Wulff, H., and Paulson, H.L. (2011). Early changes in cerebellar physiology accompany motor dysfunction in the polyglutamine disease spinocerebellar ataxia type 3. Journal of Neuroscience *31*, 13002-13014.

Sharma, A., Hoeffer, C.A., Takayasu, Y., Miyawaki, T., McBride, S.M., Klann, E., and Zukin, R.S. (2010). Dysregulation of mTOR signaling in fragile X syndrome. Journal of Neuroscience *30*, 694-702.

Skefos, J., Cummings, C., Enzer, K., Holiday, J., Weed, K., Levy, E., Yuce, T., Kemper, T., and Bauman, M. (2014). Regional alterations in purkinje cell density in patients with autism. PloS one *9*.

Softky, W.R., and Koch, C. (1993). The highly irregular firing of cortical cells is inconsistent with temporal integration of random EPSPs. Journal of Neuroscience *13*, 334-350.

Sonenberg, N., and Gingras, A.-C. (1998). The mRNA 5′ cap-binding protein eIF4E and control of cell growth. Current Opinion in Cell Biology *10*, 268-275.

Sonenberg, N., and Hinnebusch, A.G. (2009). Regulation of translation initiation in eukaryotes: mechanisms and biological targets. Cell *136*, 731-745.

Steuber, V., Mittmann, W., Hoebeek, F.E., Silver, R.A., De Zeeuw, C.I., Häusser, M., and De Schutter, E. (2007). Cerebellar LTD and pattern recognition by Purkinje cells. Neuron *54*, 121-136.

Stoodley, C.J., D'Mello, A.M., Ellegood, J., Jakkamsetti, V., Liu, P., Nebel, M.B., Gibson, J.M., Kelly, E., Meng, F., and Cano, C.A. (2017). Altered cerebellar connectivity in autism and cerebellar-mediated rescue of autism-related behaviors in mice. Nature neuroscience *20*, 1744-1751.

Stoyas, C.A., Bushart, D.D., Switonski, P.M., Ward, J.M., Alaghatta, A., Tang, M.-b., Niu, C., Wadhwa, M., Huang, H., and Savchenko, A. (2020). Nicotinamide pathway-dependent SIRT1 activation restores calcium homeostasis to achieve neuroprotection in spinocerebellar ataxia type 7. Neuron *105*, 630-644. e639.

Tang, G., Gudsnuk, K., Kuo, S.-H., Cotrina, M.L., Rosoklija, G., Sosunov, A., Sonders, M.S., Kanter, E., Castagna, C., and Yamamoto, A. (2014). Loss of mTOR-dependent macroautophagy causes autistic-like synaptic pruning deficits. Neuron *83*, 1131-1143.

Thoreen, C.C., Chantranupong, L., Keys, H.R., Wang, T., Gray, N.S., and Sabatini, D.M. (2012). A unifying model for mTORC1-mediated regulation of mRNA translation. Nature *485*, 109-113.

Tom Dieck, S., Muller, A., Nehring, A., Hinz, F.I., Bartnik, I., Schuman, E.M., and Dieterich, D.C. (2012). Metabolic labeling with noncanonical amino acids and visualization by chemoselective fluorescent tagging. Curr Protoc Cell Biol *Chapter 7*, Unit7 11.

Tsai, P.T., Hull, C., Chu, Y., Greene-Colozzi, E., Sadowski, A.R., Leech, J.M., Steinberg, J., Crawley, J.N., Regehr, W.G., and Sahin, M. (2012). Autistic-like behaviour and cerebellar dysfunction in Purkinje cell Tsc1 mutant mice. Nature *488*, 647-651.

Tsai, P.T., Rudolph, S., Guo, C., Ellegood, J., Gibson, J.M., Schaeffer, S.M., Mogavero, J., Lerch, J.P., Regehr, W., and Sahin, M. (2018). Sensitive periods for cerebellar-mediated autistic-like behaviors. Cell reports *25*, 357-367. e354.

Walter, J.T., Alvina, K., Womack, M.D., Chevez, C., and Khodakhah, K. (2006). Decreases in the precision of Purkinje cell pacemaking cause cerebellar dysfunction and ataxia. Nature neuroscience *9*, 389-397.

Wang, L.W., Berry-Kravis, E., and Hagerman, R.J. (2010). Fragile X: leading the way for targeted treatments in autism. Neurotherapeutics *7*, 264-274.

Wang, S.S.-H., Kloth, A.D., and Badura, A. (2014). The cerebellum, sensitive periods, and autism. Neuron *83*, 518-532.

Watt, A.J., Cuntz, H., Mori, M., Nusser, Z., Sjöström, P.J., and Häusser, M. (2009). Traveling waves in developing cerebellar cortex mediated by asymmetrical Purkinje cell connectivity. Nature neuroscience *12*, 463.

Wegiel, J., Flory, M., Kuchna, I., Nowicki, K., Ma, S.Y., Imaki, H., Wegiel, J., Cohen, I.L., London, E., and Wisniewski, T. (2014). Stereological study of the neuronal number and volume of 38 brain subdivisions of subjects diagnosed with autism reveals significant alterations restricted to the striatum, amygdala and cerebellum. Acta neuropathologica communications *2*, 141.

White, J.J., Arancillo, M., King, A., Lin, T., Miterko, L.N., Gebre, S.A., and Sillitoe, R.V. (2016). Pathogenesis of severe ataxia and tremor without the typical signs of neurodegeneration. Neurobiology of disease *86*, 86-98.

Wiebe, S., Nagpal, A., Truong, V.T., Park, J., Skalecka, A., He, A.J., Gamache, K., Khoutorsky, A., Gantois, I., and Sonenberg, N. (2019). Inhibitory interneurons mediate autism-associated behaviors via 4E-BP2. Proc Natl Acad Sci U S A *116*, 18060-18067.

Winslow, J.T. (2003). Mouse social recognition and preference. Current protocols in neuroscience *22*, 8.16. 11-18.16. 16.

Yakusheva, T.A., Shaikh, A.G., Green, A.M., Blazquez, P.M., Dickman, J.D., and Angelaki, D.E. (2007). Purkinje cells in posterior cerebellar vermis encode motion in an inertial reference frame. Neuron *54*, 973-985.

Yoon, S.Y., Choi, J.E., Kweon, H.S., Choe, H., Kim, S.W., Hwang, O., Lee, H., Lee, J.Y., and Kim, D.H. (2008). Okadaic acid increases autophagosomes in rat neurons: implications for Alzheimer's disease. Journal of neuroscience research *86*, 3230-3239.

Zhou, J., Blundell, J., Ogawa, S., Kwon, C.-H., Zhang, W., Sinton, C., Powell, C.M., and Parada, L.F. (2009). Pharmacological inhibition of mTORC1 suppresses anatomical, cellular, and behavioral abnormalities in neural-specific Pten knock-out mice. Journal of Neuroscience *29*, 1773-1783.

Chapter 4: Discussion

4.1 Chapter 2: The integrated stress response pathway in excitatory neurons controls autistic features.

4.1.1 p-eIF2α is significantly reduced in excitatory neurons of *Fmr1* KO mice

In this study, we found that p-eIF2α is substantially reduced in several brain regions of *Fmr1* KO mice. This phenomenon can be caused by either hypoactivation of the kinases that phosphorylate the eIF2α, or hyperactivation of the phosphatases that dephosphorylate eIF2α. We did not observe any significant alterations in the expression of the phosphatases or kinases except for p-GCN2/GCN2 which was increased compared to WT control animals. The elevated p-GCN2/GCN2 has been associated with ribosome stalling and collision, which are common in the absence of the FMRP (Ishimura, Nagy et al. 2016).

Our data further showed that diminished phosphorylated eIF2α in the brain of *Fmr1* KO mice is restricted to excitatory neurons (labeled with CAMKIIα) in the hippocampus, basolateral amygdala, and medial prefrontal cortex, and is not detected in inhibitory neurons (GAD67-positive neurons). Several previous studies used Translating Ribosome Affinity Purification (TRAP) to explore the cell-type-specific translatome in the brain of *Fmr1* KO mice. They have reported a substantial reduction in the expression of the genes harboring uORFs in the excitatory neurons in the CA1 region of the hippocampus in *Fmr1* KO mice (Ceolin, Bouquier et al. 2017, Sawicka, Hale et al. 2019). The expression of the genes containing uORFs is increased in the presence of p-eIF2α and paradoxically, when the level of the p-eIF2α is decreased, their expression is reduced.

Similarly, selective deletion of FMRP in cortical excitatory neurons using $Nex1^{Cre}/Fmr1^{Flox/y}$ conditional KOs is sufficient to increase the activity of the AKT/mTORC1 signaling pathway and gamma power in resting EEG. It also decreased the density of PV neurons and perineuronal nets (PNNs) in the auditory cortex. These findings suggest that deletion of FMRP only in excitatory neurons is sufficient to elicit the core phenotypes of *Fmr1*

KO mice (Lovelace, Rais et al. 2020). Likewise, another study reported that ablation of the *Fmr1* gene selectively in cortical excitatory but not inhibitory neurons is sufficient to produce abnormally long UP states and seizure activities (Hays, Huber et al. 2011).

Another potential explanation for the excitatory neuron-specific reduction in p-eIF2α level has been demonstrated by a recent study (Guo, Ceolin et al. 2015). This study showed that CaMKIIα, which is selectively expressed in excitatory neurons and is a direct target of FMRP (Darnell, Van Driesche et al.), is required for constitutive mGluR5 activity (Guo, Ceolin et al. 2015). This study showed that CaMKIIα phosphorylates Homer, resulting in disruption of the mGluR5-Homer interaction and causing the activation of mGluR5. Hyperactivation of mGluR5 is a key feature in *Fmr1*$^{-/y}$ mice, which signals to and enhances the activity of the PI3K-mTORC1 axis. Since CaMKIIα is an FMRP target, its levels are increased in *Fmr1*$^{-/y}$ mice (Ronesi, Collins et al. 2012, Guo, Ceolin et al. 2015). Thus, it is conceivable that increased levels of CaMKIIα in excitatory neurons of *Fmr1*$^{-/y}$ mice underlie a selective activation of the mTORC1 pathway in excitatory neurons and thereby reduction in p-eIF2α level. This potential mechanism needs to be further investigated in future studies.

4.1.2 Reduced p-eIF2α in excitatory neurons in the brain of *Fmr1* KO mice is driven by the mTORC1 pathway.

As we showed, the activity of p-eIF2α kinases and phosphatases can not explain the decreased level of p-eIF2α in *Fmr1*$^{-/y}$ mice. Therefore, other mechanisms underlie such notable changes in the integrated stress response pathway. Using different approaches, we showed that alteration in levels of p-eIF2α is driven by the mTORC1 signaling pathway. We demonstrated that selective activation of mTORC1 using NV-5138 causes a significant reduction in p-eIF2α in wild-type animals, suggesting crosstalk between the mTORC1 and eIF2α pathway. This finding is consistent with a study showing that activation of mTORC1 in non-neuronal cells

transiently decreases p-eIF2α. However, the exact molecular mechanism underlying this effect remains unknown (Gandin, Masvidal et al. 2016). Similarly, inhibition of mTORC1 by application of doxorubicin in non-neuronal cells led to phosphorylation of eIF2α (Harvey, Pöyry et al. 2019). The existence of this crosstalk in the brain was further supported by our data. We showed that selective blockade of mTORC1 using CCI-779 rescues decreased p-eIF2α in the brain lysates of *Fmr1* KO mice.

It has previously been demonstrated that the expression of the mTORC1 and p-S6 is enhanced in the brain of *Fmr1* KO mice and genetic deletion of S6K prevents the core symptoms in *Fmr1* KO mice (Bhattacharya, Kaphzan et al. 2012). We expanded these findings by showing that the enhanced phosphorylation of S6 was found exclusively in excitatory neurons in the hippocampus, prefrontal cortex, and basolateral amygdala in *Fmr1* KO mice, which is consistent with the idea that activation of the mTORC1 in excitatory neurons in the brain of the *Fmr1* KO mice decreases phosphorylated eIF2α in these neurons.

To further confirm that mTORC1 dephosphorylates p-eIF2α in excitatory neurons, cell-type-specific manipulations are required. For example, assessing p-eIF2α in excitatory neurons following the genetic deletion of mTORC1 in these neurons in *Fmr1* KO mice.

4.1.3 Normalization of p-eIF2α in excitatory neurons rescued exaggerated mGluR-LTD

In line with previous findings (Huber, Gallagher et al. 2002, Bhattacharya, Kaphzan et al. 2012, Thomson, Seo et al. 2017), we also revealed that mGluR-LTD is exaggerated in the hippocampus of *Fmr1* KO mice. In addition, excitatory-specific restoration of p-eIF2α in the brain of *Fmr1* KO mice to the wild-type level partially rescued enhanced mGluR-LTD. Consistent with our findings, forebrain-specific ablation of PERK ($Perk^{Flox/Flox}$; $CamkIIa^{Cre}$), which causes a ~ 50% reduction in p-eIF2 in the hippocampus, has been shown to elicit an elevated hippocampal mGluR-LTD (Trinh, Ma et al. 2014). This mGluR-LTD is sensitive to

anisomycin, indicating that it is protein synthesis-dependent (Trinh, Ma et al. 2014). However, the mGluR-LTD in the hippocampal sections of $GCN2^{-/-}$ mice was shown to be comparable to the wild-type animals (Costa-Mattioli, Gobert et al. 2005).

By contrast, hippocampal mGluR-LTD and the internalization of surface AMPA receptors (AMPARs), which are essential for the initialization of mGluR-LTD, were prevented by either genetically suppressing eIF2a phosphorylation or by pharmacologically blocking translation regulated by eIF2a phosphorylation (Di Prisco, Huang et al. 2014).

The discrepancy between the findings of Prisco et. al. and our results may be due to several reasons. First, whereas Prisco et. al., used hippocampal sections obtained from wild-type mice, while we recorded mGluR-LTD in the hippocampal sections prepared from *Fmr1* KO mice with full deletion of FMRP. Several proteins essential for mGluR-LTD are among the FMRP targets, and in the absence of FMRP, their expression is dramatically upregulated resulting in exaggerated mGluR-LTD. The activity-regulated cytoskeleton-associated protein (Arc), one of the targets of FMRP and a key protein in the formation of mGluR-LTD, is upregulated in the brain of *Fmr1* KO mice. (Niere, Wilkerson et al. 2012). The Arc protein is expressed normally in the brain of the mice used in Prisco's study, and Sal003-induced LTD caused by elevated p-eIF2 is not prevented by blocking Arc translation (Di Prisco, Huang et al. 2014). Another FMRP target that is essential for mGluR-LTD (Waung and Huber 2009) is microtubule-associated protein 1b (MAP1b), which is also increased in the brain of *Fmr1* KO mice (Lu, Wang et al. 2004). In contrast, Prisco's study did not observe an increase in the translation of MAP1b following activation of mGluR (Di Prisco, Huang et al. 2014).

The second source of discrepancy is the recording techniques for mGluR-LTD, namely single-cell patch clamp recording in Prisco's study versus field potential recording in our work. It has been shown that group I metabotropic glutamate receptor stimulation initiates mGluR-LTD in excitatory neurons (eLTD) and inhibitory interneurons (iLTD) through distinct

mechanisms (Valentinova and Mameli 2016). Therefore, the net outcome of the mGluR-LTD at the circuit level relies on whether the mGluR-eLTD or mGluR-iLTD is more potent. In contrast to Prisco's study, which measured the mGluR-LTD in a single pyramidal neuron in the hippocampal section, we assessed the mGluR-LTD using a field potential in the CA1 area of the hippocampus, which integrates the activities of both excitatory and inhibitory neurons.

Moreover, our finding is supported by studies demonstrating that inhibition and stimulation of translation initiation either restore the exaggerated mGluR-LTD or enhance the mGluR-LTD, respectively. For example, mice with genetic deletion of 4E-BP2, which results in overactivation of eIF4F and increased translation, exhibit enhanced mGluR-LTD (Banko, Hou et al. 2006). Genetic ablation of p70 S6 Kinase 1 (S6K1) in the brain of *Fmr1* KO mice rescued the exaggerated mGluR-LTD in these mice (Bhattacharya, Kaphzan et al. 2012).

In conclusion, loss of the FMRP results in excessive expression of the proteins required for mGluR-LTD such as Arc and MAP1b, which in turn leads to exaggerated mGluR-LTD. The expression of these proteins and the exaggerated mGluR-LTD is diminished when the level of p-eIF2α is restored to the wild-type levels.

4.1.4 Deletion of p-eIF2a in excitatory neurons but not the whole body causes autistic-like behaviors

Our findings revealed that excitatory neuron-selective ablation of p-eIF2α (~ 50 %) is sufficient to cause impaired social interactions and repetitive behaviors, which are the key autistic phenotypes. However, mice with 50 % overall deletion of p-eIF2α did not display autistic-like behaviors in comparison to their control littermates. These findings can be explained by the excitation-inhibition imbalance theory of autism. The imbalanced excitation-inhibition (E/I) notion initially emerged from clinical observations showing that up to 38 % of autistic individuals suffer from epileptic seizures and approximately 60–80 % had abnormal

EEG (Levisohn 2007). Furthermore, studies have shown that several brain circuits in autistic people are hyperexcitable (Takarae and Sweeney 2017).

An imbalanced E/I ratio has been hypothesized as one of the key underpinning mechanisms of impaired social interaction and anxiety behavior in autistic patients and animal models (Gao and Penzes 2015, Mullins, Fishell et al. 2016). Consistently, a recent study reported an increased E/I ratio in the cortical area of four autism mouse models, *Cntnap2*$^{-/-}$, *Fmr*1$^{-/y}$, *Tsc2*$^{+/-}$, and 16p11.2$^{del/+}$ (Antoine, Langberg et al. 2019). Likewise, a higher E/I ratio was detected in layer 5 pyramidal neurons of the prefrontal cortex in the mice with forebrain-specific deletion of Cacna1c protein. This mouse model had a higher amplitude and frequency of miniature excitatory synaptic currents (mEPSCs), higher mEPSC total charge, and greater levels of VGLUT1/IB (Kabir, Che et al. 2017). In a more recent study, it was shown that excitatory neuron-specific ablation of p-eIF2α increases E/I ratio as reflected by increased EPSC amplitude and frequency, and decreased IPSC frequency (Sharma, Sood et al. 2020). Based on these results, it is conceivable that E/I ratio is imbalanced in the *Eif2*α cKI$^{CamKII\alpha}$ mice. Since in the general heterozygous mice reduction of p-eIF2α occurs in all cell types, we hypothesise that other cell types cancel out the cell-type-specific effect of p-eIF2α on E/I ratio. That might explain why, unlike *Eif2*α cKI$^{CamKII\alpha}$ mice, the general het mice (*Eif2*α$^{S/A}$) did not exhibit autistic-like behaviors.

4.1.5 Excitatory-neuron-specific normalization of p-eIF2α in the brain of *Fmr1* KO mice improves core autistic behaviors

We showed that correction of the p-eIF2α levels in excitatory neurons rescues impaired social interaction, repetitive behaviors, and audiogenic seizures in the *Fmr1* KO mice. Furthermore, protein synthesis in excitatory neurons was comparable to wild-type levels. Exaggerated protein synthesis is believed to be the root cause of autistic behaviors in *Fmr1* KO mice (Bear,

Huber et al. 2004, Kelleher III and Bear 2008, Xu, Kim et al. 2020). Since phosphorylated eIF2α inhibits general protein synthesis by reducing the available trinary complex (TC) formation, exaggerated protein synthesis and the associated autistic-like behaviors in *Fmr1* KO mice can be mitigated by normalization of the p-eIF2α in excitatory neurons.

4.2 Chapter 3: 4E-BP2-dependent translation in cerebellar Purkinje cells controls spatial memory but not autism-like behaviors

4.2.1 Purkinje cell-specific deletion of 4E-BP2 does not lead to autistic-like behavior.

Previous studies have reported that genetic ablation of TSC1/2 (Tsai, Hull et al. 2012, Reith, McKenna et al. 2013) and PTEN (Cupolillo, Hoxha et al. 2016), negative regulators of mTORC1, in Purkinje cells results in autistic-like behavior in conjunction with multiple morphological and electrophysiological deficits. We showed that hyperactivation of mTORC1/eIF4E axis in Purkinje cells by deletion of 4E-BP2, a key downstream effector of mTORC1, did not lead to autism-like behaviors in mice. It is conceivable that overactivation of mTORC1 in Purkinje cells causes autistic phenotypes through other pathways downstream of mTORC1 (e.g. S6K, autophagy) rather than 4E-BP2. Genetic deletion of S6K in *Fmr1* KO mice rescued autistic-like behaviors suggesting that hyperactivated mTORC1 can cause autistic features via its downstream S6K/S6 axis (Bhattacharya, Kaphzan et al. 2012). Modulation of autophagy is the second potential mechanism. Mutations in autophagy-related genes are causally associated with autism spectrum disorders (Poultney, Goldberg et al. 2013, Sragovich, Merenlender-Wagner et al. 2017). Additionally, mTORC1 directly controls autophagy by phosphorylating Unc-51-like autophagy activating kinase (ULK1) (Kim, Kundu et al. 2011). Therefore, hyperactivation of mTORC1 as a result of TSC1/2 or PTEN deletion in PCs can inhibit ULK1 and thereby cause autism-like behavior in these mouse models.

4.2.2 Ablation of 4E-BP2 in Purkinje cells causes spatial memory impairment

We showed that selective deletion of 4E-BP2 in PCs leads to impaired spatial memory in the Morris water maze test (MWM). Whole-body genetic deletion of 4E-BP2 impairs spatial learning and memory in mice. (Banko, Poulin et al. 2005). Selective chemical destruction of PCs also impairs the acquisition phase of the MWM test (Gandhi, Kelly et al. 2000). Since we found PC loss in 4E-BP2 conditional KO mice, the impaired MWM performance in these mice could be caused by PC loss in the cerebellum. Consistent with our data, deletion of PTEN exclusively in PCs impaired spatial memory, pointing to the potential function of the 4E-BP2 in PCs in hippocampus-dependent spatial memory (Cupolillo, Hoxha et al. 2016). As we showed that deletion of 4E-BP2 in PCs did not affect contextual fear conditioning behavior, a cerebellum-independent, and hippocampus-dependent test, it can be concluded that the deficits observed in the MWM test are caused by cerebellum-specific disturbances while hippocampal functions remained intact.

4.2.3 Purkinje cell loss in 4E-BP2 cKO mice.

PC loss is a common finding in both individuals with autism and autistic animal models (Fehlow, Bernstein et al. 1993, Bauman and Kemper 2005, Cupolillo, Hoxha et al. 2016). In our study, however, PC loss was not accompanied by any autistic phenotypes. One possible explanation is that PC loss is a consequence of autism and not the cause of it. In 4E-BP2 cKO mice, PC loss does not result in autistic-like features while many autistic mouse models exhibit reduced PCs.

In our study, PC loss was observed only in lobules VI and VII. Thus, another possible explanation is that PC loss in these two lobules is not sufficient to drive autistic phenotypes.

4.3 Conclusion

Our study in chapter 2 revealed an excitatory neuron-specific reduction in p-eIF2α and a concomitant increase in global protein synthesis in a mouse model of FXS, *Fmr1* KO. Reduced p-eIF2α was causally associated with autistic-like phenotypes as genetic ablation of p-eIF2α in excitatory neurons in wild-type mice was sufficient to cause autism-like phenotype, and normalization of p-eIF2α in excitatory neurons rescued the autistic phenotype in *Fmr1* KO mice. Interestingly, we provided evidence that the reduction in p-eIF2α in excitatory neurons is driven by hyperactivation of mTORC1. Additionally, in chapter 3, we showed that genetic ablation of 4E-BP2 in cerebellar Purkinje cells impairs spatial memory in MWM and leads to a lobule-specific PC loss while it did not cause autistic-like behavior, suggesting a role for mTORC1 in cerebellar PCs in spatial memory through 4E-BP2.

4.4 References

Alone, P. V. and T. E. Dever (2006). "Direct binding of translation initiation factor eIF2γ-G domain to its GTPase-activating and GDP-GTP exchange factors eIF5 and eIF2Bϵ." Journal of Biological Chemistry **281**(18): 12636-12644.

Alpatov, R., et al. (2014). "A chromatin-dependent role of the fragile X mental retardation protein FMRP in the DNA damage response." Cell **157**(4): 869-881.

Alvarez-Castelao, B., et al. (2020). "The switch-like expression of heme-regulated kinase 1 mediates neuronal proteostasis following proteasome inhibition." Elife **9**: e52714.

Alvarez, V. A. and B. L. Sabatini (2007). "Anatomical and physiological plasticity of dendritic spines." Annu. Rev. Neurosci. **30**: 79-97.

Antar, L. N., et al. (2004). "Metabotropic glutamate receptor activation regulates fragile x mental retardation protein and FMR1 mRNA localization differentially in dendrites and at synapses." Journal of Neuroscience **24**(11): 2648-2655.

Antoine, M. W., et al. (2019). "Increased excitation-inhibition ratio stabilizes synapse and circuit excitability in four autism mouse models." Neuron **101**(4): 648-661. e644.

Armstrong, C. G., et al. (1997). "PPP1R6, a novel member of the family of glycogen-targetting subunits of protein phosphatase 1." FEBS letters **418**(1-2): 210-214.

Ashley Jr, C. T., et al. (1993). "FMR1 protein: conserved RNP family domains and selective RNA binding." Science **262**(5133): 563-566.

Bai, X., et al. (2007). "Rheb activates mTOR by antagonizing its endogenous inhibitor, FKBP38." Science **318**(5852): 977-980.

Bakker, C. E., et al. (2000). "Immunocytochemical and biochemical characterization of FMRP, FXR1P, and FXR2P in the mouse." Experimental cell research **258**(1): 162-170.

Banko, J. L., et al. (2006). "Regulation of eukaryotic initiation factor 4E by converging signaling pathways during metabotropic glutamate receptor-dependent long-term depression." Journal of Neuroscience **26**(8): 2167-2173.

Banko, J. L., et al. (2005). "The translation repressor 4E-BP2 is critical for eIF4F complex formation, synaptic plasticity, and memory in the hippocampus." Journal of Neuroscience **25**(42): 9581-9590.

Barnea-Goraly, N., et al. (2014). "A preliminary longitudinal volumetric MRI study of amygdala and hippocampal volumes in autism." Progress in Neuro-Psychopharmacology and Biological Psychiatry **48**: 124-128.

Bassell, G. J. and S. T. Warren (2008). "Fragile X syndrome: loss of local mRNA regulation alters synaptic development and function." Neuron **60**(2): 201-214.

Basu, S. N., et al. (2009). "AutDB: a gene reference resource for autism research." Nucleic acids research **37**(suppl_1): D832-D836.

Bauer, B. N., et al. (2001). "Multiple autophosphorylation is essential for the formation of the active and stable homodimer of heme-regulated eIF2α kinase." Biochemistry **40**(38): 11543-11551.

Bauman, M. L. (2010). "Medical comorbidities in autism: challenges to diagnosis and treatment." Neurotherapeutics **7**(3): 320-327.

Bauman, M. L. and T. L. Kemper (2005). "Neuroanatomic observations of the brain in autism: a review and future directions." International journal of developmental neuroscience **23**(2-3): 183-187.

Bear, M. F., et al. (2004). "The mGluR theory of fragile X mental retardation." Trends in neurosciences **27**(7): 370-377.

Berry-Kravis, E. (2002). "Epilepsy in fragile X syndrome." Developmental medicine and child neurology **44**(11): 724-728.

Bhattacharya, A., et al. (2012). "Genetic removal of p70 S6 kinase 1 corrects molecular, synaptic, and behavioral phenotypes in fragile X syndrome mice." Neuron **76**(2): 325-337.

Bidinosti, M., et al. (2010). "Postnatal deamidation of 4E-BP2 in brain enhances its association with raptor and alters kinetics of excitatory synaptic transmission." Molecular cell **37**(6): 797-808.

Bourgeron, T. (2009). "A synaptic trek to autism." Current opinion in neurobiology **19**(2): 231-234.

Boyce, M., et al. (2005). "A selective inhibitor of eIF2α dephosphorylation protects cells from ER stress." Science **307**(5711): 935-939.

Braun, K. and M. Segal (2000). "FMRP involvement in formation of synapses among cultured hippocampal neurons." Cerebral cortex **10**(10): 1045-1052.

Brown, M. R., et al. (2010). "Fragile X mental retardation protein controls gating of the sodium-activated potassium channel Slack." Nature neuroscience **13**(7): 819-821.

Brown, V., et al. (2001). "Microarray identification of FMRP-associated brain mRNAs and altered mRNA translational profiles in fragile X syndrome." Cell **107**(4): 477-487.

Carper, R. A. and E. Courchesne (2005). "Localized enlargement of the frontal cortex in early autism." Biological psychiatry **57**(2): 126-133.

Carriere, A., et al. (2011). "ERK1/2 phosphorylate Raptor to promote Ras-dependent activation of mTOR complex 1 (mTORC1)." Journal of Biological Chemistry **286**(1): 567-577.

Ceman, S., et al. (2003). "Phosphorylation influences the translation state of FMRP-associated polyribosomes." Human molecular genetics **12**(24): 3295-3305.

Ceolin, L., et al. (2017). "Cell type-specific mRNA dysregulation in hippocampal CA1 pyramidal neurons of the fragile X syndrome mouse model." Frontiers in molecular neuroscience **10**: 340.

Chen, E. and S. Joseph (2015). "Fragile X mental retardation protein: a paradigm for translational control by RNA-binding proteins." Biochimie **114**: 147-154.

Chen, E., et al. (2014). "Fragile X mental retardation protein regulates translation by binding directly to the ribosome." Molecular cell **54**(3): 407-417.

Chen, J.-J. (2000). "Heme-regulated eIF2alpha kinase." COLD SPRING HARBOR MONOGRAPH SERIES **39**: 529-546.

Chisholm, A. K., et al. (2018). "Social function and autism spectrum disorder in children and adults with neurofibromatosis type 1: a systematic review and meta-analysis." Neuropsychology Review **28**(3): 317-340.

Chuang, S.-C., et al. (2005). "Prolonged epileptiform discharges induced by altered group I metabotropic glutamate receptor-mediated synaptic responses in hippocampal slices of a fragile X mouse model." Journal of Neuroscience **25**(35): 8048-8055.

Collingridge, G. L., et al. (2010). "Long-term depression in the CNS." Nature reviews neuroscience **11**(7): 459-473.

Connor, J. H., et al. (2001). "Growth arrest and DNA damage-inducible protein GADD34 assembles a novel signaling complex containing protein phosphatase 1 and inhibitor 1." Molecular and cellular biology **21**(20): 6841-6850.

Consorthium, T. D.-B. F. X., et al. (1994). "Fmr1 knockout mice: a model to study fragile X mental retardation." Cell **78**(1): 23-33.

Contractor, A., et al. (2015). "Altered neuronal and circuit excitability in fragile X syndrome." Neuron **87**(4): 699-715.

Conturo, T. E., et al. (2008). "Neuronal fiber pathway abnormalities in autism: an initial MRI diffusion tensor tracking study of hippocampo-fusiform and amygdalo-fusiform pathways." Journal of the International Neuropsychological Society **14**(6): 933-946.

Cook Jr, E. H., et al. (1997). "Autism or atypical autism in maternally but not paternally derived proximal 15q duplication." American journal of human genetics **60**(4): 928.

Costa-Mattioli, M., et al. (2005). "Translational control of hippocampal synaptic plasticity and memory by the eIF2α kinase GCN2." Nature **436**(7054): 1166-1170.

Costa-Mattioli, M., et al. (2007). "eIF2α phosphorylation bidirectionally regulates the switch from short-to long-term synaptic plasticity and memory." Cell **129**(1): 195-206.

Costa-Mattioli, M. and P. Walter (2020). "The integrated stress response: From mechanism to disease." Science **368**(6489): eaat5314.

Courchesne, E., et al. (2011). "Brain growth across the life span in autism: age-specific changes in anatomical pathology." Brain research **1380**: 138-145.

Courchesne, E., et al. (2011). "Neuron number and size in prefrontal cortex of children with autism." Jama **306**(18): 2001-2010.

Crespi, B. J. (2010). "Revisiting Bleuler: relationship between autism and schizophrenia." The British Journal of Psychiatry **196**(6): 495-495.

Cupolillo, D., et al. (2016). "Autistic-like traits and cerebellar dysfunction in Purkinje cell PTEN knock-out mice." Neuropsychopharmacology **41**(6): 1457-1466.

D'Annessa, I., et al. (2019). "Handling FMRP and its molecular partners: Structural insights into Fragile X Syndrome." Progress in Biophysics and Molecular Biology **141**: 3-14.

d'Hulst, C., et al. (2006). "Decreased expression of the GABAA receptor in fragile X syndrome." Brain research **1121**(1): 238-245.

Dager, S. R., et al. (2007). "Shape mapping of the hippocampus in young children with autism spectrum disorder." American journal of neuroradiology **28**(4): 672-677.

Darnell, J., et al. "Fraser Ce, Stone eF, Chen C, Fak JJ, Chi Sw, Licatalosi DD, Richter JD, Darnell RB (2011) FMRP stalls ribosomal translocation on mRNAs linked to synaptic function and autism." Cell **146**(2): 247-261.

Darnell, J. C., et al. (2005). "FMRP RNA targets: identification and validation." Genes, Brain and Behavior **4**(6): 341-349.

Darnell, J. C., et al. (2011). "FMRP stalls ribosomal translocation on mRNAs linked to synaptic function and autism." Cell **146**(2): 247-261.

Davis, M. and P. J. Whalen (2001). "The amygdala: vigilance and emotion." Molecular psychiatry **6**(1): 13-34.

De Rubeis, S. and C. Bagni (2010). "Fragile X mental retardation protein control of neuronal mRNA metabolism: Insights into mRNA stability." Molecular and Cellular Neuroscience **43**(1): 43-50.

De Rubeis, S. and C. Bagni (2011). "Regulation of molecular pathways in the Fragile X Syndrome: insights into Autism Spectrum Disorders." Journal of Neurodevelopmental Disorders **3**(3): 257-269.

Deng, J., et al. (2002). "Activation of GCN2 in UV-irradiated cells inhibits translation." Current Biology **12**(15): 1279-1286.

Di Prisco, G. V., et al. (2014). "Translational control of mGluR-dependent long-term depression and object-place learning by eIF2α." Nature neuroscience **17**(8): 1073-1082.

Dictenberg, J. B., et al. (2008). "A direct role for FMRP in activity-dependent dendritic mRNA transport links filopodial-spine morphogenesis to fragile X syndrome." Developmental cell **14**(6): 926-939.

Dong, J., et al. (2000). "Uncharged tRNA activates GCN2 by displacing the protein kinase moiety from a bipartite tRNA-binding domain." Molecular cell **6**(2): 269-279.

Donnelly, N., et al. (2013). "The eIF2α kinases: their structures and functions." Cellular and molecular life sciences **70**(19): 3493-3511.

Drozd, M., et al. (2018). "Modeling fragile X syndrome in Drosophila." Frontiers in molecular neuroscience **11**: 124.

Durkin, M. S., et al. (2008). "Advanced parental age and the risk of autism spectrum disorder." American journal of epidemiology **168**(11): 1268-1276.

Eberhart, D. E., et al. (1996). "The fragile X mental retardation protein is a ribonucleoprotein containing both nuclear localization and nuclear export signals." Human molecular genetics **5**(8): 1083-1091.

Edens, B. M., et al. (2019). "FMRP modulates neural differentiation through m6A-dependent mRNA nuclear export." Cell reports **28**(4): 845-854. e845.

Eiermann, N., et al. (2020). "Dance with the devil: stress granules and signaling in antiviral responses." Viruses **12**(9): 984.

El Idrissi, A., et al. (2005). "Decreased GABAA receptor expression in the seizure-prone fragile X mouse." Neuroscience letters **377**(3): 141-146.

Ellegood, J., et al. (2015). "Clustering autism: using neuroanatomical differences in 26 mouse models to gain insight into the heterogeneity." Molecular psychiatry **20**(1): 118-125.

Engelman, J. A., et al. (2006). "The evolution of phosphatidylinositol 3-kinases as regulators of growth and metabolism." Nature Reviews Genetics **7**(8): 606-619.

Erickson, F., et al. (1997). "Functional analysis of homologs of translation initiation factor 2γ in yeast." Molecular and General Genetics MGG **253**(6): 711-719.

Evans, B. (2013). "How autism became autism: The radical transformation of a central concept of child development in Britain." History of the human sciences **26**(3): 3-31.

Faridar, A., et al. (2014). "Mapk/Erk activation in an animal model of social deficits shows a possible link to autism." Molecular autism **5**(1): 1-12.

Fatemi, S. H., et al. (2002). "Purkinje cell size is reduced in cerebellum of patients with autism." Cellular and molecular neurobiology **22**(2): 171-175.

Fehlow, P., et al. (1993). "Early infantile autism and excessive aerophagy with symptomatic megacolon and ileus in a case of Ehlers-Danlos syndrome." Padiatrie und Grenzgebiete **31**(4): 259-267.

Feinstein, A. (2011). A history of autism: Conversations with the pioneers, John Wiley & Sons.

Feng, Y., et al. (1997). "Fragile X mental retardation protein: nucleocytoplasmic shuttling and association with somatodendritic ribosomes." Journal of Neuroscience **17**(5): 1539-1547.

Ferrari, F., et al. (2007). "The fragile X mental retardation protein–RNP granules show an mGluR-dependent localization in the post-synaptic spines." Molecular and Cellular Neuroscience **34**(3): 343-354.

Ferron, L., et al. (2014). "Fragile X mental retardation protein controls synaptic vesicle exocytosis by modulating N-type calcium channel density." Nature communications **5**(1): 1-14.

Galvez, R., et al. (2005). "Olfactory bulb mitral cell dendritic pruning abnormalities in a mouse model of the Fragile-X mental retardation syndrome: further support for FMRP's involvement in dendritic development." Developmental Brain Research **157**(2): 214-216.

Gandhi, C. C., et al. (2000). "Impaired acquisition of a Morris water maze task following selective destruction of cerebellar purkinje cells with OX7-saporin." Behavioural brain research **109**(1): 37-47.

Gandin, V., et al. (2016). "mTORC1 and CK2 coordinate ternary and eIF4F complex assembly." Nature communications **7**(1): 1-15.

Gantois, I., et al. (2017). "Metformin ameliorates core deficits in a mouse model of fragile X syndrome." Nature medicine **23**(6): 674-677.

Gantois, I., et al. (2006). "Expression profiling suggests underexpression of the GABAA receptor subunit δ in the fragile X knockout mouse model." Neurobiology of disease **21**(2): 346-357.

Gao, R. and P. Penzes (2015). "Common mechanisms of excitatory and inhibitory imbalance in schizophrenia and autism spectrum disorders." Current molecular medicine **15**(2): 146-167.

Gardener, H., et al. (2011). "Perinatal and neonatal risk factors for autism: a comprehensive meta-analysis." Pediatrics **128**(2): 344-355.

Gebauer, F. and M. W. Hentze (2004). "Molecular mechanisms of translational control." Nature reviews Molecular cell biology **5**(10): 827-835.

Gholizadeh, S., et al. (2014). "Reduced phenotypic severity following adeno-associated virus-mediated Fmr1 gene delivery in fragile X mice." Neuropsychopharmacology **39**(13): 3100-3111.

Gholizadeh, S., et al. (2015). "Expression of fragile X mental retardation protein in neurons and glia of the developing and adult mouse brain." Brain research **1596**: 22-30.

Gingras, A.-C., et al. (2001). "Regulation of translation initiation by FRAP/mTOR." Genes & development **15**(7): 807-826.

Gkogkas, C. G., et al. (2013). "Autism-related deficits via dysregulated eIF4E-dependent translational control." Nature **493**(7432): 371-377.

Goldberg, J., et al. (1995). "Three-dimensional structure of the catalytic subunit of protein serine/threonine phosphatase-1." Nature **376**(6543): 745-753.

Gonzalez, D., et al. (2019). "Audiogenic seizures in the Fmr1 knock-out mouse are induced by Fmr1 deletion in subcortical, VGlut2-expressing excitatory neurons and require deletion in the inferior colliculus." Journal of Neuroscience **39**(49): 9852-9863.

Greenblatt, E. J. and A. C. Spradling (2018). "Fragile X mental retardation 1 gene enhances the translation of large autism-related proteins." Science **361**(6403): 709-712.

Gross, C., et al. (2011). "Fragile X mental retardation protein regulates protein expression and mRNA translation of the potassium channel Kv4. 2." Journal of Neuroscience **31**(15): 5693-5698.

Guo, F. and D. R. Cavener (2007). "The GCN2 eIF2α kinase regulates fatty-acid homeostasis in the liver during deprivation of an essential amino acid." Cell metabolism **5**(2): 103-114.

Guo, W., et al. (2015). "Elevated CaMKIIα and hyperphosphorylation of Homer mediate circuit dysfunction in a fragile X syndrome mouse model." Cell reports **13**(10): 2297-2311.

Hara, H. (2007). "Autism and epilepsy: a retrospective follow-up study." Brain and Development **29**(8): 486-490.

Harding, H. P., et al. (2000). "Regulated translation initiation controls stress-induced gene expression in mammalian cells." Molecular cell **6**(5): 1099-1108.

Harding, H. P., et al. (2019). "The ribosomal P-stalk couples amino acid starvation to GCN2 activation in mammalian cells." Elife **8**: e50149.

Harding, H. P., et al. (2009). "Ppp1r15 gene knockout reveals an essential role for translation initiation factor 2 alpha (eIF2α) dephosphorylation in mammalian development." Proceedings of the National Academy of Sciences **106**(6): 1832-1837.

Harding, H. P., et al. (2003). "An integrated stress response regulates amino acid metabolism and resistance to oxidative stress." Molecular cell **11**(3): 619-633.

Harris, J. (2018). "Leo Kanner and autism: a 75-year perspective." International Review of Psychiatry **30**(1): 3-17.

Harvey, R. F., et al. (2019). "Signaling from mTOR to eIF2α mediates cell migration in response to the chemotherapeutic doxorubicin." Science Signaling **12**(612): eaaw6763.

Hayashi, Y. and A. K. Majewska (2005). "Dendritic spine geometry: functional implication and regulation." Neuron **46**(4): 529-532.

Hays, S. A., et al. (2011). "Altered neocortical rhythmic activity states in Fmr1 KO mice are due to enhanced mGluR5 signaling and involve changes in excitatory circuitry." Journal of Neuroscience **31**(40): 14223-14234.

Hershey, J. W., et al. (2019). "Principles of translational control." Cold Spring Harbor Perspectives in Biology **11**(9): a032607.

Hinnebusch, A. G., et al. (2016). "Translational control by 5′-untranslated regions of eukaryotic mRNAs." Science **352**(6292): 1413-1416.

Hong, W., et al. (2014). "Antagonistic control of social versus repetitive self-grooming behaviors by separable amygdala neuronal subsets." Cell **158**(6): 1348-1361.

Hoozemans, J., et al. (2007). "Activation of the unfolded protein response in Parkinson's disease." Biochemical and biophysical research communications **354**(3): 707-711.

Hou, L., et al. (2006). "Dynamic translational and proteasomal regulation of fragile X mental retardation protein controls mGluR-dependent long-term depression." Neuron **51**(4): 441-454.

Hou, L. and E. Klann (2004). "Activation of the phosphoinositide 3-kinase-Akt-mammalian target of rapamycin signaling pathway is required for metabotropic glutamate receptor-dependent long-term depression." Journal of Neuroscience **24**(28): 6352-6361.

Huang, J. and B. D. Manning (2008). "The TSC1–TSC2 complex: a molecular switchboard controlling cell growth." Biochemical Journal **412**(2): 179-190.

Huber, K. M., et al. (2002). "Altered synaptic plasticity in a mouse model of fragile X mental retardation." Proceedings of the National Academy of Sciences **99**(11): 7746-7750.

Huber, K. M., et al. (2000). "Role for rapid dendritic protein synthesis in hippocampal mGluR-dependent long-term depression." Science **288**(5469): 1254-1256.

Huber, K. M., et al. (2015). "Dysregulation of mammalian target of rapamycin signaling in mouse models of autism." Journal of Neuroscience **35**(41): 13836-13842.

Huber, K. M., et al. (2001). "Chemical induction of mGluR5-and protein synthesis–dependent long-term depression in hippocampal area CA1." Journal of neurophysiology **86**(1): 321-325.

Hutsler, J. J. and H. Zhang (2010). "Increased dendritic spine densities on cortical projection neurons in autism spectrum disorders." Brain research **1309**: 83-94.

Ishimura, R., et al. (2016). "Activation of GCN2 kinase by ribosome stalling links translation elongation with translation initiation." Elife **5**: e14295.

Jack, A. and K. A. Pelphrey (2015). "Neural correlates of animacy attribution include neocerebellum in healthy adults." Cerebral cortex **25**(11): 4240-4247.

Jackson, R. J., et al. (2010). "The mechanism of eukaryotic translation initiation and principles of its regulation." Nature reviews Molecular cell biology **11**(2): 113-127.

Jacquemont, S., et al. (2018). "Protein synthesis levels are increased in a subset of individuals with fragile X syndrome." Human molecular genetics **27**(12): 2039-2051.

Jennings, M. D., et al. (2016). "eIF2β is critical for eIF5-mediated GDP-dissociation inhibitor activity and translational control." Nucleic acids research **44**(20): 9698-9709.

Jissendi, P., et al. (2008). "Diffusion tensor imaging (DTI) and tractography of the cerebellar projections to prefrontal and posterior parietal cortices: a study at 3T." Journal of Neuroradiology **35**(1): 42-50.

Kabir, Z., et al. (2017). "Rescue of impaired sociability and anxiety-like behavior in adult cacna1c-deficient mice by pharmacologically targeting eIF2α." Molecular psychiatry **22**(8): 1096-1109.

Kalish, B. T., et al. (2021). "Maternal immune activation in mice disrupts proteostasis in the fetal brain." Nature neuroscience **24**(2): 204-213.

Kao, D.-I., et al. (2010). "Altered mRNA transport, docking, and protein translation in neurons lacking fragile X mental retardation protein." Proceedings of the National Academy of Sciences **107**(35): 15601-15606.

Kelleher III, R. J. and M. F. Bear (2008). "The autistic neuron: troubled translation?" Cell **135**(3): 401-406.

Khandjian, E. W., et al. (1996). "The fragile X mental retardation protein is associated with ribosomes." Nature genetics **12**(1): 91-93.

Khandjian, E. W., et al. (2004). "Biochemical evidence for the association of fragile X mental retardation protein with brain polyribosomal ribonucleoparticles." Proceedings of the National Academy of Sciences **101**(36): 13357-13362.

Kim, J., et al. (2011). "AMPK and mTOR regulate autophagy through direct phosphorylation of Ulk1." Nature cell biology **13**(2): 132-141.

Kim, Y., et al. (2018). "PKR senses nuclear and mitochondrial signals by interacting with endogenous double-stranded RNAs." Molecular cell **71**(6): 1051-1063. e1056.

Kimball, S. R., et al. (1998). "Identification of interprotein interactions between the subunits of eukaryotic initiation factors eIF2 and eIF2B." Journal of Biological Chemistry **273**(5): 3039-3044.

Klann, E. and T. E. Dever (2004). "Biochemical mechanisms for translational regulation in synaptic plasticity." Nature reviews neuroscience **5**(12): 931-942.

Koekkoek, S., et al. (2005). "Deletion of FMR1 in Purkinje cells enhances parallel fiber LTD, enlarges spines, and attenuates cerebellar eyelid conditioning in Fragile X syndrome." Neuron **47**(3): 339-352.

Koelkebeck, K., et al. (2021). "Case of Asperger's Syndrome and Lesion of the Right Amygdala: Deficits in Implicit and Explicit Fearful Face Recognition." Frontiers in Psychology **12**.

Komar, A. A. and M. Hatzoglou (2011). "Cellular IRES-mediated translation: the war of ITAFs in pathophysiological states." Cell cycle **10**(2): 229-240.

Kooy, R. F. (2003). "Of mice and the fragile X syndrome." Trends in genetics **19**(3): 148-154.

Korb, E., et al. (2017). "Excess translation of epigenetic regulators contributes to fragile X syndrome and is alleviated by Brd4 inhibition." Cell **170**(6): 1209-1223. e1220.

Laggerbauer, B., et al. (2001). "Evidence that fragile X mental retardation protein is a negative regulator of translation." Human molecular genetics **10**(4): 329-338.

Lalonde, R. and C. Strazielle (2003). "The effects of cerebellar damage on maze learning in animals." The Cerebellum **2**(4): 300-309.

Lemaire, P. A., et al. (2008). "Mechanism of PKR Activation by dsRNA." Journal of molecular biology **381**(2): 351-360.

Levisohn, P. M. (2007). "The autism-epilepsy connection." Epilepsia **48**: 33-35.

Lin, W., et al. (2007). "The integrated stress response prevents demyelination by protecting oligodendrocytes against immune-mediated damage." The Journal of clinical investigation **117**(2): 448-456.

Liu, C. Y., et al. (2000). "Ligand-independent dimerization activates the stress response kinases IRE1 and PERK in the lumen of the endoplasmic reticulum." Journal of Biological Chemistry **275**(32): 24881-24885.

Liu, Z.-H., et al. (2012). "Lithium reverses increased rates of cerebral protein synthesis in a mouse model of fragile X syndrome." Neurobiology of disease **45**(3): 1145-1152.

Lovelace, J. W., et al. (2020). "Deletion of Fmr1 from forebrain excitatory neurons triggers abnormal cellular, EEG, and behavioral phenotypes in the auditory cortex of a mouse model of fragile X syndrome." Cerebral cortex **30**(3): 969-988.

Lu, R., et al. (2004). "The fragile X protein controls microtubule-associated protein 1B translation and microtubule stability in brain neuron development." Proceedings of the National Academy of Sciences **101**(42): 15201-15206.

Ma, T., et al. (2013). "Suppression of eIF2α kinases alleviates Alzheimer's disease–related plasticity and memory deficits." Nature neuroscience **16**(9): 1299-1305.

Maehama, T. and J. E. Dixon (1998). "The tumor suppressor, PTEN/MMAC1, dephosphorylates the lipid second messenger, phosphatidylinositol 3, 4, 5-trisphosphate." Journal of Biological Chemistry **273**(22): 13375-13378.

Maenner, M. J., et al. (2021). "Prevalence and characteristics of autism spectrum disorder among children aged 8 years—autism and developmental disabilities monitoring network, 11 sites, United States, 2018." MMWR Surveillance Summaries **70**(11): 1.

Manning, B. D., et al. (2002). "Identification of the tuberous sclerosis complex-2 tumor suppressor gene product tuberin as a target of the phosphoinositide 3-kinase/akt pathway." Molecular cell **10**(1): 151-162.

Marciniak, S. J., et al. (2006). "Activation-dependent substrate recruitment by the eukaryotic translation initiation factor 2 kinase PERK." The Journal of cell biology **172**(2): 201-209.

Marcotrigiano, J., et al. (1997). "Cocrystal structure of the messenger RNA 5′ cap-binding protein (eIF4E) bound to 7-methyl-GDP." Cell **89**(6): 951-961.

McKinney, B. C., et al. (2005). "Dendritic spine abnormalities in the occipital cortex of C57BL/6 Fmr1 knockout mice." American Journal of Medical Genetics Part B: Neuropsychiatric Genetics **136**(1): 98-102.

Michalon, A., et al. (2012). "Chronic pharmacological mGlu5 inhibition corrects fragile X in adult mice." Neuron **74**(1): 49-56.

Middleton, F. A. and P. L. Strick (2000). "Basal ganglia and cerebellar loops: motor and cognitive circuits." Brain research reviews **31**(2-3): 236-250.

Miyashiro, K. Y., et al. (2003). "RNA cargoes associating with FMRP reveal deficits in cellular functioning in Fmr1 null mice." Neuron **37**(3): 417-431.

Modabbernia, A., et al. (2017). "Environmental risk factors for autism: an evidence-based review of systematic reviews and meta-analyses." Molecular autism **8**(1): 1-16.

Morris, D. R. and A. P. Geballe (2000). "Upstream open reading frames as regulators of mRNA translation." Molecular and cellular biology **20**(23): 8635-8642.

Muddashetty, R. S., et al. (2007). "Dysregulated metabotropic glutamate receptor-dependent translation of AMPA receptor and postsynaptic density-95 mRNAs at synapses in a mouse model of fragile X syndrome." Journal of Neuroscience **27**(20): 5338-5348.

Muhle, R., et al. (2004). "The genetics of autism." Pediatrics **113**(5): e472-e486.

Mullins, C., et al. (2016). "Unifying views of autism spectrum disorders: a consideration of autoregulatory feedback loops." Neuron **89**(6): 1131-1156.

Musumeci, S. A., et al. (2000). "Audiogenic seizures susceptibility in transgenic mice with fragile X syndrome." Epilepsia **41**(1): 19-23.

Myrick, L. K., et al. (2015). "Independent role for presynaptic FMRP revealed by an FMR1 missense mutation associated with intellectual disability and seizures." Proceedings of the National Academy of Sciences **112**(4): 949-956.

Myrick, L. K., et al. (2015). "Human FMRP contains an integral tandem Agenet (Tudor) and KH motif in the amino terminal domain." Human molecular genetics **24**(6): 1733-1740.

Nakamoto, M., et al. (2007). "Fragile X mental retardation protein deficiency leads to excessive mGluR5-dependent internalization of AMPA receptors." Proceedings of the National Academy of Sciences **104**(39): 15537-15542.

Napoli, I., et al. (2008). "The fragile X syndrome protein represses activity-dependent translation through CYFIP1, a new 4E-BP." Cell **134**(6): 1042-1054.

Narasimhan, J., et al. (2004). "Dimerization is required for activation of eIF2 kinase Gcn2 in response to diverse environmental stress conditions." Journal of Biological Chemistry **279**(22): 22820-22832.

Nicholls, R. E., et al. (2008). "Transgenic mice lacking NMDAR-dependent LTD exhibit deficits in behavioral flexibility." Neuron **58**(1): 104-117.

Niere, F., et al. (2012). "Evidence for a fragile X mental retardation protein-mediated translational switch in metabotropic glutamate receptor-triggered Arc translation and long-term depression." Journal of Neuroscience **32**(17): 5924-5936.

Novoa, I., et al. (2001). "Feedback inhibition of the unfolded protein response by GADD34-mediated dephosphorylation of eIF2α." The Journal of cell biology **153**(5): 1011-1022.

Ofner, M., et al. (2018). Autism spectrum disorder among children and youth in Canada 2018, Public Health Agency of Canada Ottawa, ON.

Olmos-Serrano, J. L., et al. (2010). "Defective GABAergic neurotransmission and pharmacological rescue of neuronal hyperexcitability in the amygdala in a mouse model of fragile X syndrome." Journal of Neuroscience **30**(29): 9929-9938.

Osterweil, E. K., et al. (2010). "Hypersensitivity to mGluR5 and ERK1/2 leads to excessive protein synthesis in the hippocampus of a mouse model of fragile X syndrome." Journal of Neuroscience **30**(46): 15616-15627.

Pakos-Zebrucka, K., et al. (2016). "The integrated stress response." EMBO reports **17**(10): 1374-1395.

Palmen, S. J., et al. (2004). "Neuropathological findings in autism." Brain **127**(12): 2572-2583.

Palmer, M., et al. (1997). "The group I mGlu receptor agonist DHPG induces a novel form of LTD in the CA1 region of the hippocampus." Neuropharmacology **36**(11-12): 1517-1532.

Paulsen, B., et al. (2022). "Autism genes converge on asynchronous development of shared neuron classes." Nature **602**(7896): 268-273.

Pelletier, J. and N. Sonenberg (1988). "Internal initiation of translation of eukaryotic mRNA directed by a sequence derived from poliovirus RNA." Nature **334**(6180): 320-325.

Penzes, P., et al. (2011). "Dendritic spine pathology in neuropsychiatric disorders." Nature neuroscience **14**(3): 285-293.

Phan, A. T., et al. (2011). "Structure-function studies of FMRP RGG peptide recognition of an RNA duplex-quadruplex junction." Nature structural & molecular biology **18**(7): 796-804.

Pinar, C., et al. (2017). "Revisiting the flip side: long-term depression of synaptic efficacy in the hippocampus." Neuroscience & Biobehavioral Reviews **80**: 394-413.

Placzek, A. N., et al. (2016). "eIF2α-mediated translational control regulates the persistence of cocaine-induced LTP in midbrain dopamine neurons." Elife **5**: e17517.

Pop, A. S., et al. (2014). "Rescue of dendritic spine phenotype in Fmr1 KO mice with the mGluR5 antagonist AFQ056/Mavoglurant." Psychopharmacology **231**(6): 1227-1235.

Poultney, C. S., et al. (2013). "Identification of small exonic CNV from whole-exome sequence data and application to autism spectrum disorder." The American Journal of Human Genetics **93**(4): 607-619.

Qin, M., et al. (2005). "Postadolescent changes in regional cerebral protein synthesis: an in vivo study in the FMR1 null mouse." Journal of Neuroscience **25**(20): 5087-5095.

Qin, M., et al. (2013). "Altered cerebral protein synthesis in fragile X syndrome: studies in human subjects and knockout mice." Journal of Cerebral Blood Flow & Metabolism **33**(4): 499-507.

Reith, R. M., et al. (2013). "Loss of Tsc2 in Purkinje cells is associated with autistic-like behavior in a mouse model of tuberous sclerosis complex." Neurobiology of disease **51**: 93-103.

Richter, J. D. and N. Sonenberg (2005). "Regulation of cap-dependent translation by eIF4E inhibitory proteins." Nature **433**(7025): 477-480.

Riva, D. and C. Giorgi (2000). "The cerebellum contributes to higher functions during development: evidence from a series of children surgically treated for posterior fossa tumours." Brain **123**(5): 1051-1061.

Ronesi, J. A., et al. (2012). "Disrupted Homer scaffolds mediate abnormal mGluR5 function in a mouse model of fragile X syndrome." Nature neuroscience **15**(3): 431-440.

Ronesi, J. A. and K. M. Huber (2008). "Homer interactions are necessary for metabotropic glutamate receptor-induced long-term depression and translational activation." Journal of Neuroscience **28**(2): 543-547.

Ruzzo, E. K., et al. (2019). "Inherited and de novo genetic risk for autism impacts shared networks." Cell **178**(4): 850-866. e826.

Sabanov, V., et al. (2017). "Impaired GABAergic inhibition in the hippocampus of Fmr1 knockout mice." Neuropharmacology **116**: 71-81.

Santini, E., et al. (2013). "Exaggerated translation causes synaptic and behavioural aberrations associated with autism." Nature **493**(7432): 411-415.

Sato, A. (2016). "mTOR, a potential target to treat autism spectrum disorder." CNS & Neurological Disorders-Drug Targets (Formerly Current Drug Targets-CNS & Neurological Disorders) **15**(5): 533-543.

Satoh, Y., et al. (2011). "ERK2 contributes to the control of social behaviors in mice." Journal of Neuroscience **31**(33): 11953-11967.

Sawicka, K., et al. (2019). "FMRP has a cell-type-specific role in CA1 pyramidal neurons to regulate autism-related transcripts and circadian memory." Elife **8**: e46919.

Sawicka, K., et al. (2016). "Elevated ERK/p90 ribosomal S6 kinase activity underlies audiogenic seizure susceptibility in fragile X mice." Proceedings of the National Academy of Sciences **113**(41): E6290-E6297.

Saxton, R. A. and D. M. Sabatini (2017). "mTOR signaling in growth, metabolism, and disease." Cell **168**(6): 960-976.

Schaefer, G. B. and N. J. Mendelsohn (2008). "Genetics evaluation for the etiologic diagnosis of autism spectrum disorders." Genetics in Medicine **10**(1): 4-12.

Schmahmann, J. D. and D. N. Pandya (1995). "Prefrontal cortex projections to the basilar pons in rhesus monkey: implications for the cerebellar contribution to higher function." Neuroscience letters **199**(3): 175-178.

Schröder, M. and R. J. Kaufman (2005). "The mammalian unfolded protein response." Annu. Rev. Biochem. **74**: 739-789.

Schumann, C. M., et al. (2004). "The amygdala is enlarged in children but not adolescents with autism; the hippocampus is enlarged at all ages." Journal of Neuroscience **24**(28): 6392-6401.

Shah, S., et al. (2020). "FMRP control of ribosome translocation promotes chromatin modifications and alternative splicing of neuronal genes linked to autism." Cell reports **30**(13): 4459-4472. e4456.

Shahbazian, D., et al. (2010). "eIF4B controls survival and proliferation and is regulated by proto-oncogenic signaling pathways." Cell cycle **9**(20): 4106-4109.

Shahbazian, D., et al. (2006). "The mTOR/PI3K and MAPK pathways converge on eIF4B to control its phosphorylation and activity." The EMBO journal **25**(12): 2781-2791.

Sharma, A., et al. (2010). "Dysregulation of mTOR signaling in fragile X syndrome." Journal of Neuroscience **30**(2): 694-702.

Sharma, V., et al. (2020). "eIF2α controls memory consolidation via excitatory and somatostatin neurons." Nature **586**(7829): 412-416.

Siomi, H., et al. (1993). "The protein product of the fragile X gene, FMR1, has characteristics of an RNA-binding protein." Cell **74**(2): 291-298.

Smalley, S. L. (1998). "Autism and tuberous sclerosis." Journal of autism and developmental disorders **28**(5): 407-414.

Snider, R. S. and A. Maiti (1976). "Cerebellar contributions to the Papez circuit." Journal of neuroscience research **2**(2): 133-146.

Sonenberg, N. and A.-C. Gingras (1998). "The mRNA 5′ cap-binding protein eIF4E and control of cell growth." Current opinion in cell biology **10**(2): 268-275.

Sood, R., et al. (2000). "A mammalian homologue of GCN2 protein kinase important for translational control by phosphorylation of eukaryotic initiation factor-2α." Genetics **154**(2): 787-801.

Spencer, C. M., et al. (2011). "Modifying behavioral phenotypes in Fmr1KO mice: Genetic background differences reveal autistic-like responses." Autism research **4**(1): 40-56.

Sragovich, S., et al. (2017). "ADNP plays a key role in autophagy: from autism to schizophrenia and Alzheimer's disease." Bioessays **39**(11): 1700054.

Stefani, G., et al. (2004). "Fragile X mental retardation protein is associated with translating polyribosomes in neuronal cells." Journal of Neuroscience **24**(33): 7272-7276.

Takarae, Y. and J. Sweeney (2017). "Neural hyperexcitability in autism spectrum disorders." Brain sciences **7**(10): 129.

Taniuchi, S., et al. (2016). "Integrated stress response of vertebrates is regulated by four eIF2α kinases." Scientific reports **6**(1): 1-11.

Taylor, P. and J. Brameld (1999). "Mechanisms and regulation of transcription and translation." PUBLICATION-EUROPEAN ASSOCIATION FOR ANIMAL PRODUCTION **96**: 25-50.

Teske, B. F., et al. (2013). "CHOP induces activating transcription factor 5 (ATF5) to trigger apoptosis in response to perturbations in protein homeostasis." Molecular biology of the cell **24**(15): 2477-2490.

Thomson, S. R., et al. (2017). "Cell-type-specific translation profiling reveals a novel strategy for treating fragile X syndrome." Neuron **95**(3): 550-563. e555.

Todd, P. K., et al. (2003). "The fragile X mental retardation protein is required for type-I metabotropic glutamate receptor-dependent translation of PSD-95." Proceedings of the National Academy of Sciences **100**(24): 14374-14378.

Toft, A. K. H. (2019). "Impact of two autism related genes on amygdala physiology."

Toro, R., et al. (2010). "Key role for gene dosage and synaptic homeostasis in autism spectrum disorders." Trends in genetics **26**(8): 363-372.

Trinh, M. A., et al. (2014). "The eIF2α kinase PERK limits the expression of hippocampal metabotropic glutamate receptor-dependent long-term depression." Learning & memory **21**(5): 298-304.

Tsai, P. T., et al. (2012). "Autistic-like behaviour and cerebellar dysfunction in Purkinje cell Tsc1 mutant mice." Nature **488**(7413): 647-651.

Tsaytler, P., et al. (2011). "Selective inhibition of a regulatory subunit of protein phosphatase 1 restores proteostasis." Science **332**(6025): 91-94.

Udagawa, T., et al. (2013). "Genetic and acute CPEB1 depletion ameliorate fragile X pathophysiology." Nature medicine **19**(11): 1473-1477.

Utami, K. H., et al. (2020). "Elevated de novo protein synthesis in FMRP-deficient human neurons and its correction by metformin treatment." Molecular autism **11**(1): 1-11.

Vagnarelli, P. and D. R. Alessi (2018). "PP1 phosphatase complexes: undruggable no longer." Cell **174**(5): 1049-1051.

Valentinova, K. and M. Mameli (2016). "mGluR-LTD at excitatory and inhibitory synapses in the lateral habenula tunes neuronal output." Cell reports **16**(9): 2298-2307.

Veeraragavan, S., et al. (2012). "Genetic reduction of muscarinic M4 receptor modulates analgesic response and acoustic startle response in a mouse model of fragile X syndrome (FXS)." Behavioural brain research **228**(1): 1-8.

Volkmar, F. R. and B. Reichow (2013). "Autism in DSM-5: progress and challenges." Molecular autism **4**(1): 1-6.

Wang, S. S.-H., et al. (2014). "The cerebellum, sensitive periods, and autism." Neuron **83**(3): 518-532.

Wang, X., et al. (1998). "The phosphorylation of eukaryotic initiation factor eIF4E in response to phorbol esters, cell stresses, and cytokines is mediated by distinct MAP kinase pathways." Journal of Biological Chemistry **273**(16): 9373-9377.

Wang, X., et al. (2001). "Regulation of elongation factor 2 kinase by p90RSK1 and p70 S6 kinase." The EMBO journal **20**(16): 4370-4379.

Waung, M. W. and K. M. Huber (2009). "Protein translation in synaptic plasticity: mGluR-LTD, Fragile X." Current opinion in neurobiology **19**(3): 319-326.

Weiler, I. J., et al. (1997). "Fragile X mental retardation protein is translated near synapses in response to neurotransmitter activation." Proceedings of the National Academy of Sciences **94**(10): 5395-5400.

Whitney, E. R., et al. (2008). "Cerebellar Purkinje cells are reduced in a subpopulation of autistic brains: a stereological experiment using calbindin-D28k." The Cerebellum **7**(3): 406-416.

Winden, K. D., et al. (2018). "Abnormal mTOR activation in autism." Annual review of neuroscience **41**: 1-23.

Wu, C. C.-C., et al. (2020). "Ribosome collisions trigger general stress responses to regulate cell fate." Cell **182**(2): 404-416. e414.

Xu, Z.-X., et al. (2020). "Elevated protein synthesis in microglia causes autism-like synaptic and behavioral aberrations." Nature communications **11**(1): 1-17.

Yan, L. L. and H. S. Zaher (2021). "Ribosome quality control antagonizes the activation of the integrated stress response on colliding ribosomes." Molecular cell **81**(3): 614-628. e614.

Young, S. K. and R. C. Wek (2016). "Upstream open reading frames differentially regulate gene-specific translation in the integrated stress response." Journal of Biological Chemistry **291**(33): 16927-16935.

Zafeiriou, D. I., et al. (2007). "Childhood autism and associated comorbidities." Brain and Development **29**(5): 257-272.

Zalfa, F. and C. Bagni (2004). "Molecular insights into mental retardation: multiple functions for the Fragile X mental retardation protein?" Current issues in molecular biology **6**(2): 73-88.

Zhang, F., et al. (2018). "Fragile X mental retardation protein modulates the stability of its m6A-marked messenger RNA targets." Human molecular genetics **27**(22): 3936-3950.

Zhang, Y., et al. (2014). "Dendritic channelopathies contribute to neocortical and sensory hyperexcitability in Fmr1−/y mice." Nature neuroscience **17**(12): 1701-1709.

Zhou, J. and L. F. Parada (2012). "PTEN signaling in autism spectrum disorders." Current opinion in neurobiology **22**(5): 873-879.

Zhu, P. J., et al. (2011). "Suppression of PKR promotes network excitability and enhanced cognition by interferon-γ-mediated disinhibition." Cell **147**(6): 1384-1396.

Zhu, P. J., et al. (2019). "Activation of the ISR mediates the behavioral and neurophysiological abnormalities in Down syndrome." Science **366**(6467): 843-849.